Universidad de Valladolid

Escuela de Doctorado Universidad de Valladolid

PROGRAMA DE DOCTORADO EN QUÍMICA: QUÍMICA DE SÍNTESIS, CATÁLISIS Y MATERIALES AVANZADOS

TESIS DOCTORAL:

C–H Functionalization of Arenes Enabled by Cooperating Pyridone-Type Ligands: More Selective Transformations and a Dual Ligand System for Milder Reaction Conditions

Presentada por Cintya Pinilla Martín para optar al grado de Doctor/a por la Universidad de Valladolid

Dirigida por:

Ana Carmen Albéniz Jiménez

AUTORIZACIÓN DE LA DIRECTORA DE TESIS

Ana Carmen Albéniz Jiménez, Catedrática de Química Inorgánica de la Universidad de Valladolid e investigadora del I. U. CINQUIMA

CERTIFICA:

Que la memoria titulada *''C–H Functionalization of Arenes Enabled by Cooperating Pyridone-Type Ligands: More Selective Transformations and a Dual Ligand System for Milder Reaction Conditions''* ha sido realizada en el I. U. CINQUIMA y el Área de Química Inorgánica de la Facultad de Ciencias de la Universidad de Valladolid por Cintya Pinilla Martín, alumna del programa de doctorado *"Doctorado en Química: Química de Síntesis, Catálisis y Materiales Avanzados"* y autoriza su presentación para que sea calificada como Tesis Doctoral.

Valladolid, a 28 de septiembre de 2023

La Directora de la Tesis

Fdo: Ana Carmen Albéniz Jiménez

La Tesis Doctoral titulada *''C-H Functionalization of Arenes Enabled by Cooperating Pyridone-Type Ligands: More Selective Transformations and a Dual Ligand System for Milder Reaction Conditions''* ha sido realizada gracias al apoyo económico del MICINN/AEI (proyectos CTQ-2016-80913-P y PID2019-111406GB-I00), de la Junta de Castilla y León-FEDER y Fondo Social Europeo (proyectos VA051P17, VA062G18, VA224P20, ayuda para contratos predoctorales EDU/556/2019, de 5 de junio, VA087-18). La asistencia a algunos congresos ha sido objeto de ayudas por parte de la ST de Castilla de la RSEQ. La realización de una estancia breve ha sido financiada por la Universidad de Valladolid (movilidad doctorandos: ayudas para estancias breves en el desarrollo de tesis doctorales, convocatoria 2022).

Hasta el momento, el trabajo presentado en esta Tesis ha dado lugar a la siguiente publicación:

''Palladium-Catalyzed Ortho C-H Arylation of Unprotected Anilines: Chemo- and Regioselectivity Enabled by the Cooperating Ligand [2,2'-Bipyridin]-6(1H)-one''

Pinilla, C.; Salamanca, V.; Lledós, A.*; Albéniz, A. C.* *ACS Catalysis* **2022**, *12*, 14527-14532. DOI: 10.1021/acscatal.2c05206

Agradecimientos

Me gustaría dedicar estas palabras a todas aquellas personas que me han acompañado durante la tesis doctoral, ya que cada una de ellas han aportado su granito de arena para que llegara este momento.

En primer lugar, a la Profesora Ana Carmen Albéniz por acogerme en su grupo de investigación y dejarme formar parte de él. Gracias por la paciencia durante las largas reuniones de las que he aprendido mucha química, pero también por los trucos y consejos.

A todos los profesores del departamento por estar siempre disponibles para echarme una mano ya fuera en el uso de equipos, tramitación de papeles o dudas en general. Sobre todo a JM, que siempre tiene soluciones a todos los imprevistos que puedan ocurrir.

Gracias a todos los compis que han pasado por el lab 21, desde los que me han enseñado las bases de todo lo que sé: Beto, Rodri y Vanesa, los que ya no están por aquí: Javi y Mario, hasta mis últimos compañeros Sozan, Virginia y Miguel. A Sarah, por las largas charlas dentro y fuera del laboratorio. También a todos con los que he compartido estos años por el quifima Andrea, Jose Ramón, Olmo, María P., María B., Noelia, Sandra, Javi, Leo, Marconi y Sergio.

A la cuadrilla que hemos formado estos últimos años: Miguel, Nacho, Fran, Jaime, Safer, Wonka, Carlos, Marta, Rebeca y Damián. Por todos los cafés, las (necesarias) cervezas, casas rurales y congresos que han hecho todo más divertido.

To Prof. Cristina Nevado, for the opportunity to join her group in the University of Zurich. To all my lab mates Iván, Hamish, Eleen, Johannes, Xiaoyong, Georgia, Leonardo, in special to my beer-mates at the Irchel bar: the bad influence from Marc and Ced, and also Jaime, Jorge, Sergio, Marc L, Robin and Michal. To the best flat mates ever: Doriane and Debora, for all the help at home and at the university. I would also like to thank Marc, Doriane, Debora and Helena for all the hikes we have done discovering the beauty of Switzerland. I hope we will meet again maybe in another city, in other lab, but always with a beer, glühwein or an Aperol.

Gracias a mis primeritos compis químicos, que llevan aguantándome DIEZ años desde que en septiembre de 2013 empezamos la carrera. Por todos los viajes, fiestas, comidas, cenas y todos los momentos compartidos. Laura, David, Bea, Ana y

Gaby, espero que sigamos conociendo mundo y gastronomía juntos por muchos muchos años más.

A las de toda la vida, Vero, Isa, Estefanía, Sonia, Isa, Marina, Moni, Anabel, Eva y, aunque este un poco más lejos, Alba. Por seguir saliendo, festejando y charlando para recargar las pilas.

Por último, los más importantes, los que han celebrado cada una de las buenas noticias pero que también han sufrido conmigo la cara B del doctorado: ***mi familia****. Gracias a mis padres, por apoyarme en cada decisión que he tomado y darme un empujoncito siempre que lo he necesitado. A María, por estar ahí en lo bueno y en lo malo, por tener siempre un rato para escucharme y alegrarme, o también enfadarme, pero para eso están las hermanas. A Darío, mi compañero de vida y aventuras. Habéis sido lo que me ha dado fuerza para continuar hasta el final. Simplemente gracias.*

A mi Abuela y a Yaya, allá dónde estéis. A mi Abuelo. Vuestra sabiduría forma parte de mí, y gracias a vosotros soy quien soy hoy en día.

Table of contents

Preface

Preface

The development of more sustainable and environmentally friendly chemical processes is one of the main challenges in chemistry nowadays. In that context, the main goal of this thesis is to improve the reaction conditions in C–C coupling processes that involve a C–H activation step and achieve selective transformations. The formation of new C–C bonds is a versatile tool in the synthesis of interesting compounds such as drugs, pesticides, cosmetics and so on. Focusing on palladium-catalysed reactions, they generally involve an organometallic compound and an organic halide derivative. Both reagents have to be synthesised from the corresponding hydrocarbons. To improve the step economy of the processes, several efforts have been made during the last decades in order to use the raw materials as reagents, avoiding their prefunctionalization. The new strategies require a C–H activation step in their mechanism but this is not easy due to the low reactivity of the C–H bonds. To achieve those high energy demanding processes, cooperating ligands have been developed with the role of assisting during the C–H activation of the reactants. The work in this thesis is focused on the use of cooperating ligands in C–C coupling reactions with C–H activation.

Chapter 1 contains a general introduction of C–C coupling processes involving a C–H activation step. The different alternatives to the conventional couplings used in the literature and the most relevant mechanisms described for the C–H activation step are included. Some of the strategies developed to control the regioselectivity of the reactions are also commented.

Chapter 2 and *Chapter 3* describes the use of the cooperating ligand 2,2'-bipiridin-6(1*H*)-one in the direct arylation of arenes. In *Chapter 2*, the chemo- and regioselective arylation of primary anilines in the aromatic ring is achieved. By using the cooperating ligand, the competitive amination reaction (Buchwald-Hartwig reaction) is not occurring, and the C–C coupling product is obtained without the need of protecting the amine group. An exhaustive computational study of the reaction mechanism explaining the selectivity observed was done in collaboration with Prof. Agustí Lledós from Universidad Autónoma de Barcelona.

The direct arylation of simple arenes by a dual ligand system is described in *Chapter 3*. The use of the cooperating ligand in combination with PCy_3 allows to use milder conditions than the reported ones. Several functional groups are tolerated in the arene and in the aryl halide derivative. The preliminary mechanistic studies show an operating bimetallic catalytic cycle.

Finally, *Chapter 4* describes the study of the cooperating ability of 6-hydroxypicolinic acid and amido-pyridine type ligands. Both of them have a similar scaffold to 2,2'-bipiridin-6(1*H*)-one or the widely reported *N*-monoprotected amino acids (MPAAs). In that way, we hypothesize those ligands meet the necessary requirements to assist during the C–H activation step in different processes.

The dissertation contains an *Appendix* with a list of abbreviations and an index of the compounds described. The references are presented as footnotes in every chapter and collected in the appendix as a list. A brief summary of the results in Spanish is also included.

Chapter 1

1 Introduction

1.1 C–C CROSS COUPLING REACTIONS WITH C–H ACTIVATION

Since their discovery in the 1970s, Pd-catalysed C–C cross coupling reactions have become one of the most relevant reactions in synthetic chemistry. The formation of a new carbon-carbon bond between two different carbon-containing molecules is a powerful tool due to the large variety of compounds that can be synthesised. The importance of this strategy was recognised by the Nobel Prize in chemistry awarded in 2010 to Professors Richard F. Heck, Ei-ichi Negishi and Akira Suzuki.[1]

There is a huge number of different C–C cross coupling reactions depending on the nature of the reagents and the metals that have been used as catalysts. Focusing on Pd-catalysed reactions, one of the first references found in the literature is the coupling between an organic halide (R–X) and an olefinic compound, the so called Mizoroki-Heck reaction.[2] Soon, new processes were developed where an organometallic compound (M–R') is the coupling partner of the halide derivative (R–X) (Equation 1.1). Based on the metal used in the M–R' molecule, the reaction receives diverse names: MgXR'

[1] Wu, X.-F.; Anbarasan, P.; Neumann, H.; Beller, M. *Angew. Chem. Int. Ed.* **2010**, *49*, 9047-9050.
[2] a) Mizoroki, T.; Ozaki, M. A. *Bull. Chem. Soc. Jpn.* **1971**, *44*, 581-584. b) Heck, R. F. *J. Am. Chem. Soc.* **1968**, *90*, 5518-5526. c) Heck, R. F. *Org. React.* **1982**, *27*, 345-390.

(Kumada),[3] ZnXR' (Negishi),[4] R_2BR' (Suzuki-Miyaura),[5] R_3SnR' (Stille),[6] R_3SiR' (Hiyama).[7] Furthermore, the coupling of alkynes and organic halides, the Sonogashira reaction, generally uses a Cu cocatalyst.[8]

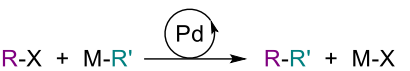

Equation 1.1.

The main disadvantage of the conventional C–C cross couplings is the need to previously synthesise the reagents. From hydrocarbons as starting materials, their prefunctionalization needs at least one step to prepare the organic halide and two steps to synthesise the organometallic compound. In this context, several efforts have been made in the last decades to find more efficient processes.[9]

The most studied strategy is to use the hydrocarbons directly as reagents, leading to a more step-economic process. Those reactions involve a C–H activation step and avoid the requirement of prefunctionalizing the reagents. However, the poor reactivity and elevated strength of the C–H bonds makes the transformation high energy demanding. Moreover, the selectivity to functionalize one C–H bond among the large amount of them in the starting material is a real challenge.

In the last decades, a large number of research groups have focused their studies on C–H activation processes. A quick search in SciFinder[n][10] with the keywords ''C–H activation'' leads to 1941 references only in 2022 (Figure 1.1). The huge number of articles clearly demonstrates the synthetic importance of the topic.

[3] Kumada, M. *Pure Appl. Chem.* **1980**, *52*, 669-679.
[4] Negishi, E.-I., *Ass. Chem. Res.* **1982**, *15*, 340-348.
[5] a) Miyaura, N.; Yanagi, T.; Suzuki, A. *Synth. Commun.* **1981**, *11*, 513-519. b) Miyaura, N.; Suzuki, A. *Chem. Rev.* **1995**, *95*, 2457-2483.
[6] a) Stille, J. K. *Angew. Chem. Int. Ed.* **1986**, *25*, 508-524. b) Stille, J. K. *Angew. Chem.* **1986**, *98*, 504-519.
[7] a) Hiyama, T.; Shirakawa, E. *Top. Curr. Chem.* **2002**, *219*, 61-85. b) Hiyama, T.; *J. Organomet. Chem.* **2002**, *653*, 58-61.
[8] a) Sonogashira, K.; Tohda, Y.; Hagihara, N. *Tetrahedron Lett.* **1975**, 4467-4470. b) Sonogashira, K. in *Comprehensive organic Synthesis* (Eds.: B. M. Trost, I. Fleming), Pergamon Press, Oxford, **1991**, *3*, 521-549.
[9] Campeau, L.-C.; Hazari, N. *Organometallics* **2019**, *38*, 3-35.
[10] https://scifinder.cas.org (accessed June 5, 2023).

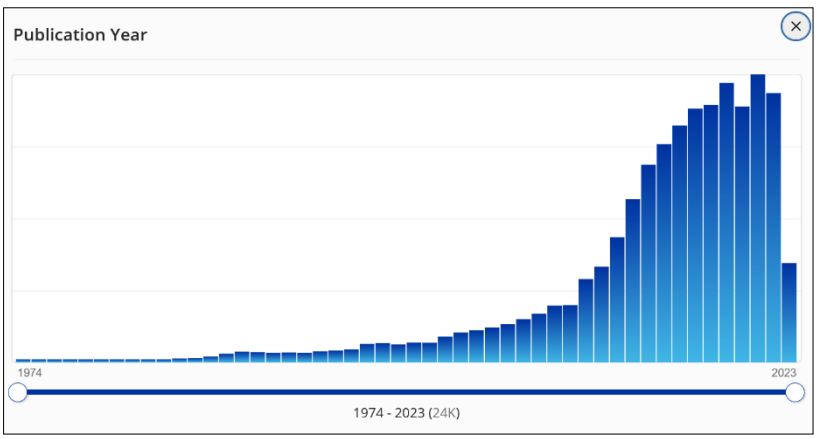

Figure 1.1. Increment in the number of articles published from 1974 to 2023. Data taken from SciFinder^{n} using ‘’C–H activation’’ as key words.

One of the metals most used as catalyst for these strategies is palladium. The progress in the field lets to functionalize alkanes,[11] make enantioselective transformations,[12] or even introduce other procedures such as mechanochemistry[13] or photocatalysis[14] to obtain the desired coupling product. Several efforts have been made to make the process even more sustainable,[15] such as the development of reusable catalyst,[16] the use of earth abundant metals as catalysts,[17] or the development of suitable conditions for room temperature reactions.[18]

We will focus this introduction on palladium-catalysed C–H activation of arenes as hydrocarbons, the substrates used in this thesis work. Depending on the reagent in the conventional cross-coupling reaction that is going to be replaced with the corresponding hydrocarbon, we can differentiate three types of processes (Figure 1.2).

[11] He, J.; Wasa, M.; Chan, K. S. L.; Shao, Q.; Yu, J.-Q. *Chem. Rev.* **2017**, *117*, 8754-8786.
[12] Newton, C. G.; Wang, S.-G.; Oliveira, C. C.; Cramer, N. *Chem. Rev*. **2017**, *117*, 8908-8976.
[13] Seo, T.; Kubota, K.; Ito, H. *J. Am. Chem. Soc*. **2023**, *145*, 12, 6823-6837.
[14] a) Kalyani, D.; McMurtrey, K. B.; Neufeldt, S. R.; Sanford, M. S. *J. Am. Chem. Soc*. **2011**, *133*, 18566-18569. b) Liang, L.; Xie, M. S.; Wang, H. X.; Niu, H. Y.; Qu, G. R.; Guo, H. M. *J. Org. Chem.* **2017**, *82*, 5966-5973. c) Sahoo, M. K.; Rana, J.; Subaramanian, M.; Balaraman, E. *ChemistrySelect* **2017**, *2*, 7565-7569.
[15] Dhawa, U.; Kaplaneris, N.; Ackermann, L. *Org. Chem. Front*., **2021**, *8*, 4886-4913.
[16] Mandal, T.; Mondal, M.; Choudhury, J. *Organometallics* **2021**, *40*, 2443-2449.
[17] Gandeepan, P.; Müller, T.; Zell, D.; Cera, G.; Warratz, S.; Ackermann, L. *Chem. Rev*. **2019**, *119*, 2192-2452.
[18] Yadav, P.; Velmurugan, N.; Luscombe, C. K. *Synthesis* **2023**, *55*, 1-26.

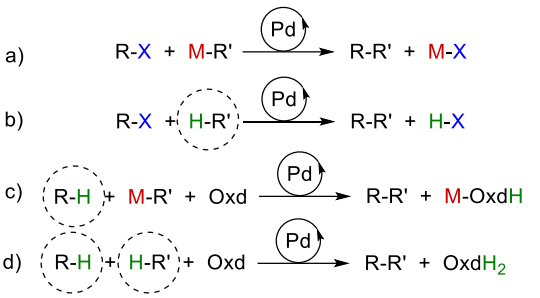

Figure 1.2. a) Traditional cross-coupling. b) Cross-coupling between a halide and a hydrocarbon. c) and d) oxidative cross-coupling.

In the conventional reaction we can assume an electrophilic behaviour of the halide derivative and a nucleophilic one for the organometallic reactant (Figure 1.2, a). By substituting the organometallic derivative by the corresponding hydrocarbon (Figure 1.2, b), we can consider that the electronic properties do not change, the hydrocarbon will behave as nucleophile. This strategy has been widely used for the synthesis of biaryls,[19] and it has been studied in our research group, for example, the direct arylation of toluene (Equation 1.2).[20]

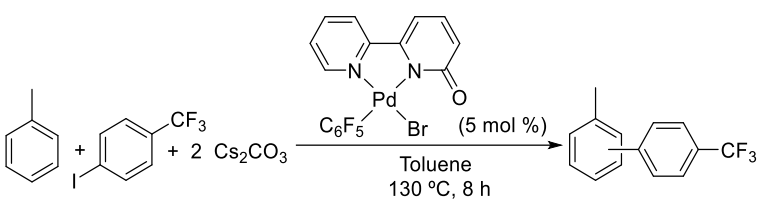

Equation 1.2.

When the organic halide is replaced, the two reagents will behave as nucleophiles, so an oxidant is required as reactant in the reaction medium (Figure 1.2, c). Usually, a boronic acid is used as organometallic reagent.[21] A recent example can be found in the oxidative arylation of benzylic carboxylates using oxygen as oxidant, whose mechanism has been studied by Stahl *et al*. (Equation 1.3).[22]

---

[19] Vicente, R.; Kapdi, A. R.; Ackermann, L. *Angew. Chem. Int. Ed*. **2009**, *48*, 9792-9826.
[20] a) Salamanca, V.; Toledo, A.; Albéniz, A. C. *J. Am. Chem. Soc*. **2018**, *140*, 17851-17856. b) Salamanca, V.; Albéniz, A. C. *Org. Chem. Front*., **2021**, *8*, 1941-1951.
[21] a) Luan, Y.-X.; Zhang, T.; Yao, W.-W.; Lu,, K.; Kong, L.-Y.; Lin, Y.-T.; Ye, M. *J. Am. Chem. Soc*. **2017**, *139*, 1786-1789. b) Wang, D.; Salazar, C. A.; Stahl, S. S. *Organometallics*, **2021**, *40*, 2198-2203.
[22] Salazar, C. A.; Gair, J. J.; Flesch, K. N.; Guzei, I. A.; Lewis, J. C.; Stahl, S. S. *Angew. Chem. Int. Ed.*, **2020**, *59*, 10873-10877.

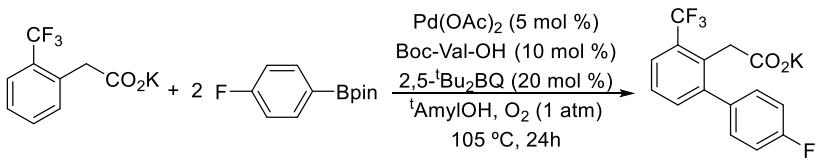

Equation 1.3.

In the last strategy (Figure 1.2, d), both reagents are replaced by hydrocarbons and again an oxidant is needed to recover the active catalyst. This type of reactions can be divided in two main groups: the coupling between an arene and an olefin (Fujiwara-Moritani or oxidative Heck reaction),[23] and between two arenes.[24] The oxidative Heck reaction of arenes and polyfluoroarenes has been studied recently in our research group; one example is the reaction between toluene and *tert*-butyl acrylate using oxygen as oxidant (Equation 1.4).[25]

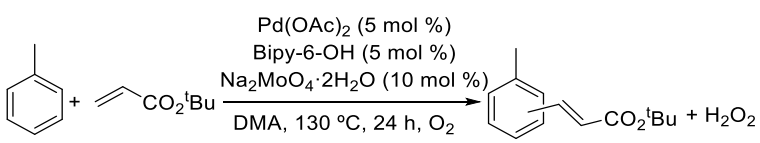

Equation 1.4.

In the case of the oxidative coupling between two arenes, one of the first publications was the reaction of indoles and simple arenes developed by Fagnou. The reaction conditions require a slight excess of copper acetate as oxidant (Equation 1.5).[26]

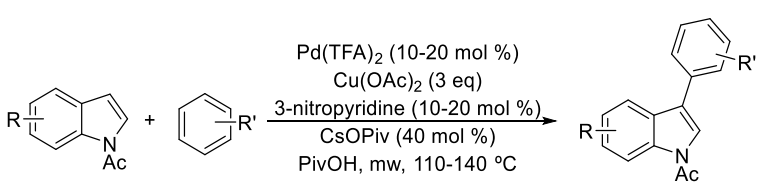

Equation 1.5.

[23] a) Kancherla,S.; Jorgensen, K. B.; Fernández-Ibáñez, M. A. *Synthesis* **2019**, *51*, 643-663. b) Ali, W.; Prakash, G.; Maiti, D. *Chem. Sci.* **2021**, *12*, 2735-2759. c) Ortiz-de-Elguea, V.; Carral-Menoyo, A.; Simón-Vidal, L.; Martinez-Nunes, M.; Barbolla, I.; Lete, M. G.; Sotomayor, N.; Lete, E. *ACS Omega*, **2021**, *6*, 29483-29494.
[24] Yang, Y.; Lan, J.; You, J. *Chem. Rev*. **2017**, *117*, 8787-8863.
[25] Villalba, F.; Albéniz, A. C. *Adv. Synth.Catal*. **2021**, *363*, 4795-4804.
[26] Stuart, D. R. ; Fagnou, K. *Science* **2007**, *316*, 1172-1175.

Comparing the mechanism of the conventional couplings and the alternatives described above, we can find elementary steps that are not modified but some others that change depending on the reagent that is replaced. The catalytic cycle for conventional cross coupling reactions can be simplified in three different steps (Scheme 1.1, a). First of all, oxidative addition of the halide derivative to the Pd(0) species forming a Pd(II) complex [PdL_nRX]. Then, transmetallation from the organometallic compound (M-R') to the catalyst obtaining a Pd(II) complex with the two organic groups coordinated [PdL_nRR']. Finally, the reductive elimination step takes place affording the corresponding C–C coupling product and Pd(0) species to restart the catalytic cycle. When the organometallic reagent is substituted by a hydrocarbon, the transmetallation step is replaced by a C–H activation step (Scheme 1.1, b). The oxidative addition and reductive elimination steps remain the same. In the simplified mechanism of oxidative cross coupling, two C–H cleavage steps are needed when both hydrocarbons are used as reagents (Scheme 1.1, c). The Pd(0) released after the reductive elimination of the coupling product needs to be oxidized to regenerate the Pd(II) active species. Thus, an oxidant as reagent and an oxidation step are also required.

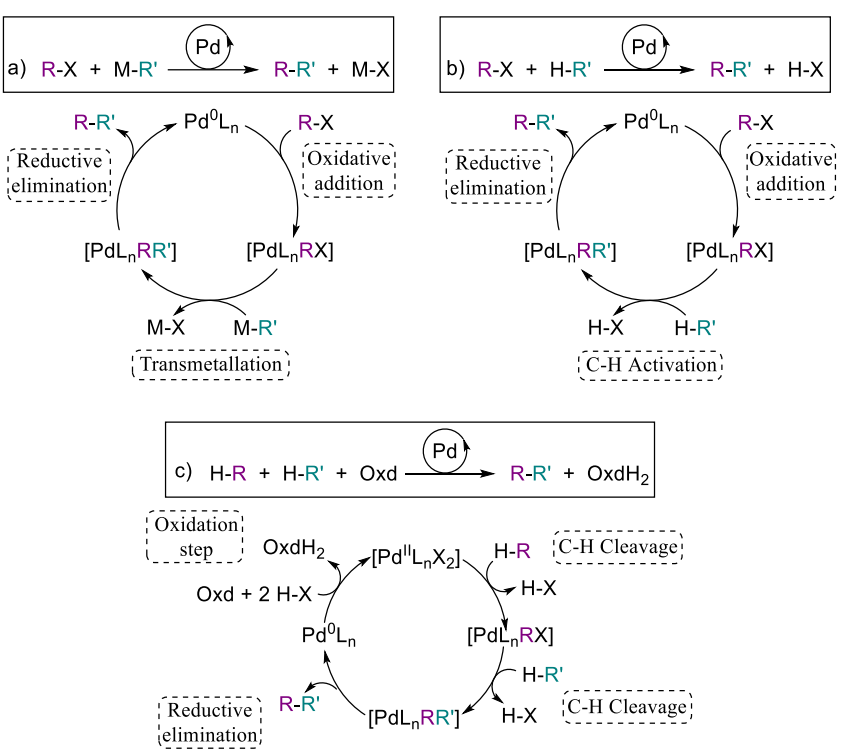

Scheme 1.1. Simplified catalytic cycles of: a) Conventional C–C cross coupling reactions. b) C–C cross coupling reactions of an organic halide and an arene (i.e. direct arylation). c) C–C oxidative cross coupling reactions of arenes.

On the other hand, there are several examples in the literature that propose a Pd(II)-Pd(IV) mechanism for specific C–C coupling transformations.[27] The different reactivity of Pd(IV) species allows to achieve synthetic strategies that a conventional Pd(0)-Pd(II) cycle is not able to do. Some Pd(IV) complexes have been isolated and proved to be effective in coupling processes.[28] An interesting example was published by Fernández-Ibáñez *et al*. in 2014 in the direct arylation of amino acid derivatives.[29] After the coordination and C–H activation of the substrate, the oxidative addition of the aryl halide takes place forming a Pd(IV) intermediate. Finally, the reductive elimination releases the desired product (Figure 1.3). The mechanism is supported by the isolation of some of the intermediates. However a Pd(II)/Pd(IV) mechanism in direct arylations is only accessible for the right combination of ligands and substrates and the more common Pd(0)/Pd(II) generally operates.

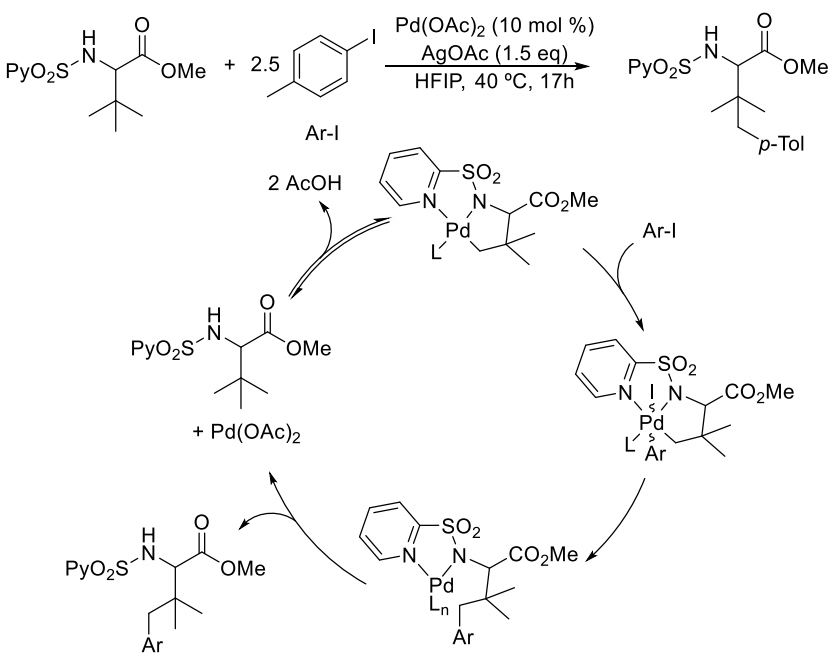

Figure 1.3. Proposed catalytic cycle for the direct arylation of amino acid derivatives *via* Pd(II)/Pd(IV) mechanism.

---

[27] a) Xu, L.-M.; Li, B.-J.; Yang, Z.; Shi, Z.-J., *Chem. Soc. Rev*. **2010**, *39*, 712-733. b) Juliá-Hernández, F.; Arcas, A.; Vicente, J. *Chem. Eur. J.*, **2011**, *18*, 7780-7786. c) Topczewski, J. J.; Sanford, M. S. *Chem. Sci.*, **2015**, *6*, 70-76. d) Liu, S.; Zhuang, Z; Qiao, J. X.; Yeung, K.-S.; Su, S.; Cherney, E. C.; Ruan, Z.; Ewing, W. R.; Poss, M. A.; Yu, Y.-Q. *J. Am. Chem. Soc*. **2021**, *143*, 21657-21666.

[28] a) Arcas, A.; Juliá-Hernández, F.; Bautista, D.; Vicente, J. *Angew. Chem. Int. Ed.*, **2011**, *50*, 6896-6899. b) Whitehurst, W. G.; Gaunt, M. J., *J. Am. Chem. Soc.* **2020**, *142*, 14169-14177.

[29] Poveda, S.; Alonso, I.; Fernández-Ibáñez, M. A. *Chem. Sci*., **2014**, *5*, 3873-3882.

1.2 REGIOSELECTIVITY OF THE C–H FUNCTIONALIZATION

One of the main problems of the reactions involving hydrocarbons as reagents is to make the process selective to one C–H bond. The challenge of the regioselectivity has been tackled by developing different approaches to control it. The use of directing groups is a common strategy,[30] where usually the substrate is functionalized with a coordinating group previously to the coupling reaction. The directing group (DG) coordinates to palladium and directs the functionalization to a C–H bond close to it *via* a chelate-assisted C–H activation. Finally, the removal of the DG leads to the desired product (Scheme 1.2).

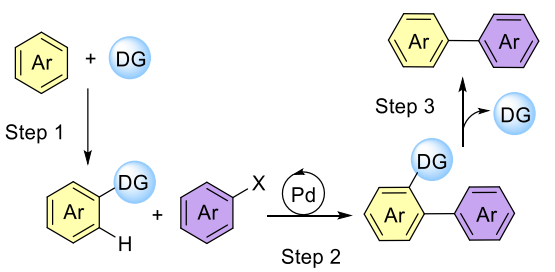

Scheme 1.2. General scheme for C–H functionalization of arenes with directing groups.

There are many examples using this strategy to make the reactions more regioselective. A recent example of the use of directing groups in C–H arylation of arenes catalysed by palladium is the work reported by Sun *et al*. in 2017.[31] They use thioamides as directing groups to achieve the C–H arylation selectively in the *ortho* position to the functional group (Scheme 1.3). In the catalytic cycle, they proposed that the thioamide coordinates to the palladium and the *ortho* C–H activation occurs. After the transmetallation and reductive elimination steps the product is released with the directing group attached.

[30] a) Neufeldt, S. R.; Sanford, M. S. *Acc. Chem. Res.* **2012,** *45*, 936-946. b) Tang, K.-X.; Wang, C.-M.; Gao, T.-H.; Chen., L.; Fan, L.; Sun, L.-P. *Adv. Synth. Catal*. **2019**, *361*, 26-38. c) Tomberg, A.; Muratore, M. E.; Johansson, M. M.; Terstiege, I.; Sköld, C.; Norrby, P.-O. *iScience*, **2019**, *20*, 373-391. d) Murali, K.; Machado, L. A.; Carvalho, R. L.; Pedrosa, L. F.; Mukherjee, R.; Da Silva, E. N.; Maiti, D. *Chem. Eur. J.* **2021**, *27*, 12453-12508. e) Urruzuno, I.; Andrade-Sampedro, P.; Correa, A. *Eur. J. Org. Chem*. **2023**, *26*, e202201489.
[31] Tang, K.-X.; Wang, C.-M.; Gao, T.-H.; Pan, C.; Sun, L.-P. *Org. Chem. Front*. **2017**, *4*, 2167-2169.

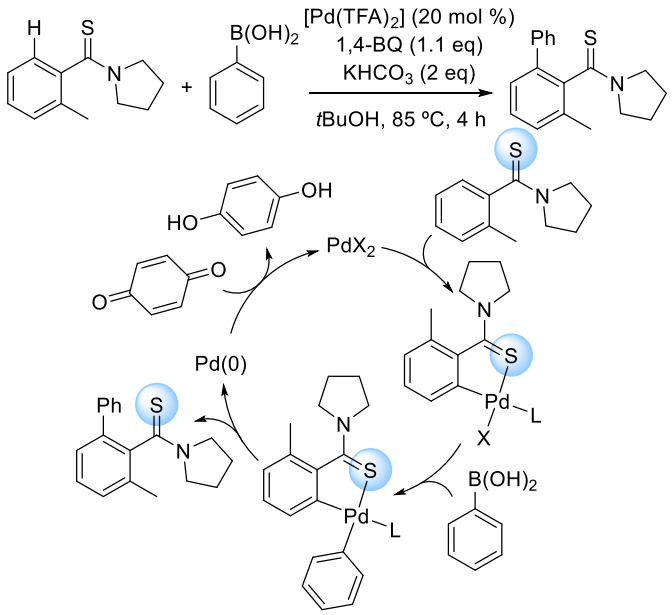

Scheme 1.3. C–H arylation of benzothioamides with boronic acids using the thioamide as directing group.

The additional two steps to add and remove the DG reduce the step-economy of the process. To alleviate this problem, the concept of transient directing groups (TDG) appeared, described as an *in situ* generation and deconstruction of the directing group.[32] Here, a functional group of the starting material is transformed in the reaction medium to a more coordinating group. Then, the substrate is able to coordinate to the metal centre and the C–H activation takes place. Finally, the directing group is removed and the product is released without additional steps. An example is the use of glycine to form an imine TDG from an aldehyde or a ketone. This was pioneered by Yu *et al.* in the C(sp^3)–H functionalization of carbonyl derivatives,[33] and has also been used in the direct arylation of aryl ketones as reported in 2017 by Xu and Jin (Scheme 1.4).[34] The imine, formed in the reaction media by the reaction between the ketone and the amino acid, coordinates to palladium previously to the C–H activation step. The coupling product formed undergoes hydrolysis of the imine and releases the desired product.

[32] a) Gandeepan, P.; Ackermann, L. *Chem*, **2018**, *4*, 199-222. b) Jacob, C.; Maes, B. U. W.; Evano, G. *Chem. Eur. J.* **2021**, *27*, 13899-13952. c) Xu, W.; Zhang, Y.; Wu, Y.; Wuan, J.; Lu, X.; Zhou, Y.; Zhang F.-L. *J. Org. Chem.* **2022**, *87*, 10807-10814.
[33] Zhang, F.-L.; Hong, K.; Li, T.-J.; Park, H.; Yu, J.-Q. *Science*, **2016**, *351*, 252-256.
[34] Xu, J.; Liu, Y.; Wang, Y.; Li, Y.; Xu, X.; Jin, Z. *Org. Lett*. **2017**, *19*, 1562-1565.

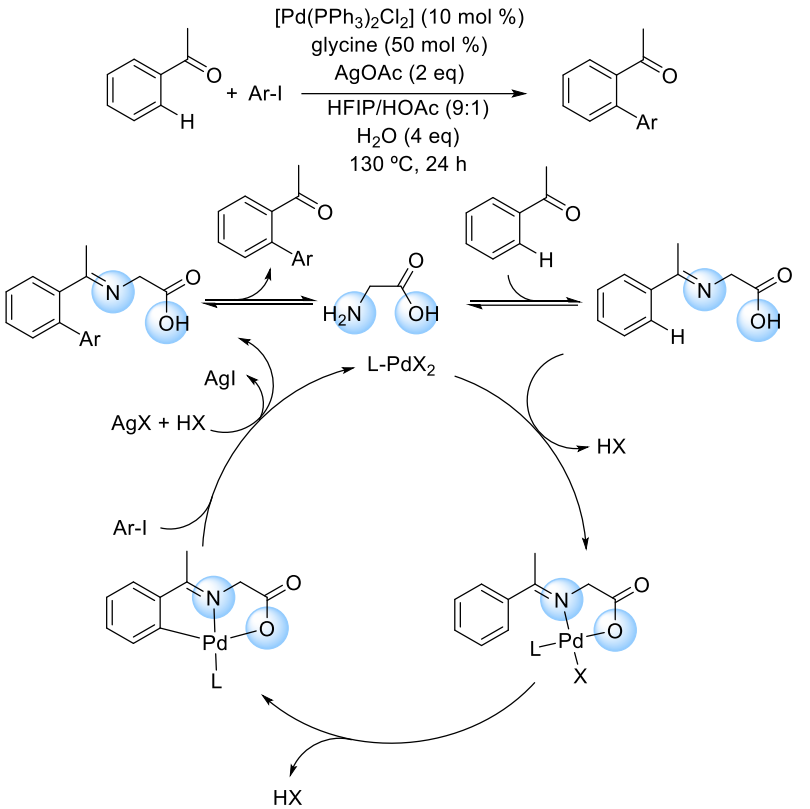

Scheme 1.4. Direct C–H arylation of aromatic ketones enabled by glycine as transient directing group.

A different approach to control the regioselectivity of the reaction is to use template ligands.[35] Those ligands are previously synthesised with a designed scaffold to direct the C–H functionalization to a specific bond. The ligand can influence the regioselectivity in two different ways: by steric hindrance or by involvement of non-covalent interactions between the metal centre and the substrate. One of the first groups developing template ligands was the Yu's group. In 2020 they reported a pincer-type palladium complex as template in the functionalization of remote C–H bonds (Figure 1.4, a).[36] In this reaction two different palladium complexes are involved. The substrate (quinoline derivatives) coordinates by the nitrogen to the pincer complex. Meanwhile, another palladium complex with a *N*-mono protected aminoacid ligand (MPAA)

[35] a) Zhang, Z.; Tanaka, K.; Yu, J.-Q. *Nature*, **2017**, *543*, 538–542. b) Achar, T. K.; Ramakrishna, K.; Pal, T.; Porey, S.; Dolui, P.; Biswas, J. P.; Maiti, D. *Chem. Eur. J.*, **2018**, *24*, 17906-17910. c) Achar, T. P.; Biswas, J. P.; Porey, S.; Pal, T.; Ramakrishna, K.; Maiti, S.; Maiti, D. *J. Org. Chem.* **2019**, *84*, 8315-8321.

[36] Shi, H.; Lu, Y.; Weng, J.; Bay, K. L.; Chen, X.; Tanaka, K.; Verma, P.; Houk, K. N.; Yu, J.-Q. *Nat. Chem.* **2020**, *2*, 399-404.

coordinates to a free nitrile group of the pincer ligand. In that intermediate, the MPAA ligand is close to the quinoline and the C–H activation takes place (Figure 1.4, b). Then, the decoordination of the nitrile group and the insertion of a norbornene molecule (the use of norbornene to control the regioselectivity will be discussed in the following pages) results in the C–H activation of a remote position, that will be functionalized in the final product.

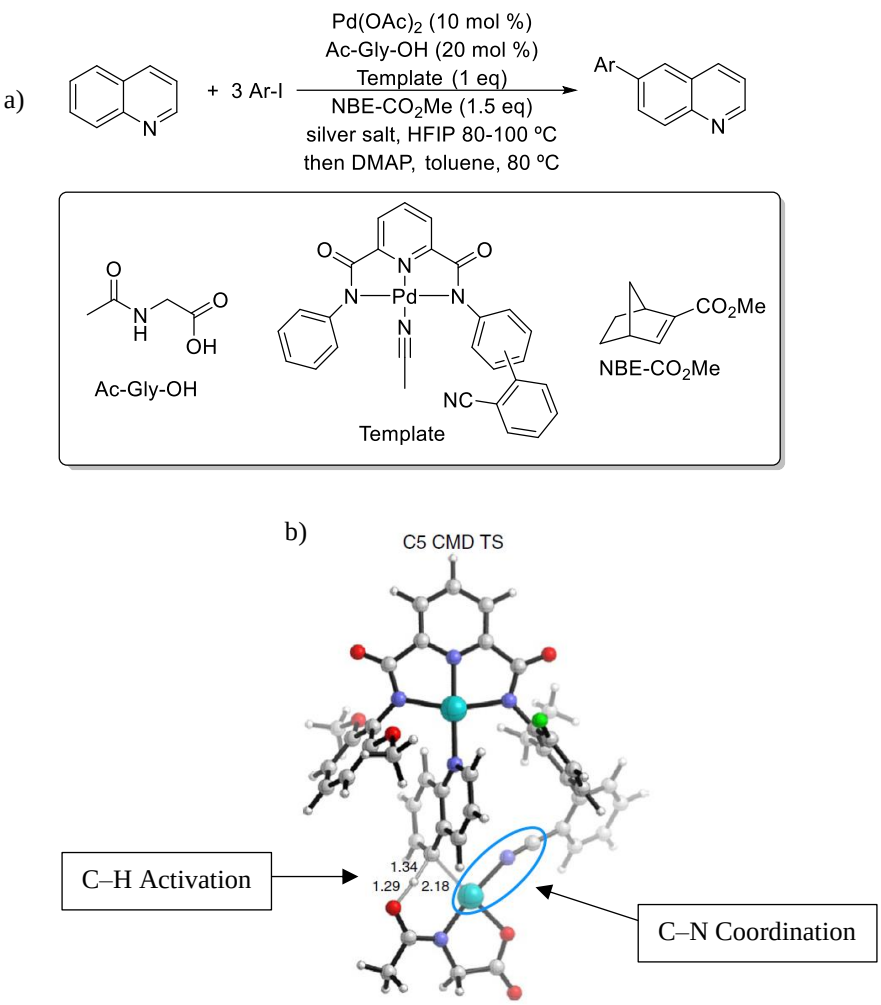

Figure 1.4. a) General reaction for the functionalization of quinolines in a remote position. b) Transition state of the C–H activation and nitrile coordination by the second palladium complex. Images taken from the original publication.

A recent example has been published by Čorić in 2022,[37] where they developed the functionalization of C–H bonds close to small alkyl groups (Scheme 1.5, a). The authors confirm by computational studies that the regioselectivity is achieved due to weak interactions in the selectivity-determining C–H activation transition state between the substrate and the ligand (Scheme 1.5, b).

a)

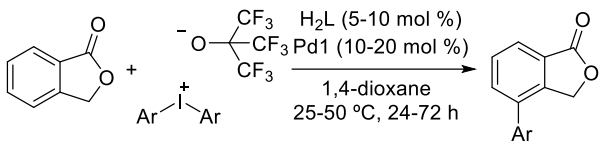

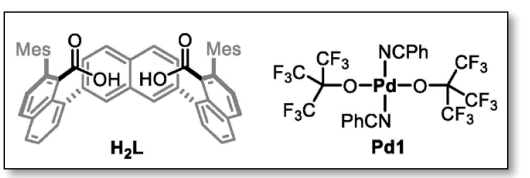

b)

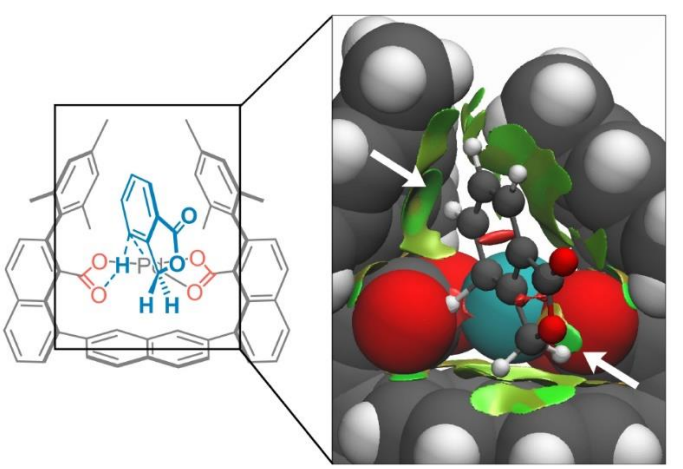

Scheme 1.5. a) Site-selective C–H arylation of arenes *ortho* to small alkyl groups. b) Transition state of the C–H activation where the selectivity is determined by the ligand scaffold. Images taken from the original publication.

The addition of non-innocent ligands that can be inserted into a Pd–C bond and results in the functionalization of a specific C–H bond of the substrate are called transient mediator groups. One of the best known examples is the use of norbornene or its derivatives, and was first developed by Catellani for the functionalization of arenes.[38]

[37] Dhankhar, J.; Hofer, M. D.; Linden, A.; Čorić, I. *Angew. Chem. Int. Ed.* **2022**, *61*, e2022054.
[38] a) Catellani, M.; Chiusoli, G. P.; Costa, M. *J. Organomet. Chem.* **1995**, *500*, 69-80. b) Catellani, M. *Synlett* **2003**, 298-313. c) Della Ca',N.; Fontana, M.; Motti, E.; Catellani, M. *Acc. Chem. Res.* **2016**, *49*, 1389-1400.

Since then, there are many examples of the use of norbornene in this way, such as the works published by Yu, Dong, Maiti and Chen.[39] Recently, Fernández-Ibáñez *et al*. have published the direct arylation of anisole derivatives selectively in the *meta* position *via* a Pd(II)-Pd(IV) mechanism (Scheme 1.6)[40].

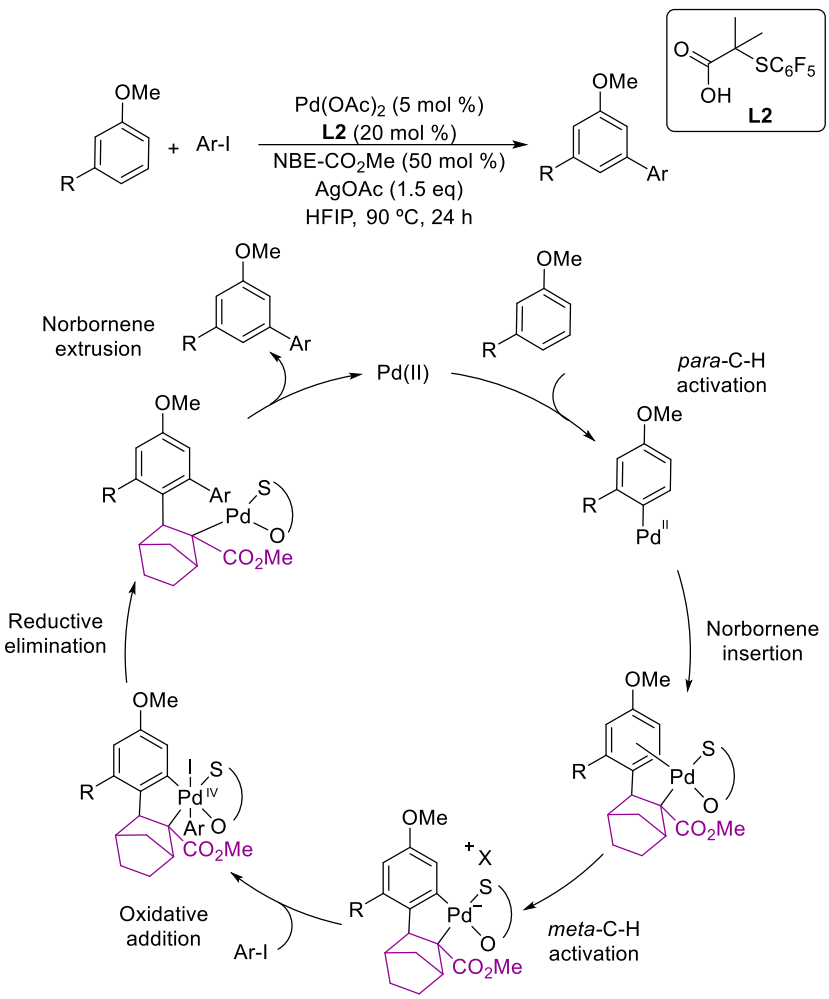

Scheme 1.6. *Meta*-C–H arylation of anisole derivatives using norbornene as transient mediator group.

[39] a) Wang, X.-C.; Gong, W.; Fang, L.-Z.; Zhu, R.-Y.; Li, S.; Engle, K. M.; Yu, J.-Q. *Nature*, **2015**, *519*, 334-338. b) Dong, Z.; Wang, J.; Dong, G. *J. Am. Chem. Soc*. **2015**, *137*, 5887-5890. c) Dutta, U.; Porey, S.; Pimparkar, S.; Mandal, A.; Grover, J.; Koodan, A.; Maiti, D. *Angew. Chem. Int. Ed.* **2020**, *59*, 20831-20836. d) Liu, S.; Wang, Q.; Huang, F.; Wang, W.; Yang, C.; Liu, J. Chen, D. *Org. Chem. Front.* **2022**, *9*, 129-139.

[40] Sukowski, V.; Borselen, M. V.; Mathew, S.; Fernández-Ibáñez, M. A. *Angew. Chem., Int. Ed.* **2022**, *61*, e202201750.

The proposed mechanism begins with the *para*-C–H activation of the anisole derivative. Later, the norbonene is inserted in the Pd–C bond and the *meta*-C–H activation occurs. In this step, the regioselectivity of the reaction has changed due to the insertion of the norbonene. The oxidative addition of the aryl halide gives rise to a Pd(IV) intermediate that, after the reductive elimination of the coupling product and the norbornene extrusion, release the starting Pd(II) complex and close the catalytic cycle.

1.3 C–H ACTIVATION MECHANISMS

The C–H activation is usually the turnover limiting step and it is responsible of the global rate of the C–H functionalization reaction. It is worth understanding the mechanism and the transition state for this step in order to know how to accelerate it and develop more sustainable processes. In the last years, several mechanisms have been described for the palladium-catalysed C–H activation reactions.[41] The most relevant studies are mentioned below.

Electrophilic aromatic substitution (S_EAr):[42] The most widely accepted mechanism for direct arylation processes several years ago. It consists of an electrophilic attack of the metal centre to an electron-rich arene forming an areniun ion intermediate (Wheland intermediate, Equation 1.6). An external base will accept the proton from the arene with no interaction with the metal centre. It was proposed mostly for aryls containing electron-donating substituents.

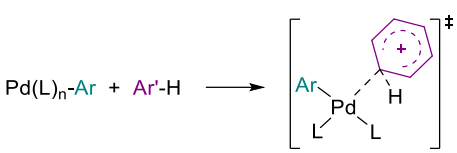

Equation 1.6.

C–H Oxidative addition: The metal complex, often a low-valent and electron rich complex, reacts as nucleophile and cleaves the C–H bond usually in a concerted manner (Equation 1.7). Both groups, the aryl and the hydrogen, remain coordinated to the metal after the C–H bond cleavage and the metal centre is oxidized in two units. There are only a few examples of this process in palladium chemistry,[43] but it has often been described for ruthenium, rhodium or iridium complexes.[44]

---

[41] Altus, K. M.; Love, J. A. *Commun. Chem.* **2021**, *4*, Article number 173.
[42] a) Jia, C.; Piao, D.; Oyamada, J.; Lu, W.; Kitamura, T.; Fujiwara, Y. *Science*, **2000**, *287*, 1992-1995. b) Martín-Matute, B.; Mateo, C.; Cárdenas, D. J; Echavarren, A. M. *Chem. Eur. J*. **2001**, *7*, 2341-2348. c) Lane, B. S.; Brown, M. A.; Sames, D. *J. Am. Chem. Soc.* **2005**, *127*, 8050-8057.
[43] Capito, E.; Browna, J. M.; Ricci, A. *Chem. Commun*. **2005**, 1854-1856.
[44] a) Murai, S.; Kakiuchl, F.; Seklne, S.; Tanaka, Y.; Kamatani, A.; Sonoda M.; Chatani, N. *Nature*, **1993**, *336*, 529-531. b) Zhang, X.; Kanzelberger, M.; Emge, T. J.; Goldman, A. S. *J. Am. Chem. Soc*. **2004**, *126*, 13192-13193. c) Pabst, T. P.; Chirik, P. J. *Organometallics*, **2021**, *40*, 7, 813-831.

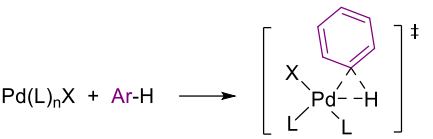

Equation 1.7.

σ-bond metathesis:[45] Common for early-transition metals and lanthanide metallocene compounds in high oxidation states. The reaction proceeds *via* a four-centered transition state (Equation 1.8). The interaction between the metal and the aryl occurs at the same time that between the X group and the hydrogen. The formation of two new bonds (M–C and X–H) is simultaneous to the cleavage of the other two bonds (M–X and C–H).

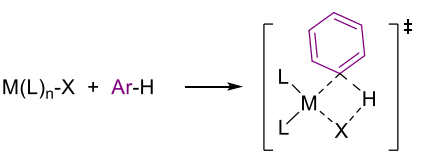

Equation 1.8.

Concerted metalation-deprotonation (CMD):[46] The C–H bond cleavage is assisted by a base (usually carbonate or carboxylate) coordinated to the metal centre (Equation 1.9).

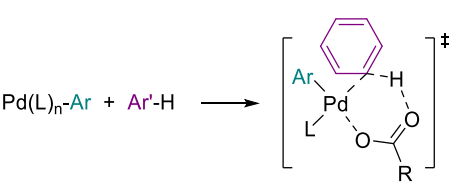

Equation 1.9.

[45] a) Thompson, M. E.; Baxter, S. M.; Bulls, A. R.; Burger, B. J.; Nolan, M. C.; Santarsiero, B. D.; Schaefer, W. P.; Bercaw, J. E. *J. Am. Chem. Soc.* **1987**, *109*, 203-219. b) Sadow, A. D.; Tilley, T. D. *J. Am. Chem. Soc*. **2005**, *127*, 643-656. c) Waterman, R. *Organometallics*, **2013**, *32*, 7249-7263. d) Soller, B. S.; Salzinger, S.; Jandl, C.; Pöthig, A.; Rieger, B. *Organometallics*, **2015**, *34*, 2703-2706. e) Parker, K.; Weragoda, G. K.; Canty, A. J.; Polyzos, A.; Ryzhov, V.; O'Hair, R. A. J. *Organometallics*, **2020**, *39*, 4027-4036. f) Perutz,R. N.; Sabo-Etienne, S.; Weller, A. S. *Angew. Chem. Int. Ed*. **2022**, *61*, e202111462.

[46] a) Fagnou, K.; Lapointe, D. *Chem. Lett.* **2010**, *39*, 1118-1126. b) Akermann, L. *Chem. Rev*. **2011**, *111*, 1315-1345. c) McMullin, C. L.; Davies, D. L.; Macgregor, S. A. *Chem. Rev*. **2017**, *117*, 8649-8709. d) Sampson, J.; Wang, L.; Carrow, B. P. *Isr. J. Chem*. **2020**, *60*, 230-258.

This mechanism is the most common and widely accepted for the C–H activation of arenes by palladium complexes nowadays. One of the first examples describing a CMD-type transition state was published by Davies and Macgregor while doing a computational study of the cyclometallation mechanism of *N*,*N*-dimethylbenzylamine.[47] They found that the hydrogen abstraction occurs via six-membered transition state (TS) with a coordinated acetate. They used the term AMLA (ambiphilic metal ligand activation) to highlight the importance of an electrophilic complex and a nucleophilic base.[48] In the same year, Maseras and Echavarren reported the mechanism of a palladium-catalysed intramolecular arylation in where they describe a similar TS with a coordinated carboxylate.[49] Fagnou also developed the direct arylation of polyfluorobenzenes and other aromatic substrates through a CMD mechanism and he did an extensive analysis of the TS of the C–H activation.[50] Since then, the CMD mechanism has gained importance in the field and it is proposed as possible mechanism for many C–H functionalization processes.

The standard CMD was proposed to operate when C–H bonds with low pK_a or electron poor arenes and palladium complexes with low electrophilicity are involved. Later, Carrow reported the C–H alkenylation of electron rich heteroarenes using a thioether-palladium catalyst.[51] Mechanistic studies showed that the C–H activation occurs again through a concerted mechanism but with some differences from the standard CMD. In that context, Carrow described the electrophilic concerted-metallation deprotonation mechanism (*e*CMD).[52] This mechanism is favoured for non-acidic C–H bonds, electron rich arenes and electrophilic catalysts. Moreover, the C–H and Pd–C bond lengths in the transition state are shorter than the ones expected for the standard CMD (Figure 1.5). That means the formation of the Pd–C bond is faster than the C–H cleavage. These differences show that, by selecting the correct catalyst for each substrate, the functionalization of electron poor or electron rich arenes can be achieved through CMD or *e*CMD, within a broader mechanistic continuum for C–H activation processes.

---

[47] Davies, D. L.; Donald, S. M. A.; Macgregor, S. A. *J. Am. Chem. Soc*. **2005**, *127*, 13754-13755.
[48] Boutadla, Y.; Davies, D. L.; Macgregor, S. A.; Poblador-Bahamonde, A. I. *Dalton Trans*, **2009**, 5820-5831.
[49] García-Cuadrado, D.; Braga, A. A. C.; Maseras, F.; Echavarren, A. M. *J. Am. Chem. Soc*. **2006**, *128*, 1066-1067.
[50] a) Lafrance, M.; Rowley, C. N; Woo, T. K.; Fagnou, K. *J. Am. Chem. Soc*. **2006**, *128*, 8754-8756. b) Gorelsky, S. I.; Lapointe, D.; Fagnou, K. *J. Am. Chem. Soc*. **2008**, *130*, 10848-10849. c) Gorelsky, S. I.; Lapointe, D.; Fagnou, K. *J. Org. Chem*. **2012**, *77*, 658-668.
[51] Gorsline, B. J.; Wang, L.; Ren, P.; Carrow, B. P. *J. Am. Chem. Soc*. **2017**, *139*, 9605-9614.
[52] Wang, L.; Carrow, B. P. *ACS Catal*. **2019**, *9*, 6821-6836.

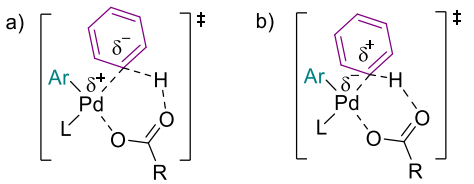

Figure 1.5. Transition state comparison: a) standard CMD and b) *e*CMD.

1.4 METAL-LIGAND COOPERATION (MLC)

As commented before, the main challenges in C–H activation processes are to overcome the low reactivity of the C–H bonds and reach the site-selectivity of the functionalization. The development of new catalysts to achieve those objectives is essential. In this way, the concept of metal-ligand cooperation appeared to describe metal complexes with ligands that play a dual role during the reaction mechanism.[53] The cooperating ligand coordinated to the metal centre can interact with the substrate and undergo reversible structural changes. Those processes can decrease the activation energy in elementary steps related with the substrate activation and accelerate the main reaction.

One example of metal-ligand cooperation is the pincer complexes developed by Milstein *et al*.[54] The ligand is deprotonated by an external base and loses the aromaticity, forming more reactive species. The new complex can activate unusual Y–H bonds in order to recover the aromaticity (Scheme 1.7).

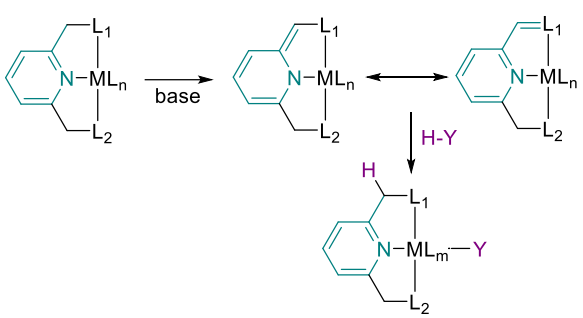

Scheme 1.7. Metal-ligand cooperation by aromatization-dearomatization.

An example of the acceptorless dehydrogenation of C–C single bonds by metal ligand cooperation was reported by Nozaki *et al*.[55] The hydroxycyclopentadienyl ligand was found to cooperate in the release of dihydrogen after C–H activation of the alkane. Then, the alkene is formed after the *β*-H elimination step as can be seen in Scheme 1.8.

[53] a) Khusnutdinova, J. R.; Milstein, D. *Angew. Chem. Int. Ed.* **2015**, *54*, 12236-12273. b) Higashi, T.; Kusumoto, S.; Nozaki, K. *Chem. Rev.* **2019**, *119*, 18, 10393-10402.
[54] Gunanathan, C.; Milstein, D. *Acc. Chem. Res.* **2011**, *44*, 588-602.
[55] Kusumoto, S.; Akiyama, M.; Nozaki, K. *J. Am. Chem. Soc.* **2013**, *135*, 18726-18729.

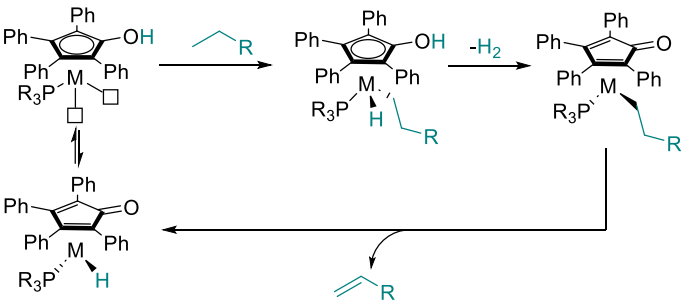

Scheme 1.8. Metal-ligand cooperation in acceptorless dehydrogenation of C–C single bonds.

An interesting example of MLC in palladium catalysis are the SCS pincer ligands developed by Martin-Vaca and Bourissou for the Conia-ene reaction.[56] In this case, the ligand backbone accepts an acidic proton from the substrate before the cyclization takes place, as shown in Scheme 1.9. Then, the proton is transferred to the final product again and the palladium complex is regenerated.

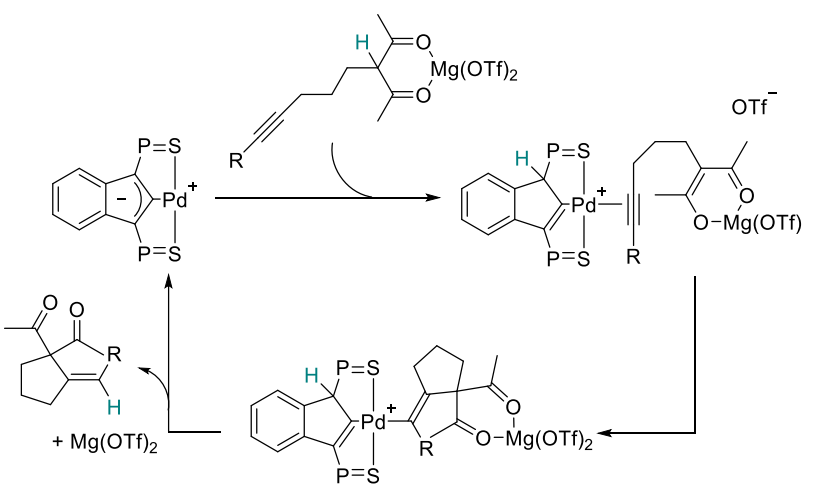

Scheme 1.9. Proposed mechanism for the Conia-ene reaction assisted by a SCS pincer ligand.

Focusing on palladium-catalysed C–H activation reactions *via* a CMD mechanism, a clear example of MLC is the acyl mono-*N*-protected aminoacids (MPAAs) introduced by Yu *et al.*[57] It has been demonstrated by computational studies and experimental procedures that MPAAs ligands can cooperate during the C–H activation

[56] Clerc, A.; Marelli, E.; Adet, N.; Monot, J.; Martín-Vaca, B.; Bourissou, D. *Chem. Sci*., **2021**, *12*, 435-441.
[57] Shao, Q.; Wu, K.; Zhuang, Z.; Qian, S.; Yu, J.-Q. *Acc. Chem. Res*. **2020**, *53*, 833-851.

step.[58,59] The ligand is coordinated in a chelate dianionic manner and the acyl group assists in the C–H cleavage. Comparing to the original CMD mechanism, the added base does not have to previously approach and coordinate to the metal since the ligand is acting as a base (Figure 1.6). In this way, the transition state is lower in energy as the entropic factor is more favourable. If the C–H activation is the turnover limiting step of the process, the rate of the reaction will be increased as the activation energy of the reaction profile will be smaller.

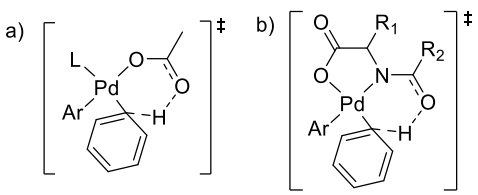

Figure 1.6. Transition states for: a) C–H cleavage assisted by an external base (carbonate or carboxylate) and b) C–H cleavage assisted by the ligand (MPAA).

2-pyridone and its derivatives have been also used as cooperating ligands in C–H functionalization reactions by Yu's group.[60] The pyridine coordinates as a monodentate ligand to palladium and the ketone group can act as internal base and assist in the C–H cleavage transition state (Figure 1.7, a). To achieve more stable complexes during the C–H activation step, our group started to use bipyridone derivatives. Those ligands will coordinate as chelates leading to more robust palladium complexes. The role of the pyiridone is the abstraction of the hydrogen during the C–H functionalization regaining the aromaticity of the ring (Figure 1.7, b). The accelerating effect of the [2,2′-bipyridin]-6(1H)-one (bipy-6-OH) has been demonstrated by experimental and

[58] a) Cheng, G. J.; Yang, Y. F.; Liu, P.; Chen, P.; Sun, T. Y.; Li, G.; Zhang, X.; Houk, K. N.; Yu J.-Q.; Wu, Y. D. *J. Am. Chem. Soc*., **2014**, *136*, 894-897. b) Haines, B. E.; Yu; J.-Q.; Musaev, D. G. *ACS Catal*., **2017**, *7*, 4344-4354. c) Wedi, P.; Farizyan, M.; Bergander, K.; Mück-Lichtenfeld C.; Gemmeren, M. *Angew. Chem. Int. Ed*., **2021**, *60*, 15641-15649. d) Mukherjee, K.; Grimblat, N.; Sau, S.; Ghosh, K.; Shankar, M.; V. Gandon ; Sahoo, A. K. *Chem. Sci*., **2021**, *12*, 14863-14870. e) Xu, L. P.; Zhuang, Z.; Qian, S.; Yu, J.-Q.; Musaev, D. G. *ACS Catal*., **2022**, *12*, 4848-4858.

[59] Fernández-Moyano, S.; Salamanca, V.; Albéniz, A. C. *Chem. Sci*., **2023**,*14*, 6688-6694.

[60] a) Wang, P.; Verma, P.; Xia, G.; Shi, J.; Qiao, J. X.; Tao, S.; Cheng, P. T. W.; Poss, A.; Farmer, M. E.; Yeung, K.-S.; Yu, J.-Q. *Nature*, **2017**, *551*, 489-494. b) Zhu, R.-Y.; Li, Z.-Q.; Park, H. S.; Senanayake, C. H.; Yu, J.-Q. *J. Am. Chem. Soc*. **2018**, *140*, 3564-3568. c) Fan, Z.; Bay, K. L.; Chen, X.; Zhuang, Z.; Park, H. S.; Yeung, K.-S.; Houk, K. N.; Yu, J.-Q. *Angew. Chem., Int. Ed.* **2020**, *59*, 4770-4777. d) Li, Y.-H. Ouyang, Y.; Chekshin, N.; Yu, J.-Q. *ACS Catal.* **2022**, *12*, 10581-10586.

computational studies in the direct arylation of arenes and oxidative Heck reactions.[20,25] Recently, this kind of ligands has been also used by Yu's group.[61]

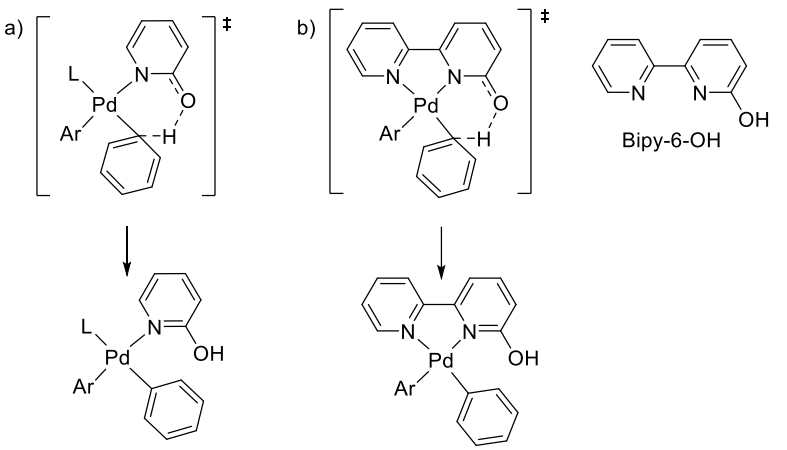

Figure 1.7. Transition states for: a) 2-pyridone assisted C–H activation and b) bipy-6-OH assisted C-H activation.

The use of bipy-6-OH as cooperating ligand has been expanded during this thesis. We have developed the chemo- and regioselective direct arylation of aniline derivatives (*Chapter 2*) and we have improved the reaction conditions in the direct arylation of arenes with no directing groups (*Chapter 3*). In the same context, we have studied the cooperating ability of several ligands with a similar scaffold that we hypothesised could assist in the C–H activation step (*Chapter 4*).

[61] a) Wang, Z.; Hu, L.; Chekshin, N.; Zhuang, Z.; Qian, S.; Qiao, J. X.; Yu, J.-Q. *Science* **2021**, *374*, 1281-1285. b) Chan, H. S. S.; Yang, J.-M.; Yu, J.-Q. *Science.* **2022**, *376*, 1481-1487. c) Hu, L.; Meng, G.; Yu, J.-Q. *J. Am. Chem. Soc*. **2022**, *144*, 20550-20553.

Chapter 2

2 Palladium-Catalysed Ortho C–H Arylation of Unprotected Anilines

2.1 INTRODUCTION

Anilines are attractive substrates for C–H functionalization. Many biologically relevant compounds have the aniline motif in their structure, so there is a lot of interest in developing efficient derivatization methods of the parent aniline that can be used in the synthesis of more complex molecules. The functionalization by direct transformation of the C–H bonds of the aryl ring of aniline into C–C bonds allows the synthesis of useful derivatives in a lower number of steps. Most metal-catalysed processes of this type use *N*-protected anilines as substrates.[62] Tertiary anilines, anilides or anilines bearing *N*-bound directing groups such as 2-piridyl have been functionalized in a number of ways. For example, the alkenylation of protected anilines using the Fujiwara-Moritani or oxidative Heck reaction of arenes has been reported,[63,64] as well as arylation (Scheme

[62]a) Tischler, M. O.; Tóth, M. B.; Novák, Z. *Chem. Rec*. **2017**, *17*, 184-199. b) Leitch, J. A.; Frost, C. G. *Synth*. **2018**, *50*, 2693-2706.
[63]a) Boele, M. D. K.; Van Strijdonck, G. P. F.; De Vries, A. H. M.; Kamer, P. C. J.; De Vries, J. G.; Van Leeuwen, P. W. N. M. *J. Am. Chem. Soc*. **2002**, *124*, 1586-1587. b) Mizuta, Y.; Obora, Y.; Shimizu, Y.; Ishii, Y. *ChemCatChem* **2012**, *4*, 187-191. c) Yao, Q. J.; Xie, P. P.; Wu, Y. J.; Feng, Y. L.; Teng, M. Y.; Hong, X.; Shi, B. F. *J. Am. Chem. Soc*. **2020**, *142*, 18266-18276.
[64]Naksomboon, K.; Poater, J.; Bickelhaupt, F. M.; Fernández- Ibáñez, M. A. *J. Am. Chem. Soc*. **2019**, *141*, 6719-6725.

2.1),[65,66,67,68] alkylation,[69] alkynylation,[70] or acylation reactions.[71] The presence of the protecting group directs the *ortho* selectivity observed in most cases, *via* a chelate-assisted C–H activation. Also, the careful design of the protecting group allows the selective synthesis of other regioisomers.[65,72]

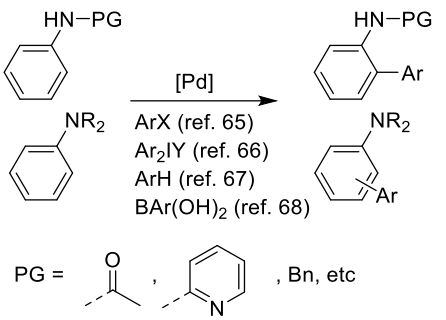

Scheme 2.1 C–H arylation of protected secondary and tertiary anilines

The use of unprotected primary anilines in C–H activation reactions is rare. Fernández-Ibáñez reported the *para*-selective palladium-catalysed alkenylation of anilines and a few examples of the functionalization of *ortho*-disubstituted primary anilines were included.[64] *Ortho*-substituted aryl anilines have been used as substrates in Pd-catalysed C–H functionalization but in that case the $–NH_2$ group directs the first C–H functionalization to the aryl substituent rather than the aniline ring (Equation 2.1).[73]

---

[65]Direct arylation using ArX: a) Daugulis, O.; Zaitsev, V. G.Angew. *Chem. Int. Ed*. **2005**, *44*, 4046-4048. b) Scarborough, C. C.;McDonald, R. I.; Hartmann, C.; Sazama, G. T.; Bergant, A.; Stahl, S. S. *J. Org. Chem*. **2009**, *74*, 2613-2615. c) Wan, C.; Zhao, J.; Xu, M.; Huang, J. *J. Org. Chem*. **2014**, *79*, 4751-4756. d) Kwak, S. H.; Gulia, N.; Daugulis, O. *J. Org. Chem*. **2018**, *83*, 5844-5850. e) Lichte, D.; Pirkl, N.; Heinrich, G.; Dutta, S.; Goebel, J. F.; Koley, D.; Goossen, L. J. *Angew, Chem, Int. Ed*. **2022**, *61*, e202210009.

[66]Arylation using diaryliodonium salts: a) Kalyani, D.; Deprez, N. R.; Desai, L. V.; Sanford, M. S. *J. Am. Chem. Soc*. **2005**, *127*, 7330-7331. b) Phipps, R. J.; Gaunt, M. J. *Science*, **2009**, *323*, 1593-1597. c) Ciana, C. L.; Phipps, R. J.; Brandt, J. R.; Meyer, F. M.; Gaunt, M. J. *Angew. Chem. Int. Ed*. **2011**, *50*, 458-462.

[67]Oxidative arylation with arenes: a) Li, B. J.; Tian, S. L.; Fang, Z.; Shi, Z. J. *Angew. Chem. Int. Ed*. **2008**, *47*, 1115-1118. b) Yeung, C. S.; Zhao, X.; Borduas, N.; Dong, V. M. *Chem. Sci*. **2010**, 1, 331-336. c) Brasche, G.; García-Fortanet, J.; Buchwald, S. L. *Org. Lett*. **2008**, *10*, 2207-2210.

[68]Oxidative arylation with arylboronic derivatives: a) Nishikata, T.; Abela, A. R.; Huang, S.; Lipshutz, B. H. *J. Am. Chem. Soc*. **2010**, *132*, 4978-4979. b) Koley, M.; Dastbaravardeh, N.; Schnürch, M.; Mihovilovic, M. D. *ChemCatChem* **2012**, *4*, 1345-1352.

[69]Ghorai, D.; Finger, L. H.; Zanoni, G.; Ackermann, L. *ACS Catal*. **2018**, *8*, 11657-11662.

[70]Deng, K. Z.; Jia, W. L.; Fernández-Ibáñez, M. A. *Chem. Eur. J*. **2022**, *28*, e202104107.

[71]Chan, C. W.; Zhou, Z.; Yu, W. Y. *Adv. Synth. Catal*. **2011**, *353*, 2999-3006.

[72]Tang, R. -Y.; Li, G.; Yu, J. -Q. *Nature* **2014**, *507*, 215-220.

[73]Raju, S.; Hsiao, H. C.; Thirupathi, S.; Chen, P. L.; Chuang, S. C. *Adv. Synth. Catal.* **2019**, *361*, 683-689.

Then, the second C–H activation occurs in the aniline ring giving rise to the phenanthrene derivative.

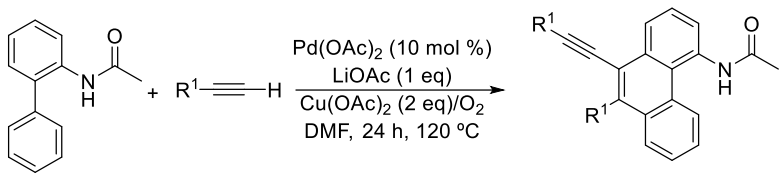

Equation 2.1.

To our knowledge, no examples of palladium-catalysed direct arylation of unprotected anilines have been reported. This is not surprising since the combination of an aryl halide and $ArNH_2$ could easily produce the Buchwald-Hartwig amination product leading to the N–H functionalization and the corresponding secondary aniline. Therefore, the *N*-protection is the common practice. It would be very interesting to develop a chemoselective catalytic system that could functionalize the aryl ring with no interference of the amino group, so the protection-deprotection additional steps could be avoided.

A few methods for the arylation of primary anilines have been reported, based on radical reactions of aryl diazo derivatives, or arylhydrazines, both rather hazardous reagents.[74] *Ortho* arylation of anilines has been achieved *via* the *in situ* generation of benzyne intermediates.[75] Daugulis *et al*. described such a reaction using ArCl as benzyne precursor in the presence of a strong lithium base, which was applied to a large number of anilines (Equation 2.2).[76]

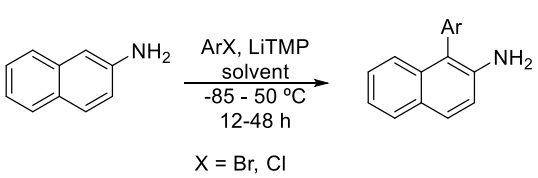

Equation 2.2.

[74]a) Wetzel, A.; Ehrhardt, V.; Heinrich, M. R. *Angew. Chem. Int. Ed.* **2008**, *47*, 9130-9133. b) Jiang, T.; Chen, S. Y.; Zhuang, H.; Zeng, R. S.; Zou, J. P. *Tetrahedron Lett.* **2014**, *55*, 4549-4552.
[75]Pirali, T.; Zhang, F.; Miller, A. H.; Head, J. L.; McAusland, D.; Greaney, M. F. *Angew. Chem. Int. Ed.* **2012**, *51*, 1006-1009.
[76]Truong, T.; Daugulis, O. *Org. Lett.* **2012**, *14*, 5964-5967.

This chapter describes a palladium catalytic system that brings about the selective *ortho*-arylation of unprotected anilines (Equation 2.3). The use of the ligand bipy-6-OH is crucial. It is responsible of the activity of the catalyst by playing a cooperating role in the C–H cleavage.[20] It is also important in determining the selectivity of the process by favouring the C–C *vs.* the C–N coupling (chemoselectivity) and also the *ortho*-regioselectivity.

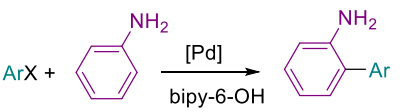

Equation 2.3

2.2 RESULTS AND DISCUSSION

2.2.1 C–H arylation of unprotected anilines

The well-defined complex [Pd(bipy-6-OH)Br(C_6F_5)] (**1**) was tested in the reaction of aniline with *p*-$CF_3C_6H_4I$ (Equation 2.4), an aryl halide that allows the easy monitorization of the reaction by ^{19}F NMR. Following our previous work,[20] in the first experiment we used pinacolone as solvent and a moderate excess of aniline (ten-fold). The reaction goes to completion in 24 h and good yields of the *ortho*-arylated aniline were obtained. Similar results can be achieved in a much shorter time (6 h) using DMA (entries 1 and 2, Table 2.1), so this solvent was selected for our experiments. The reaction is equally effective when an equimolar mixture of palladium acetate and bipy-6-OH was used as precatalyst (entry 3, Table 2.1). The presence of the cooperating ligand is necessary, and no conversion was observed when no ligand was added, when the pyridone moiety is not present in the ligand (bipy), or when it is in a position far from the metal (bipy-4-OH) so it is not able to play a cooperating role (entries 4-6, Table 2.1). In contrast, the ligand phen-2-OH is also effective, although the reaction is slower. The amount of reactant aniline can be reduced to almost the stoichiometric amount at the expense of a moderate reduction of the yield and a much longer reaction time (entry 8, Table 2.1).

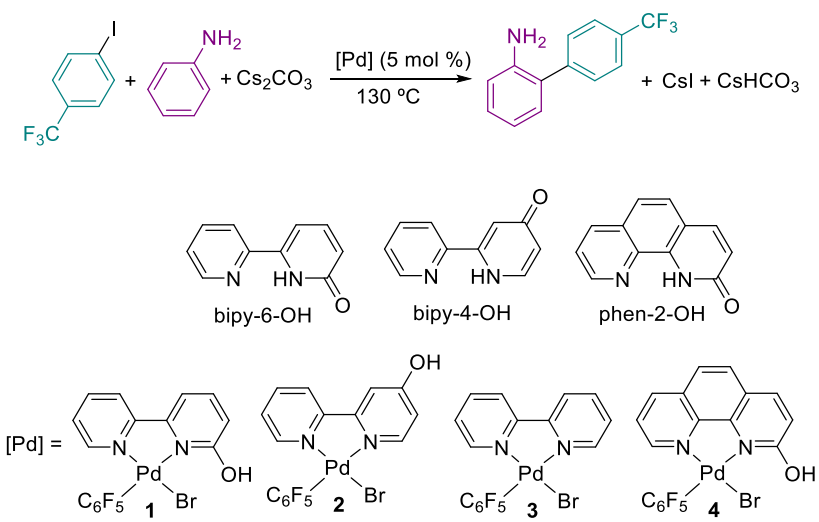

Equation 2.4

Table 2.1 Arylation of aniline with using different catalysts according to Equation 2.4.[a]

Entry	[Pd]	Crude yield, % (conv., %), 6 h[b]	Crude yield, % (conv., %), 24 h[b]
1[c]	**1**	46 (51)	92 (100)
2	**1**	83 (100)	-
3	$Pd(OAc)_2$ + bipy-6-OH	86 (100)	-
4	$Pd(OAc)_2$	2 (5)	7 (18)
5	**2**	7 (30)	12 (53)
6	**3**	10 (46)	15 (94)
7	**4**	7 (8)	87 (98)
8[d]	**1**	13 (20)	74 (100)

[a]Reaction conditions: *p*-$CF_3C_6H_4I$ (0.34 mmol), aniline (3.4 mmol), [Pd] (5 mol %), Cs_2CO_3 (0.68 mmol), DMA (2.7 mL); 130 °C. [b]Crude yields determined by ^{19}F NMR of the reaction mixture. Mixture of regioisomers o:m:p = 25:1:1. The reduction of the aryliodide (ArH) and the homocoupling (Ar-Ar) are the observed byproducts. [c]Pinacolone as solvent. [d]Aniline (0.37 mmol).

The *ortho* arylated product was the major one and only 5% of the Buchwald-Hartwig amination product (*N*-arylation) was detected in the crude mixture. In fact, the amination product was obtained cleanly when the same base (Cs_2CO_3) and similar solvent (DMF) than those in Equation 2.4 were used, but a different Pd-catalyst: a mixture of a Pd(0) precursor and XPhos (Equation 2.5). Thus, the Pd/bipy-6-OH catalyst system can be used in combination with other catalysts for the orthogonal functionalization of aniline by C–C and C–N coupling.

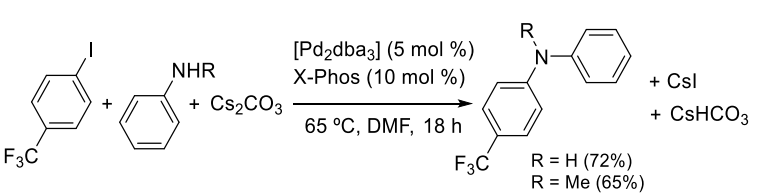

Equation 2.5

The selective *ortho* arylation can be extended to primary anilines with different substitution patterns in the aromatic ring (*ortho*-, *meta*- and *para*-substituted). Also, electron-withdrawing and electron-donating groups are tolerated in the aniline and in the aryl halide (Scheme 2.2).

Scheme 2.2 Arylation of anilines with complex **1.**

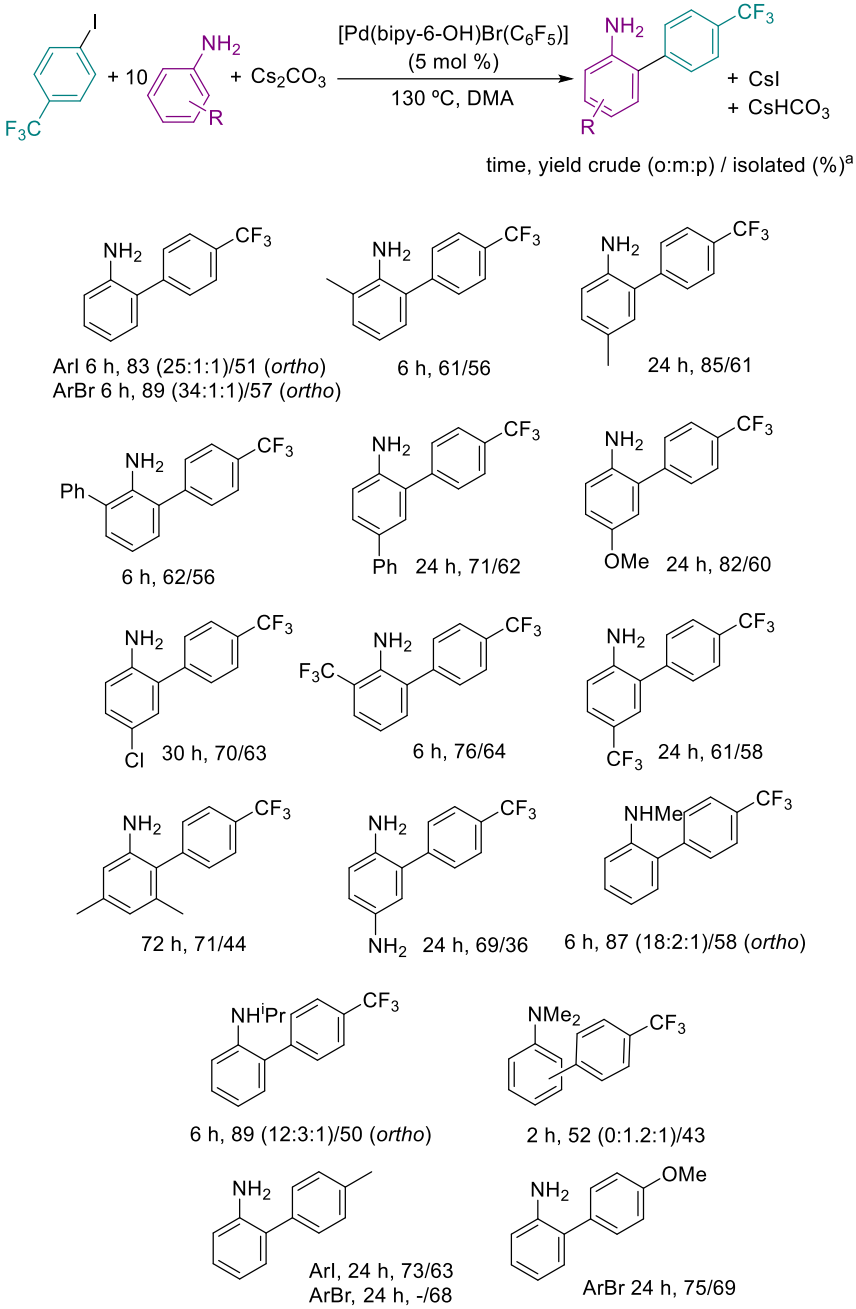

[a]Reactions conditions given in Table 2.1

Only monoarylation was observed in all cases and the *ortho*-arylated anilines were obtained in good to moderate yields, with the only exception of the tertiary

dimethylaniline. Some of the derivatives shown can be interesting precursors of biologically active compounds as, for example, in the synthesis of biphenylbenzamide microbiocidal agents,[77] carbazole alkaloids,[78] and dyes.[79] Again, in the few cases that it was observed, the C–N coupling product only accounts for about 2-5 % of the crude yield. Note that when *ortho*-phenyl aniline is used as substrate only the functionalization of the aniline ring occurs and the aryl substituent remains unaltered, in contrast to other reactions in the literature that use the 2-anilino as directing group as in the example shown in Equation 2.1.[73]

Scheme 2.2 also shows the arylation products of several secondary and tertiary anilines. We observed that the regioselectivity is eroded as the *N*-substitution increases. But, whereas the *ortho* isomer is still the major one for secondary anilines, the arylation of the *N*, *N*-dimethyl aniline only affords a mixture of the *meta* and *para* isomers.

2.2.2 Mechanistic experiments

Experimental studies

Mechanistic experiments were carried out to gather information on the catalytic cycle and the origin of the selectivity observed. The reaction shown in Equation 2.6 was used as a model. Complex **1** is transformed under catalytic conditions (DMA, excess of aniline) into the amino derivative **5**, which was independently synthesised (Equation 2.7) and characterized by X-ray diffraction (Figure 2.1).

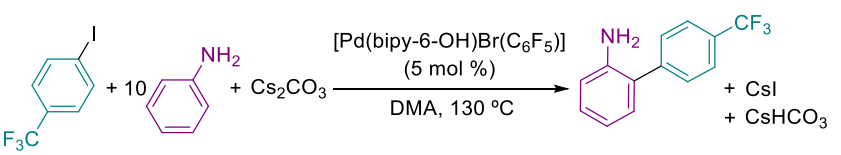

Equation 2.6

[77]Rieck, H.; Dunkel, R.; Elbe, H. L.; Wachendorff-Neumann, U.; Mauleer-Machnik, A.; Kuck, K. H. US 7186862 B2, 2007.
[78]a) Dhanak, D.; Knight, S. D.; Moore, M. L.; Newlander, K.A. WO 2006/005063 A2, 2006. b) Schmidt, A. W.; Reddy, K. R.; Knölker , H. J. *Chem. Rev.* **2012**, *112*, 3193-3328. c) Suzuki, C.; Hirano, K.; Satoh, T.; Miura, M. *Org. Lett.* **2015**, *17*, 1597-1600.
[79]Braun, H.J.; Chassot, L. US 6500213 B1, 2002.

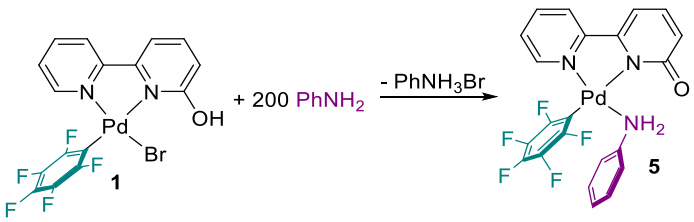

Equation 2.7

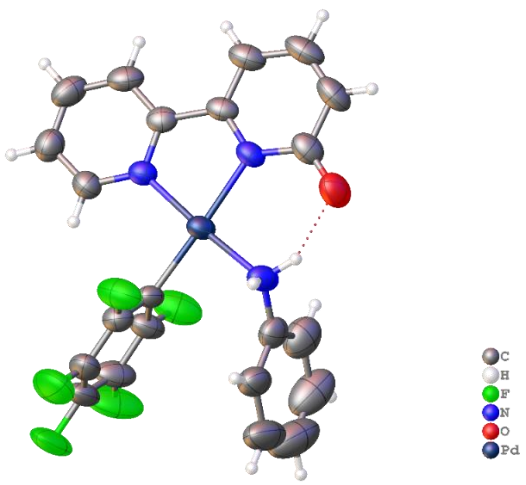

Figure 2.1 . X-ray molecular structure of [Pd(bipy-6-O)(C_6F_5)($PhNH_2$)] (**5**). ORTEP plot (40% probability ellipsoids) is shown.

The analogous complex [Pd(bipy-6-O)(*p*-$CF_3C_6H_4$)($PhNH_2$)] (**6**) was also prepared by ligand substitution (Equation 2.8) and was fully characterized by NMR and X-ray diffraction (Figure 2.2).

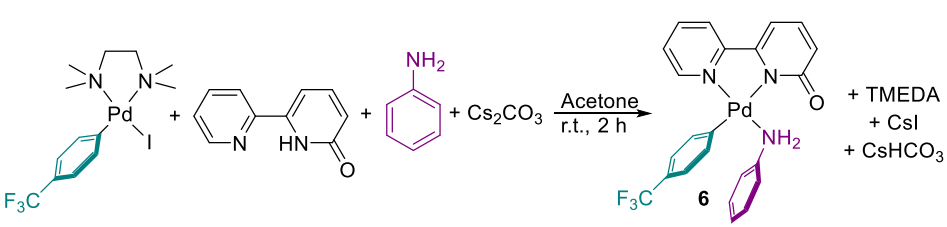

Equation 2.8.

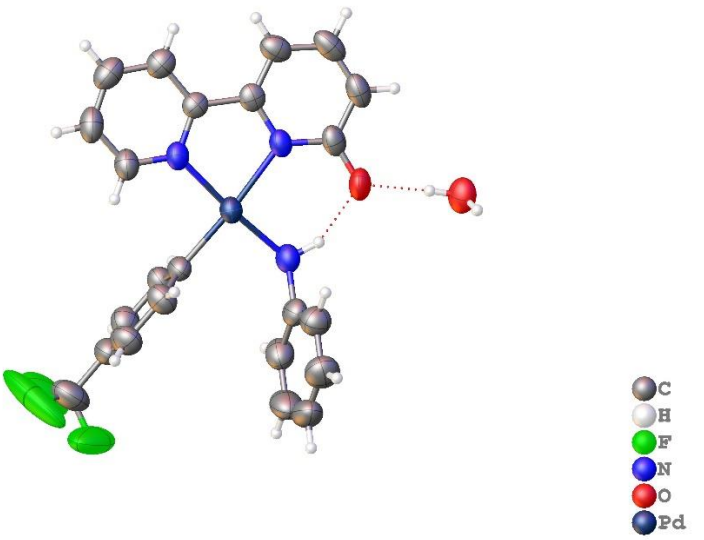

Figure 2.2 X-ray molecular structure of [Pd(Bipy-6-O)(C_6H_4-p-CF_3)($PhNH_2$)] (**6**). ORTEP plot (40% probability ellipsoids) is shown. The complex crystallizes with a water molecule.

Complex **6** proved to be catalytically competent for the reaction in Equation 2.6 (90% yield in 6 h). It also decomposes under catalytic conditions to the *ortho* arylated aniline (Equation 2.9, Figure 2.3), so the presence of **6** is plausible in the catalytic reaction.

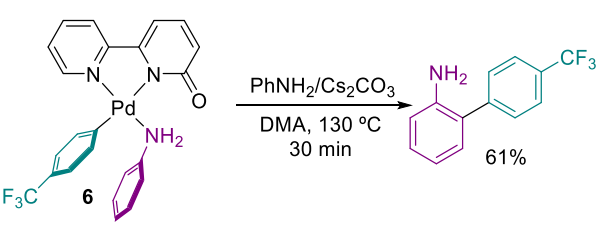

Equation 2.9

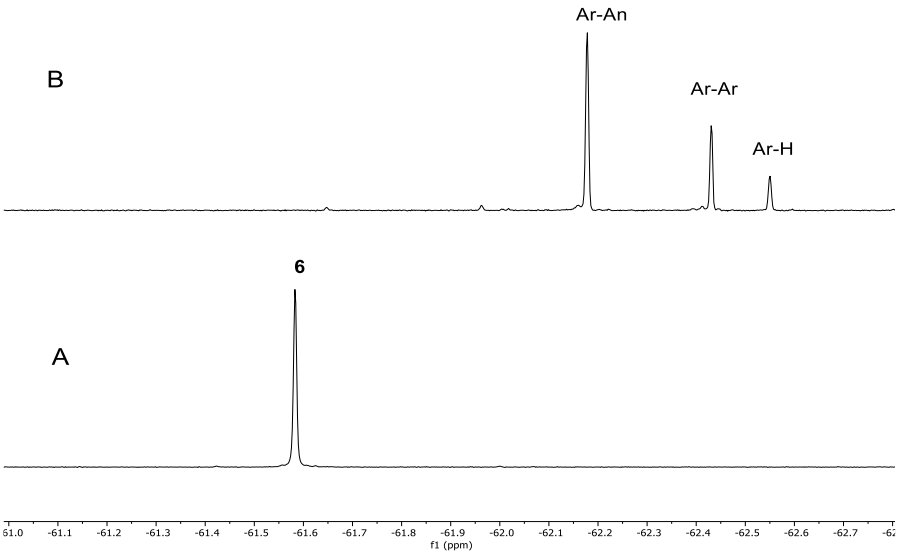

Figure 2.3 ^{19}F NMR spectra (470.168 MHz): A) Complex **6** in DMA with 200 equivalents of $PhNH_2$ and 1 equivalent of Cs_2CO_3. B) Sample A after heating at 130 °C for 30 min (mol ratio Ar-An : Ar-Ar : Ar-H = 5 : 1 : 1).

Kinetic experiments show that the rate of the reaction exhibits a first-order dependence on the catalyst (**1**) and a zero order on the concentration of the aryl halide (see experimental part, Figure 2.16). The reaction rate is also insensitive to the concentration of aniline in the excess range used for this reactant in the catalysis (about ten-fold). As it can be seen in Equation 2.7, under these conditions the coordination equilibrium is completely shifted to the aniline-coordinated species (see NMR spectra in Figure 2.11 in the experimental part).

The kinetic isotope effect was determined in separate experiments and the value found is large (KIE = 4.2 ± 0.2, Scheme 2.3 and Figure 2.15, experimental part) pointing to the C–H activation as the turnover limiting step.

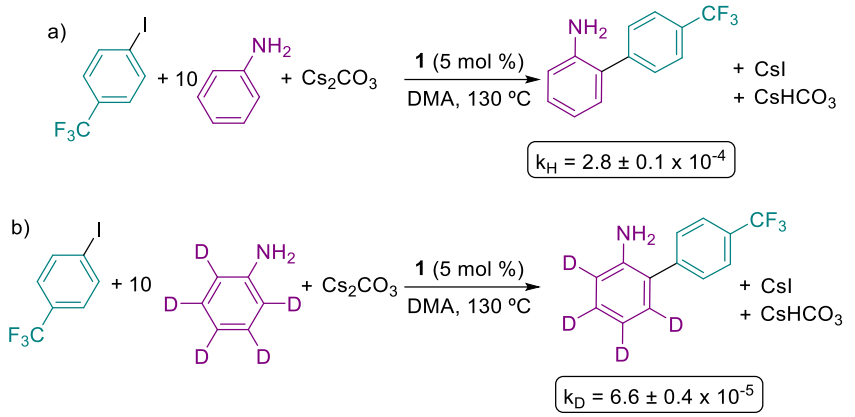

KIE = k_H ($C_6H_5NH_2$)/ k_D ($C_6D_5NH_2$) = 4.2 ± 0.2

Scheme 2.3. KIE determination experiments: a) aniline as reactant, b) deuterated aniline as reactant.

The reaction in Equation 2.6 was also carried out in the presence of D_2O. Since the H/D exchange in the protonated ligand is facile (Figure 2.13, experimental part), a reversible C–H activation should lead to the incorporation of deuterium in the final substituted aniline (Scheme 2.4). No deuterium incorporation was observed supporting an irreversible C–H cleavage.

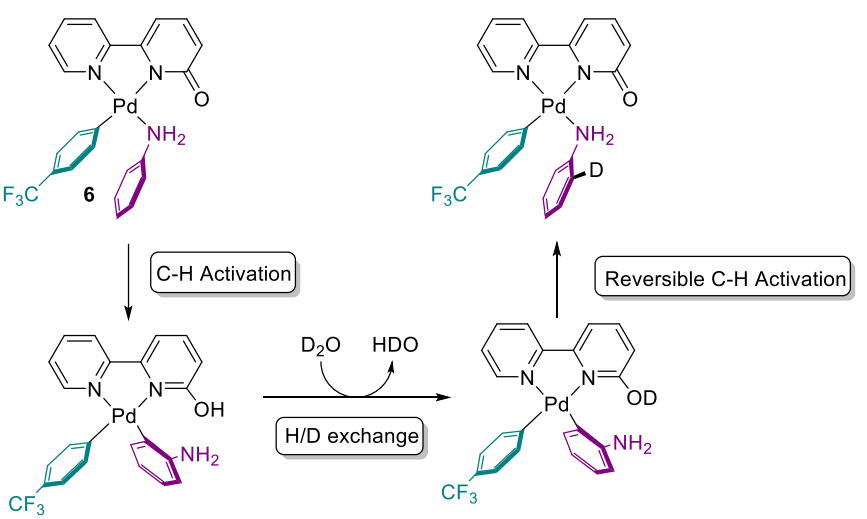

Scheme 2.4. Possible H/D exchange pathway through a reversible C–H activation.

Since the regioselectivity of the reaction depends on the substitution of the aniline nitrogen, the coordination ability of the *N*-substituted anilines and aniline was

determined in case there was a clear trend with this feature. The equilibrium constants of their coordination to the model palladium complex $(NBu_4)_2[Pd_2(\mu\text{-}Br)_2(C_6F_5)_4]$ were measured (Equation 2.10), taking advantage of the distinct patterns of complexes **I** and **II** in ^{19}F NMR (Figure 2.4).

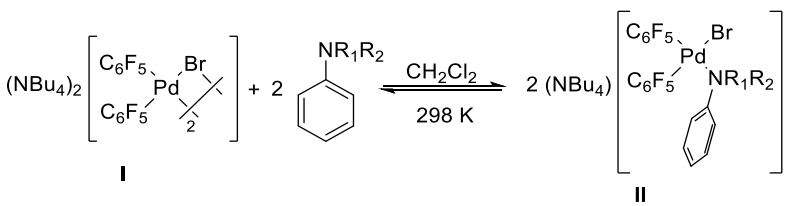

Equation 2.10

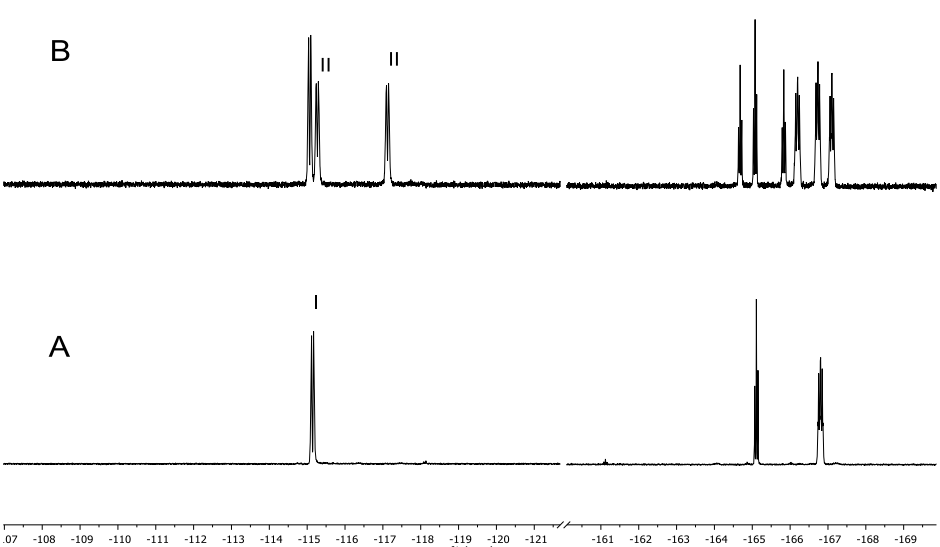

Figure 2.4 ^{19}F NMR spectra (470.168 MHz): A) Complex **I** in dichloromethane. B) Sample A after adding 10 equivalents of aniline.

The Keq values (Table 2.3) show a clear decrease in coordination ability of the anilines as the bulkiness of the *N*-substitution increases, $PhNMe_2$ being the least coordinating one.

Table 2.2 Coordination equilibrium constants (K_{eq}) and selectivity for different anilines.[a]

Entry	R_1, R_2	K_{eq} (L mol^{-1})	Ratio o:m:p	Regioselectivity (% *ortho*)
1	H	118 ± 4	25:1:1	93
2	H, Me	1.2 ± 0.4	18:2:1	86
3	H, ^{i}Pr	0.027 ± 0.016	12:3:1	75
4	Me	1.7x10^{-5} ± 0.6x10^{-5}	0:1.2:1	1

[a]Since the *ortho* isomer was not detected for $PhNMe_2$, a maximum of 1 % corresponding to the NMR integration uncertainty was assumed.

A plot of log (Keq) *vs.* log (regioselectivity) was created, taken the selectivity as the percentage of *ortho* isomer observed in the arylation reaction. Although a linear decrease was observed for aniline and the secondary anilines, no correlation was observed for all the anilines tested (Figure 2.5).

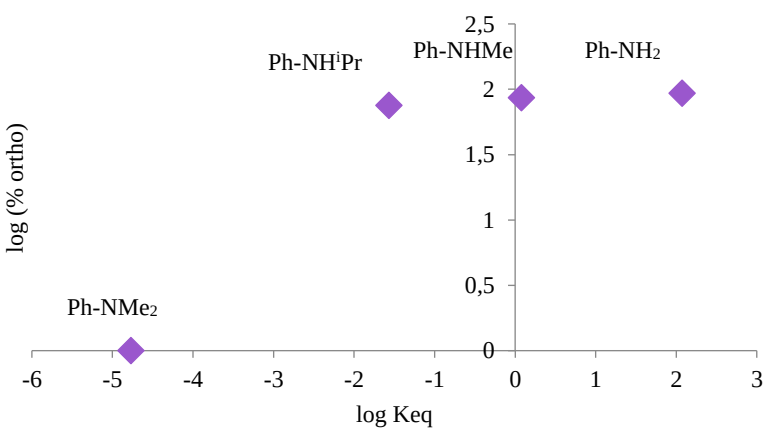

Figure 2.5 Plot of log(K_{eq}) (coordination equilibirum) *vs.* log(regioselectivity) in the arylation of different anilines. Data from Table 2.2.

Thus, all the experiments above give information about the basic features of the reaction: a) it is chemoselective towards C−C coupling *vs.* C−N coupling; b) it shows *ortho* regioselectivity for primary and secondary anilines but not for the tertiary one and this is not correlated to the coordination ability of the anilines; c) the reaction has a turnover-limiting C−H cleavage.

Computational studies

With the experimental mechanistic information at hand, the reaction mechanism has been investigated by computational methods. A thorough exploration of several routes, with location of intermediates and transition states, was carried out using the M06 functional with basis set BS1 and including solvation in the optimizations through the SMD implicit solvent method. Using this method, preliminary DFT calculations were carried out trying to shed light on the regioselectivity observed and the energy barriers for the C–H activation step for each isomer were studied. The energy barriers found were 26.3 kcal mol^{-1} for the *ortho* isomer, 26.6 kcal mol^{-1} for the *para* and 30.6 kcal mol^{-1} for the *meta*. Those results did not reproduce the ratio of isomers observed experimentally so, in collaboration with professor Agustí Lledós from the Universidad Autónoma de Barcelona, additional single point calculations were performed on all optimized structures employing the domain based local pair natural orbital coupled cluster approach (DLPNO-CCSD(T)) and an extended basis set (def2-TZVP) (see computational details in the experimental part). This method can be considered the state-of-the-art for providing energies of systems of this size and it has proved to be very effective in obtaining accurate reaction thermodynamics and barrier heights,[80] including palladium-catalysed cross-coupling reactions.[81] All the Gibbs energies collected in the text have been obtained adding to the DLPNO-CCSD(T)/def2-TZVp electronic energies thermal and entropic corrections as well as solvation energies (ΔG(solv)) obtained at M06/BS1 level. However, as can be seen in Figure 2.6, even with this method, the simple model (no carbonate salts or explicit solvent molecules) does not reproduce the experimental results, since it predicts a turnover limiting reductive elimination instead of the observed C–H cleavage and it disfavours the *ortho* regioisomer, which is the one observed experimentally.

[80]Sparta, M.; Riplinger, C.; Neese, F. *J. Chem. Theory Comput*. **2014**, *10*, 1099-1108.
[81]Cusumano, A. Q.; Stoltz, B. M.; Goddard, III, W. A. *J. Am. Chem. Soc.* **2020**, *142*, 13917-13933.

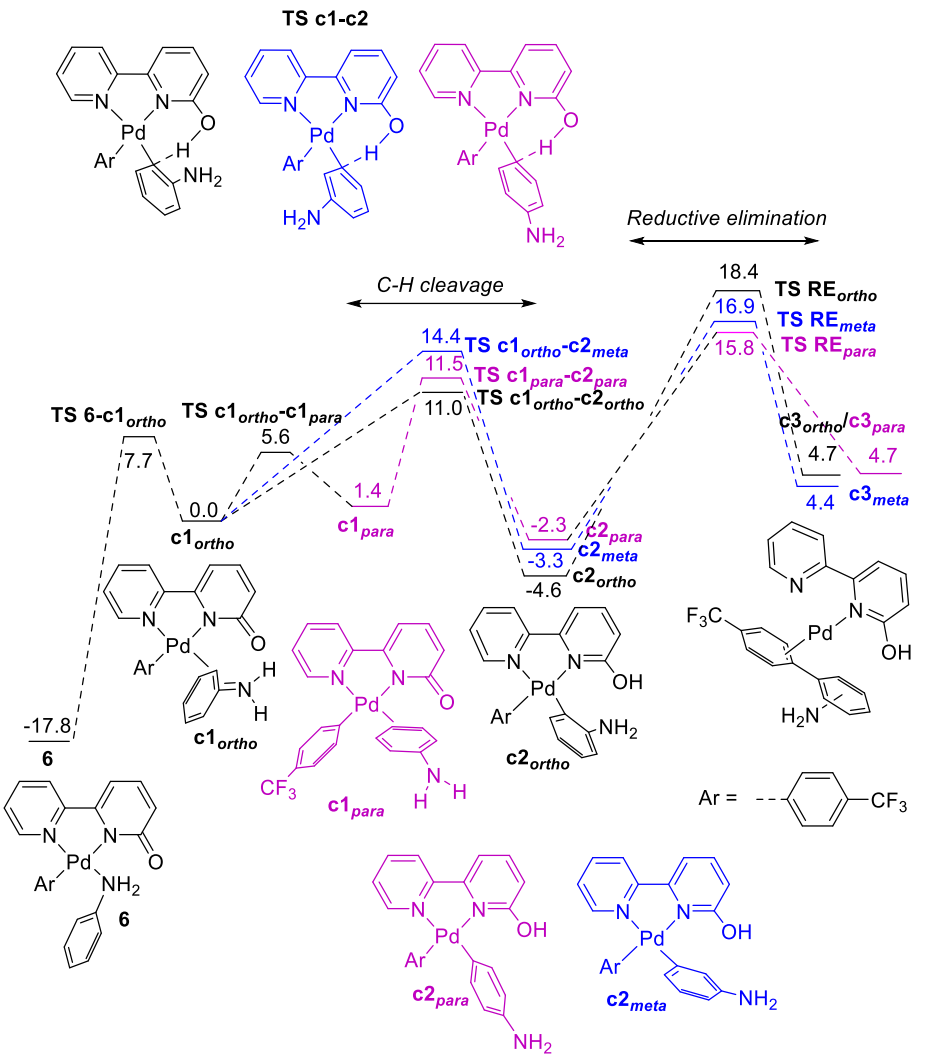

Figure 2.6. Gibbs energy profile for the arylation reaction of aniline (C–H cleavage and reductive elimination steps) using a simple model, not taking into account carbonate salts or solvent molecules. Data for the three regioisomers are shown. Energies in kcal mol^{-1}. No minimum has been found for a **c1**$_{meta}$ intermediate.

It was found that the choice of model is crucial to reproduce the basic features of the reaction. The simplest model, consisting in just the palladium, the ligand (bipy-6-OH), the aryl and aniline fails in accounting for the experimental results. To improve it, the model was enlarged adding other species present in the reaction medium, such as carbonate and cesium ions and solvent molecules. Figure 2.7 shows the comparison of activation energies for the C–N reductive elimination in an amido aryl palladium complex, leading to the Buchwald-Hartwig amination product, and the C–H activation on the same complex. The simplest model (Model 1, Figure 2.7) does not account for the

chemoselectivity observed. It was found that the smallest model able to reproduce the prevalence of C–C coupling over C–N coupling must involve, in addition to the cesium carbonate, several explicit DMA solvent molecules (Model 4, Figure 2.7). This has been the model employed in all the calculations. All the models tried are represented in Figure 2.19 in the experimental part.

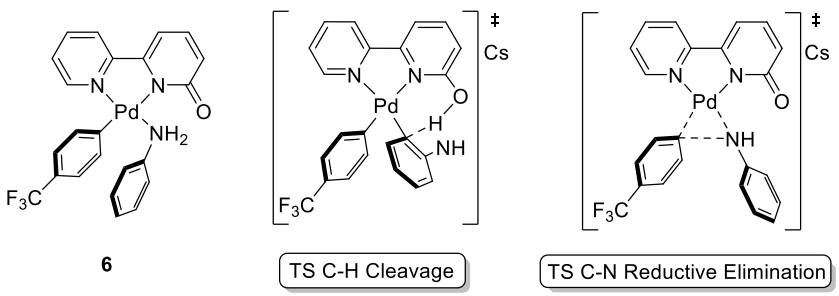

	TS C–H cleavage (TS c1NH$_{ortho}$-c2NH$_{ortho}$)	**TS C–N reductive elimination**
Model 1	(11.0)	(5.8) ΔΔG **-5.2** kcal mol^{-1}
Model 4	(12.1)	(14.1) ΔΔG **2.0** kcal mol^{-1}

Figure 2.7. Optimized structures for the transition states of the competing C–H bond cleavage (**TS c1NH$_{ortho}$-c2NH$_{ortho}$**) and the C–N reductive elimination in an amido palladium complex **6NH** using different chemical models. Relative Gibbs energies of both transition states (ΔΔG) are also shown in blue (kcal mol^{-1}). A negative value implies a lower TS for C–N reductive elimination than for the *ortho* C–H cleavage. Only model 4 agrees with the experimental evidence. In parenthesis Gibbs activation barriers (kcal mol^{-1}, taking **c1$_{ortho}$** as reference).

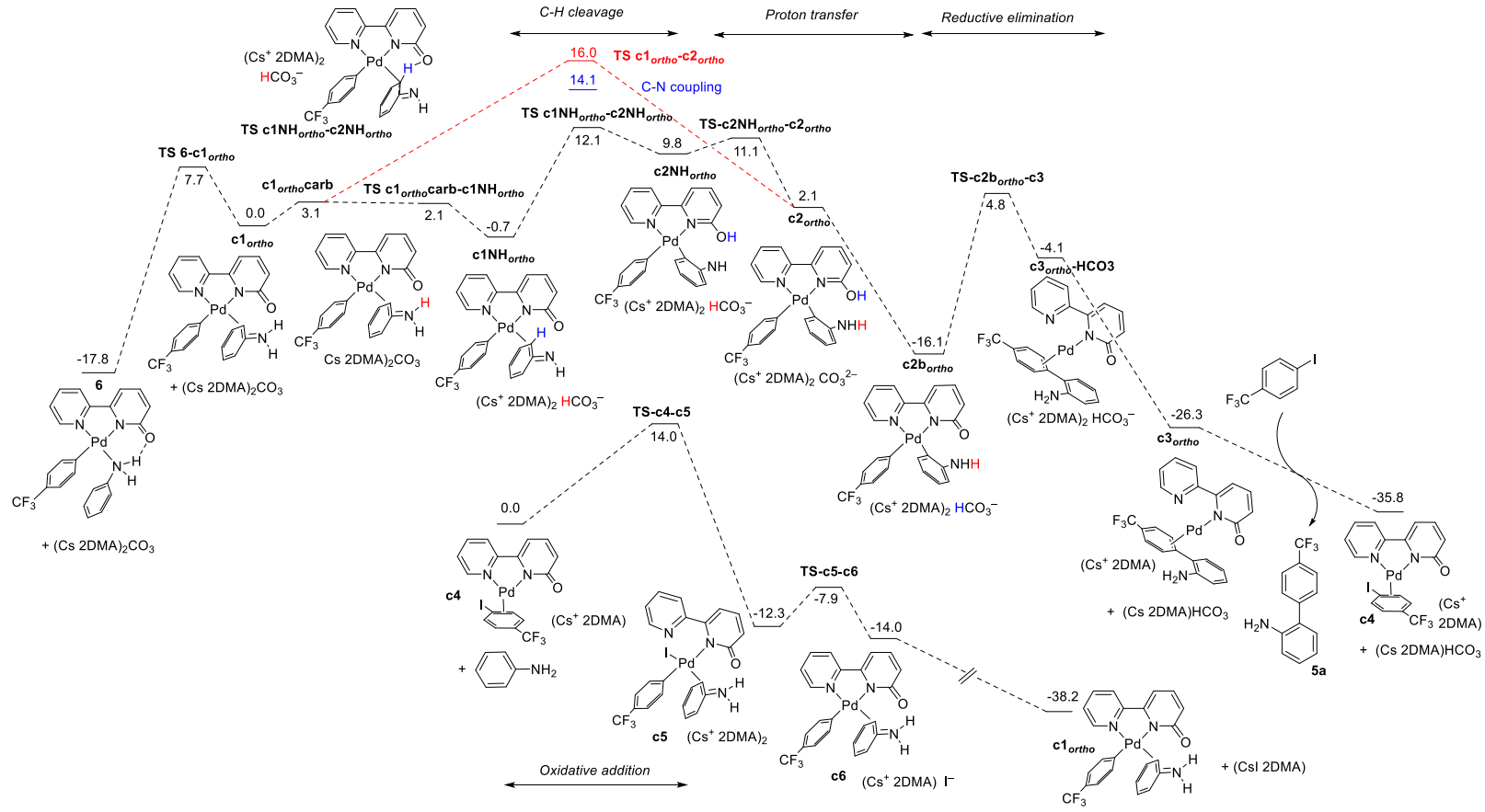

Figure 2.8. Gibbs energy profile for the Pd-catalysed arylation of aniline in the ortho position, assisted by the ligand bipy-6-O. Energies in kcal mol^{-1}.

Figure 2.8 shows a complete profile for the reaction yielding the *ortho* arylated product. The computed catalytic cycle is also represented in Scheme 2.5. The rearrangement of the aniline from a *N*– to a *C*–bound mode transforms complex **6** into **c1*ortho***. At this point, the deprotonation of the aniline is facile to give **c1NH*ortho*** which undergoes C–H cleavage (*via* **TS-c1NH*ortho*-c2NH*ortho*)** with a lower energy barrier than that from **c1*ortho*** (**TS-c1*ortho*c2*ortho***; Gibbs energy barriers of 12.1 *vs.* 16 kcal mol^{-1} respectively). Therefore, an anionic route on an amido-type intermediate is preferred. A series of proton transfer steps occur on biaryl intermediate **c2NH*ortho*** with the involvement of the pair HCO_3^-/CO_3^{2-}, which eventually leads to **c2b*ortho***. In this way the *ortho* C–H proton ends up in the carbonate, with a notable stabilization of the system. From **c2b*ortho*** a reductive elimination follows through transition state **TS-c2b*ortho*-c3**, leading to the arylation product and the Pd(0) intermediate **c4**. In the presence of aniline, the oxidative addition occurs leading to **c1*ortho*** that closes the cycle. The conversion of **c1*ortho*** into **6** has a lower energy barrier than the C–H cleavage and therefore **6** is the plausible resting state of the reaction, outside the catalytic cycle. The equilibrium between **6** and **c1*ortho*** controls the actual concentration of palladium in the catalytic cycle and leads to an energetic span of 29.9 kcal mol^{-1} for the reaction, consistent with the reaction conditions needed. A microkinetic simulation of this pathway is also consistent with the conversions observed experimentally (see experimental part for details).

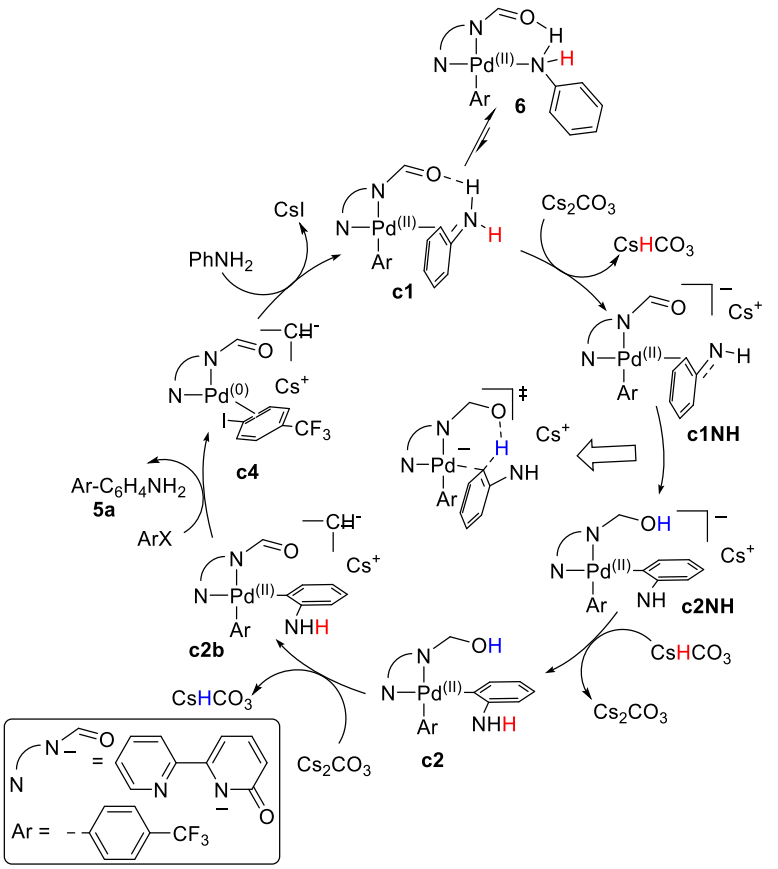

Scheme 2.5. Plausible catalytic cycle for the ortho arylation of anilines.

The energy barriers for the other two regioisomers were also calculated. Both the neutral (implying NH_2 in the aniline) and the anionic (with NH) were computed. The C–H cleavage *via* the neutral pathway (**c1** to **c2**) is preferred to the anionic one (**c1NH** to **c2NH**) for the *meta* C–H activation, with Gibbs energy barriers of 19.0 and. 25.7 kcal mol^{-1}, respectively, whereas the anionic route is slightly preferred for the *para* C–H activation (19.4 *vs*. 19.7 kcal mol^{-1} Gibbs energy barriers, Figure 2.9). The lowest energy pathway for each of these two regioisomers is less favoured than the *ortho* arylation by 6.9 kcal mol^{-1} (*meta*) and 7.3 kcal mol^{-1} (*para*). Therefore, the facile deprotonation of the aniline by the carbonate anion, forming an amido type intermediate in these reactions is important to drive the regioselectivity toward *ortho* arylation. This is possible for primary and secondary anilines but not for the tertiary *N*,*N*-dimethyl aniline where the *ortho* isomer was not observed.

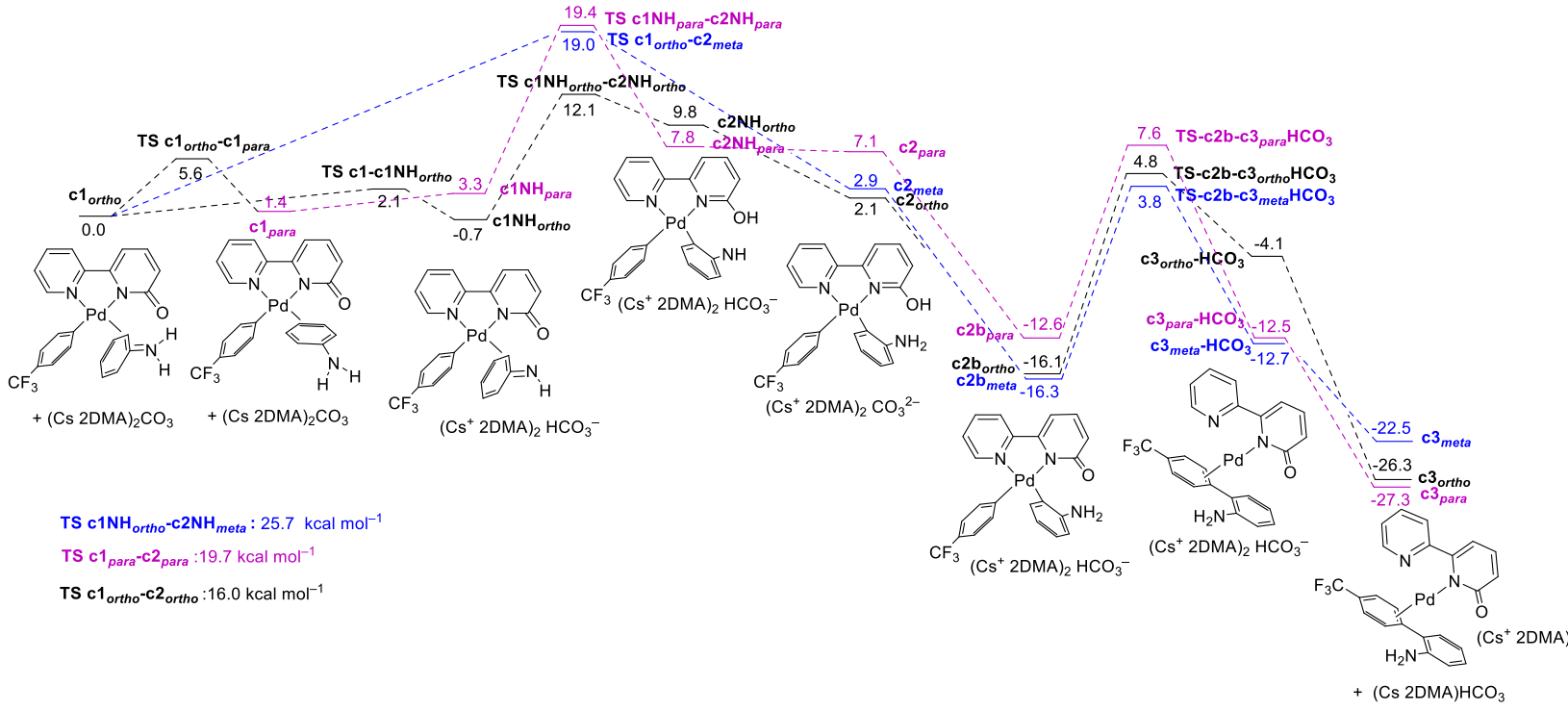

Figure 2.9. Gibbs energy profiles for the preferred C–H activation pathway (amido-type or anilino-type intermediates) and reductive elimination steps for aniline in the *ortho* (black), the *meta* (blue) and the *para* (magenta) positions. For simplicity, only the *ortho* isomer has been drawn for all the intermediates. Energies in kcal mol^{-1}. The energies of the C–H cleavage transition states not depicted in the profile are also shown. No minimum has been found for a c1$_{meta}$ intermediate.

Other alternatives such as a Pd(II)/Pd(IV) mechanism where the C–H activation occurs first on a Pd(II) complex followed by an oxidative addition of ArX can be thought of. This route is less favourable because the aryl halide is not a strong enough oxidant to oxidize a Pd(II) aryl complex to a Pd(IV) derivative. DFT calculations on this step shows that the energy barrier would be about 46 kcal mol^{-1} (Figure 2.21). Experimentally, when either complex **5** or a benzylamine palladacycle were heated with *p*-$CF_3C_6H_4I$ in DMA at 130 °C no C–C cross coupling product was observed (Scheme 2.6, see experimental part for further details).

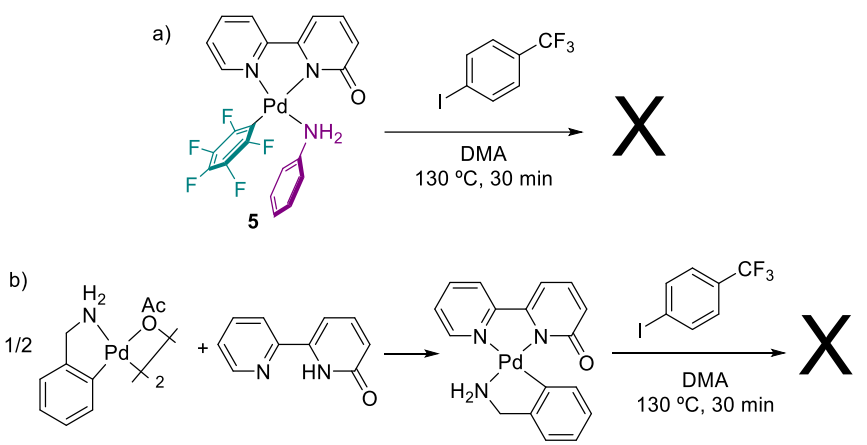

Scheme 2.6. Pd(II)/Pd(IV) experiments**:** a) from **5**, b) from benzilamine palladacylce.

The C–N coupling route to give the Buchwald-Hartwig amination product was also calculated. The deprotonation of the aniline in complex **6** is facile and the amido version of complex **6** is found 0.6 kcal mol^{-1} below the neutral form, pointing out the existence of an amino-amido equilibrium in the presence of carbonate in the reaction medium (Figure 2.10). The aryl-amido reductive elimination barrier is 14.1 kcal mol^{-1}. This value is 2 kcal mol^{-1} higher than the barrier for C–H *ortho* cleavage in the aniline (12.1 kcal mol^{-1}, Figure 2.8), which makes the *ortho* C–H functionalization preferred in good agreement with the experimental chemoselectivity. In contrast to bulky phosphine ligands, the ligand bipy-6-OH does not favour the reductive elimination step, which, eventually, is an advantage for chemoselectivity.

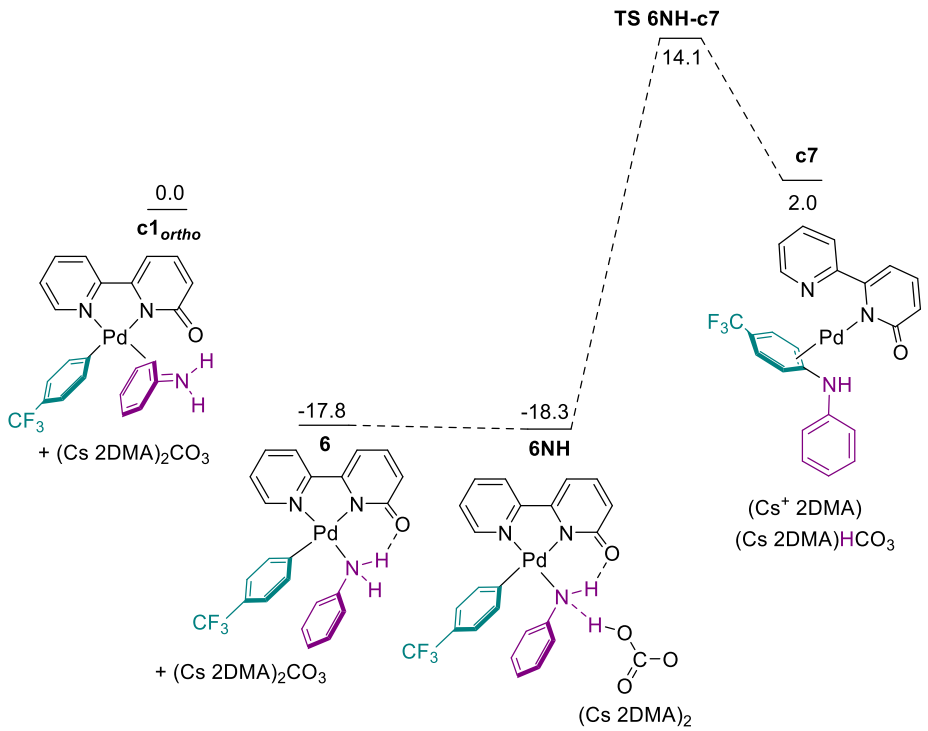

Figure 2.10. Gibbs energy profile for the formation of the Buchwald-Hartwig amination product (C–N coupling) from complex **6**. Energies (referenced to $c1_{ortho}$, also shown for clarity) in kcal mol^{-1}.

2.3 CONCLUSIONS

Unprotected anilines can be selectively arylated in the *ortho* position using the Pd/bipy-6-OH catalyst system, avoiding the protection-deprotection additional steps commonly used in the literature. The best reaction conditions found were DMA as co-solvent, cesium carbonate as base at 130 ºC. Substituted anilines with different electronic properties (electron-donating or electron-withdrawing) or even with bulky substituents can be functionalized using the described reaction conditions. The *ortho* isomer was obtained selectively for all the primary and secondary anilines but for tertiary anilines no *ortho* coupling product was formed. It has been demonstrated by mechanistic studies that the cooperating role of the bipy-6-OH in the C–H cleavage step is crucial for the chemoselectivity, affording the C–C coupling product. Moreover, the computational studies have shown a high discriminating barrier for reductive elimination that eliminates the competition of the C–N coupling product (amination). The regioselectivity of primary and secondary anilines can be explained by the operation of an anionic route where the C–H activation occurs on an amido complex which favours the *ortho* isomer. This route is not possible for tertiary anilines, that cannot be deprotonated and lead to a different regioisomeric mixture.

2.4 EXPERIMENTAL PART

2.4.1 General considerations

^{1}H, $^{13}C\{^{1}H\}$ and ^{19}F NMR spectra were recorded on Agilent MR-500, Agilent MR-400 or Bruker AV-400 spectrometers at the Laboratorio de Técnicas Instrumentales (LTI) of the UVa. Chemical shifts (in δ units, ppm) were referenced to $SiMe_4$ (^{1}H and ^{13}C) and $CFCl_3$ (^{19}F). The spectral data were recorded at 298 K unless otherwise noted. Homonuclear (^{1}H-COSY and ^{1}H-NOESY) and heteronuclear (^{1}H-^{13}C HSQC, ^{1}H-^{13}C HMBC, ^{19}F-^{13}C HSQC and ^{19}F-^{13}C HMBC) experiments were used to help with the signal assignments. The GC-MS analyses were performed in a Thermo-Scientific Focus DSQ II GC/MS apparatus. The intensities are reported as percentages relative to the base peak after the corresponding *m/z* value. HRMS analyses were carried out on a Bruker Maxis Impact mass spectrometer at the Laboratorio de Técnicas Instrumentales (LTI) of the UVa. Elemental analyses were carried out in a Carlo Erba 1108 microanalyzer (at the Vigo University, Spain). Infrared spectra were recorded (in the range 4000-200 cm^{-1}) on a Perkin-Elmer FT-IR Spectrum Frontier with an ATRdiamond accessory.

Solvents were dried using a solvent purification system SPS PS-MD-5 (ether, hexane and CH_2Cl_2) or distilled from appropriate drying agents under nitrogen prior to use and stored over 3 Å or 4 Å molecular sieves (toluene, DMA, acetone).

4-Iodobenzotrifluoride, 4-iodotoluene, 4-bromoanisole, cesium carbonate, tetramethylethylenediamine (TMEDA), palladium acetate and all the anilines are commercially available and were purchased from Sigma-Aldrich, Acros Organics, Alfa Aesar or Fluorochem. Commercial reagents were used as received unless otherwise noted. The anilines were distilled or recrystallized and kept under a N_2 atmosphere before use.

[Pd(bipy-6-OH)Br(C_6F_5)] (**1**),[20] [[Pd(bipy-4-OH)Br(C_6F_5)] (**2**),[20] [Pd(bipy)Br(C_6F_5)] (**3**),[20,82] [PdBr(C_6F_5)(phen-2-OH)] (**4**),[25] $(NBu_4)_2[Pd_2(\mu\text{-}Br)_2(C_6F_5)_4]$,[82] $[Pd_2(dba)_3].CHCl_3$,[83] [Pd(C_6H_4-*p*-CF_3)I(TMEDA)][84] and [2,2'-bipyridin]-6(1*H*)-one (bipy-6-OH),[20,85] were prepared according to the procedures in the literature.

---

[82] Espinet, P.; Albéniz, A. C.; Usón, R.; Forniés, J.; Nalda, J. A.; Lozano, M. *J. Inorg. Chim. Acta*, **1989**, *156*, 251-256.
[83] Ishii, Y.; Hasegawa, S.; Kimura, S.; Itoh, K. *J. Organomet. Chem.* **1974**, *73*, 411-418.
[84] Yamashita, M.; Cuevas Vicario, J.; Hartwig, J. F. *J. Am. Chem. Soc.* **2003**, *125*, 16347-16360.
[85] Tomon, T.; Koizumi, T.; Tanaka, K. *Eur. J. Inorg. Chem*. **2005**, 285-293.

2.4.2 *Synthesis of palladium complexes*

[Pd(bipy-6-O)(C_6F_5)($PhNH_2$)] (5). [Pd(bipy-6-OH)Br(C_6F_5)] (95.8 mg, 0.182 mmol) was dissolved in dichloromethane (25 mL). Aniline (50 μL, 0.547 mmol), Cs_2CO_3 (60 mg, 0.182 mmol) and $AgBF_4$ (35.5 mg, 0.182 mmol) were added while stirring. The reaction mixture was stirred for 20 h at room temperature. The yellow solution was filtered through kieselgur and the solvent was removed. Cold EtOH was added (15 mL) and the yellow solid was filtered, washed with cold EtOH and air-dried. Yield: 61 mg (62%).

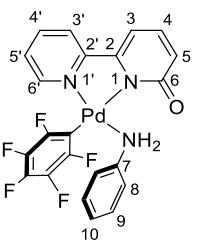

^{1}H NMR (500.13 MHz, δ, $CDCl_3$): 8.65 (br, 2H, H^{NH2}), 7.87 (m, 2H, $H^{3'}$, $H^{4'}$), 7.64 (d, J = 6.5 Hz, 1H, $H^{6'}$), 7.45 (dd, J = 7.2, 8.7 Hz, 1H, H^4), 7.09 (m, 3H, $H^{5'}$, H^9), 7.02 (t, J = 6.2 Hz, 1H, H^{10}), 6.94 (d, J = 7.1 Hz, 1H, H^3), 6.84 (d, J = 7.5 Hz, 2H, H^8), 6.66 (d, J = 8.9 Hz, 1H, H^5). ^{13}C{^{1}H} NMR (125.78 MHz, δ, $CDCl_3$): 174.1 (C^6), 160.7 ($C^{2'}$), 151.4 ($C^{6'}$, C^2), 147.5 (C^{Fortho})*, 142.5 (C^7), 138.9 ($C^{4'}$), 137.9 (C^{Fpara} *, C^4), 136.2 (C^{Fmeta})*, 129 (C^9), 124.5 (C^{10}, $C^{5'}$),122.9 (C^5), 121.6 ($C^{3'}$), 120.8 (C^8), 106.7 (C^3). ^{19}F NMR (470.168 MHz, δ, $CDCl_3$): -119.9 (m, 2F, F_{ortho}), 158.39 (t, J = 19.1 Hz, 1F, F_{para}), 161.27 (m, 2F, F_{meta}). Anal. Calculated for $C_{22}H_{14}F_5N_3OPd$ C, 49.13 %; N, 7.81 %; H, 2.62 %; found: C, 49.41 %; N, 7.68 %; H, 2.80 %.

*The chemical shifts of the C_6F_5 carbon resonances were determined by HSQC ^{13}C-^{19}F.

[Pd(bipy-6-O)(C_6H_4-*p*-CF_3)($PhNH_2$)] (6). Bipy-6-OH (24.1 mg, 0.14 mmol) was dissolved in acetone (25 mL) and Cs_2CO_3 (46.0 mg, 0.14 mmol) was added. The suspension was stirred at room temperature for 10 min. Then, aniline (39 μL, 0.42 mmol) and [Pd(C_6H_4-*p*-CF_3)I(TMEDA)] (69 mg, 0.14 mmol) were added. The mixture was stirred at room temperature for 2 h. The yellow suspension was filtered through kieselgur and the solvent was removed. Cold Et_2O (5 mL) was added and the yellow solid was filtered, washed with cold hexane (2 x 2 mL) and air-dried. Yield: 60 mg (83%).

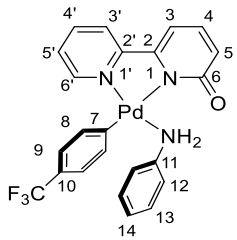

^{1}H NMR (500.13 MHz, δ, $CDCl_3$): 8.29 (br, 2H, H^{NH2}), 7.87 (d, J = 8.1 Hz, 1H, $H^{3'}$), 7.79 (td, J = 8.0, 1.5 Hz, 1H, $H^{4'}$), 7.59 (d, J = 5.5 Hz, 1H, $H^{6'}$), 7.43 (dd, J = 8.7, 6.9 Hz, 1H, H^{4}), 7.33 (m, J = 7.5 Hz, 2H, H^{8}), 7.21(m, J = 7.5 Hz, 2H, H^{9}), 7.09 (t, J = 8.0 Hz, 2H, H^{13}), 7.04 (t, J = 6.7 Hz, 1H, $H^{5'}$), 6.99 (t, J = 7.2 Hz, 1H, H^{14}), 6.93 (d, J = 6.7 Hz, 1H, H^{3}), 6.78 (d, J = 7.6 Hz, 2H, H^{12}), 6.64 (d, J = 8.9, 1H, H^{5}). ^{13}C{^{1}H} NMR (125.78 MHz, δ, $CDCl_3$): 174.1 (C^{6}), 164.2 (C^{7}), 160.2 ($C^{2'}$), 151.1 ($C^{6'}$), 150.6 (C^{2}), 142.2 (C^{11}), 138.2 ($C^{4'}$), 137.9 (C^{4}), 134.7 (C^{8}), 128.8 (C^{13}), 126.2 (q, $^{2}J_{C-F}$ = 32 Hz, C^{10}), 125.9 (q, $^{1}J_{C-F}$ = 178 Hz, CF_3), 124.3 ($C^{5'}$), 123.9 (C^{14}), 123.2 (q, $^{3}J_{C-F}$ = 3.5 Hz, C^{9}), 121.7 (C^{5}), 121.5 ($C^{3'}$, C^{12}), 106.3 (C^{3}). ^{19}F NMR (470.168 MHz, δ, $CDCl_3$): -61.91 (s, CF_3). Anal. Calculated for $C_{22}H_{18}F_3N_3OPd$: C, 53.55 %; N, 8.15 %; H, 3.52 %; found: C, 53.50 %; N, 8.08 %; H, 3.70 %.

[Pd(bipy-6-O)(C_6F_5)(PhNHMe)] (7). [Pd(bipy-6-OH)Br(C_6F_5)] (106 mg, 0.202 mmol) was dissolved in dichloromethane (25 mL). N-methylaniline (65.5 μL, 0.606 mmol), Cs_2CO_3 (65.8 mg, 0.202 mmol) and $AgBF_4$ (39.3 mg, 0.202 mmol) were added to the solution while stirring. The reaction mixture was stirred for 20 h at room temperature. The yellow solution was filtered through kieselgur and the solvent was removed. Cold EtOH (15 mL) was added and the yellow solid was filtered, washed with cold EtOH (5 mL) and air-dried. Yield: 65 mg (58%). The solid is a mixture of complex **7** and a minor isomer (5%) as shown by ^{1}H and ^{19}F NMR. Only complex **7** was completely characterized.

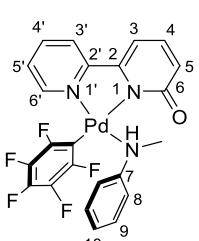

^{1}H NMR (500.13 MHz, δ, $CDCl_3$): 13.81 (br, H, H^{NH}), 7.84 (m, 2H, $H^{4'}$, $H^{3'}$), 7.46 (dd, J = 8.7, 7.1 Hz, 1H, H^{4}), 7.43 (d, J = 5.7 Hz, 1H, $H^{6'}$), 7.17 (t, J = 6.9 Hz, 2H, H^{9}), 7.09 (t, J = 7.2 Hz, 1H, H^{10}), 7.04 (t, J = 6.6 Hz, 1H, $H^{5'}$), 6.99 (d, J = 8.3 Hz, 2H, H^{8}), 6.95

(dd, J = 7.2, 1 Hz, 1H, H^3), 6.68 (dd, J = 8.7, 1 Hz, 1H, H^5), 2.9 (d, J = 5.3 Hz, 3H, H^{Me}). $^{13}C\{^1H\}$ NMR (125.78 MHz, δ, $CDCl_3$): 174.2 (C^6), 160.4 ($C^{2'}$), 151.4 (C^2), 151.3 ($C^{6'}$), 148.5 (C^7), 147.7 (C^{Fortho})*, 146.9 (C^{Fortho})*, 138.8 ($C^{4'}$), 138.2 (C^{Fpara})*, 138 (C^4), 136.2 (C^{Fmeta})*, 135.9 (C^{Fmeta})*, 128.8 (C^9), 124.6 (C^{10}), 124.6 ($C^{5'}$), 122.7 (C^5), 121.8 ($C^{3'}$), 119.6 (C^8), 106.9 (C^3), 37.7 (C^{Me}). ^{19}F NMR (470.168 MHz, δ, $CDCl_3$): -120.01 (m, 1F, F_{ortho}), -120.2 (m, 1F, F_{ortho}), -158.64 (t, J = 20.1 Hz, 1F, F_{para}), -161 (m, 1F, F_{meta}), -161.86 (m, 1F, F_{meta}). Anal. Calculated for $C_{23}H_{16}F_5N_3OPd$: C, 50.06 %; N, 7.62 %; H, 2.92 %; found: C, 49.77 %; N, 7.22 %; H, 2.82 %.

*The chemical shifts of the C_6F_5 carbon resonances were determined by HSQC ^{13}C-^{19}F

2.4.3 Catalytic reactions

General procedure for the direct arylation of anilines.

[Pd(bipy-6-OH)Br(C_6F_5)] (**1**) (9.0 mg, 0.017 mmol) and cesium carbonate (222 mg, 0.68 mmol) were introduced in a Schlenk flask under a nitrogen atmosphere. Then, 4-iodobenzotrifluoride (51 μL, 0.34 mmol), the corresponding aniline (3.4 mmol) and dry DMA (2.7 mL) were added to the flask. The reaction mixture was stirred at 130 ºC and checked by ^{19}F NMR of the crude mixture after 2 h, 6 h or 24 h depending on the aniline. When total conversion was observed, the solvent was evaporated in vacuo and the organic product was extracted with a mixture of *n*-hexane (3 mL) and ethyl acetate (0.3 mL). The extract was filtered through kieselgur and evaporated to dryness. The ratio of isomers was checked again by ^{19}F NMR and GC-MS. The product was purified by column chromatography using silica gel and a mixture of *n*-hexane:EtOAc = 9:1 as eluent.

The reaction with aryl halides other than 4-iodobenzotrifluoride were carried out in the same way. Those products that could not be completely purified by column chromatography were subjected to preparative TLC (*n*-hexane:EtOAc = 9:1). The yields and characterization data for the products obtained are collected below. For known compounds the spectral data conforms to those in the literature (references are given).

Aniline as arene. ArX = ***p*-$CF_3C_6H_4I$**. The product was obtained as a yellow oil, mixture of three isomers in a ratio o:m:p = 25:1:1. Yield: 0.061 g (76 %). The major isomer (*ortho*) was separated by column chromatography (0.041 g, 51 % yield). The characterization of 4'-(trifluoromethyl)-[1,1'-biphenyl]-2-amine, 4'-(trifluoromethyl)-

[1,1'-biphenyl]-4-amine and 4'-(trifluoromethyl)-[1,1'-biphenyl]-3-amine has been reported before.[¡Error! Marcador no definido.]

***N*-methylaniline** as arene. ArX = ***p*-$CF_3C_6H_4I$**. The product was obtained as a yellow oil, mixture of three isomers in the ratio o:m:p = 18:2:1. Yield: 0.068 g (79 %). The major isomer (*ortho*) was separated by column chromatography (0.05 g, 58 % yield).

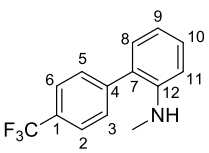

N-Methyl-4'-(trifluoromethyl)[1,1'-biphenyl]-2-amine:[86] ^{1}H NMR (500.13 MHz, δ, $CDCl_3$): 7.70 (m, 2H, H^2, H^6), 7.56 (m, 2H, H^3, H^5), 7.31 (ddd, J = 8.3, 7.4, 1.6 Hz, 1H, H^{10}), 7.08 (dd, J = 7.4, 1.5 Hz, 1H, H^8), 6.80 (td, J = 7.4, 1.6 Hz, 1H, H^9), 6.73 (d, J = 8.3 Hz, 1H, H^{11}), 3.86 (br, 1H, H^{NH}), 2.81 (s, 3H, Me). $^{13}C\{^1H\}$ NMR (125.78 MHz, δ, $CDCl_3$): 145.9 (C^{12}), 143.3 (C^4), 129.9 (C^8), 129.8 (C^3, C^5), 129.5 (C^{10}), 129.3 (q, $^2J_{C\text{-}F}$ = 33.6 Hz, C^1), 126.0 (C^7), 125.8 (q, $^3J_{C\text{-}F}$ = 3.8 Hz, C^2, C^6), 124.2 (q, $^1J_{C\text{-}F}$ = 272 Hz, CF_3), 117.1 (C^9), 110.2 (C^{11}), 30.8 (Me). ^{19}F NMR (470.168 MHz, δ, $CDCl_3$): -62.51 (s, CF_3). MS (EI, 70 eV): m/z (%) 251 (50) [M^+], 235 (10), 202 (7), 181 (35), 152 (10).

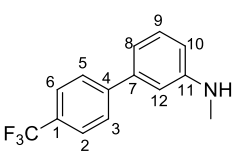

N-Methyl-4'-(trifluoromethyl)[1,1'-biphenyl]-3-amine:[87] ^{1}H NMR (500.13 MHz, δ, $CDCl_3$): 7.67 (br, 4H, H^2, H^3, H^5, H^6), 7.28 (t, J = 7.7 Hz, 1H, H^9), 6.93 (d, J = 7.5 Hz, 1H, H^8), 6.79 (br, 1H, H^{12}), 6.66 (d, J = 7.9 Hz, 1H, H^{10}), 3.87 (br, 1H, H^{NH}), 2.90 (s, 3H, Me). $^{13}C\{^1H\}$ NMR (125.78 MHz, δ, $CDCl_3$): 129.9 (C^9), 127.5 (C^3, C^5), 125.6 (C^2, C^6), 116.4 (C^8), 112.5 (C^{10}), 110.9 (C^{12}), 30.4 (Me). ^{19}F NMR (470.168 MHz, δ, $CDCl_3$): -62.37 (s, CF_3). MS (EI, 70 eV): m/z (%) 251 (100) [M^+], 201 (15), 152 (20).

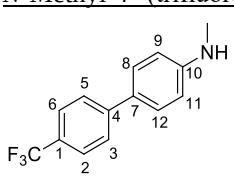

N-Methyl-4'-(trifluoromethyl)[1,1'-biphenyl]-4-amine:[88] ^{1}H NMR (500.13 MHz, δ, $CDCl_3$): 7.63 (br, 4H, H^2, H^3, H^5, H^6), 7.47 (d, J = 8.6 Hz, 2H, H^8, H^{12}), 6.70 (d, J = 8.8 Hz, 2H, H^9, H^{11}), 3.87 (br, 1H, H^{NH}), 2.90 (s, 3H, Me). $^{13}C\{^1H\}$ NMR (125.78 MHz, δ, $CDCl_3$): 149.3 (C^{10}), 144.6 (C^4), 128.1 (C^8, C^{12}), 126.2 (C^3, C^5), 125.6 (C^2, C^6), 123.1 (CF_3), 112.9 (C^9, C^{11}), 30.8 (Me). ^{19}F NMR (470.168 MHz, δ, $CDCl_3$): -62.22 (s, CF_3). MS (EI, 70 eV): m/z (%) 251(100) [M^+], 235 (10), 181(40).

---

[86] Chen, H.; Wang, L.; Han, J. *Chem. Commun*., **2020**, *56*, 5697-5700.
[87] Benting, J.; Desbordes, P.; Gary, S.; Greul, J.; Tsuchiya, T.; Wachendorff-Neumann, U. US 9206137 B2, 2015.
[88] Parrish, C. A.; Adams, N. D.; Auger, K. D.; Burgess, J. L.; Carson, J. D.; Chaudhari, A. M.; Copeland, R. A.; Diamond, M. A.; Donatelli, C. A.; Duffy, K. J.; Faucette, L. F.; Finer, J. T.; Huffman, W. F.; Hugger, E. D.; Jackson, J. R.; Knight, S. D.; Luo, L.; Moore, M. L.; Newlander, K. A.; Ridgers, L. H.; Sakowicz, R.; Shaw, A. N.; Sung, C. M.; Sutton, D.; Wood, K. W.; Zhang, Y.-S.; Zimmerman, M. N.; Dhanak, D. *J. Med. Chem.* **2007**, *50*, 4939-4952.

***N*-isopropylaniline** as arene. ArX = ***p*-$CF_3C_6H_4I$**. The product was obtained as a yellow oil, mixture of three isomers in the ratio o:m:p = 12:3:1. Yield: 0.062 g (65 %). The major product (*ortho*) was separated by column chromatography (0.048 g, 50 % yield).

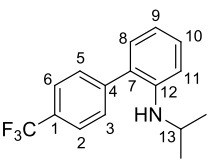

<u>*N*-Isopropyl-4'-(trifluoromethyl)[1,1'-biphenyl]-2-amine:</u> ^{1}H NMR (500.13 MHz, δ, $CDCl_3$): 7.70 (m, 2H, H^2, H^6), 7.54 (m, 2H, H^3, H^5), 7.26 (t, J = 7.39 Hz, 1H, H^{10}), 7.05 (d, J = 7.34 Hz, 1H, H^8), 6.75 (m, 3H, H^9, H^{11}), 3.63 (br, 2H, H^{NH}, H^{13}), 1.15 (d, J = 5.89 Hz, 6H, Me). $^{13}C\{^1H\}$ NMR (125.78 MHz, δ, $CDCl_3$): 144.1 (C^{12}), 143.5 (C^4), 130.4 (C^8), 129.7 (C^3, C^5), 129.4 (C^{10}), 129.2 (q, $^2J_{C\text{-}F}$ = 34 Hz, C^1), 126.0 (C^7), 125.8 (q, $^3J_{C\text{-}F}$ = 4 Hz, C^2, C^6), 124.2 (q, $^1J_{C\text{-}F}$ = 273 Hz, CF_3), 116.7 (C^9), 111.4 (C^{11}), 44.2 (C^{13}), 22.9 (Me). ^{19}F NMR (470.168 MHz, δ, $CDCl_3$): -62.49 (s, CF_3). IR (neat) cm^{-1}: 3422, 2968, 1504, 1320, 1119. HRMS (ESI-TOF): Calcd. for $C_{16}H_{17}F_3N$ $(M+H)^+$ 280.1308, found 280.1313. Rf (SiO_2, *n*-hexane:EtOAc = 8:2) = 0.72.

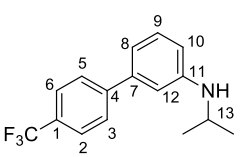

<u>*N*-Isopropyl-4'-(trifluoromethyl)[1,1'-biphenyl]-3-amine:</u> ^{1}H NMR (500.13 MHz, δ, $CDCl_3$): 7.66 (m, 4H, H^2, H^3, H^5, H^6), 7.25 (t, J = 8.0 Hz, 1H, H^9), 6.89 (d, J = 7.9 Hz, 1H, H^8), 6.77 (s, 1H, H^{12}), 6.63 (d, J = 7.9 Hz, 1H, H^{10}), 3.68 (br, 2H, H^{NH}, H^{13}), 1.25 (d, J = 6.1 Hz, 6H, Me). ^{19}F NMR (470.168 MHz, δ, $CDCl_3$): -62.38 (s, CF_3). MS (EI, 70 eV): m/z (%) 279 (40) $[M^+]$, 264 (100), 248 (20).

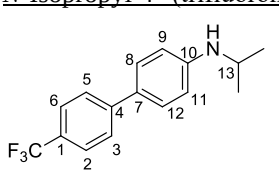

<u>*N*-Isopropyl-4'-(trifluoromethyl)[1,1'-biphenyl]-4-amine:</u> ^{1}H NMR (500.13 MHz, δ, $CDCl_3$): 7.62 (m, 4H, H^2, H^3, H^5, H^6), 7.44 (m, J = 8.5 Hz, 2H, H^8, H^{12}), 6.6 (m, J = 8.4 Hz, 2H, H^9, H^{11}), 3.68 (br, 2H, H^{NH}, H^{13}), 1.25 (d, J = 6.0 Hz, 6H, Me). $^{13}C\{^1H\}$ NMR (125.78 MHz, δ, $CDCl_3$): 147.4 (C^{10}), 144.7 (C^4), 128.1 (C^8, C^{12}), 128.0 (C^7), 126.1 (C^3, C^5), 125.8 (C^1), 125.6 (C^2, C^6), 123.2 (CF_3)*, 113.5 (C^9, C^{11}), 44.7 (C^{13}), 22.8 (Me). ^{19}F NMR (470.168 MHz, δ, $CDCl_3$): -62.23 (s, CF_3). MS (EI, 70 eV): m/z (%) 279 (40) $[M^+]$, 264 (100), 248 (20). *The chemical shift was determined by HSQC ^{13}C-^{19}F.

***N, N*-dimethylaniline** as arene. ArX = ***p*-$CF_3C_6H_4I$**. The product was obtained as a yellow oil, mixture of two isomers in the ratio m:p = 1.2:1. Yield: 0.039 g (43%). The products could not be completely separated by column chromatography.

N, *N*-Dimethyl-4'-(trifluoromethyl)[1,1'-biphenyl]-3-amine:[89] ^{1}H NMR (500.13 MHz, δ, $CDCl_3$): 7.68 (m, 4H, H^2, H^3, H^5, H^6), 7.33 (t, J = 7.9 Hz, 1H, H^9), 6.93 (d, J = 7.3 Hz, 1H, H^8), 6.89 (m, 1H, H^{12}), 6.79 (d, J = 9.1 Hz, 1H, H^{10}), 3.02 (s, 6H, Me). $^{13}C\{^{1}H\}$ NMR (125.78 MHz, δ, $CDCl_3$): 150.9 (C^{11}), 145.9 (C^4), 140.8 (C^7), 129.5 (C^9), 129.1 (q, $^{2}J_{C\text{-}F}$ = 31 Hz, C^1), 127.5 (C^3, C^5), 125.5 (q, $^{3}J_{C\text{-}F}$ = 3.8 Hz, C^2, C^6), 124.3 (q, $^{1}J_{C\text{-}F}$ = 271 Hz, CF_3), 115.8 (C^8), 112.3 (C^{10}), 111.1 (C^{12}), 40.1 (Me). ^{19}F NMR (470.168 MHz, δ, $CDCl_3$): -62.37 (s, CF_3). MS (EI, 70 eV): m/z (%) 264 (100) [M^+], 221 (10), 201 (20), 152 (25).

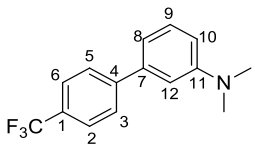

N, *N*-Dimethyl-4'-(trifluoromethyl)[1,1'-biphenyl]-4-amine:[89] ^{1}H NMR (500.13 MHz, δ, $CDCl_3$): 7.63 (m, 4H, H^2, H^3, H^5, H^6), 7.56 (d, J = 8.7 Hz, 2H, H^8, H^{12}), 7.28 (d, J = 8.9 Hz, 2H, H^9, H^{11}), 2.84 (s, 6H, Me). $^{13}C\{^{1}H\}$ NMR (125.78 MHz, δ, $CDCl_3$): 150.5 (C^{10}), 144.6 (C^4), 140.8 (C^7), 128 (q, J = 32.9 Hz, C^1), 127.9 (C^8, C^{12}), 126.2 (C^3, C^5), 125.5 (q, J = 2.7 Hz, C^2, C^6), 124.4 (CF_3)*, 112.8 (C^9, C^{11}), 40.4 (Me). ^{19}F NMR (470.168 MHz, δ, $CDCl_3$): -62.23 (s, CF_3). MS (EI, 70 eV): m/z (%) 265 (20) [M^+], 251 (50), 201 (15), 152 (15). *The chemical shift was determined by HSQC ^{13}C-^{19}F.

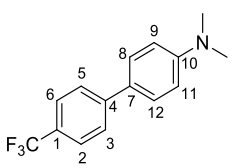

2-Toluidine as arene. ArX = ***p*-$CF_3C_6H_4I$**. The product was obtained as a yellow oil. Yield: 0.048 g (56 %). Rf (SiO_2, *n*-hexane:EtOAc = 8:2) = 0.42.

3-Methyl-4'-(trifluoromethyl)-[1,1'-biphenyl]-2-amine: ^{1}H NMR (500.13 MHz, δ, $CDCl_3$): 7.71 (d, J = 8.3 Hz, 2H, H^2, H^6), 7.59 (d, J = 8.3 Hz, 2H, H^3, H^5), 7.10 (d, J = 7.4 Hz, 1H, H^{10}), 6.98 (d, J = 7.5 Hz, 1H, H^8), 6.78 (t, J = 7.7 Hz, 1H, H^9), 3.68 (br, 2H, H^{NH2}), 2.23 (s, 3H, Me). $^{13}C\{^{1}H\}$ NMR (125.78 MHz, δ, $CDCl_3$): 143.7 (C^4), 141.3 (C^{12}), 130.4 (C^{10}), 129.6 (C^3, C^5), 129.3 (q, $^{2}J_{C\text{-}F}$ = 32 Hz, C^1), 128.2 (C^8), 125.7 (q, $^{3}J_{C\text{-}F}$ = 3.8 Hz, C^2, C^6, C^7), 124.0 (q, $^{1}J_{C\text{-}F}$ = 273 Hz, CF_3), 122.8 (C^{11}), 118.4 (C^9), 17.9 (Me). ^{19}F NMR (470.168 MHz, δ, $CDCl_3$): -62.52 (s, CF_3). IR (neat) cm^{-1}: 3388, 2922, 1609, 1464, 1322, 1118. HRMS (ESI-TOF): Calcd. for $C_{14}H_{13}F_3N$ $[M+H]^+$ 252.0995, found 252.1001. The regiochemistry of the product was unequivocally determined by the observation of a positive NOE effect H^{NH2}-$H^{3,5}$ in a NOESY NMR experiment.

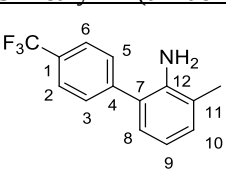

4-Toluidine as arene. ArX = ***p*-$CF_3C_6H_4I$**. The product is obtained as a yellow oil. Yield: 0.052 g (61 %).

[89] Dai, W.; Yang, B.; Xu, S.; Wang, Z. *J. Org. Chem.* **2021**, *86*, 2235-2243.

5-Methyl-4'-(trifluoromethyl)-[1,1'-biphenyl]-2-amine:[90] 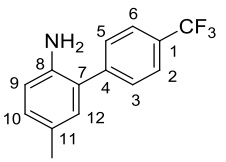 ^{1}H NMR (500.13 MHz, δ, $CDCl_3$): 7.70 (d, J = 8.3 Hz, 2H, H^2, H^6), 7.60 (d, J = 8.3 Hz, 2H, H^3, H^5), 7.02 (d, J = 8.1 Hz, 1H, H^{10}), 6.94 (s, 1H, H^{12}), 6.72 (d, J = 8.1 Hz, 1H, H^9), 3.61 (br, 2H, H^{NH2}), 2.29 (s, 3H, Me). $^{13}C\{^{1}H\}$ NMR (125.78 MHz, δ, $CDCl_3$): 143.5 (C^4), 140.8 (C^8), 130.8 (C^{12}), 129.8 (C^{10}), 129.4 (C^3, C^5), 129.2 (q, $^{2}J_{C-F}$ = 32 Hz, C^1), 128.2 (C^{11}), 126.1 (C^7), 125.7 (q, $^{3}J_{C-F}$ = 3.7 Hz, C^2, C^6), 124.3 (q, $^{1}J_{C-F}$ = 272 Hz, CF_3), 116.1 (C^9), 20.4 (Me). ^{19}F NMR (470.168 MHz, δ, $CDCl_3$): -62.6 (s, CF_3). MS (EI, 70 eV): m/z (%) 251 (100) [M^+], 180 (20), 106 (20). The regiochemistry of the product was unequivocally determined by the observation of a positive NOE effect between H^{12}-H^{Me}, H^{10}-H^{Me} and H^{NH2}-$H^{3,5}$ in a NOESY NMR experiment.

2-Phenylaniline as arene. ArX = ***p*-$CF_3C_6H_4I$**. The product is obtained as a yellow solid. m.p.: 73.5-74.8 ºC. Yield: 0.060 g (56 %). Rf (SiO_2, *n*-hexane:EtOAc = 8:2) = 0.56.

3-Phenyl-4'-(trifluoromethyl)-[1,1'-biphenyl]-2-amine: 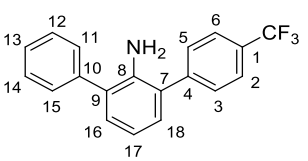 ^{1}H NMR (500.13 MHz, δ, $CDCl_3$): 7.71 (d, J = 8.1 Hz, 2H, H^2, H^6), 7.64 (d, J = 8.1 Hz, 2H, H^3, H^5), 7.48 (m, 4H, H^{11}, H^{12}, H^{14}, H^{15}), 7.37 (tt, J = 6.6, 1.5 Hz, 1H, H^{13}), 7.15 (dd, J = 7.7, 1.5 Hz, 1H, H^{16}), 7.10 (dd, J = 7.7, 1.5 Hz, 1H, H^{18}), 6.90 (t, J = 7.7 Hz, 1H, H^{17}), 3.81 (br, 2H, H^{NH2}). $^{13}C\{^{1}H\}$ NMR (125.78 MHz, δ, $CDCl_3$): 143.6 (C^4), 140.6 (C^8), 139.4 (C^{10}), 130.4 (C^{16}), 129.7 (q, $^{2}J_{C-F}$ = 31 Hz, C^1, C^3, C^5, C^{18}), 129.3 (C^{11}, C^{15}), 128.9 (C^{12}, C^{14}), 128.3 (C^9), 127.4 (C^{13}), 126.4 (C^7), 125.8 (q, $^{3}J_{C-F}$ = 3.5 Hz, C^2, C^6), 124.1 (q, $^{1}J_{C-F}$ = 274 Hz, CF_3), 118.4 (C^{17}). ^{19}F NMR (470.168 MHz, δ, $CDCl_3$): -62.52 (s, CF_3). IR (neat) cm^{-1}: 3463, 3370, 3065, 1601, 1435, 1318, 1106. HRMS (ESI-TOF): Calcd. for $C_{19}H_{15}F_3N$ $[M+H]^+$ 314.1151, found 314.1142. The regiochemistry of the product was unequivocally determined by the observation of a positive NOE effect H^{NH2}-$H^{11,15}$, H^{NH2}-$H^{3,5}$ in a NOESY NMR experiment.

4-Phenylaniline as arene. ArX = ***p*-$CF_3C_6H_4I$**. The product is obtained as a yellow oil. Yield: 0.066g (62 %). Rf (SiO_2, *n*-hexane:EtOAc = 8:2) = 0.38.

5-Phenyl-4'-(trifluoromethyl)-[1,1'-biphenyl]-2-amine: ^{1}H NMR (500.13 MHz, δ, $CDCl_3$): 7.74 (d, J = 7.9 Hz, 2H, H^2, H^6), 7.66 (d, J = 7.9 Hz, 2H, H^3, H^5), 7.57 (d, J = 7.2 Hz, 2H, H^{14}, H^{18}), 7.47 (dd, J = 8.3, 2.3 Hz, 1H, H^{10}), 7.40 (t, J = 7.2 Hz, 2H, H^{15},

[90] Zuo, Z.; Liu, J.; Nan, J.; Fan, L.; Sun, W.; Wang, Y.; Luan, X. *Angew. Chem. Int. Ed*. **2015**, 54, 15385-15389.

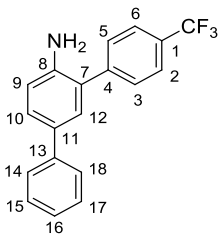

H^{17}), 7.38 (d, J = 2.3 Hz, 1H, H^{12}), 7.29 (t, J = 7.2 Hz, 1H, H^{16}), 6.86 (d, J = 8.3 Hz, 1H, H^{9}), 3.97 (br, 2H, H^{NH2}). $^{13}C\{^{1}H\}$ NMR (125.78 MHz, δ, $CDCl_3$): 143.2 (C^4), 142.7 (C^8), 140.7 (C^{13}), 132.0 (C^{11}), 129.5 (C^3, C^5), 129.4 (q, $^2J_{C-F}$ = 32 Hz, C^1), 129.0 (C^{12}), 128.7 (C^{15}, C^{17}), 127.9 (C^{10}), 126.5 (C^{16}), 126.4 (C^7, C^{14}, C^{18}), 125.8 (q, $^3J_{C-F}$ = 3.6 Hz, C^2, C^6), 124.1 (q, $^1J_{C-F}$ = 274 Hz, CF_3), 116.4 (C^9). ^{19}F NMR (470.168 MHz, δ, $CDCl_3$): -62.56 (s, CF_3). IR (neat) cm^{-1}: 3485, 3390, 2922, 1615, 1483, 1323, 1158. HRMS (ESI-TOF): Calcd. for $C_{19}H_{15}F_3N$ $[M+H]^+$ 314.1151, found 314.1157. The regiochemistry of the product was unequivocally determined by the observation of a positive NOE effect H^{NH2}-H^9, H^{NH2}-$H^{3,5}$ in a NOESY NMR experiment

4-Methoxyaniline as arene. ArX = ***p*-$CF_3C_6H_4I$.** The product is obtained as a yellow oil. It was completely characterized. Yield: 0.055 g (60 %). Rf (SiO_2, *n*-hexane:EtOAc = 8:2) = 0.27.

<u>5-Methoxy-4'-(trifluoromethyl)-[1,1'-biphenyl]-2-amine:</u> ^{1}H NMR (500.13 MHz, δ, $CDCl_3$): 7.68 (d, J = 8.0 Hz, 2H, H^2, H^6), 7.61 (d, J = 8.0 Hz, 2H, H^3, H^5), 6.82 (d, J = 1.5 Hz, 2H, H^9, H^{10}), 6.73 (d, J = 1.5 Hz, 1H, H^{12}), 4.43 (br, 2H, H^{NH2}), 3.78 (s, 3H, H^{OMe}). $^{13}C\{^{1}H\}$ NMR (125.78 MHz, δ, $CDCl_3$): 153.6 (C^{11}), 142.9 C^4), 135.2 (C^8), 129.6 (q, $^2J_{C-F}$ = 33 Hz, C^1), 129.5 (C^3, C^5), 128.2 (C^7), 125.7 (q, $^3J_{C-F}$ = 3.6 Hz, C^2, C^6), 124.1 (q, $^1J_{C-F}$ = 274 Hz, CF_3), 118.1 (C^9), 115.7 (C^{12}), 115.1 (C^{10}), 55.8 (OMe). ^{19}F NMR (470.168 MHz, δ, $CDCl_3$): -62.55 (s, CF_3). IR (neat) cm^{-1}: 3362, 2937, 1615, 1497, 1321, 1117. HRMS (ESI-TOF): Calcd. for $C_{14}H_{13}F_3NO$ $[M+H]^+$ 268.0944, found 268.0949. The regiochemistry of the product was unequivocally determined by the observation of a positive NOE effect H^{OMe}-H^{10}, H^{OMe}-H^{12}, $H^{3,5}$-H^{12} in a NOESY NMR experiment.

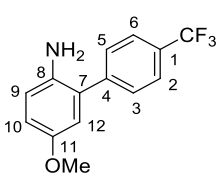

4-Chloroaniline as arene. ArX = ***p*-$CF_3C_6H_4I$**. The product is obtained as a yellow oil. Yield: 0.058 g (63 %). Rf (SiO_2, *n*-hexane:EtOAc = 8:2) = 0.33.

<u>5-Chloro-4'-(trifluoromethyl)-[1,1'-biphenyl]-2-amine:</u> ^{1}H NMR (500.13 MHz, δ, $CDCl_3$): 7.71 (m, J = 8.0 Hz, 2H, H^2, H^6), 7.55 (m, J = 8.0 Hz, 2H, H^3, H^5), 7.15 (dd, J = 8.4, 2.5 Hz, 1H, H^{10}), 7.09 (d, J = 2.5 Hz, 1H, H^{12}), 6.70 (d, J = 8.5 Hz, 1H, H^9), 3.73 (br, 2H, H^{NH2}). $^{13}C\{^{1}H\}$ NMR (125.78 MHz, δ, $CDCl_3$): 142 (C^8, C^4), 129.9 (q, $^2J_{C-F}$ = 32 Hz, C^1), 129.8 (C^{12}), 129.3 (C^3, C^5), 128.9 (C^{10}), 127.2 (C^7), 125.9 (q, $^3J_{C-F}$ = 3.7 Hz, C^2, C^6), 124.0 (q, $^1J_{C-F}$ = 270 Hz, CF_3), 123.4 (C^{11}), 116.9 (C^9). ^{19}F NMR (470.168

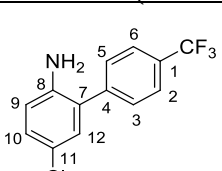

MHz, δ, $CDCl_3$): -62.62 (s, CF_3). IR (neat) cm^{-1}: 3474, 3383, 2926, 1617, 1486, 1321, 1106. HRMS (ESI-TOF): Calcd. for $C_{13}H_{10}ClF_3N$ $[M+H]^+$ 272.0448, found 272.0452. The regiochemistry of the product was unequivocally determined by the observation of a positive NOE effect H^{NH2}-H^9, H^{NH2}-$H^{3,5}$ in a NOESY NMR experiment.

2-Trifluoromethylaniline as arene. ArX = ***p*-$CF_3C_6H_4I$**. The product is obtained as a yellow oil. Yield: 0.066 g (64 %). R_f (SiO_2, *n*-hexane:EtOAc = 8:2) = 0.63.

<u>3-Trifluoromethyl-4'-(trifluoromethyl)-[1,1'-biphenyl]-2-amine:</u> ^1H NMR (500.13

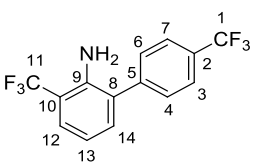

MHz, δ, $CDCl_3$): 7.74 (d, J = 8.3 Hz, 2H, H^3, H^7), 7.56 (d, J = 8.3 Hz, 2H, H^4, H^6), 7.49 (d, J = 7.9 Hz, 1H, H^{12}), 7.29 (d, J = 7.9 Hz, 1H, H^{14}), 6.86 (t, J = 7.9 Hz, 1H, H^{13}), 4.22 (br, 1H, H^{NH2}). $^{13}C\{^1H\}$ NMR (125.78 MHz, δ, $CDCl_3$): 141.9 (C^5), 141.6 (C^9), 133.8 (C^{14}), 130.2 (q, $^2J_{C-F}$ = 32 Hz, C^2), 129.7 (C^4, C^6), 127.7 (C^8), 126.6 (q, $^3J_{C-F}$ = 5.2 Hz, C^{12}), 126.1 (q, $^3J_{C-F}$ = 3.8 Hz, C^3, C^7), 124.7 (q, $^1J_{C-F}$ = 273 Hz, C^{11}), 123.9 (q, $^1J_{C-F}$ = 272 Hz, C^1), 117.3 (C^{13}), 114.2 (q, ^2J = 30 Hz, C^{10}). ^{19}F NMR (470.168 MHz, δ, $CDCl_3$): -62.67 (s, 3F, F^1), -62.92 (s, 3F, F^{11}). IR (neat) cm^{-1}: 3517, 3423, 2927, 1619, 1461, 1321, 1067. HRMS (ESI-TOF): Calcd. for $C_{14}H_8F_6N$ $[M-H]^-$ 304.0566, found 304.0560. The regiochemistry of the product was unequivocally determined by the observation of a positive NOE effect H^{NH2}-$H^{4,6}$ in a NOESY NMR experiment.

4-Trifluoromethylaniline as arene. ArX = ***p*-$CF_3C_6H_4I$**. The product is obtained as a yellow oil. R_f (SiO_2, *n*-hexane:EtOAc = 8:2) = 0.36. Yield: 0.058 g (56 %).

<u>5-Trifluoromethyl-4'-(trifluoromethyl)-[1,1'-biphenyl]-2-amine:</u> ^1H NMR (500.13

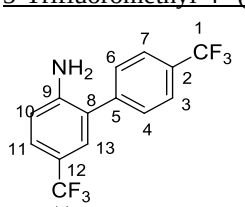

MHz, δ, $CDCl_3$): 7.73 (d, J = 8.1 Hz, 2H, H^3, H^7), 7.57 (d, J = 8.1 Hz, 2H, H^4, H^6), 7.41 (dd, J = 8.6, 2.0 Hz, 1H, H^{11}), 7.35 (d, J = 2.0 Hz, 1H, H^{13}), 6.80 (d, J = 8.6 Hz, 1H, H^{10}), 4.10 (br, 2H, H^{NH2}). $^{13}C\{^1H\}$ NMR (125.78 MHz, δ, $CDCl_3$): 146.4 (C^9), 141.8 (C^5), 130.1 (q, $^2J_{C-F}$ = 32 Hz, C^2), 129.4 (C^4, C^6), 127.5 (q, $^3J_{C-F}$ = 3.7 Hz, C^{13}), 126.3 (q, $^3J_{C-F}$ = 3.7 Hz, C^{11}), 126.0 (q, $^3J_{C-F}$ = 3.1 Hz, C^3, C^7), 125.3 (C^8), 124.6 (q, $^1J_{C-F}$ = 271 Hz, C^{14}), 124.1 (q, $^1J_{C-F}$ = 273 Hz, C^1), 120.7 (q, $^2J_{C-F}$ = 34 Hz, C^{12}), 115.3 (C^{10}). ^{19}F NMR (470.168 MHz, δ, $CDCl_3$): -61.30 (s, 3F, F^{14}), -62.67 (s, 3F, F^1). IR (neat) cm^{-1}: 3500, 3410, 2929, 1625, 1320, 1103. HRMS (ESI-TOF): Calcd. for $C_{14}H_{10}F_6N$ $[M+H]^+$ 306.0712, found 306.0712. The regiochemistry of the product was unequivocally determined by the observation of a positive NOE effect H^{NH2}-$H^{4,6}$, H^{NH2}-H^{10} in a NOESY NMR experiment.

1,4-Diaminobenzene as arene. ArX = ***p*-$CF_3C_6H_4I$**. The product is obtained as a brown oil. R_f (SiO_2, *n*-hexane:EtOAc = 8:2) = 0.26. Yield = 0.031 g (36 %).

<u>4′-(Trifluoromethyl)[1,1′-biphenyl]-2,5-diamine</u>: ^{1}H NMR (500.13 MHz, δ, $CDCl_3$):

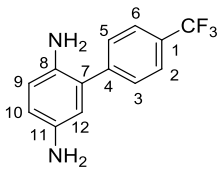

7.67 (d, J = 8.4 Hz, 2H, H^2, H^6), 7.55 (d, J = 8.4 Hz, 2H, H^3, H^5), 6.76 (dd, J = 8.8, 2.4 Hz, 1H, H^9), 6.68 (m, 2H, H^{10}, H^{12}), 4.49 (br, 4H, H^{NH2}). ^{13}C{^{1}H} NMR (125.78 MHz, δ, $CDCl_3$): 142.8 (C^4), 136.9 (C^{11}), 135.0 (C^8), 129.4 (C^3, C^5, C^1)*, 127.5 (C^7), 125.7 (C^2, C^6), 124.1 (CF_3)*, 119.0 (C^{10}), 118.4 (C^9), 117.5 (C^{12}). ^{19}F NMR (470.168 MHz, δ, $CDCl_3$): -62.53 (s, CF_3). HRMS (ESI-TOF): Calcd. for $C_{13}H_{12}F_3N_2$ $[M+H]^+$ 253.0947, found 253.0951. *The chemical shifts were determined by HSQC ^{13}C-^{19}F and HMBC ^{13}C-^{19}F.

Aniline as arene. ArX = ***p*-$CH_3C_6H_4I$**. The product is obtained as a colorless oil. Yield: 0.039 g (63 %).

<u>4'-Methyl-[1,1'-biphenyl]-2-amine:</u>[91] ^{1}H NMR (500.13 MHz, δ, $CDCl_3$): 7.35 (d, J = 8.3

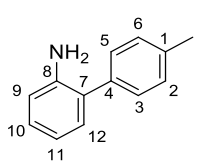

Hz, 2H, H^3, H^5), 7.26 (d, J = 8.3 Hz, 2H, H^2, H^6), 7.13 (m, 2H, H^{10}, H^{12}), 6.83 (td, J = 7.5, 1.1 Hz, 1H, H^{11}), 6.76 (dd, J = 7.9, 1.1 Hz, 1H, H^9), 3.75 (br, 2H, H^{NH2}), 2.39 (s, 3H, Me). ^{13}C{^{1}H} NMR (125.78 MHz, δ, $CDCl_3$): 142.9 (C^8), 136.9 (C^1), 136.4 (C^4), 130.5 (C^{12}), 129.5 (C^2, C^6), 128.9 (C^3, C^5), 128.3 (C^{10}), 128.0 (C^7), 119.0 (C^{11}), 115.9 (C^9), 21.2 (Me). MS (EI, 70 eV): m/z (%) 183 (100) $[M^+]$, 167 (45) 152 (15). The regiochemistry of the product was unequivocally determined by the observation of a positive NOE effect $H^{3,5}$-H^{12}, $H^{10,12}$-H^{11}, H^{10}-H^9 H^{NH2}-H^9 in a NOESY NMR experiment.

Aniline as arene. ArX = ***p*-(OMe)C_6H_4Br**. The product is obtained as a white solid. Yield: 0.047 g (69 %).

<u>4'-Methoxy-[1,1'-biphenyl]-2-amine:</u>[92] ^{1}H NMR (500.13 MHz, δ, $CDCl_3$): 7.37 (m, 2H,

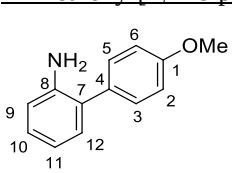

H^3, H^5), 7.14 (ddd, J = 7.9, 7.4, 1.6 Hz, 1H, H^{10}), 7.11 (dd, J = 7.4, 1.5 Hz, 1H, H^{12}), 6.97 (m, 2H, H^2, H^6), 6.82 (td, J = 7.4, 1.3 Hz, 1H, H^{11}), 6.77 (dd, J = 7.6, 1.1 Hz, 1H, H^9), 3.92 (br, 2H, H^{NH2}), 3.85 (s, 3H, OMe). ^{13}C{^{1}H} NMR (125.78 MHz, δ, $CDCl_3$): 158.8 (C^1), 143.3 (C^8), 131.7 (C^4), 130.5 (C^{12}), 130.2 (C^3, C^5), 128.2 (C^{10}), 127.6

[91] Gillespie, J. E.; Morrill, C.; Phipps, R. J. *J. Am. Chem. Soc.* **2021**, *143*, 9355-9360.
[92] Maity, A.; Frey, B. L.; Hoskinson, N. D.; Powers, D. C. *J. Am. Chem. Soc*. **2020**, *142*, 4990-4995.

(C^7), 118.8 (C^{11}), 115.7 (C^9), 114.2 (C^2, C^6), 55.3 (OMe). MS (EI, 70 eV): m/z (%) 199 (100) [M^+], 184 (45), 168 (30).

Amination of 4-iodobenzotrifluoride with anilines

The procedure used follows the conditions reported in the literature with small variations.[93]

$Pd_2dba_3.CHCl_3$ (25.8 mg, 0.025mmol), Xphos (23.8 mg, 0.050 mmol) and cesium carbonate (231.3 mg, 0.71 mmol) were introduced in a Schlenk flask in a nitrogen atmosphere. Then, the corresponding aniline (0.5 mmol) and DMF (0.25 mL) were added. The reaction mixture was stirred for 10 min at room temperature. Then 4-iodobenzotrifluoride (75 µL, 0.5 mmol) was added. The mixture was stirred at 65 ºC for 18 h and checked by ^{19}F NMR of the crude mixture. The crude was purified by column chromatography using silica gel and a mixture of *n*-hexane:EtOAc = 1:1.

N-Phenyl-4-(trifluoromethyl)benzenamine.[94] The product was obtained as a brown oil. Yield: 0.072 g (61 %).

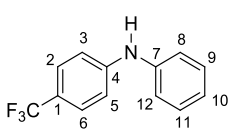

^1H NMR (500.13 MHz, δ, $CDCl_3$): 7.45 (d, J = 8.6 Hz, 2H, H^2, H^6), 7.33 (t, J = 7.4 Hz, 2H, H^9, H^{10}), 7.15 (d, J = 7.4 Hz, 2H, H^8, H^{12}), 7.05 (m, 3H, H^3, H^5, H^{10}), 5.91 (br, 1H, H^{NH}). $^{13}C\{^1H\}$ NMR (125.78 MHz, δ, $CDCl_3$): 146.9 (C^4), 141.2 (C^7), 129.6 (C^9, C^{11}), 126.7 (q, $^3J_{C\text{-}F}$ = 4 Hz, C^2, C^6), 124.6 (q, $^1J_{C\text{-}F}$ = 270 Hz, CF_3), 122.9 (C^{10}), 121.7 (q, $^2J_{C\text{-}F}$ = 31 Hz, C^1), 120.1 (C^8, C^{12}), 115.3 (C^3, C^5). ^{19}F NMR (470.168 MHz, δ, $CDCl_3$): -61.48 (s, CF_3). MS (EI, 70 eV): m/z (%) 237 (100) [M^+], 167 (40).

N-Methyl-N-phenyl-4-(trifluoromethyl)benzenamine.[95] The product was obtained as a brown oil. Yield: 0.052 g (41 %).

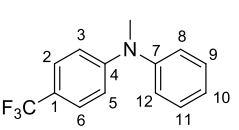

^1H NMR (500.13 MHz, δ, $CDCl_3$): 7.41 (m, 4H, H^2, H^6, H^8, H^{12}), 7.20 (m, 3H, H^9, H^{10}, H^{11}), 6.85 (d, J = 8.9 Hz, 2H, H^3, H^5), 3.35 (s, 3H, Me). $^{13}C\{^1H\}$ NMR (125.78 MHz, δ, $CDCl_3$): 151.5 (C^4), 147.7 (C^7), 129.7 (C^8, C^{12}), 126.2 (q, $^3J_{C\text{-}F}$ = 3.5 Hz, C^2, C^6), 125.2 (C^9, C^{11}), 124.9 (C^{10}),

[93] a) Ohshita, K.; Ishiyama, H.; Oyanagi, K.; Nakatab, H.; Kobayashi, J. *Bioorg. Med. Chem.* **2007**, *15*, 3235-3240. b) Surry, D. S.; Buchwald, S. L. *Angew. Chem. Int. Ed.* **2008**, *47*, 6338-6361.
[94] a) Sharma, C.; Srivastava, A. K.; Sharma, K. S.; Joshi, R. K. *Org. Biomol. Chem.*, **2020**,*18*, 3599-3606. b) Srivastava, A. K.; Sharma, C.; Joshi, R. K. *Green Chem*., **2020**, *22*, 8248-8253.
[95] a) Li, J.; Huang, C.; Wen, D.; Zheng, Q.; Tu, B.; Tu, T. *Org. Lett.* **2021**, *23*, 687-691. b) Tröndle, S.; Freytag, M.; Jones, P. G.; Tamm, M. *Eur. J. Inorg. Chem.* **2019**, 2569-2576.

124.8 (q, $^{1}J_{C-F}$ = 264 Hz, CF_3), 119.8 (q, $^{2}J_{C-F}$ = 27 Hz, C^1), 114.7 (C^3, C^5), 40.2 (Me). ^{19}F NMR (470.168 MHz, δ, $CDCl_3$): -61.26 (s, CF_3). MS (EI, 70 eV): m/z (%) 251 (100) [M^+], 232 (10), 167 (20).

2.4.4 Mechanistic experiments

Behavior of complex 1 with aniline.

Complex **1** (5.3 mg, 0.01 mmol) was added into an NMR tube along with a sealed glass capillary filled with DMSO-d_6 as a NMR reference. Then, 0.6 mL of dry DMA were added. The corresponding aniline was added to the tube and the Pd:aniline molar ratio is specified in the spectra. The species formed in solution at room temperature were examined by ^{19}F NMR.

The spectroscopic data of the identified species are given below.

1: Mixture of isomers A and B. Isomer A: ^{19}F NMR (470.168 MHz, δ, DMA/DMSO-d^6 capillary): -119.29 (m, 2F, F_{ortho}), -166.52 (t, J = 19.1 Hz, 1F, F_{para}), -168.36 (m, 2F, F_{meta}). Isomer B: ^{19}F NMR (470.168 MHz, δ, DMA/DMSO-d^6 capillary): -119.54 (m, 2F, F_{ortho}), -161.70 (t, J = 21.8 Hz, 1F, F_{para}), -164.42 (m, 2F, F_{meta}).

5: ^{19}F NMR (470.168 MHz, δ, DMA/DMSO-d^6 capillary): -118.50 (m, 2F, F_{ortho}), -161.83 (t, J = 20.1 Hz, 1F, F_{para}), -164.02 (m, 2F, F_{meta}).

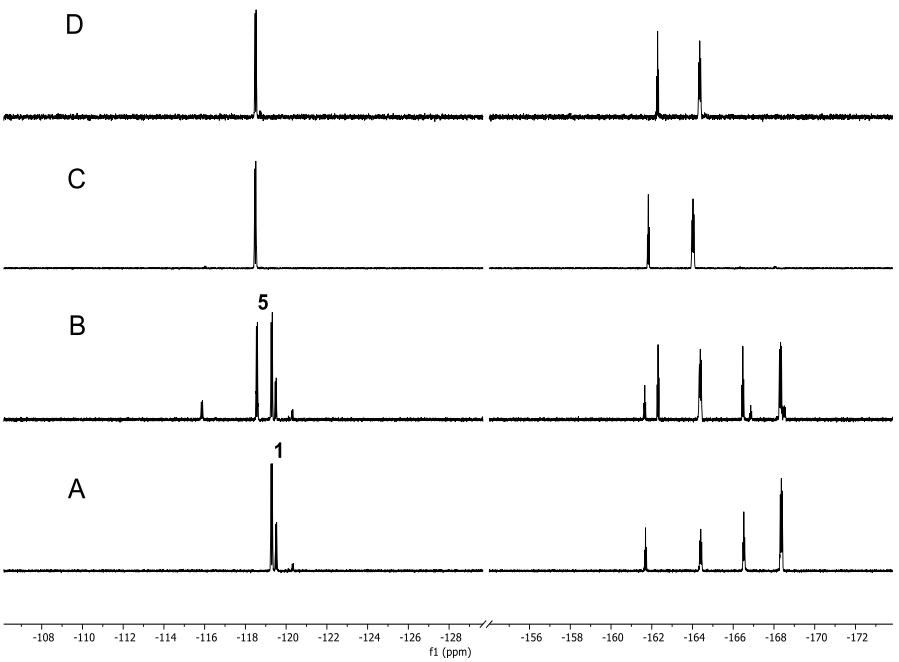

Figure 2.11 ^{19}F NMR spectra (470.168 MHz): A) Complex **1** in DMA (mixture of isomers). B) Sample A after adding 10 equivalents of aniline. C) Sample A after adding 200 equivalents of aniline. D) Complex **5** in DMA.

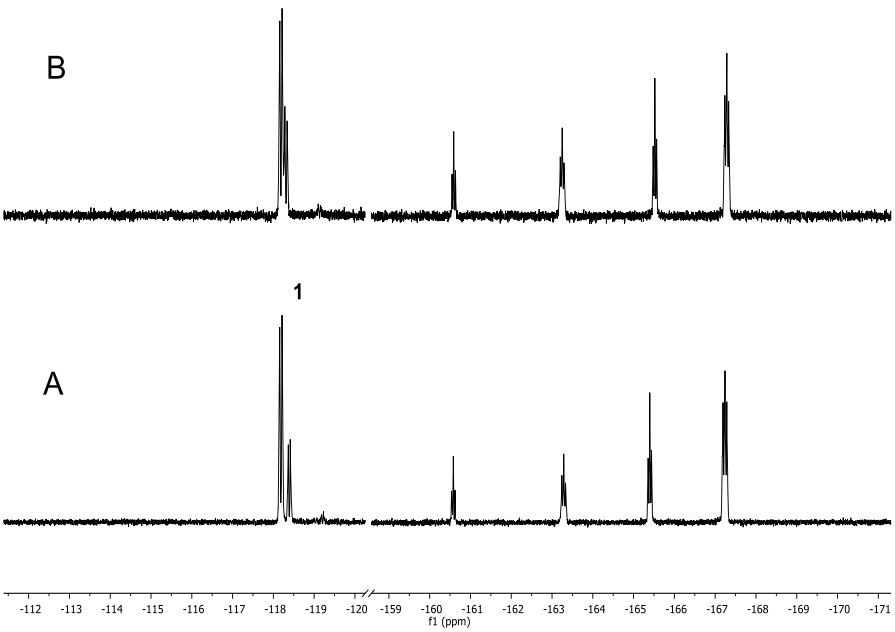

Figure 2.12 ^{19}F NMR spectra (470.168 MHz): A) Complex **1** in DMA (mixture of isomers). B) Sample A after adding 200 equivalents of *N*, *N*-dimethylaniline.

Thermal decomposition of complex 6 under catalytic conditions.

Complex **6** (5.2 mg, 0.01 mmol) and Cs_2CO_3 (3.3 mg, 0.01 mmol) were added into an NMR tube along with a sealed glass capillary filled with DMSO-d_6 as a NMR reference. Then, 0.6 mL of DMA and aniline (183 µL, 2 mmol) were added. The species formed in solution at room temperature were examined by ^{19}F NMR. Then, the mixture was heated at 130 °C for the specified time (Figure 2.3).

The spectroscopic data of the identified species are given below.

6: ^{19}F NMR (470.168 MHz, δ, DMA/DMSO-d^6 capillary): -61.58 (s, CF_3).

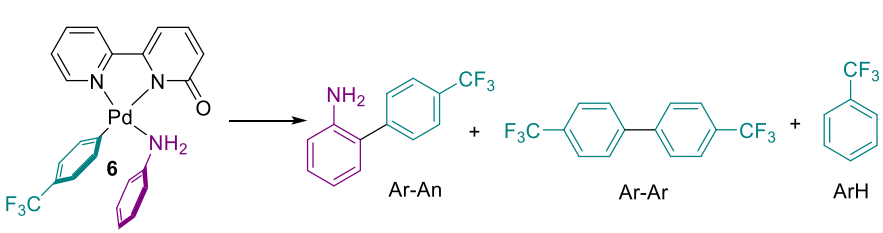

H-D exchange in complexes 1 and 6 with deuterium oxide.

The palladium complex (0.01 mmol) was added into an NMR tube along with a sealed glass capillary filled with DMSO-d_6 as a NMR reference. Then, 0.6 mL of dry DMA and deuterium oxide (1μL) were added to the tube.

The H-D exchange was observed at room temperature by ^{1}H NMR for the resonances specified below.

1: Mixture of isomers A and B. Isomer A: ^{1}H NMR (500.13 MHz, δ, DMA/DMSO-d^6 capillary): 13.40 (br, 1H, OH). Isomer B: ^{1}H NMR (500.13 MHz, δ, DMA/DMSO-d^6 capillary): 10.9 (br, 1H, OH).

6: ^{1}H NMR (500.13 MHz, δ, DMA/DMSO-d^6 capillary): 9.38 (br, 2H, NH_2).

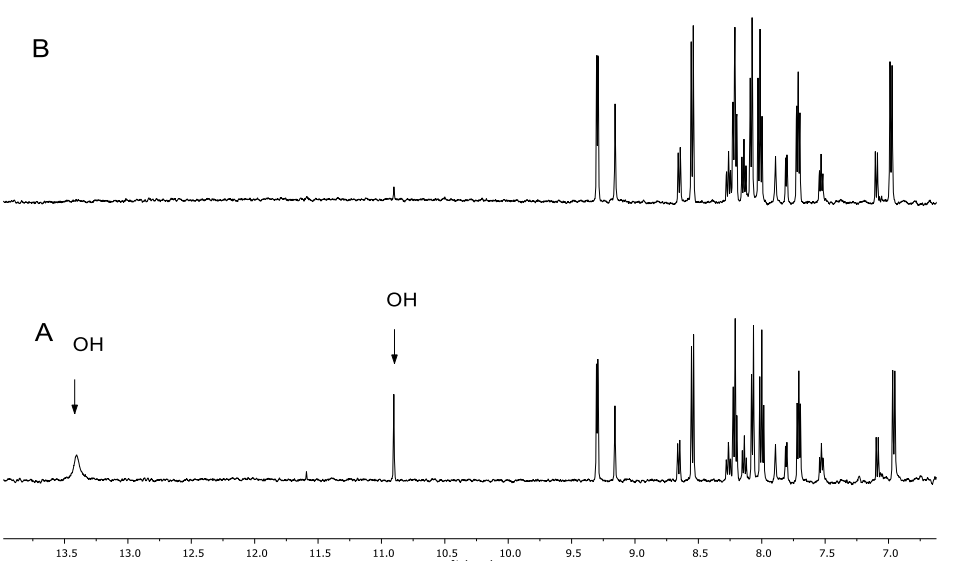

Figure 2.13 ^{1}H NMR spectra (500.13 MHz): A) Complex **1** in DMA. B) Sample A after adding D_2O.

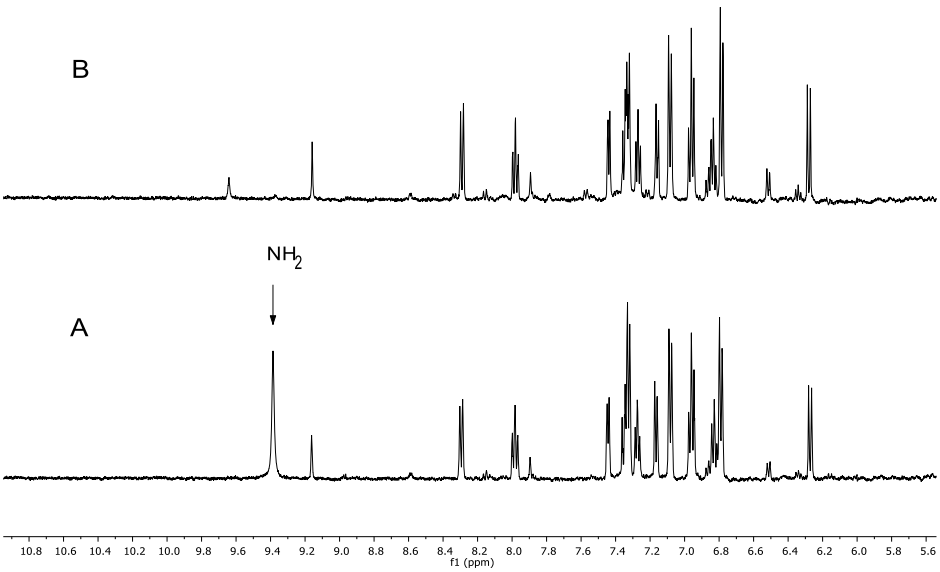

Figure 2.14 ^{1}H NMR spectra (500.13 MHz): A) Complex **6** in DMA. B) Sample A after adding D_2O.

Determination of equilibrium constants for the coordination of anilines and comparison with the regioselectivity observed.

Samples of 400 µL of a 4.72 10^{-3} M solution of $(NBu_4)_2[Pd_2(\mu\text{-}Br)_2(C_6F_5)_4]$ (**I**) in dichloromethane were placed in 1 mL volumetric flasks. A different known quantity of the chosen aniline was added to each sample and the volumetric flasks were filled with CH_2Cl_2. 0.6 mL of the final solution were introduced into a NMR tube along with a sealed glass capillary filled with acetone-d_6 as NMR reference. The species formed in the solution at room temperature were examined by ^{19}F NMR. The equilibrium concentrations of complexes **I** and **II** (Equation 2.10) were determined by integration of ^{19}F NMR signals. The values of K_{eq} and errors were determined as an average of three measurements.

$$K_{eq}=\frac{[II]^2}{[I]\,[Aniline]^2}$$

Table 2.3 Equilibrium constants (K_{eq}) for the coordination of different anilines.

Entry	R_1, R_2	K_{eq} (L mol^{-1})
1	H	118 ± 4
2	H, Me	1.2 ± 0.4
3	H, ^{i}Pr	0.027 ± 0.016
4	Me	$1.7x10^{-5} \pm 0.6x10^{-5}$

Probing the intermediacy of Pd(IV) species.

We checked the possibility of a formation of a Pd(IV) intermediate in our reaction using two model Pd(II) aryl complexes.

a) [Pd(bipy-6-O)(C_6F_5)($PhNH_2$)] (**5**). Complex **5** (0.01 mmol) was placed into an NMR tube along with a sealed glass capillary filled with DMSO-d6 as NMR lock signal. Then, 0.6 mL of dry DMA and *p*-$CF_3C_6H_4I$ (0.02 mmol) were added. The mixture was heated at 130 °C for 30 min. The species formed were examined by ^{19}F NMR. We did not observed any C–C cross coupling product (*p*-$CF_3C_6H_4$–C_6F_5) and only a small amount of C_6F_5H (7 %) from decomposition of **5** was found.

b) [Pd(κ^2-N,C-$NH_2CH_2C_6H_4$)(bipy6-O)]. This complex was prepared by reaction of [Pd(μ-OAc)(κ^2-N,C-$NH_2CH_2C_6H_4$)]$_2$ synthesised as reported in the literature,[96] with the stoichiometric amount of bipy-6-OH (Scheme 2.6).

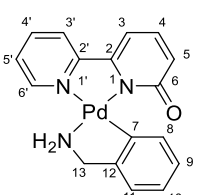

^1H NMR (500.13 MHz, δ, $CDCl_3$): 8.91 (d, J = 5.4 Hz, 1H, $H^{3'}$), 7.91 (m, 2H, $H^{5'}$, $H^{6'}$), 7.40 (m, 2H, $H^{4'}$, H^4), 7.22 (d, J = 6.5 Hz, 1H, H^{11}), 7.09 (m, 3H, H^8, H^9, H^{10}), 6.96 (d, J = 6.5 Hz, 1H, H^3), 6.64 (d, J = 8.6 Hz, 1H, H^5), 5.62 (br, 2H, H^{NH2}), 4.28 (t, J = 5.6 Hz, 2H, H^{13}).

The same procedure described above (a) was used for the reaction of this complex with *p*-$CF_3C_6H_4I$. No reaction was observed (Scheme 2.6).

[96] Fuchita Y.; Tsuchiya, H.; Miyafuji, A. *Inorg. Chim. Acta*. **1995**, 233, 91-96.

2.4.5 Kinetic data

Determination of the KIE

Two Schlenk flasks equipped with a septum cap and a Teflon stirring bar were charged with [Pd(bipy-6-OH)Br(C_6F_5)] (**1**) (9 mg, 0.017 mmol) and cesium carbonate (222 mg, 0.68 mmol) in a nitrogen atmosphere. 4-iodobenzotrifluoride (51 μL, 0.34 mmol) was added to each flask. Then, aniline (3.4 mmol, 310 μL) was added to one flask and aniline-2,3,4,5,6-d5 to the other. Finally, DMA (2.7 mL) was added to each flasks ([ArI]0 = 0.12 M). The Schlenk flasks were heated at 130 °C with constant stirring. At the indicated time, an aliquot was taken and analyzed by ^{19}F NMR adding 0.5 mL of $CDCl_3$ as NMR lock signal. The concentration of the product was determined by integration of the distinct trifluoromethyl signals of reagents and products. The ratio of initial rate constants for both experiments (k_H/k_D) give the reported KIE value (see below).

Table 2.4 Time and product concentration data for the KIE determining experiments.[a]

Aniline		Anilne-d_5	
Time (min)	**[Product] (M)**	**Time (min)**	**[Product] (M)**
15	0.0036	30	0.0024
30	0.0085	60	0.0036
60	0.0182	90	0.0049
75	0.0219	120	0.0061
90	0.0255	150	0.0085
105	0.0291	180	0.0109
		210	0.0134
		270	0.0182

[a]Initial concentrations: $[ArI]_0$ = 0.12 M; $[PhNH_2]_0$ = 1.2 M

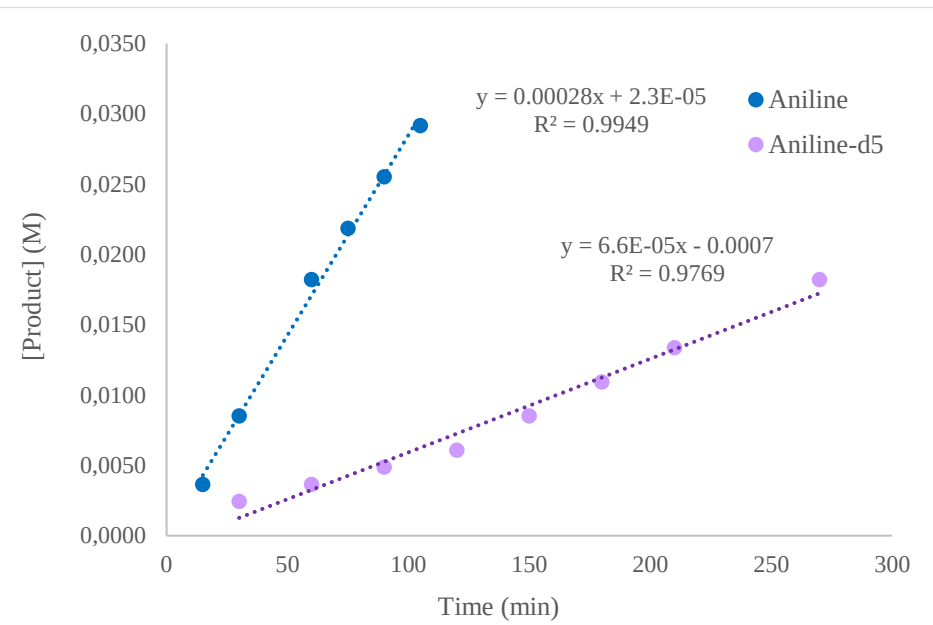

Figure 2.15. Concentration-time plots of the direct arylation of aniline and aniline-d_5.

The ratio of initial reaction rate constants gives the KIE value:

$k_H = 2.8 \pm 0.1 \times 10^{-4}$; $k_D = 6.6 \pm 0.4 \times 10^{-5}$. KIE = $k_H/k_D = 4.2 \pm 0.4$

Kinetic experiments of the direct arylation of aniline

A Schlenk flask equipped with a septum cap and a Teflon stirring bar were charged, in a nitrogen atmosphere, with [Pd(bipy-6-OH)Br(C_6F_5)] (**1**) and cesium carbonate. Then, 4-iodobenzotrifluoride, aniline and DMA (2.7 mL) were added. The Schlenk flask was heated at 130 °C with constant stirring. At the indicated time, an aliquot was taken and analyzed by ^{19}F NMR adding 0.5 mL of $CDCl_3$ as NMR lock signal. The concentration of the product was determined by integration of the distinct trifluoromethyl signals of reagents and products.

The variable time normalization analysis (VTNA) reported by Burés,[97] was used to determine the order on the reactants for the catalytic reaction. Four experiments were performed each time varying one of the reagent's initial concentration (Table 2.5). The resulting plots are represented in Figure 2.16.

Table 2.5 Initial concentration values for the kinetic experiments.

Experiment	[Cat] (M)	[ArI] (M)	[Aniline] (M)
1	0.006	0.1214	1.2143
2	0.003	0.1214	1.2143
3	0.006	0.2429	1.2143
4	0.006	0.1214	1.7586

[97] a) Burés, J. *Angew. Chem. Int. Ed.* **2016**, *55*, 16084-16087. b) Burés, J., A. *Angew. Chem. Int. Ed.* **2016**, *55*, 2028-2031.

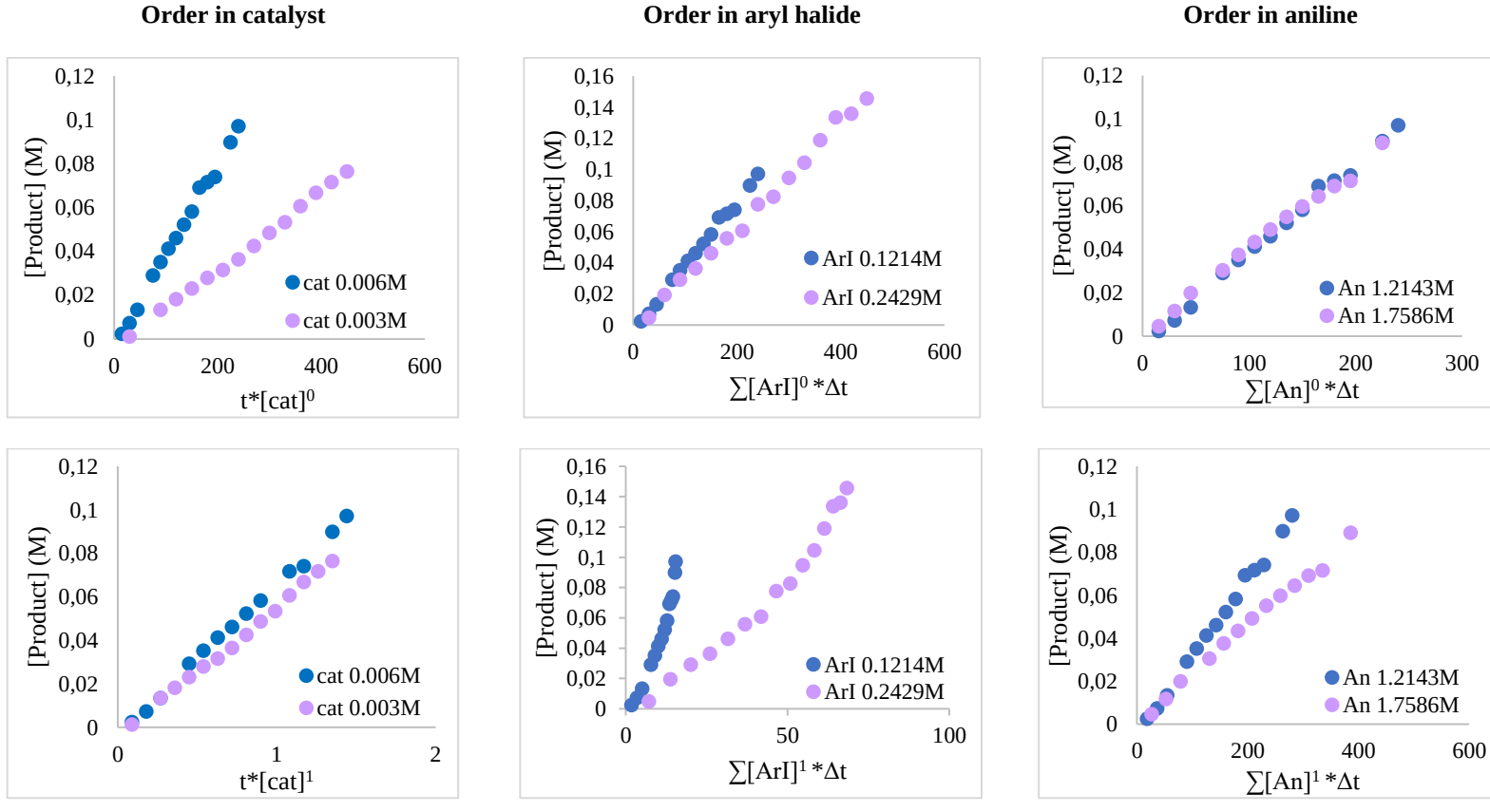

Figure 2.16 Plots derived from the variable time normalization analysis (VTNA). Overlay of plots from two different experiments gives the order in the reagent whose initial concentration is changed (power value in abscissa axis).

Table 2.6 Kinetic data (product concentration at different times) for experiments 1-4 (Table 2.5).

Experiment	Time (min)	[Product] (M)
[Cat] = 0.006 M [ArI] = 0.1214 M [An] = 1.2143 M	15	0.0024
	30	0.0073
	45	0.0134
	75	0.0291
	90	0.0352
	105	0.0413
	120	0.0461
	135	0.0522
	150	0.0583
	165	0.0692
	180	0.0716
	195	0.0741
	225	0.0899
	240	0.0971
[Cat] = 0.003 M [ArI] = 0.1214 M [An] = 1.2143 M	30	0.0012
	60	0.0012
	90	0.0134
	120	0.0182
	150	0.0231
	180	0.0279
	210	0.0316
	240	0.0364
	270	0.0425
	300	0.0486
	330	0.0534
	360	0.0607
	390	0.0668
	420	0.0716
	450	0.0765
[Cat] = 0.006 M [ArI] = 0.2429 M [An] = 1.2143 M	30	0.0049
	60	0.0194
	90	0.0291
	120	0.0364
	150	0.0461
	180	0.0559
	210	0.0607
	240	0.0777
	270	0.0826

	300	0.0947
	330	0.1044
	360	0.1190
	390	0.1336
	420	0.1360
	450	0.1457
[Cat] = 0.006 M [ArI] = 0.1214 M [An] = 1.7586 M	15	0.0047
	30	0.0117
	45	0.0199
	75	0.0305
	90	0.0375
	105	0.0434
	120	0.0492
	135	0.0551
	150	0.0598
	165	0.0645
	180	0.0692
	195	0.0715
	225	0.0891

2.4.6 Data for X-Ray structure determinations

Crystals suitable for X-ray analyses were obtained by slow evaporation of the solvent of a solution of complex [Pd(bipy-6-O)(C_6F_5)($PhNH_2$)] (**5**) in CH_2Cl_2 at room temperature or a solution of complex [Pd(bipy-6-O)(C_6H_4-*p*-CF_3)(κ-N-aniline)] (**6**) in CH_2Cl_2 at -20 °C. In each case, the crystal was attached to a glass fiber and transferred to an Agilent Supernova diffractometer with an Atlas CCD area detector. Data collection was performed with Mo Kα radiation (0.71073 Å) at 298 K. Data integration and empirical absorption correction were carried out using the CrysAlisPro program package.[98] The structures were solved by direct methods and refined by full-matrix least squares against F^2 with SHELX,[99] using Olex2.[100] The non-hydrogen atoms were refined anisotropically and hydrogen atoms were constrained to ideal geometries and refined with fixed isotropic displacement parameters. Refinement proceeded smoothly to give the residuals shown in Table S5. Complex **6** crystallized with a water molecule, hydrogen-bonded to the pyridone oxygen (Figure 2.2). Both crystal structures have deposited in the CCDC database (CCDC-2165844 and CCDC-2165845).

[98] CrysAlisPro Software system, version 1.171.33.51, **2009**, Oxford Diffraction Ltd, Oxford, UK.
[99] Sheldrick, G. M. *Acta Cryst.* **2015**, *C71*, 3-8.
[100] Dolomanov, O. V.; Bourhis, L. J.; Gildea, R. J.; Howard J. A. K.; Puschmann, H. *J. Appl. Crystallogr.* **2009**, *42*, 339-341.

Table 2.7 Crystal data and structure refinement for complexes **5** and **6**.

	5	**6**
Empirical formula	$C_{22}H_{14}N_3OF_5Pd$	$C_{23}H_{20}N_3O_2F_3Pd$
Formula weight	537.76	515.80
Temperature/K	298	298
Crystal system	triclinic	triclinic
Space group	P-1	P-1
a/Å	7.6417(8)	7.0887(4)
b/Å	10.5945(9)	11.1373(7)
c/Å	12.9337(13)	14.2923(8)
α/°	94.254(8)	86.703(5)
β/°	90.812(9)	83.477(5)
γ/°	103.361(8)	82.420(5)
Volume/$Å^3$	1015.43(17)	1110.23(11)
Z	2	2
$\rho_{calc}g/cm^3$	1.759	1.543
μ/mm^{-1}	0.979	0.879
F(000)	532.0	516.0
Crystal size/mm^3	0.435 × 0.247 × 0.063	0.282 × 0.197 × 0.154
Radiation	MoKα (λ = 0.71073)	MoKα (λ = 0.71073)
2Θ range for data collection/°	6.692 to 58.998	6.694 to 58.93
Index ranges	$-10 \le h \le 9$, $-10 \le k \le 14$, $-17 \le l \le 17$	$-7 \le h \le 9$, $-11 \le k \le 14$, $-19 \le l \le 18$
Reflections collected	7073	8624
Independent reflections	4621 [R_{int} = 0.0304, R_{sigma} = 0.0690]	5189 [R_{int} = 0.0287, R_{sigma} = 0.0579]
Data/restraints/parameters	4621/0/289	5189/0/292
Goodness-of-fit on F^2	1.053	1.063
Final R indexes [I>=2σ (I)]	R_1 = 0.0454, wR_2 = 0.0750	R_1 = 0.0463, wR_2 = 0.0956
Final R indexes [all data]	R_1 = 0.0753, wR_2 = 0.0899	R_1 = 0.0698, wR_2 = 0.1133
Largest diff. peak/hole / e $Å^{-3}$	0.76/-0.59	0.76/-0.68

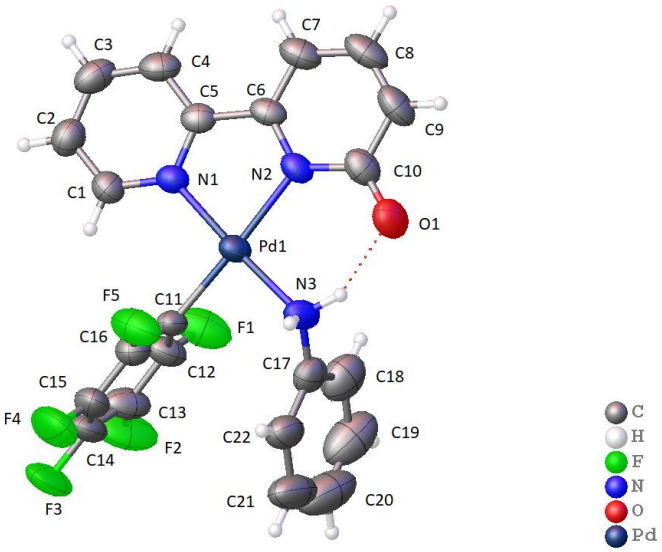

Figure 2.17. X-ray molecular structure of **5** (ORTEP 40 % probability ellipsoids).

Table 2.8. Selected bond lengths for complex **16.** Numbering scheme in Figure 2.17.

Bond	**d (Å)**
Pd-N_1	2.015
Pd-N_2	2.077
Pd-N_3	2.059
Pd-C_{11}	2.006
N_3-C_{17}	1.411
C_{10}-O_1	1.264

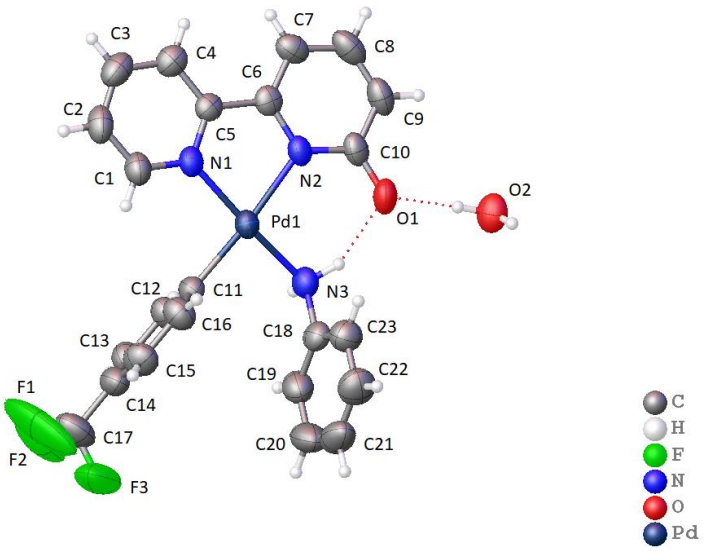

Figure 2.18. X-ray molecular structure of **6** (ORTEP 40 % probability ellipsoids).

Table 2.9. Selected bond lengths for complex **6.** Numbering scheme in Figure 2.18.

Bond	**d (Å)**
Pd-N_1	2.034
Pd-N_2	2.117
Pd-N_3	2.064
Pd-C_{11}	1.993
N_3-C_{18}	1.445
C_{10}-O_1	1.284

2.4.7 Computational details

Preliminary DFT calculations using the M06 functional and the methods described below on the simple models were carried out at the UVa. Calculations on the extended models, benchmarking and the final reaction profiles were calculated by Prof. Agustí Lledós at the UAB.

Computational methods

Geometry optimizations and thermochemical corrections: Density Functional Theory (DFT) calculations

Exploration of the potential energy surface, with location of minima and transition states has been carried out using the Gaussian16 software[101] at DFT level of theory with the M06 functional.[102] Basis set 1 (BS1) was employed in the optimizations, consisting of the 6-31+G(d) basis set for C, O, N, F and H,[103] and LANL2TZ(f) basis set for Pd and Cs[104] with the corresponding Hay-Wadt effective core potential (ECP).[105] All structure optimizations were carried out in solvent phase with no symmetry restrictions. Solvent effects have been considered in all the optimizations through a cluster/continuum solvation model,[106] that includes the continuum model SMD[107] for the experimental solvent, *N*, *N*-dimethylacetamide (DMA, ε = 37.781 at 25 ºC), and a few (4) explicit DMA molecules. For each structure several conformational isomers, which differ in the

[101] Gaussian 16, Revision C.01, Frisch, M. J.; Trucks, G. W.; Schlegel, H. B.; Scuseria, G. E.; Robb, M. A.; Cheeseman, J. R.; Scalmani, G.; Barone, V.; Petersson, G. A.; Nakatsuji, H.; Li, X.; Caricato, M.; Marenich, A. V.; Bloino, J.; Janesko, B. G.; Gomperts, R.; Mennucci, B.; Hratchian, H. P.; Ortiz, J. V.; Izmaylov, A. F.; Sonnenberg, J. L.; Williams-Young, D.; Ding, F.; Lipparini, F.; Egidi, F.; Goings, J.; Peng, B.; Petrone, A.; Henderson, T.; Ranasinghe, D.; Zakrzewski, V. G.; Gao, J.; Rega, N.; Zheng, G.; Liang, W.; Hada, M.; Ehara, M.; Toyota, K.; Fukuda, R.; Hasegawa, J.; Ishida, M.; Nakajima, T.; Honda, Y.; Kitao, O.; Nakai, H.; Vreven, T.; Throssell, K.; Montgomery, J. A., Jr.; Peralta, J. E.; Ogliaro, F.; Bearpark, M. J.; Heyd, J. J.; Brothers, E. N.; Kudin, K. N.; Staroverov, V. N.; Keith, T. A.; Kobayashi, R.; Normand, J.; Raghavachari, K.; Rendell, A. P.; Burant, J. C.; Iyengar, S. S.; Tomasi, J.; Cossi, M.; Millam, J. M.; Klene, M.; Adamo, C.; Cammi, R.; Ochterski, J. W.; Martin, R. L.; Morokuma, K.; Farkas, O.; Foresman, J. B.; Fox, D. J. Gaussian, Inc., Wallingford CT, **2016**.

[102] (a) Zhao, Y.; Truhlar, D. G. J. *Chem. Phys.* **2006**, *125*, 194101-194118. (b) Zhao, Y.; Truhlar, D. G. *Theor. Chem. Acc.* **2006**, *120*, 215-241.

[103] (a) Francl, M. M; Petro, W. J.; Hehre, W. J.; Binkley, J. S.; Gordon, M. S.; DeFrees, D. J.; Pople, J. A. *J. Chem. Phys.* **1982**, *77*, 3654- 3665. (b) Clark, T.; Chandrasekhar, J.; Schleyer, P. V. R. J. *J. Comput. Chem.* **1983**, *4*, 294-301.

[104] (a) Ehlers, A. W.; Böhme, M.; Dapprich, S.; Gobbi, A.; Höllwarth, A.; Jonas, V.; Köhler, K. F.; Stegmann, R.; Veldkamp, A.; Frenking, G. *Chem. Phys. Lett.* **1993,** *208*, 111-114. (b) Roy, L. E.; Hay, P. J.; Martin, R. L. J. *J. Chem. Theory Comput.* **2008**, *4*, 1029-1031.

[105] Hay, P. J.; Wadt, W. R. *J. Chem. Phys.* **1985**, *82*, 270-283.

[106] Norjmaa, G.; Ujaque, G.; Lledós. *Top. Catal.* **2022**, *65*, 118-140.

[107] Marenich, A. V.; Cramer, C. J.; Truhlar, D. G. *J. Phys. Chem. B* **2009**, *113*, 6378-6396.

positions of the cesium and carbonate ions, as well as of DMA solvent molecules, were computed. The lowest energy isomers are collected in the text.

Vibrational frequency calculations were performed for all the optimized geometries to characterize the stationary points as either minima (without imaginary frequencies) or transition states (with one imaginary frequency). Connectivity of the transition state structures was confirmed by relaxing the transition state geometry towards both the reactant and the product. Thermal and entropic corrections were calculated at 403.15 K (the experimental temperature) from the unscaled harmonic vibrational frequencies at this level of theory.

Single point DLPNO-CCSD(T) energy calculations

To obtain accurate electronic energies, single point calculations were performed on all the M06 optimized structures with the domain based local pair natural orbital coupledcluster ((DLPNO-CCSD(T)) method[108] as implemented in ORCA package.[109] The def2-TZVP basis set[110] and the RIJCOSX approximation[111] along with def2-ECP for Pd and Cs[112] were used in all single point calculations.

Gibbs energies in solution

All the energies reported are Gibbs energies in solution at 403.15 K. They were calculated by combining the electronic energy computed by means of single point DLPNO-CCSD(T) electronic energy calculations ($E_{el/gas}^{DLPNO-CCSD(T)/SP}$) with the thermal and entropic corrections evaluated at the geometry optimization level of theory (M06) ((G-E)$^{M06/opt}$) and Gibbs energies of solvation (ΔG_{solv}), computed as the energy difference between the single point energy calculated at M06 level of theory with and without the SMD continuum model ($E_{el/solv}^{M06} - E_{el/gas}^{M06}$). A correction of 2.56 kcal mol^{-1} ($\Delta G^{0\rightarrow *}$) was applied to all Gibbs energy values to change the standard state from the gas

[108] (a) Riplinger, C.; Neese, F. *J. Chem. Phys.* **2013**, *138*, 034106. (b) Riplinger, C.; Sandhoefer, B.; Hansen, A.; Neese, F. *J. Chem. Phys.* **2013**, *139*, 134101. (c) Riplinger, C.; Pinski, P.; Becker, U.; Valeev, E. F.; Neese, F.. *J. Chem. Phys.* **2016**, 144, 024109.
[109] a) Neese, F. WIREs Comput. Mol. Sci. 2012, 273-78. (b) Neese, F. WIREs Comput. Mol. Sci. 2018, 8, e1327.
[110] (a) Schäfer, A.; Horn, H.; Ahlrichs, R. *J. Chem. Phys.* **1992**, *97*, 2571-2577. (b) Weigend, F.; Ahlrichs, R. *Phys. Chem. Chem. Phys.* **2005**, *7*, 3297-3305. (c) Weigend, F. *Phys. Chem. Chem. Phys.* **2006**, *8*, 1057-1065.
[111] Neese, F.; Wennmohs, F.; Hansen, A.; Becker, U. *Chem. Phys.* **2009**, *356*, 98-109.
[112] (a) Andrae, D.; Häussermann, U.; Dolg, M.; Stoll, H.; Preuss, H. *Theoret. Chim. Acta* **1990**, *77*, 123-141. (b) Leininger, T.; Nicklass, A.; Kuechle, W.; Stoll, H.; Dolg, M.; Bergner, A. *Chem. Phys. Lett.* **1996**, *255*, 274-280.

phase (1 atm) to solution (1M) at 430.15 K.[113] In this way, the Gibbs energy in DMA solution for each species is computed as:

$$G_{sol} = E_{el/gas}^{DLPNO-CCSD(T)/SP} + (G - E_{el})^{M06/opt} + (E_{el/solv}^{M06} - E_{el/gas}^{M06}) + \Delta G^{0\rightarrow *}$$

3D chemical structures were generated using CYLview.[114]

Benchmarking of the chemical and computational models

Initially, single point calculations were performed using the functional employed in the optimizations (M06), adding long-range dispersion effects (M06-D3) and an extended basis set (BS2), considering the simple model commonly employed in this kind of studies (the palladium ion and its ligands: complex **6**). DLPNO-CCSD(T) calculations were used as a benchmark. Table 2.10 collects the Gibbs energy barriers obtained for the two steps of the reaction: C–H bond activation and C–C reductive elimination, at different levels of calculation. Optimized geometries, obtained with M06/BS1 were used in the single point calculations.

Table 2.10. Gibbs energy barriers, using different computational methods, for the C–H bond activation and C–C reductive elimination steps using a simple model, not taking into account neither carbonate salt nor explicit solvent molecules.[a]

	M06/BS1	**M06-D3/BS2**	**DLPNO-CCSD(T)/BS2**
		C-H Bond Activation step	
ortho	27.1	26.3	28.8
meta	32.4	30.9	32.2
para	27.9	27.0	29.3
		C-C Reductive Elimination step	
ortho	27.6	27.5	36.2
meta	26.9	26.5	34.7
para	26.3	26.2	33.6

[a]Energies, in kcal mol^{-1}, are given taking complex **6** as reference (0.0 kcal mol^{-1}).

The spectroscopic data of the identified species are given below.

[113] Bryantsev, V. S.; Diallo, M. S.; Goddard III, W. A. Calculation of Solvation Free Energies of Charged Solutes Using Mixed Cluster/Continuum Models. *J. Phys. Chem. B* **2008**, *112*, 9709-9719.

[114] Legault, C. Y. CYLview20; Université de Sherbrooke, **2020**; http://www.cylview.org

These results reveal that, although M06 barriers for the C–H bond activation step are only a little lower than those for DLPNO-CCSD(T) (about 2 kcal mol^{-1}), the energies of the reductive elimination step show a marked deviation (about 8 kcal mol^{-1}). From these results DLPNO-CCSD(T) was chosen as the method at choice to estimate accurate energies.

Another important feature of the reaction is the prevalence of the C–C coupling over the Buchwald-Hartwig C–N coupling. To benchmark the chemical model to be included in the calculations we scrutinized how this model affects the relative barriers of the C–H cleavage and C–N coupling steps. To do that, complexity was introduced in the model sequentially. Four models were checked. Model 1 is the simplest model: deprotonated complex **6** (**6NH**), adding a cesium cation to make a neutral system. In model 2 a [Cs+,HCO3-] ion pair was also added, complemented with two explicit DMA molecules in model 3 to solvate the cesium cations, and four explicit DMA molecules in model 4. 3D structures of all the transition states and their relative DLPNO-CCSD(T) Gibbs energies are depicted in Figure 2.19. The C–H bond cleavage *vs.* C–N coupling competition is notably influenced by the model chosen. The transition state for the C–N coupling moves from being 5.2 kcal mol^{-1} lower than the C–H cleavage with model 1 to 2.0 kcal mol^{-1} above it with model 4. Indeed, model 4, consisting of complex **6**, a carbonate anion and two cesium cations and four DMA molecules is the simplest one able to reproduce the experimental results and it has been adopted in most of the calculations collected in the paper.

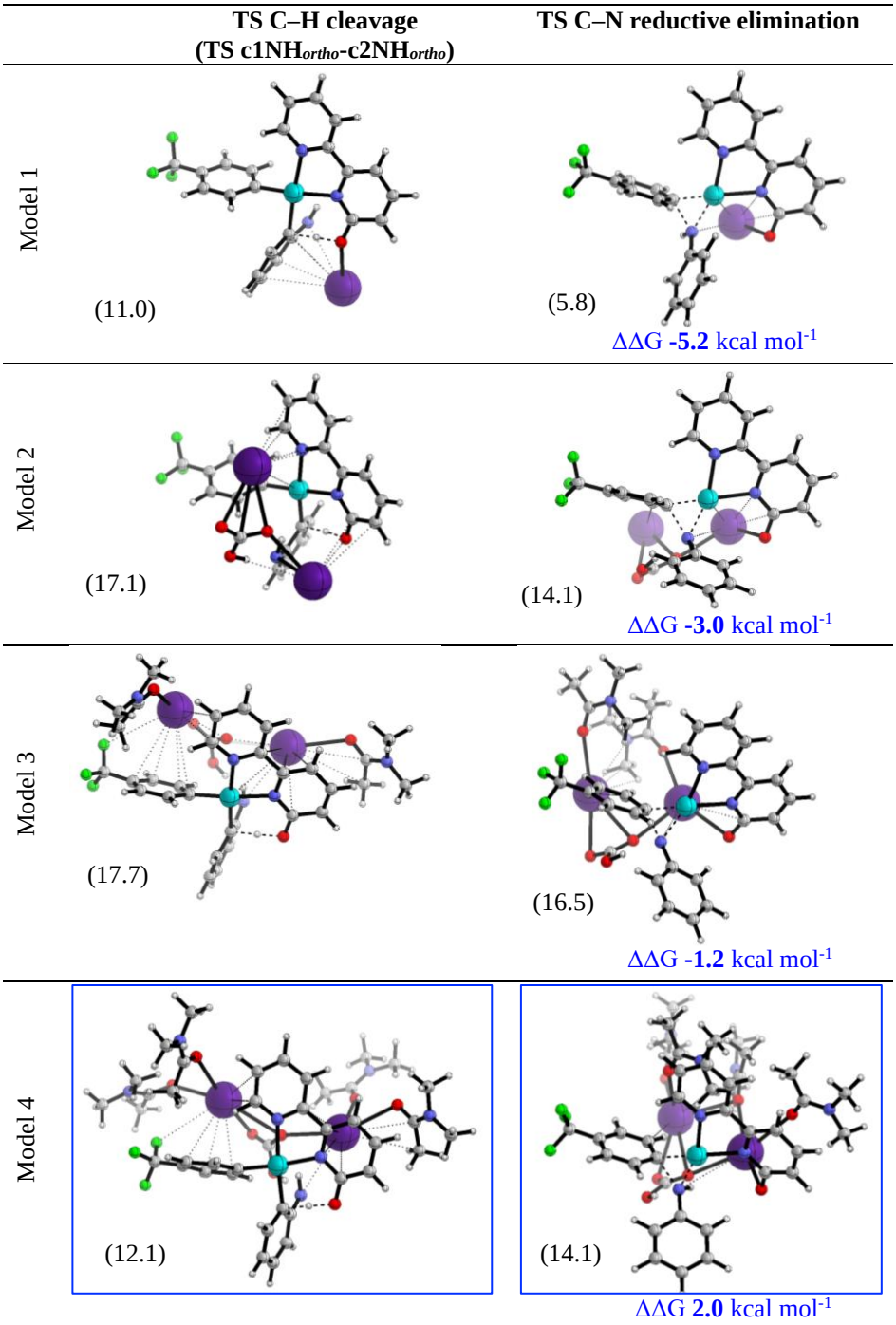

Figure 2.19. Optimized structures for the transition states of the competing C–H bond cleavage (**TS c1NH$_{ortho}$-c2NH$_{ortho}$**) and the C–N reductive elimination in an amido palladium complex **6NH** using different chemical models. Relative Gibbs energies of both transition states (ΔΔG) are also shown in blue (kcal mol^{-1}). A negative value implies a lower TS for C–N reductive elimination than for the *ortho* C–H cleavage. Only model 4 agrees with the experimental evidences. In parenthesis Gibbs activation barriers (kcal mol^{-1}, taking **c1**$_{ortho}$ as reference).

Microkinetic modeling

A simple kinetic simulation of the reaction profile in Figure 2.8 was carried out using the COPASI software. [115]

The kinetic model is given below. Experimental concentrations were used. Equilibrium and rate constants for the kinetic model were calculated from the calculated energy differences between intermediates (ΔG) or intermediates and transition states ($\Delta G^{\ddagger}$) according to the following equations:

Equilibrium constants: $K = e^{-\Delta G/RT}$ Rate constants: $k = (k_B T/h)e^{-\Delta G^{\ddagger}/RT}$

This model reproduces the experimental conversions collected.

Kinetic model and rate constants.

a) Equilibrium **6-c1**$_{ortho}$:

6 $\rightleftharpoons$ **c1**$_{ortho}$

$k_1 = 0.13\ s^{-1}$, $k_{-1} = 5.7x10^{8}\ s^{-1}$ $K_1 = 2.3x10^{-10}$, $\Delta G = 17.7$ kcal mol^{-1}

b) Deprotonation:

c1$_{ortho}$ + Cs_2CO_3 $\rightleftharpoons$ **c1NH**$_{ortho}$ + $CsHCO_3$

$k_2 = 6.1x10^{11}\ M^{-1}\ s^{-1}$, $k_{-2} = 2.5x10^{11}\ M^{-1}\ s^{-1}$; $K_2 = 2.4$, $\Delta G = -0.7$ kcal mol^{-1}

c) C–H cleavage:

c1NH$_{ortho}$ $\rightleftharpoons$ **c2NH**$_{ortho}$

$k_3 = 9.7x10^{5}\ s^{-1}$, $k_{-3} = 4.8x10^{11}\ s^{-1}$; $K_3 = 2x10^{-6}$, $\Delta G = 10.5$ kcal mol^{-1}

d) Fast proton transfer reactions:

c2NH$_{ortho}$ + $CsHCO_3$ $\rightleftharpoons$ **c2**$_{ortho}$ + Cs_2CO_3

$k_4 = 8.4x10^{12}\ M^{-1}\ s^{-1}$, $k_{-4} = 5.6x10^{8}\ M^{-1}\ s^{-1}$ $K_4 = 1.5x10^{4}$, $\Delta G = -7.7$ kcal mol^{-1}

c2$_{ortho}$ + Cs_2CO_3 $\rightleftharpoons$ **c2b**$_{ortho}$ + $CsHCO_3$

$k_5 = 8.4x10^{12}\ M^{-1}\ s^{-1}$, $k_{-5} = 1.1x10^{3}\ M^{-1}\ s^{-1}$ $K_5 = 7.6x10^{9}$, $\Delta G = -18.2$ kcal mol^{-1}

e) Reductive elimination:

c2b$_{ortho}$ $\rightleftharpoons$ **c3**$_{ortho}$

$k_6 = 40\ s^{-1}$, $k_{-6} = 1.2x10^{-4}\ s^{-1}$; $K_6 = 3.3x10^{5}$, $\Delta G = -10.2$ kcal mol^{-1}

f) Arylhalide coordination:

c3$_{ortho}$ + ArI $\rightleftharpoons$ **c4** + ArAnil

---

[115] COmplex PAthway Simulator (COPASI) is an easily available free software: Hoops, S.; Sahle, S.; Gauges, R.; Lee, C.; Pahle, J.; Simus, N.; Singhal, M; Xu, L.; Mendes, P.; Kummer, U. COPASI–A COmplex PAthway SImulator *Bioinformatics*, **2006**, *22*, 3067-3074.

$k_7 = 8.4x10^{12}\ M^{-1}\ s^{-1}$, $k_{-7} = 6x10^{7}\ M^{-1}\ s^{-1}$; $K_7 = 1.4x10^{5}$, $\Delta G = -9.5$ kcal mol^{-1}

g) Oxidative addition:

c4 + Anil → **c1**$_{ortho}$ + CsI $k_8 = 2.2x10^{5}\ M^{-1}\ s^{-1}$

Initial concentrations:

$[\mathbf{6}]_0 = 0.006$ M

$[ArI]_0 = 0.12$ M

$[Anil]_0 = 1.2$ M

$[Cs_2CO_3]_0 = 0.24$ M

$[\mathbf{c1}_{otho}]_0 = [\mathbf{c1NH}_{otho}]_0 = [\mathbf{c2NH}_{otho}]_0 = [\mathbf{c2}_{otho}]_0 = [\mathbf{c2}_{otho}\mathbf{b}]_0 = [\mathbf{c3}_{otho}]_0 = [\mathbf{c4}]_0 = 0$

Figure 2.20 shows the evolution of the concentration of the product *vs.* time and reproduces the conversions observed experimentally (see Table 2.6). As expected from the very small equilibrium constant (**6-c1**$_{ortho}$), complex **6** is the most abundant species throughout the reaction and only a small fraction of palladium is in the actual catalytic cycle (almost 0 in the graph).

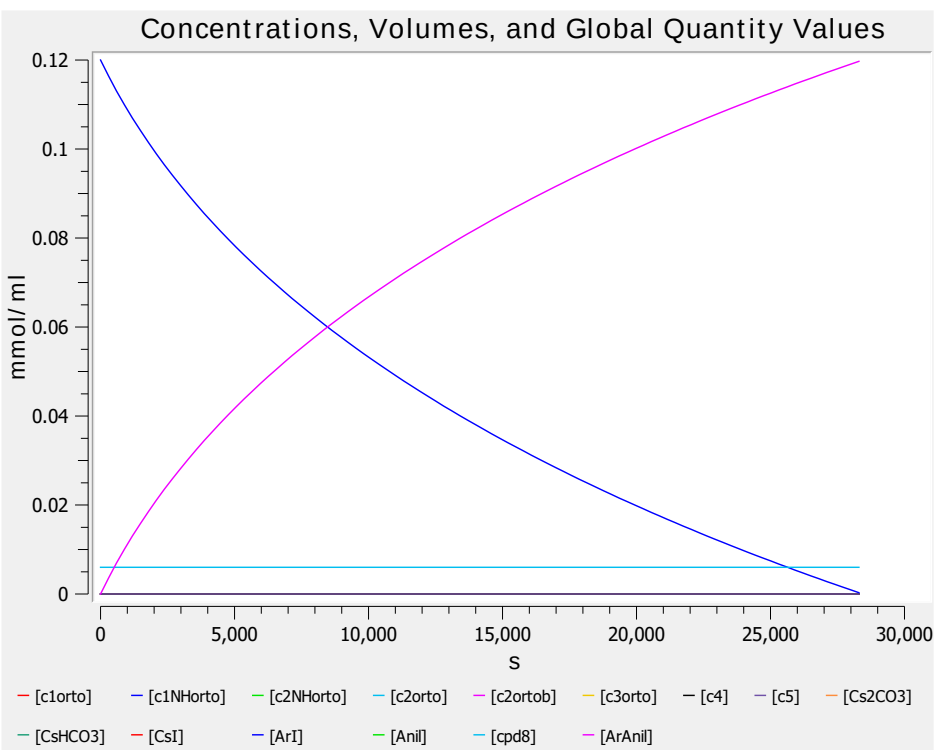

Figure 2.20. Evolution of concentration (M) over time (s) for the reaction in Equation 2.6. Experimental product formation: 0.072 M of product after 3 h (10800 s). The concentrations of aniline and carbonates have been omitted for clarity.

Probing the intermediacy of Pd(IV) species.

The most stable plausible Pd(IV) intermediate that could be formed in the reaction was calculated. It is [Pd(bipy-6-O)(*o*-$NH_2C_6H_4$)(*p*-$CF_3C_6H_4$)I($PhNH_2$)] with a deprotonated ligand and a coordinated aniline, i.e. the combination of the most donor ligands. The Gibbs energy barrier for the oxidative addition of *p*-$CF_3C_6H_4I$ on the preceding Pd(II) complex is 46.7 kcal mol^{-1} (Figure 2.21) much higher than those found for the Pd(0)/Pd(II) mechanism in Figure 2.8. This makes a route where the C–H activation occurs first followed by an oxidative addition of the aryl halide to give a Pd(IV) species less probable in the arylation of anilines.

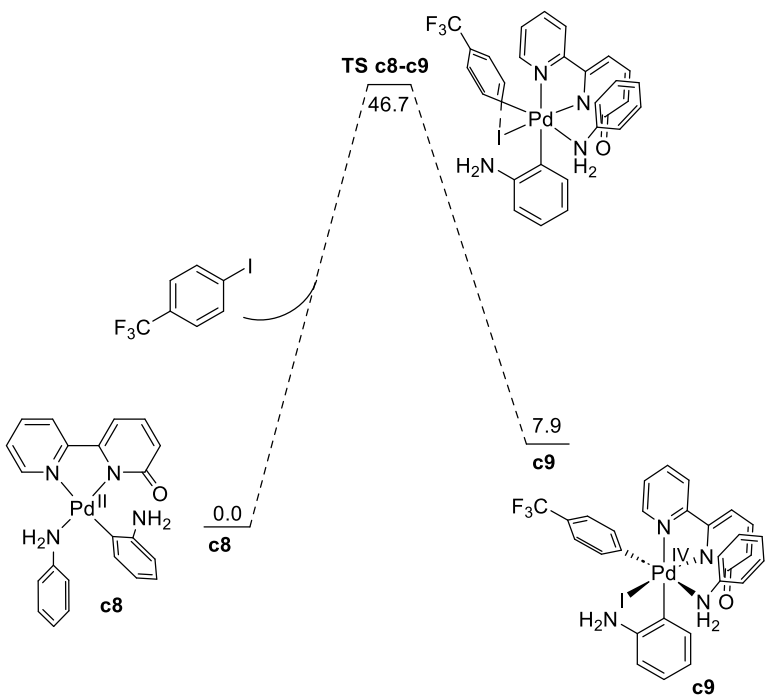

Figure 2.21. Gibbs energy profile for the oxidative addition of the aryl iodide to a Pd(II) complex to give a Pd(II) derivative. Energies in kcal mol^{-1}.

Chapter 3

3 Palladium-Catalysed Direct C–H Arylation of Simple Arenes Enabled by a Dual Ligand System

3.1 INTRODUCTION

The concept of dual ligand catalysis appeared to describe reactions where two complementary ligands are used instead of developing and synthesizing a complex ligand with specific properties. The combination of two known ligands, each of them with a specific role in the reaction mechanism, results in the acceleration of the full reaction. In the last decade, some examples have been reported in C–H functionalization reactions. One of the first articles using this strategy in palladium catalysis was the C–H olefination of arenes developed by van Gemmeren *et al.* in 2018.[116] They used a MPAA (*N*-acetyl glycine) as cooperating ligand in the C–H activation step *via* a CMD mechanism and a pyridine derivative ligand to achieve good reactivity using simple arenes as limiting reagents. (Figure 3.1). The same group has extended this approach to other reactions such

[116] a) Chen, H.; Wedi, P.; Meyer, T.; Tavakoli, G.; Gemmeren, M. v. *Angew. Chem. Int. Ed.* **2018**, *57*, 2497-2501. b) Wedi, P.; Farizyan, M.; Bergander, K.; Mgck-Lichtenfeld, C.; Gemmeren, M. V. *Angew. Chem. Int. Ed*. **2021**, *60*, 15641-15649.

as the cyanation,[117] and alkynylation,[118] of simple arenes.[119] The olefination of arenes using a combination of a MPAA and a thioether as ligands has also been reported.[120]

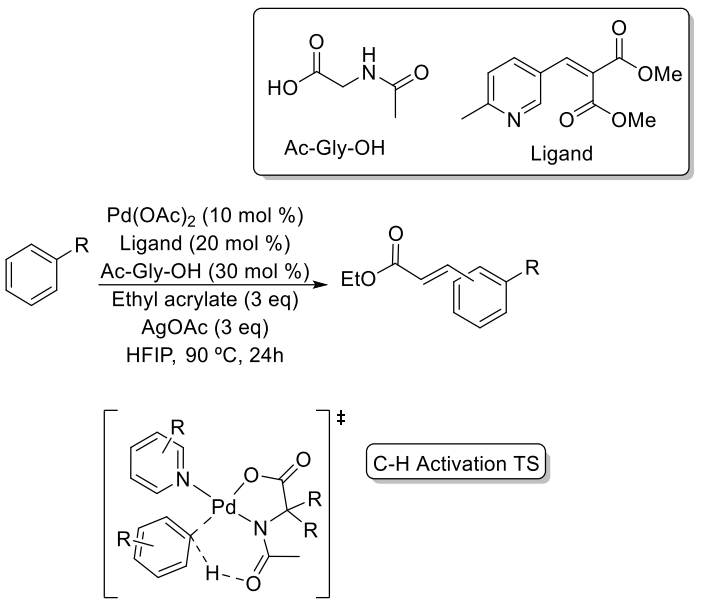

Figure 3.1. Reported conditions for the C–H olefination of arenes via a dual ligand system and proposed TS for the C–H activation step.

The use of two pyridine derivatives as ligands together with norbornene has been also studied in direct arylation of arenes in the Yu's group (Equation 3.1).[121] The norbornene is responsible of the regioselectivity due to its ability to insert in the Pd–C bond as commented in the general introduction. The role of the pyridine ligands is not clear, however they proposed it can promote other catalytic steps such as the oxidative addition.

[117] Chen, H.; Mondal, A.; Wedi, P.; Gemmeren, M. v. *ACS Catal.* **2019**, *9*, 1979-1984.
[118] Mondal, A.; Chen, H.; Flämig, L.; Wedi, P.; Gemmeren, M. v. *J. Am. Chem. Soc.* **2019**, *141*, 18662-18667.
[119] Kaltenberger, S.; Gemmeren, M. v. *Acc. Chem. Res.* **2023**, *56*, 2459-2472.
[120] Yin, B.; Fu, M.; Wang, L.; Liu, J.; Zhu, Q. *Chem. Commun.*, **2020**, *56*, 3293-3296.
[121] a) Liu, L.-Y.; Qiao, Y. X.; Yeung, K.-S.; Ewing, W. R.; Yu, Y.-Q. *J. Am. Chem. Soc.* **2019**, *141*, 14870-14877. b) Liu, L.-Y.; Qiao, J. X.; Yeung, K.-S. Ewing, W. R.; Yu, Y.-Q. *Angew. Chem. Int. Ed.*, **2020**, *53*, 13831-13835.

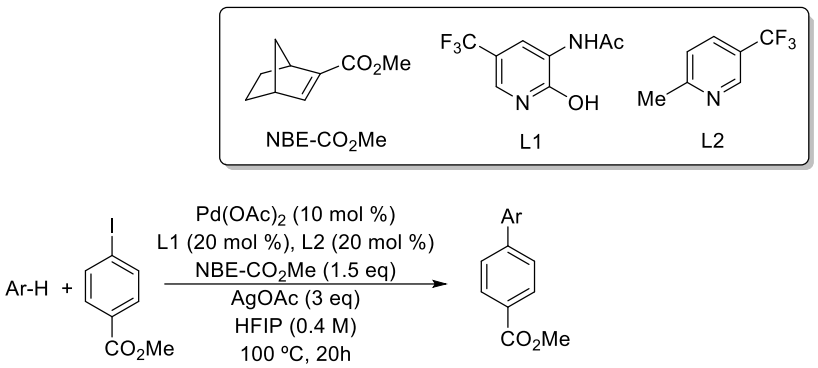

Equation 3.1.

Other examples of dual ligand chemistry are the use of MPAAs ligands along with pyridone-type ligands. Their accelerating effect has been proved in the olefination of ketone derivatives,[122] and in the chalcogenation of arenes.[123] In the last case, the C–H activation is proposed to be assisted by the MPAA ligand and the pyridone is forming hydrogen bonds while coordinated to palladium (Figure 3.2).

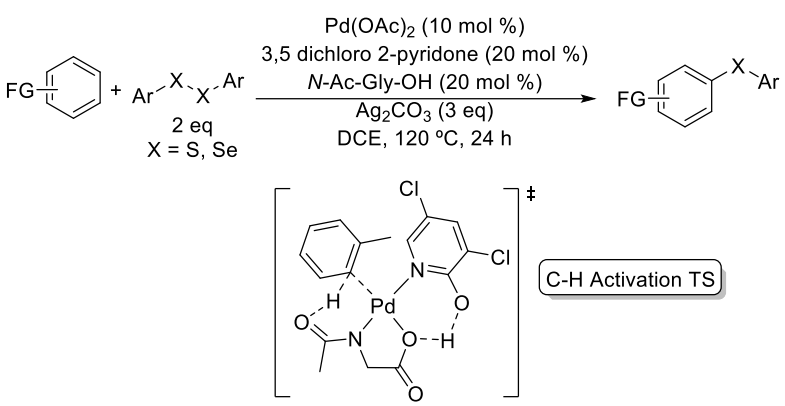

Figure 3.2. Reported conditions for the chalcogenation of arenes and proposed TS for the C–H activation step.

The olefination of pyridine has been published recently by Yu *et al.* using a bipyridone as cooperating ligand in the C–H cleavage step.[124] It is also considered as

[122] Park, H. S.; Fan, Z.; Zhu, R.-Y.; Yu, J.-Q. *Angew. Chem. Int. Ed.***, 2020**, *59*, 12853-12859.
[123] Sinha, S. K.; Panja, S.; Grover, J.; Hazra, P.S.; Pandit, S.; Bairagi, Y.; Zhang, X.; Maiti, D. *J. Am. Chem. Soc*. **2022**, *144*, 12032-12042.
[124] Meng, G.; Wang, Z.; Chan, H. S. S.; Chekshin, N.; Li, Z.; Wang, P.; Yu, J.-Q. *J. Am. Chem. Soc*. **2023**, *145*, 8198-8208.

dual ligand system due to the two functions of the pyridine substrate: in addition to be a reagent, it has an important role as coordinating ligand during the catalytic cycle.

De Vos *et al.* has developed the direct arylation of *N*-heterocyclic compounds assisted by 2-pyridone combined with a phosphine ligand, which allows to use a large variety of functional groups in the reagent scaffold (Equation 3.2).[125] Their rationale is to use an additional ligand to avoid coordination of the heterocyclic substrates to the catalyst by the heteroatom and therefore favouring the C–H activation. They confirm experimentally by analysis of the catalyst mixture by EXAFS the presence of species where both ligands are coordinated under the reaction conditions. In the same way, those reports which contain mechanistic studies on dual ligand systems propose the coordination of both ligands to the same palladium centre during the C–H activation step as shown in Figure 3.1 and Figure 3.2.

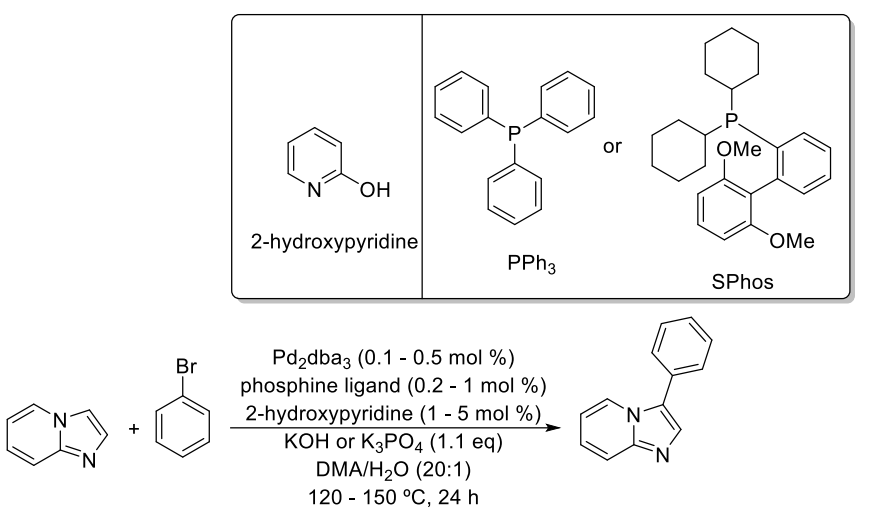

Equation 3.2.

Looking for milder reaction conditions in the functionalization of arenes with no-directing groups, this chapter describes a dual-ligand approach. The use of the bipy-6-OH ligand together with tricyclohexylphosphine allows the direct arylation of simple arenes at lower temperatures than those reported using only bipy-6-OH. Phosphines as ligands in cross-coupling processes are very common and useful, and how their features can improve reaction steps such as oxidative addition or reductive elimination has been

[125] a) Beckers, I.; Bugaev, A.; De Vos, D. *Chem. Sci*., **2023**, *14*, 1176-1183. b) Beckers, I.; De Vos, D. *iScience*, **2023**, *26*, 105790.

widely studied and it is well understood.[9, 126] Also, phosphines were one of the first type of ligands used in C–H activation reactions, in particular in direct arylation of arenes.[50, 127] Thus, the combination of a cooperative ligand that can favour the C–H activation and a phosphine which makes the product forming step easy is, in principle, a good choice. In addition, the studies that are described in this chapter show that this system is mechanistically different than the catalyst with just one ligand and a cooperative bimetallic mechanism as plausible reaction pathway.

The general catalytic cycle for direct arylation reactions has been described in the general introduction (Scheme 1.1, b) where all catalytic steps occur on a metal center. However, a few works in the literature describe a bimetallic mechanism and the cooperation between two different palladium species. A clear example is the mechanism described for the direct arylation of pyridine *N*-oxides reported by Hartwig *et al.*[128] They proved that the oxidative addition and reductive elimination steps occur on a palladium complex with a coordinated P^tBu_3. Nevertheless, the C–H activation step takes place in a palladium complex with a metalated phosphine ligand. The transmetallation between the two catalytic species leads to the palladium intermediate prior to the reductive elimination step that releases the coupling product (Scheme 3.1).

---

[126] a) Barder, T. E.; Walker, S. D.; Martinelli, J. R.; Buchwald, S. L. *J. Am. Chem. Soc.* **2005**, *127*, 4685-4696. b) Martin, R.; Buchwald, S. L. *Acc. Chem. Res.* **2008**, *41*, 1461-1473.

[127] a) Sun, H.-Y.; Gorelsky, S. I.; Stuart, D. R.; Campeau, L.-C.; Fagnou, K. *J. Org. Chem*. **2010**, *75*, 8180-8189. b) Liegault, B.; Petrov, I.; Gorelsky, S. I.; Fagnou, K. *J. Org. Chem*. **2010**, *75*, 1047-1060. c) Yamajala, K. D. B.; Patil, M.; Banerjee, S. *J. Org. Chem*. **2015**, *80*, 3003-3011. d) Yuen; O. Y; Charoensak, M.; So, C. M.; Kuhakarn C.; Kwong, F. Y. *Chem. Asian J.*, **2015**, *10*, 857-861. e) Ji, Y.; Plata, R. E.; Regens, C. S.; Hay, M.; Schmidt, M.; Razler, T.; Qiu, Y.; Geng, P.; Hsiao, Y.; Rosner, T.; Eastgate, M. D.; Blackmond, D. G. *J. Am. Chem. Soc*. **2015**, *137*, 13272-13281.

[128] a) Tan, Y.; Barrios-Landeros, F.; Hartwig, J. F. *J. Am. Chem. Soc*. **2012**, *134*, 3683-3686. b) Gorelsky, S. I. *Organometallics*, **2012**, *31*, 4631-4634.

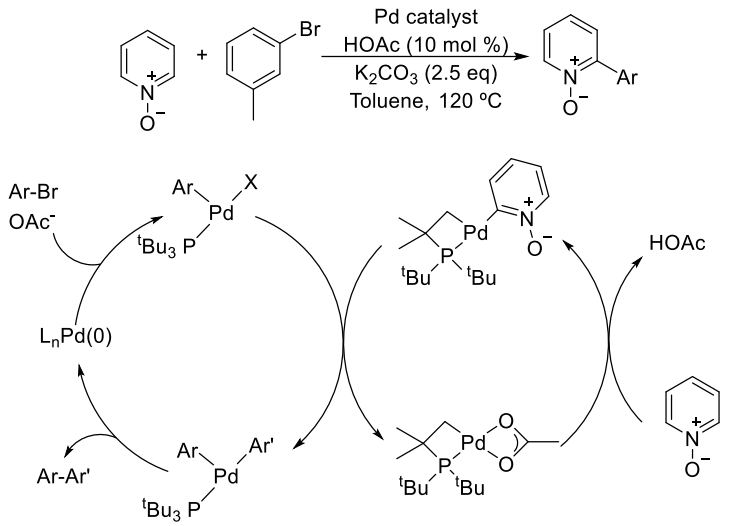

Scheme 3.1. Direct arylation of pyridine *N*-oxides *via* a bimetallic mechanism.

Stahl *et al.* reported in 2014 the first example of a second-order palladium dependence observed in an oxidative biaryl coupling (Scheme 3.2).[129] At high catalyst concentrations they found a first-order dependence on the catalyst and an elevated KIE value meaning that the turnover limiting step is the C–H activation. However, at lower catalyst concentrations a second-order on palladium was observed, proving a bimetallic mechanism and a turnover limiting transmetallation.

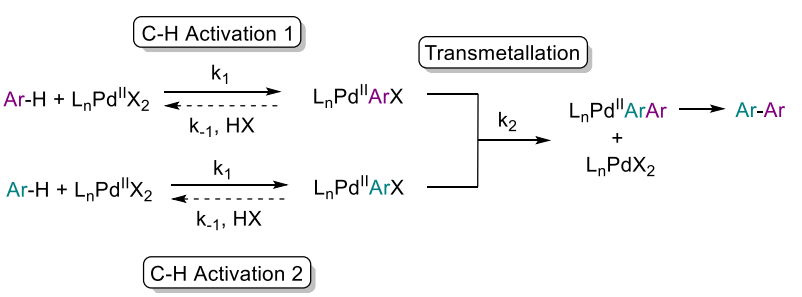

Scheme 3.2. Proposed bimetallic mechanism for the aerobic oxidative coupling of arenes.

Similar experiments were done in the direct arylation of arenes published by Hong *et al.*[130] In this case the two active species have different coordinated ligands. The oxidative addition and reductive elimination steps occur in the diimine palladium

[129] Wang, D.; Izawa, Y.; Stahl, S. S. *J. Am. Chem. Soc*. **2014**, *136*, 9914-9917.
[130] a) Kim, J.; Hong, S. H. *ACS Catal.* **2017**, *7*, 3336-3343. b) Kim, D.; Choi, G.; Kim, W.; Kim, D.; Kang, Y. K.; Hong, S. H. *Chem. Sci*., **2021**, *12*, 363-373.

complex and the C–H activation step is assisted by a pivalate molecule coordinated to the other metal centre (Scheme 3.3). In the same way as before, a second-order dependence was observed at low catalyst concentrations.

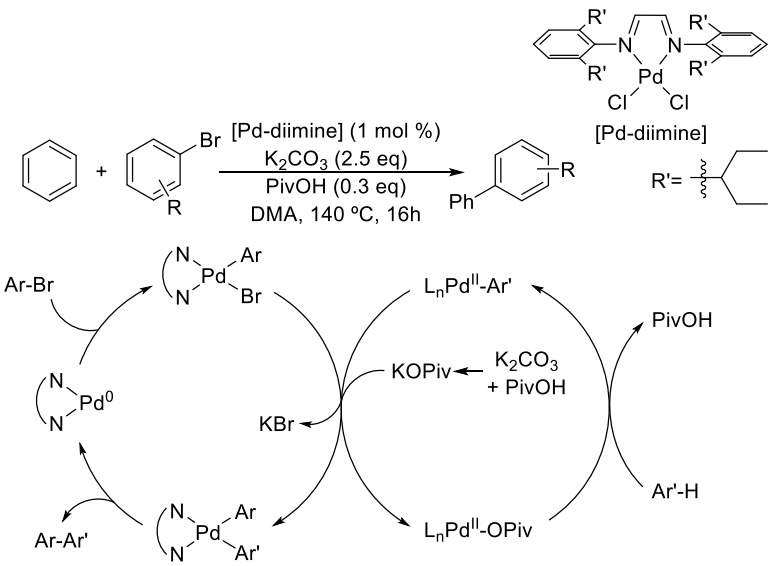

Scheme 3.3. Ligand promoted direct arylation of arenes *via* a cooperative bimetallic mechanism.

3.2 RESULTS AND DISCUSSION

3.2.1 C–H arylation of simple arenes.

The direct arylation of toluene has been studied in our research group before.[20] Using bipy-6-OH as cooperating ligand, the best reported reaction conditions require an aryl iodide as coupling partner, pinacolone as co-solvent and 130 ºC. Looking for milder conditions we decided to test the effect of adding a phosphine ligand in the reaction medium. Phosphines are known to stabilize palladium species and are able to decrease the energy barrier of elementary catalytic steps such as oxidative addition or reductive elimination, depending on their electronic and steric properties.

The coupling between toluene and *p*-$CF_3C_6H_4X$ (an aryl that allows the easy monitorization of the reaction by ^{19}F NMR) was chosen as model reaction. Toluene was used as solvent at 130 ºC and cesium carbonate as base (Equation 3.3).

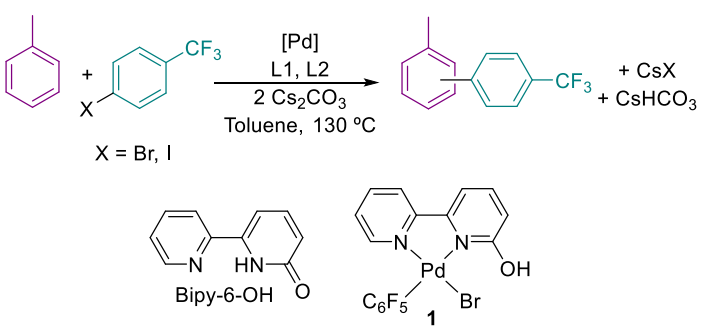

Equation 3.3.

The reaction described in the literature using bipy-6-OH as the only ligand and toluene as solvent produced a 91 % of the coupling product after 24 h for the iodo aryl (entry 1, Table 3.1). A mixture of bipy-6-OH and a phosphine ligand was then used. The reaction conditions chosen for the dual ligand system were 5 mol % of palladium salt, 2.5 mol % of bipy-6-OH (half of the quantity used in the reported reaction) and 5 mol % of phosphine. PCy_3 was tested first and the reaction is clearly accelerated with the ligand mixture and it is complete in 6 h (90% yield *vs*. 22 % in the absence of PCy_3, entries 1 and 2, Table 3.1). The corresponding and less expensive bromoaryl was also tried and a respectable 59 % of the coupling product was obtained after 6 h, faster than the reaction in absence of PCy_3 (16 % after 6 h, entries 3 and 4, Table 3.1). PPh_3, P^tBu_3 were also tested but PCy_3 is the phosphine that gave the best results (entries 4-6, Table 3.1). When

no bipy-6-OH was used, the reaction did not take place (entry 7, Table 3.1), proving that this cooperating ligand is necessary for the C–H activation of toluene. [Pd_2dba_3] or [$PdCl_2(NCMe)_2$] were used as palladium source and no better results were obtained than for $Pd(OAc)_2$ (entries 8 and 9, Table 3.1). The use of a preformed complex with the bipy-6-OH coordinated (**1**) gave similar results as the mixture $Pd(OAc)_2$+ligand (entry 10, Table 3.1). The amount of PCy_3 was modified showing that an excess did not make any difference, but a smaller amount of phosphine gave worse results (entries 11 and 12, Table 3.1). Finally, decreasing the temperature to 100 ºC slowed the reaction rate down and, even after 24 h, the reaction was not complete (entry 13, Table 3.1).

Table 3.1. Arylation of toluene with *p*-$CF_3C_6H_4Br$ using different catalysts according to Equation 3.3.[a]

Entry	[Pd] (mol %)	L1 (mol %)	L2 (mol %)	Crude yield, %, (Conv, %), 6 h[b]	Crude yield, %, (Conv, %), 24 h[b]
1[c, d]	$Pd(OAc)_2$ (5)	Bipy-6-OH (5)	-	20 (22)	91 (100)
2[d]	$Pd(OAc)_2$ (5)	Bipy-6-OH (2.5)	PCy_3 (5)	90 (100)	
3	$Pd(OAc)_2$ (5)	Bipy-6-OH (5)	-	16 (16)	75 (75)
4	$Pd(OAc)_2$ (5)	Bipy-6-OH (2.5)	PCy_3 (5)	59 (65)	90 (100)
5	$Pd(OAc)_2$ (5)	Bipy-6-OH (2.5)	PPh_3 (5)	5 (10)	35 (63)
6	$Pd(OAc)_2$ (5)	Bipy-6-OH (2.5)	P^tBu_3 (5)	14 (17)	31 (38)
7	$Pd(OAc)_2$ (5)	-	PCy_3 (10)	3 (6)	3 (7)
8	[Pd_2dba_3] (5)	Bipy-6-OH (2.5)	PCy_3 (5)	34 (88)	52 (100)
9	[$PdCl_2(NCMe)_2$] (5)	Bipy-6-OH (2.5)	PCy_3 (5)	13 (19)	36 (48)
10	$Pd(OAc)_2$ (2.5) **1** (2.5)	-	PCy_3 (5)	71 (87)	86 (100)
11	$Pd(OAc)_2$ (5)	Bipy-6-OH (2.5)	PCy_3 (7.5)	59 (72)	83 (100)
12	$Pd(OAc)_2$ (5)	Bipy-6-OH (2.5)	PCy_3 (2.5)	19 (22)	57 (68)
13[e]	$Pd(OAc)_2$ (5)	Bipy-6-OH (2.5)	PCy_3 (5)	25 (28)	48 (55)

[a]Reaction conditions: *p*-$CF_3C_6H_4Br$ (0.34 mmol), Cs_2CO_3 (0.68 mmol), toluene (3 mL). [b]Crude yields determined by ^{19}F NMR of the reaction mixture. The reduction or the arylbromide (ArH) and the homocoupling (Ar-Ar) are the observed byproducts. [c]Data from the literature. [d]*p*-$CF_3C_6H_4I$ as aryl halide. [e]At 100 ºC.

Since the yield obtained at 100 ºC was moderate after 24 h, we decided to try to improve it using a co-solvent. This strategy has been used before in the research group to accelerate the arylation of toluene, being pinacolone the best solvent. In the direct arylation of anilines DMA was used in a similar way (*Chapter 2*).

Adding DMA as co-solvent the reaction is complete after 90 min at 130 ºC and after 3 h at 100 ºC (entries 1 and 2, Table 3.2), much faster than before (Table 3.1) so the accelerating effect of the DMA is clear. By decreasing the temperature to 90 ºC, excellent yields are obtained after 24 h, but at 80 ºC poor yields were observed (entries 3 and 4,Table 3.2). When DMA is added as solvent and a smaller excess of toluene is used (about ten-fold, entry 5, Table 3.2), the yield decreased dramatically and the amount of byproducts was higher than in entry 2. The use of pinacolone did not give any better results (entries 6 and 7, Table 3.2).

Table 3.2. Co-solvent and temperature screening in the direct arylation of toluene.[a]

Entry	Co-solvent[b]	Toluene:ArBr ratio [c]	T (°C)	Crude yield, %, (Conv, %), 6 h[d]	Crude yield, %, (Conv, %), 24 h[d]
1	DMA	41:1	130	88 (100)[e]	
2	DMA	41:1	100	90 (94)[f]	
3	DMA	41:1	90	42 (44)	96 (100)
4	DMA	41:1	80	15 (15)	33 (25)
5	DMA	10:1	100	0 (0)	29 (40)
6	Pinacolone	41:1	100	7 (56)	19 (88)
7	Pinacolone	10:1	100	13 (62)	23 (94)

[a]Reaction conditions: *p*-$CF_3C_6H_4Br$ (0.34 mmol), $Pd(OAc)_2$ (5 mol %), bipy-6-OH (2.5 mol %), PCy_3 (5 mol %), Cs_2CO_3 (0.68 mmol). [b]Toluene (1.5 mL), co-colvent (1.5 mL): entries 1-4 and 6. Co-solvent (3 mL): entries 5 and 7. [d]Crude yields determined by ^{19}F NMR of the reaction mixture. The reduction or the arylbromide (ArH) and the homocoupling (Ar-Ar) are the observed byproducts. [e]After 90 min. [f]After 3 h.

With the best conditions of solvent and temperature (DMA as co-solvent and 100 ºC, Equation 3.4) several ligands and complexes were tried. The absence of PCy_3 or bipy-6-OH results in no evolution of the reaction, both ligands are necessary under those conditions (entries 1-3, Table 3.3). Only byproducts are observed when bipy is used as ligand, so the ketone moiety in the cooperating ligand is clearly necessary for the success of the reaction (entry 4, Table 3.3). The use of bipy-4-OH, a ligand with the same electronic properties as bipy-6-OH but with the ketone group in a position far from the metal and not able to assist in the C–H cleavage, did not give any desired product (entry 5, Table 3.3). Slight modifications in the bipy scaffold resulted in the loss of the activity (entries 6 and 7, Table 3.3). MPAA-type ligands and 2-pyridone were also tried and gave

no coupling product (entries 8-10, Table 3.3). Different phosphines were tested again under those reaction conditions: PPh_3 and P^tBu_3 let to moderate or low yields (entries 11 and 12, Table 3.3); however XPhos produced similar results to PCy_3 but in longer reaction times (6 h *vs.* 3 h, entries 1 and 13, Table 3.3). In addition, tricyclohexylphosphonium tetrafluoroborate salt, more air-stable than PCy_3 and easily deprotonated under the reaction conditions, gave also excellent yields (entries 14, Table 3.3). Different ligand concentrations were also tested: a 5 mol % of bipy-6-OH has almost no effect; however, increasing or decreasing the molar ratio of PCy_3 results in lower rates (entries 15-18, Table 3.3).

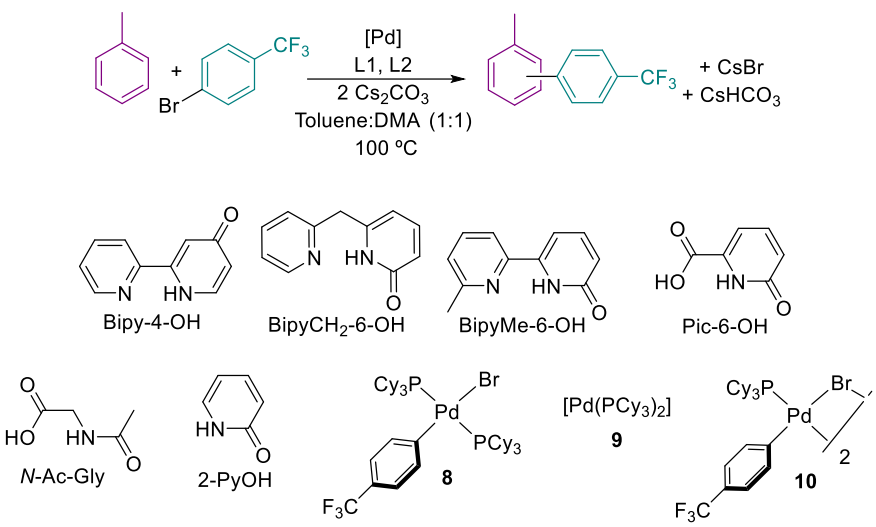

Equation 3.4.

Table 3.3. Catalyst screening at 100 ºC and using DMA as co-solvent.[a]

Entry	[Pd] (mol %)	L1 (mol %)	L2 (mol %)	Crude yield, %, (Conv, %), 6h[b]	Crude yield, %, (Conv, %), 24h[b]
1	$Pd(OAc)_2$ (5)	Bipy-6-OH (2.5)	PCy_3 (5)	90 (94)[c]	
2	$Pd(OAc)_2$ (5)	Bipy-6-OH (5)	-	0 (100)	
3	$Pd(OAc)_2$ (5)	-	PCy_3 (10)	0 (100)	
4	$Pd(OAc)_2$ (5)	Bipy (2.5)	PCy_3 (5)	0 (22)	0 (100)
5	$Pd(OAc)_2$ (5)	Bipy-4-OH (2.5)	PCy_3 (5)	0 (0)	0 (100)
6	$Pd(OAc)_2$ (5)	BipyCH_2-6-OH (2.5)	PCy_3 (5)	3 (10)	8 (16)
7	$Pd(OAc)_2$ (5)	BipyMe-6-OH (2.5)	PCy_3 (5)	0 (4)	3 (14)
8	$Pd(OAc)_2$ (5)	Pic-6-OH (2.5)	PCy_3 (5)	1 (7)	3 (13)
9	$Pd(OAc)_2$ (5)	*N*-Ac-Gly (2.5)	PCy_3 (5)	0 (5)	0 (10)
10	$Pd(OAc)_2$ (5)	2-PyOH (2.5)	PCy_3 (5)	3 (12)	5 (21)
11	$Pd(OAc)_2$ (5)	Bipy-6-OH (2.5)	PPh_3 (5)	38 (45)	41 (49)
12	$Pd(OAc)_2$ (5)	Bipy-6-OH (2.5)	P^tBu_3 (5)	4 (9)	14 (19)
13	$Pd(OAc)_2$ (5)	Bipy-6-OH (2.5)	XPhos (5)	80 (85)	88 (92)
14	$Pd(OAc)_2$ (5)	Bipy-6-OH (2.5)	$HPCy_3$ BF_4 (5)	93 (97)[c]	
15	$Pd(OAc)_2$ (5)	Bipy-6-OH (5)	PCy_3 (5)	78 (84)[c]	
16	$Pd(OAc)_2$ (5)	Bipy-6-OH (5)	PCy_3 (10)	31 (40)	85 (91)
17	$Pd(OAc)_2$ (5)	Bipy-6-OH (2.5)	PCy_3 (7.5)	46 (54)	78 (89)
18	$Pd(OAc)_2$ (5)	Bipy-6-OH (2.5)	PCy_3 (2.5)	35 (38)	79 (87)
19	$Pd(OAc)_2$ (2.5)	Bipy-6-OH (2.5)	**8** (2.5)	72 (75)	
20	$Pd(OAc)_2$ (2.5)	Bipy-6-OH (2.5)	**9** (2.5)	92 (95)	
21	$Pd(OAc)_2$ (2.5)	Bipy-6-OH (2.5)	**10** (1.75)	27 (35)	87 (98)
22	$Pd(OAc)_2$ (2.5)	Bipy-6-OH (2.5)	**10** (1.75) $HPCy_3$ BF_4 (1.75)	98 (98)[c]	

[a]Reaction conditions: *p*-$CF_3C_6H_4Br$ (0.34 mmol), Cs_2CO_3 (0.68 mmol), toluene (1.5 mL), DMA (1.5 mL). [b]Crude yields determined by ^{19}F NMR of the reaction mixture. The reduction or the arylbromide (ArH) and the homocoupling (Ar-Ar) are the observed byproducts. [c]After 3h.

We decided to try preformed complexes with two PCy_3 coordinated to palladium. The well-defined Pd(II) complex **8** was synthesised by ligand substitution (see the experimental part for more information) and the Pd(0) complex **9** was commercially available. Both were tried in combination with the mixture $Pd(OAc)_2$ + bipy-6-OH obtaining excellent yields but in longer reaction times than using the free phosphine (6 h, entries 19 and 20 *vs.* 3 h, entry 1, Table 3.3). We also tried a palladium complex with only one PCy_3 coordinated (**10**) but again longer reaction times were needed to achieve full conversion (entry 21, Table 3.3). However, when a small excess of free phosphine (1.75 %) is used with **10** full conversion is obtained after 3 h (entry 22, Table 3.3).

The direct arylation of toluene using this catalyst system can be extended to several aryl bromides as coupling partners (Scheme 3.4). Different electronic properties are tolerated and electron-donating or electron-withdrawing functional groups can be present in the aryl halide. Functional groups like aldehydes that are more reactive, gave the coupling product in good yields too. Longer reaction times were used to ensure the complete conversion of the reactants when the reaction cannot be followed by NMR of the crude mixture. The reaction is not selective and a mixture of three isomers (*ortho*, *meta* and *para*) was obtained in all cases although the regioselectivity of the reaction changes slightly depending on the aryl bromide used.

Scheme 3.4. Direct arylation of toluene with different aryl bromides.

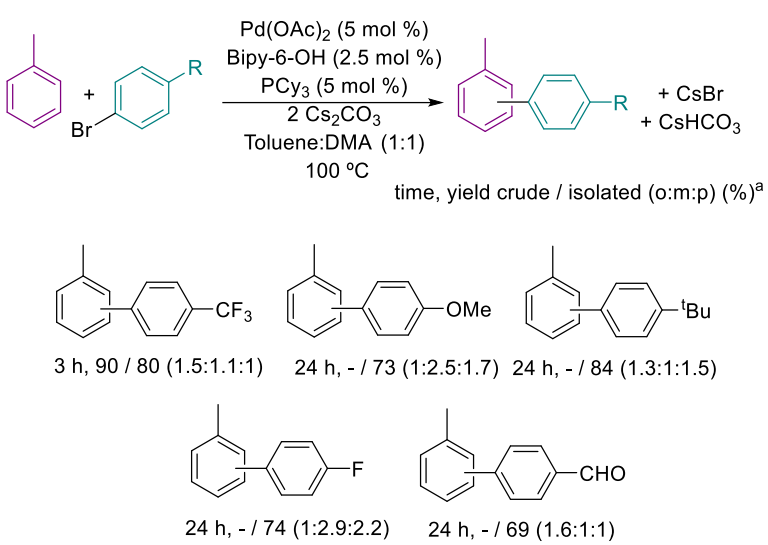

[a]Reaction conditions given in Table 3.3.

Different arenes were also tested (Scheme 3.5). Trifluorotoluene, ethyl benzoate and *N*,*N*-dimethylaniline gave moderate to good yields of the *meta* isomer as major product. The reaction is completely *meta* regioselective for pyridine. On the other hand, with anisole and fluorobenzene the *ortho* product was preferred. There is no correlation between the electronic properties of the arene and the regioselectivity of the reaction. In the case of anisole, the best results were observed when only 10 equivalents of the arene. In the case of ethyl benzoate, the regioselectivity decreased when DMA was used as co-solvent.

Scheme 3.5. Direct arylation of several arenes.

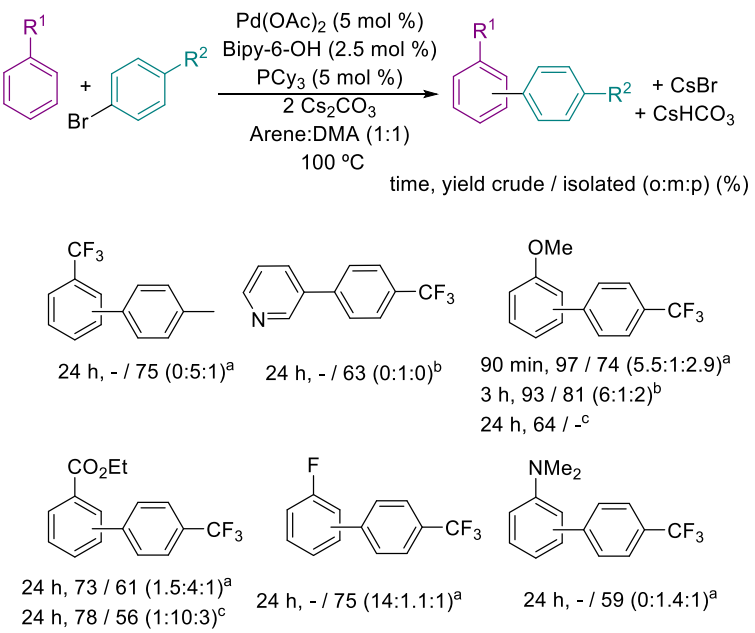

Reaction conditions: [a]Given in Table 3.3. [b]Arene (3.4 mmol), DMA (3 mL). [c]Arene (3 mL).

The reaction is also working when aryl chlorides were used (Scheme 3.6) substrates that are rarely active in direct arylation reactions. Electron-donating and electron-withdrawing groups were tested in the halide derivative obtaining good to excellent results.

Scheme 3.6. Direct arylation of arenes with different aryl chlorides.

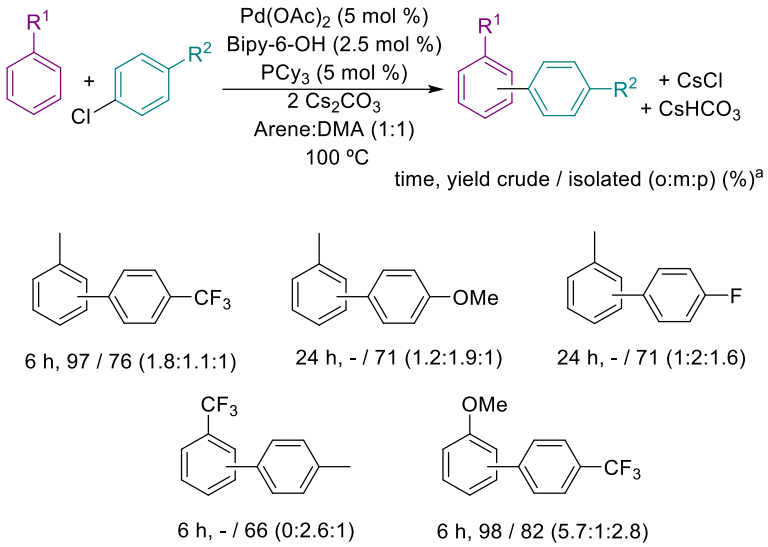

[a]Reaction conditions given in Table 3.3.

The reaction did not take place with some other arenes or aryl halides that were tried. In the case of aniline, the competitive C–N coupling product was obtained as only product, indicating that this dual system is more effective in the C–N reductive elimination step (see *Chapter 2*). Benzonitrile as arene did not give any coupling product, neither was observed when, *p*-bromobenzonitrile or *p*-bromobenzoic acid were used as aryl bromides in the direct arylation of toluene. *p*-Bromochlorobenzene as aryl halide gave a mixture of mono- and ditolyl products.

3.2.2 Mechanistic studies

In order to shed light into the reaction mechanism, several experiments were carried out. First of all, to gather information about the active catalytic species, we studied the species formed from the mixture $Pd(OAc)_2$ + 2 PCy_3 (Equation 3.5).[131] We observed the coordination of two phosphines to palladium acetate resulting in the complex $[Pd(OAc)_2(PCy_3)_2]$ and the Pd(0) complex **9** was also formed by the oxidation of one phosphine. Therefore, Pd(0) species can be easily formed from the precatalytic mixture. Also, the preformed complex **9** is also efficient in the catalytic reaction of this

[131] Hattori, H.; Ogiwara, Y.; Sakai, N. *Organometallics* **2022**, 41, 1509-1518.

dual-ligand system (entry 20, Table 3.3), which points to the involvement of Pd(0) phosphino complexes in the catalytic cycle.

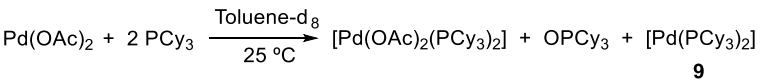

Equation 3.5.

Kinetic experiments were carried out using the reaction between toluene and an aryl halide as model (Equation 3.6.). Using the variable time normalization analysis (VTNA) reported by Burés,[97] the results showed a first-order dependence on the catalyst and a zero order dependence on the concentration of the aryl bromide or aryl chloride (see experimental part, Figure 3.29 and Figure 3.30 respectively). A large kinetic isotope effect was observed (KIE = 4.0 ± 0.5, Figure 3.28) when two separate experiments were carried out using toluene and toluene-d_8, meaning that the C–H activation is the turnover limiting step.

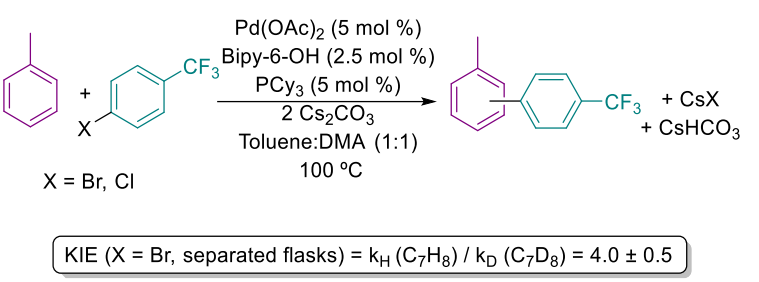

Equation 3.6.

Several mechanistic schemes are possible for this dual system. They have to explain the advantage of both ligands and take into account the fact that the optimal metal to ligand mol ratio is Pd:bipy-6-OH:PCy_3 = 1: 0.5: 1. Moreover, considering the reduction to Pd(0) mentioned above, the actual phosphine amount can even be smaller. Also, the kinetic experiments show that the C–H activation step is turnover limiting and that the C–H cleavage is assisted by the cooperating bipy-6-O (see entries 1, 3, 4 and 5, Table 3.3).

As a dual ligand approach, our first thought about the reaction mechanism was that a series of ligand exchange steps were taking place in the catalytic cycle, and the role of each ligand would be different. As can be seen in Scheme 3.7, the phosphine

would be coordinated during the oxidative addition step, then the bipy-6-OH would take its place to assist the C–H activation step and finally, the phosphine would coordinate again to give the reductive elimination releasing the coupling product.

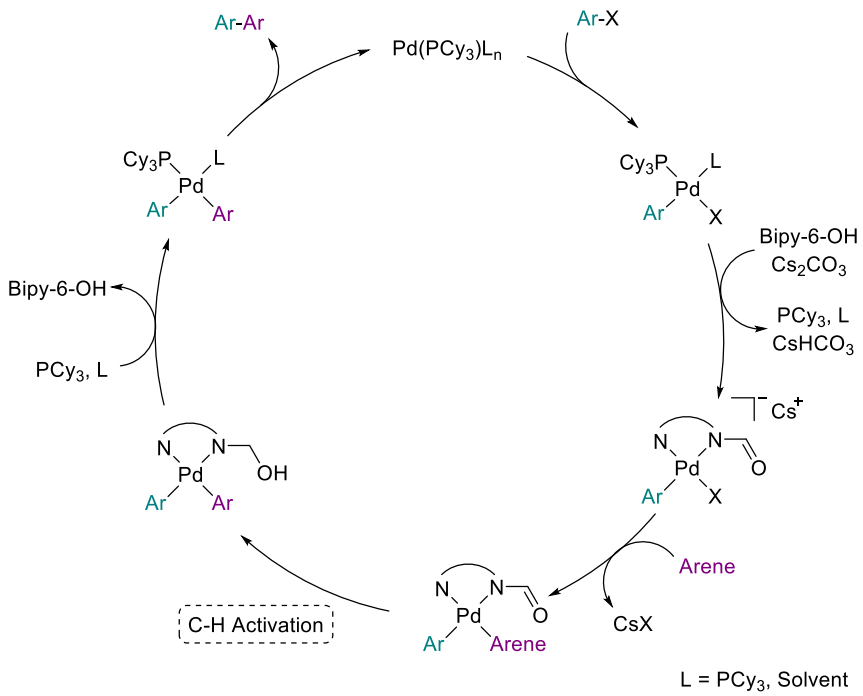

Scheme 3.7. Plausible monometallic catalytic cycle.

Ligand exchange experiments were done to support or discard the reaction mechanisms proposed. The well-defined complex **1**, as model of the intermediates in the cycle, was examined under catalytic conditions (toluene:DMA (1:1) as solvent) in the presence of 2 equivalents of PCy_3 (Equation 3.7). Complex **1** in DMA or in the toluene:DMA solvent mixture forms two isomers attributed to the cis and trans arrangement, as has been reported before.[25] A complex with two PCy_3 coordinated (**11**) was formed and free bipy-6-OH was observed a few minutes after the addition of the phosphine, proving the easy substitution of the bipy-6-OH ligand (Figure 3.3, see ^{1}H and $^{31}P\{^{1}H\}$ NMR spectra in the experimental part, Figure 3.14 and Figure 3.15 respectively). The same experiment was carried out in $CDCl_3$ and when equimolar amounts of **1** and PCy_3 were mixed only half of the starting material reacted to give **11** with the liberation of bipy-6-OH, as observed by ^{1}H NMR (Figure 3.16 in the experimental part). The addition of more PCy_3 in the ratio shown in Equation 3.7 led to the complete disappearance of **1**.

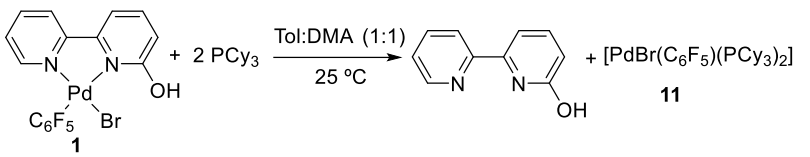

Equation 3.7.

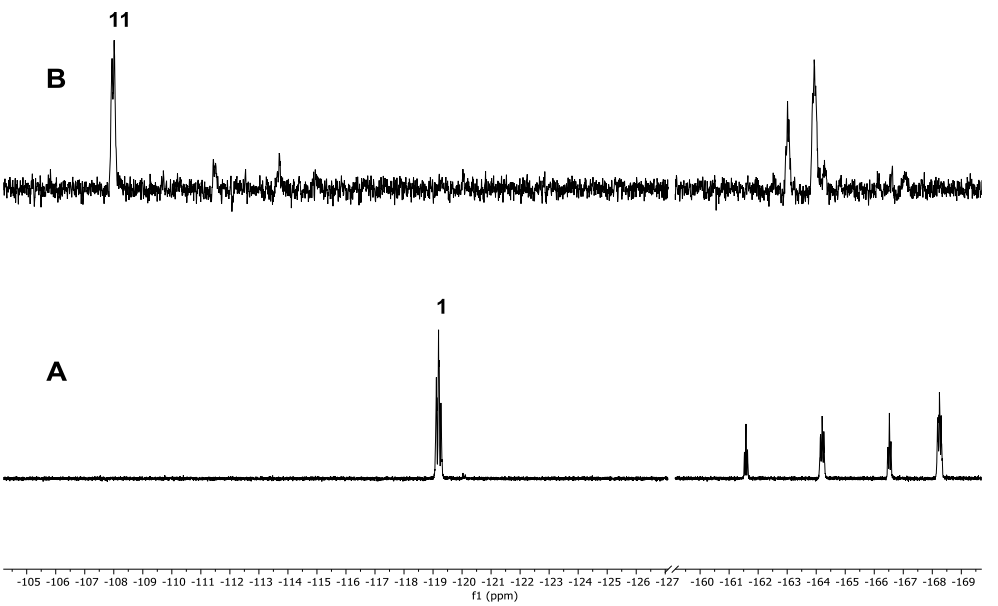

Figure 3.3. ^{19}F NMR spectra (470.168 MHz). A) Complex **1** in toluene:DMA (1:1) as a mixture of isomers. B) Sample A after adding 2 equivalents of PCy_3.

The same experiment was carried out using the preformed complex **12**, where the coordinating ligand is deprotonated (bipy-6-O, Equation 3.8). It is known by independent experiments reported before that the coordination ability of the ligand is better when it is deprotonated.[20] One hour after the addition of the phosphine, the formation of a new complex is observed by ^{1}H, ^{19}F and $^{31}P\{^{1}H\}$ NMR (Figure 3.4, Figure 3.5 and Figure 3.19) that we tentatively assigned to a complex with bipy-6-O, PCy_3 and a pentafluorophenyl group coordinated (**13**). The reaction evolved to the formation of complex **11** after heating the mixture at 100 ºC for 30 min. It is clear that the substitution of the bipy-6-O by PCy_3 is more difficult than for bipy-6-OH, however it is occurring under the catalytic conditions.

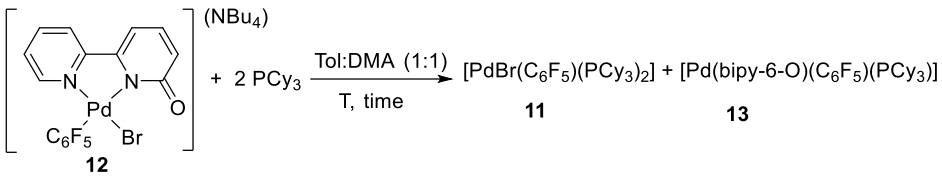

Equation 3.8.

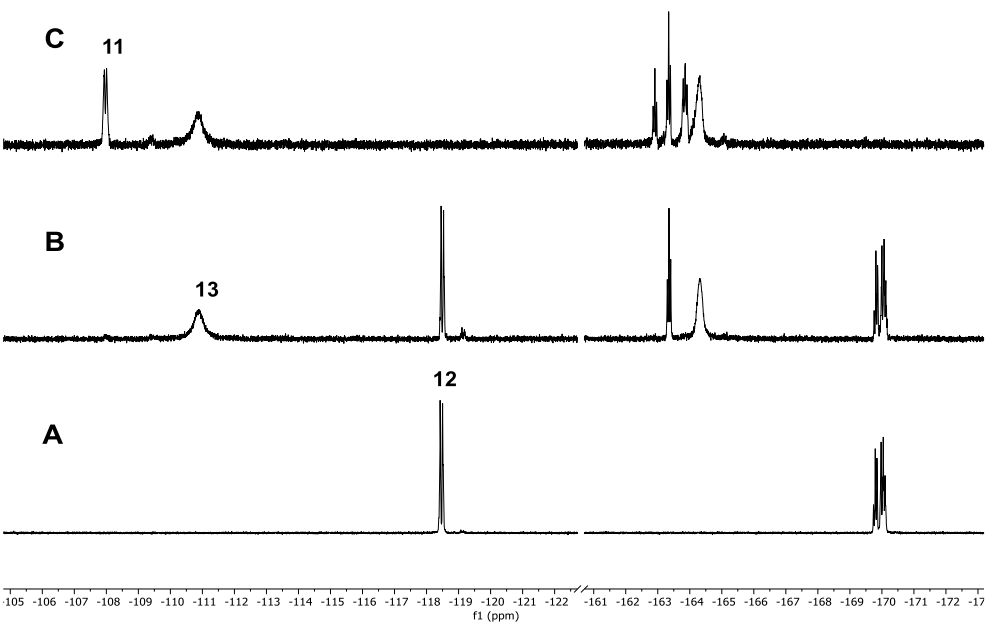

Figure 3.4. ^{19}F NMR spectra (470.168 MHz). A) Complex **12** in toluene:DMA (1:1). B) Sample A after adding 2 equivalents of PCy_3, 1 hour at room temperature C) Sample B after heating for 30 min at 100 ºC.

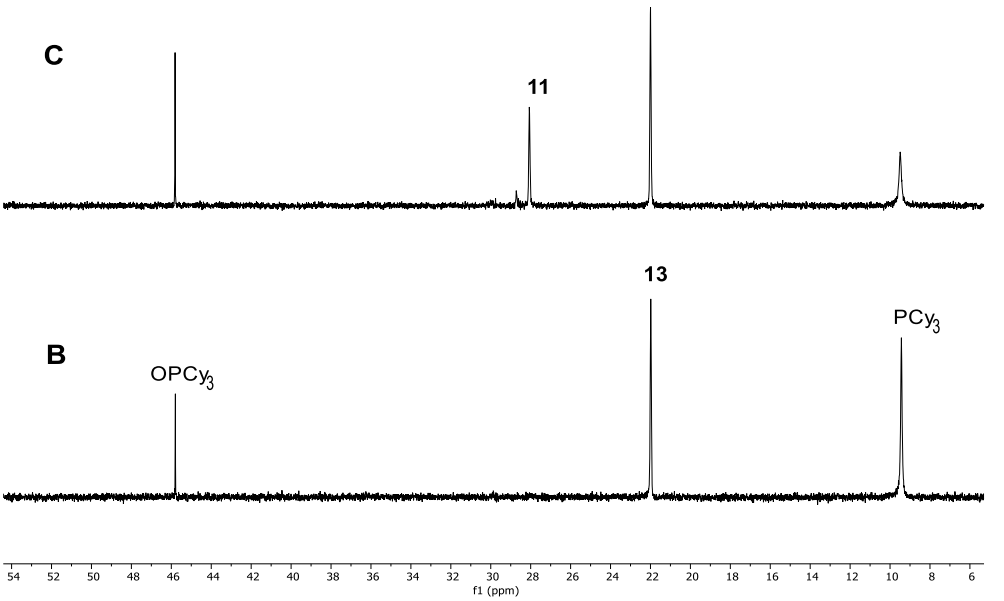

Figure 3.5. $^{31}P\{^{1}H\}$ NMR spectra (202.31 MHz). B) Complex **12** + 2 equivalents of PCy_3 in toluene:DMA (1:1), 1 hour at room temperature after the addition. C) Sample A after heating for 30 min at 100 ºC.

We also tried the reverse reaction, the substitution of a coordinated PCy_3 by the bipy-6-OH ligand. Bipy-6-OH was added to complex **8** in toluene:DMA (1:1) and no changes in the reaction mixture were observed (Equation 3.9). The addition of cesium carbonate to deprotonate the ligand gave similar results. Finally, after heating for 30 min at 100 ºC some decomposition of **8** was observed, however no other palladium complexes could be identified (Figure 3.20 and Figure 3.21 in the experimental part).

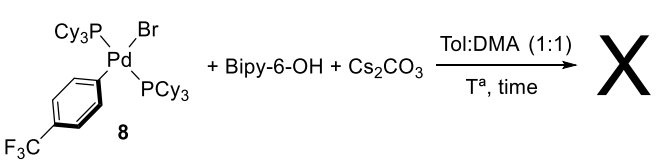

Equation 3.9.

These experiments clearly show that the coordination ability of the ligands present in the catalysis follows the trend PCy_3 > bipy-6-O > bipy-6-OH. An excess of phosphine will deactivate the catalyst by occupying the coordinating position of the bipy-

6-OH. In those conditions, the assistance of the cooperating ligand in the C–H activation step could not happen and the reaction does not evolve to the coupling product.

With those results it is clear that a monometallic catalytic cycle with ligand exchange steps as represented in Scheme 3.7 can be ruled out. The ligand substitution occurs just in one way: the phosphine taking the coordination positions of the bipy-6-OH. It has been proved that neither the bipy-6-OH nor the monoanionic bipy-6-O can displace the coordinated phosphine. Therefore, in the presence of PCy_3, the coordination of the cooperating ligand is more difficult and the reaction should be slower. In addition, if we focus on the C–H activation step, the turnover determining step, the intermediates and the transition state will be the same as in the reactions of direct arylation of arenes using just bipy-6-OH described before at 130 ºC.[20] So, the reaction should have a similar rate. However, this is not happening, and without the phosphine at 100 ºC the reactions did not take place (entry 2, Table 3.3), so different intermediates and transition state for the C–H activation must be operating.

A bimetallic mechanism is also possible when using two ligands in the experimental optimal ratio, each ligand coordinated to a different palladium centre. As it is shown in Scheme 3.8, on one cycle the phosphine would be coordinated to half of the metal centres and the oxidative addition would take place. On the other cycle, the bipy-6-O bound to the remaining palladium atoms would cooperate in the C–H cleavage and after a transmetallation step between both metal centres, the organic groups coordinated to the phosphine complex, would undergo the reductive elimination step, leading to the final product.

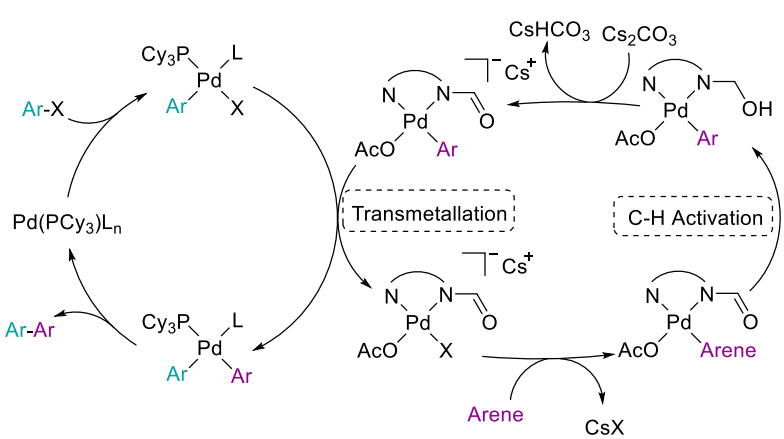

Scheme 3.8. Proposed bimetallic catalytic cycle.

We decided to carry out several experiments to test a transmetallation step between two different palladium complexes and to probe the proposed bimetallic mechanism (Scheme 3.8). Complex **14** was prepared in situ by bromide abstraction and deprotonation of **1** using silver carbonate. After filtration of the insoluble silver byproducts, complex **8** was added to the solution of **14** and heated at 100 ºC (Scheme 3.9); 14 % of the coupling product C_6F_5-Ar was observed, along with [PdBr(C_6F_5)(PCy_3)$_2$] (**11**) as a result of the substitution of the bipyridine ligand by the phosphine (Figure 3.6).

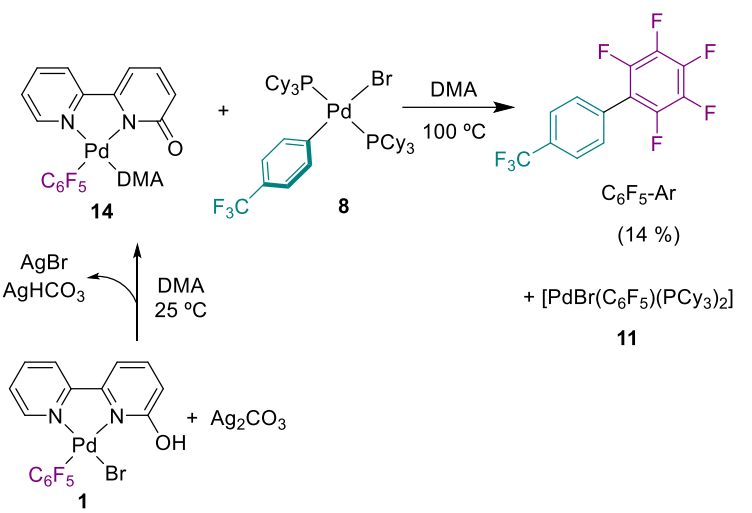

Scheme 3.9. Transmetallation experiment between complexes **14** and **8**.

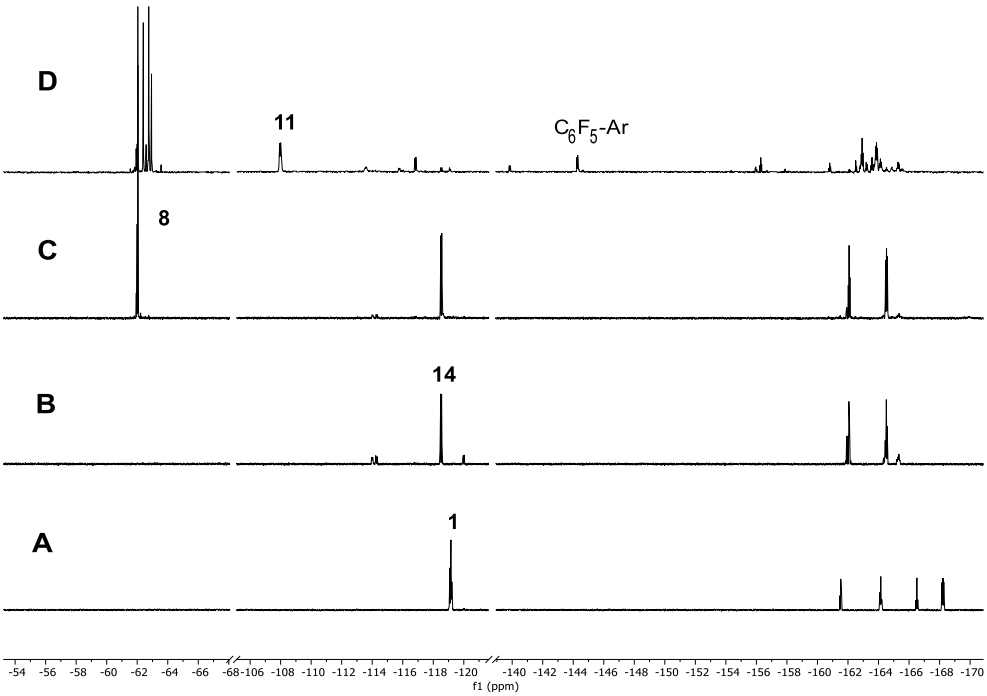

Figure 3.6. ^{19}F NMR spectra (470.168 MHz). A) Complex **1** in DMA (mixture of isomers)**.** B) Sample A + Ag_2CO_3 in DMA. C) Sample B after adding complex **8**. D) Sample C after heating for 30 min at 100 °C. (C_6F_5-Ar 14 %).

The same experiment was carried out in the presence of cesium carbonate simulating the catalytic conditions. However, the amount of coupling product observed decreased to a 4 % (see Figure 3.23 in the experimental part).

Since a fraction of the added phosphine is consumed in the reduction of $Pd(OAc)_2$ as shown in the experiment in Equation 3.5, the actual amount of PCy_3 under catalytic conditions would lead to phosphine complex with a ratio PCy_3/Pd < 2. Therefore, the palladium complex with only one PCy_3 coordinated (**10**) was tested as transmetallation partner of **14**. The experiment was done in the same way as before: first the *in situ* formation of **14**, then the addition of **10** and finally heating the mixture at 100 ºC (Scheme 3.10). After 3 h, 48 % of the coupling product was formed (Figure 3.7). Similar results were obtained when cesium carbonate was added to the mixture in a comparative experiment (45 % of C_6F_5-Ar, Figure 3.26).

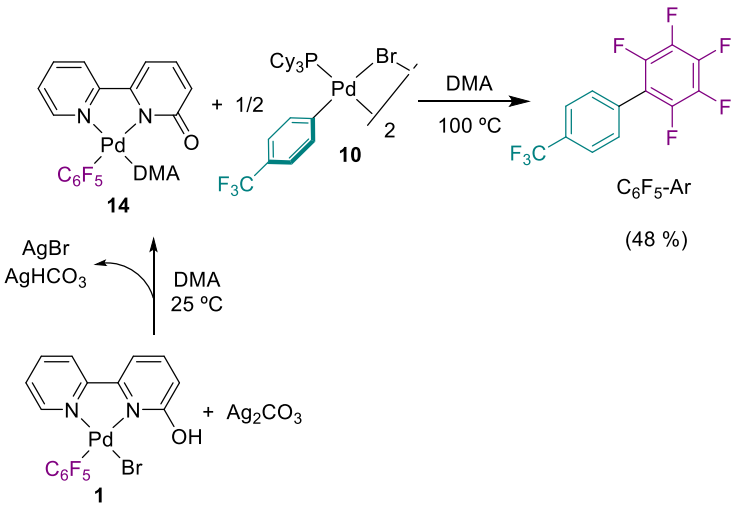

Scheme 3.10. Transmetallation experiment between **14** and **10**.

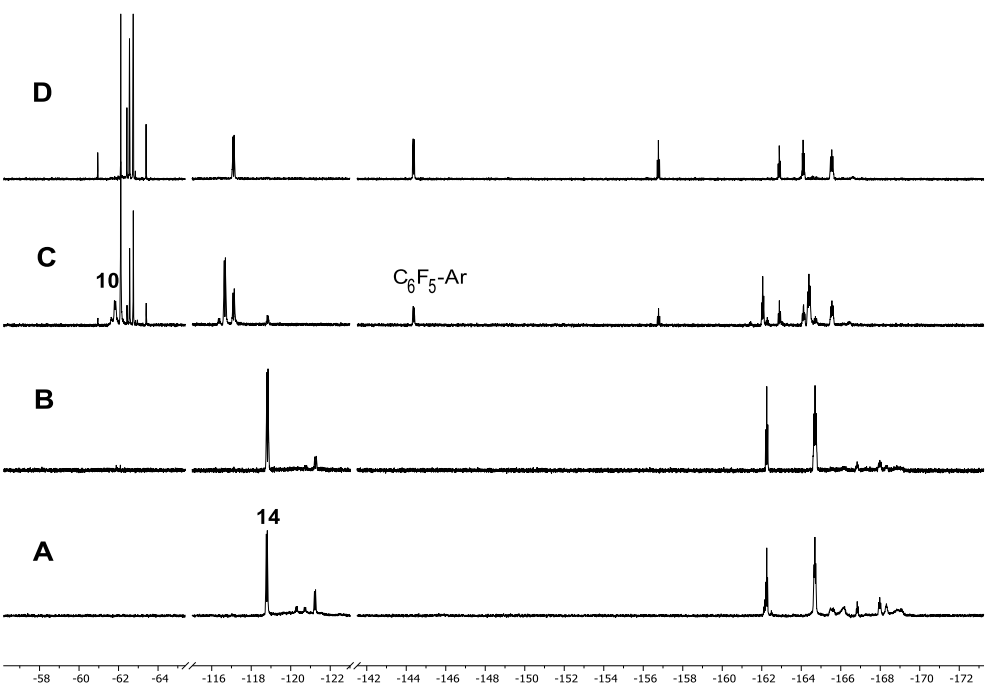

Figure 3.7. ^{19}F NMR spectra (470.168 MHz). A) Complex **14** in DMA. B) Sample A after adding complex **10** (not soluble). C) Sample B after heating for 30 min at 100 °C. (C_6F_5-Ar 12 %). D) Sample C after heating for 3 h at 10 ºC (C_6F_5-Ar 48 %).

These experiments show that a transmetallation step between a bipyridone-coordinated palladium and a phosphine-containing complex is possible and it is a plausible elementary step in the catalytic cycle. An excess of phosphine disfavours this process, which is more efficient for a monophosphine derivative. The optimal mol ratio for the catalytic reactions ($Pd(OAc)_2$:bipy-6-OH:PCy_3 = 1: 0.5: 1) show an scenario

consistent with half of the palladium ligated to the cooperating ligand Pd(II)-bipy-6-O and half of the metal forming monophosphine Pd(0)/PCy_3 after reduction of the Pd(II) with one equivalent of PCy_3 which is transformed into $OPPh_3$, as observed independently.

The nature of the intermediates in the C–H activation.

When this dual bipy-6-OH/PCy_3 catalytic system is compared to that enabled by the cooperating bipy-6-OH only, there are some differences that are worth mentioning. First, the dual system is active for aryl chlorides whereas the monoligand system is not, even at the higher temperature used for the reaction (130 ˚C). This points to the involvement of PCy_3 in the oxidative addition step. The bipy-6-OH-only system shows no significant differences in reactivity for arenes with electron-withdrawing or electron-donating groups and the regioselectivity observed favours the meta isomer in all cases. In contrast, the dual system shows an effect of the electronic properties of the arene in the reaction rate as determined by the monitoring of the initial rate of the direct arylation of toluene, ethyl benzoate and anisole. The k_{obs} of each experiment is shown in Table 3.4. It seems that electron-donating groups (anisole) accelerate the reaction while electron-withdrawing groups (ethyl benzoate) slow down the global rate. In the former case, the *ortho*/*para* selectivity is favoured.

Table 3.4. Rate constant for the different arenes.

Arene	k_{obs} (M min^{-1})	Time to get full conversion
Anisole	$3.1 \pm 0.3\ 10^{-4}$	90 min
Toluene	$2.3 \pm 0.1\ 10^{-4}$	3 h
Ethyl benzoate	$5.8 \pm 0.7\ 10^{-5}$	24 h

These data point to more electrophilic palladium intermediates involved in the C–H activation step. Thus, in the dual system, this elementary step could happen in a palladium complex with the bipy-6-O coordinated, responsible of the C–H bond activation and, for example, an acetate (**c2**, Figure 3.8) instead of the more electron rich complex **c5** (Figure 3.9) with an aryl group which is involved in the monoligand catalytic cycle.

DFT calculations of the C–H activation step on a simple model (see computational details in the experimental part) shows an energetic span of 26.9 kcal mol^{-1} *via* **c2** (Figure 3.8). The calculated barrier for the C–H activation *via* intermediate **c5** was found to be higher (28.4 kcal.mol^{-1}, Figure 3.9). Comparing both transition states, it can be seen that the C–H and C–Pd bond distances for the **TS c2-c3** are slightly shorter than those in **TS c4-c5** (Figure 3.8 and Figure 3.9), indicating that the mechanism for the C–H activation has a *e*CMD character.[52] This is in agreement with the higher rate observed for electron rich arenes. Thus, we can conclude that because the oxidative addition step is happening in a phosphine complex and not in the bipy-6-OH complex, the nature of the intermediates in the turnover limiting C–H activation step is modified, lowering the overall barrier of the reaction and making the whole system more active.

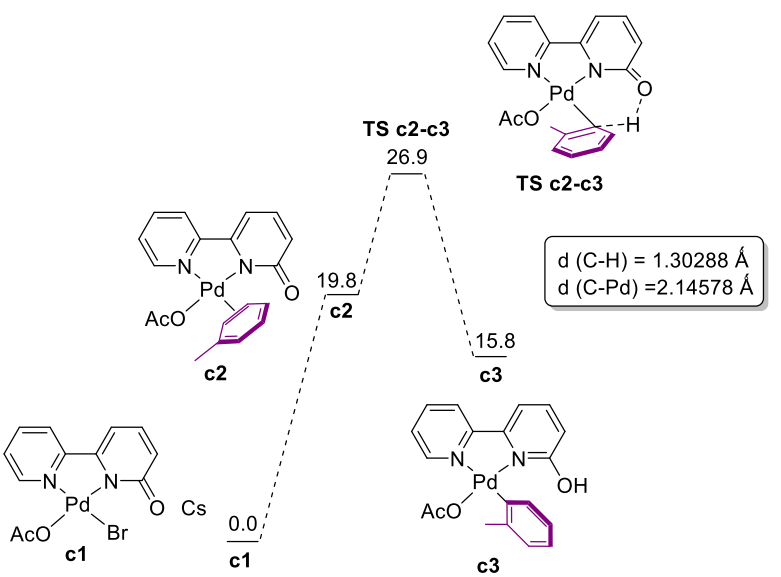

Figure 3.8. Gibbs energy profile for the C–H activation step from intermediate **c2** (energies in kcal mol^{-1}). Conditions: DMA as solvent, 100 ºC.

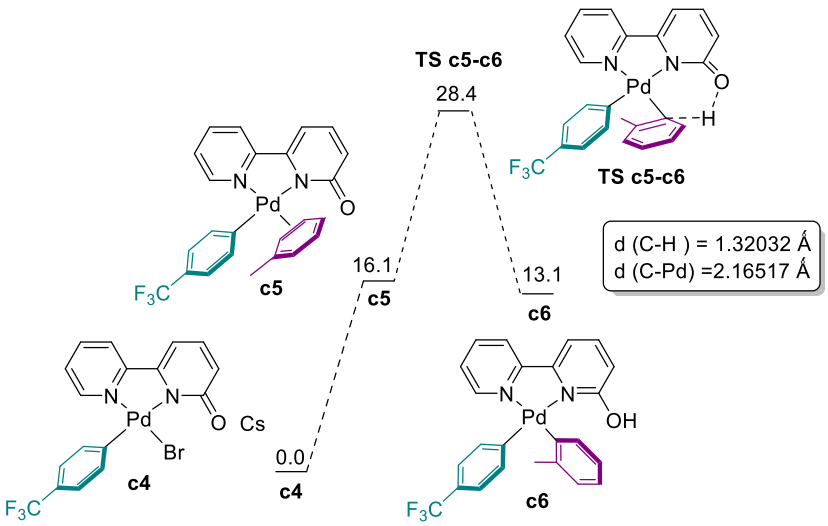

Figure 3.9. Gibbs energy profile for the C–H activation step from intermediate **c5** (energies in kcal mol^{-1}). Conditions: DMA as solvent, 100 ºC.

The plausible catalytic cycle is represented in Scheme 3.11. It is a bimetallic process through two different palladium complexes: on one cycle a palladium with a PCy_3 coordinated and on the other, the bipy-6-OH-containing complex. The oxidative addition of the aryl bromide occurs on the phosphine complex. Meanwhile, the coordination and C–H activation of toluene takes place in the bipy-6-OH complex. After the deprotonation of the ligand, which is known to occur fast in the presence of Cs_2CO_3, the transmetallation give raise to the phosphine complex with the two aryl groups coordinated. The reductive elimination of the coupling product gives the Pd(0) complex that reenters the catalytic cycle.

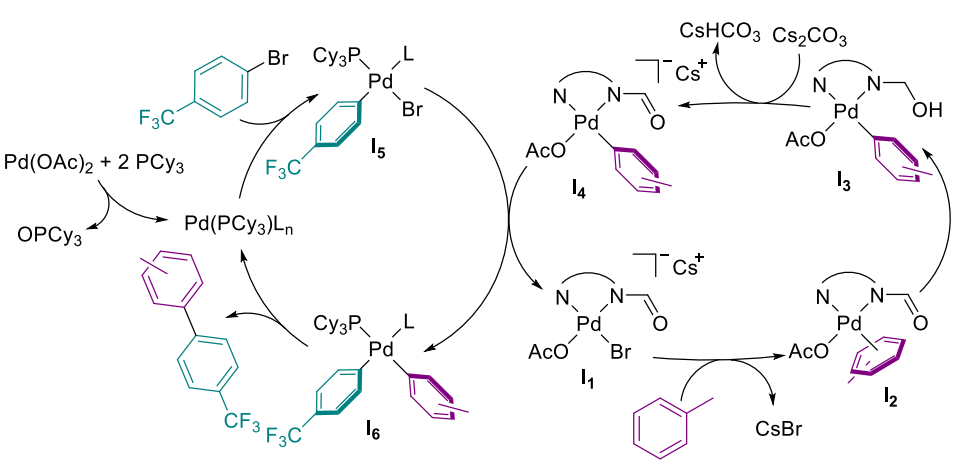

Scheme 3.11. Proposed catalytic cycle for the *ortho* arylation of toluene.

The regioselectivity of the reaction vary depending on the arene as can be expected, since the energy barrier for the C–H activation step in each position in the ring would not be the same, and the difference between them determines the regioisomer ratio. However, it is worth mentioning that when toluene is used as arene, the regioselectivity is also changing depending on the aryl halide used. It seems that the rate of the transmetallation step could be different for each regioisomer of the intermediate **I4**, and this determines the selectivity even if it is not the rate limiting step of the catalytic cycle (Scheme 3.4). This has been observed before in the bimetallic system described by Hong *et al.*[130] For this, we should think the different mechanisms that can make possible the interconversion between the **I4** isomers. A reversible C–H activation step would equilibrate the isomers and the rate of the transmetallation step would be responsible for the isomers' ratio. We cannot rule this out since the common experiment to check the reversibility of the C–H cleavage, the use of D_2O and the analysis of the deuteration in the coupling product, is not possible here due to the sensitivity of the catalytic system to the presence of water. So far, there is no evidence of a reversible C–H activation step in similar system, as it was found after deuteration experiments in *Chapter 2* for aniline and also in previous studies published by the group, on the C–H activation of toluene.[25] The deprotonation of the complex after the C–H cleavage (**I3**) is known to occur fast and results in a very stable complex (**I4**), making more difficult the possibility of a reversible C–H activation step.

We explored other mechanisms for the reorganization of **I4** isomers. The possibility of a second C–H activation will result in a different **I4** isomer as can be seen in Figure 3.10. From the *ortho* intermediate (**c3**) and after the deprotonation of the ligand (**c3Cs-*ortho***), the activation of a C–H in the *meta* position takes place, forming a benzyne-type intermediate. Finally, the meta isomer (**c3Cs-*meta***) is obtained after the protonation of the Pd–C bond in *ortho*.

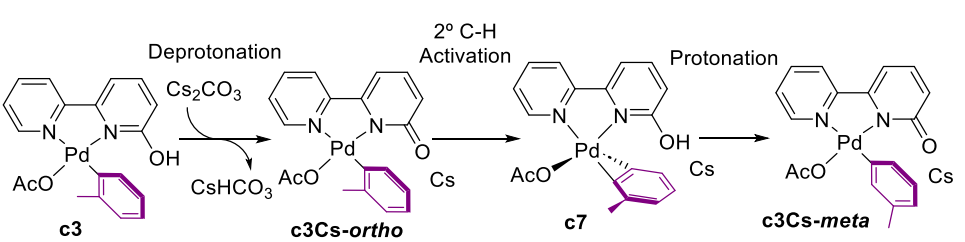

Figure 3.10. Possible isomer interconversion mechanism through a second C–H activation of the coordinated aryl.

DFT calculations were done on this route and a really high energy barrier was found for the second C–H activation of the aryl (Scheme 3.12). The deprotonation of **c3** resulted in a really stable complex as was expected, **c3Cs**, and the energy barrier for the transition state of this C–H cleavage was found to be 45.2 kcal mol^{-1}, so this pathway can be ruled out.

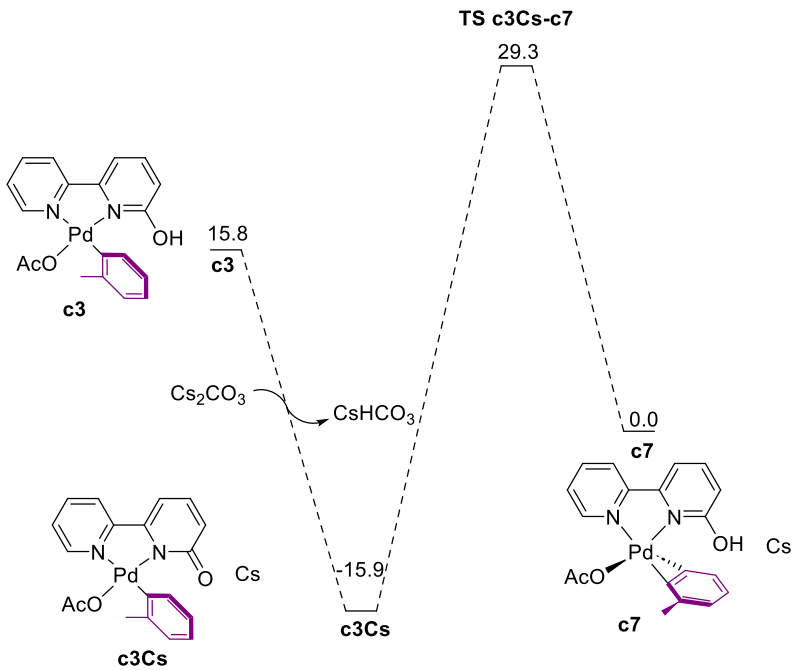

Scheme 3.12. Gibbs energy profile for a second C–H activation of toluene (energies in kcal mol^{-1}). Conditions: DMA as solvent, 100 ºC.

Finally, the decomposition by protonation of the aryl in the intermediate **I4** externally (HCO_3^- or another adventitious proton source) would release the arene molecule that can be activated again. The fastest isomer undergoing the transmetallation step would be the major isomer, as the other would decompose in the reaction medium. In conclusion, the observed isomer ratio in the final product would be determined by the transmetallation step rate, that also depends on the aryl halide used. That can explain why a different ratio of regioisomers is observed for the same arene but different aryl halides.

3.3 CONCLUSIONS

A dual ligand approach has been developed for the direct arylation of simple arenes. The use of the cooperating ligand bipy-6-OH in collaboration with PCy_3 allows to use milder reaction conditions than the reported ones in the literature with only bipy-6-OH (lower temperatures by 30 ˚C). Electron-donating and electron-withdrawing groups are tolerated in the arene and aryl halide scaffold. In addition, aryl chlorides can be used as coupling partner. The reaction rate depends directly on the electronic properties of the arene and a higher reaction rate was observed for electron rich arenes (anisole). A monometallic catalytic cycle where ligand exchange occurs can be ruled out since experiments shows a higher preference for PCy_3 coordination that does not allow the coordination of bipy-6-OH in both neutral or monoanionic forms. Mechanistic studies allow to propose a bimetallic reaction mechanism where a bipy-6-OH palladium complex and a PCy_3-containing complex operates simultaneously. The oxidative addition and reductive elimination steps occur through a phosphine-coordinated complex whereas the C–H activation step takes place in the bipy-6-O palladium complex. The transmetallation step between those two species has been demonstrated by independent experiments. The palladium species responsible for the C–H activation are more electrophilic than in the monoligand systems and an *e*CMD mechanism is possible as supported by computational studies and the higher reactivity of electron rich arenes. The regioselectivity of the reaction depends on the arene and aryl halide used, and the isomer ratio observed seems to be influenced by the rate of the transmetallation step.

The advantage of the dual ligand system is that it allows to change the nature of the intermediates in the turnover limiting C–H activation step by shifting the aryl halide reactivity to a different complex. This lowers the overall barrier of the reaction and makes the whole system more active.

3.4 EXPERIMENTAL PART

3.4.1 General considerations

^{1}H, $^{13}C\{^{1}H\}$, $^{19}P\{^{1}H\}$ and ^{19}F NMR spectra were recorded on Agilent MR-500, Agilent MR-400 or Bruker AV-400 spectrometers at the Laboratorio de Técnicas Instrumentales (LTI) of the UVa. Chemical shifts (in δ units, ppm) were referenced to $SiMe_4$ (^{1}H and ^{13}C), $CFCl_3$ (^{19}F) and H_3PO_4 (85%, ^{31}P). The spectral data were recorded at 298 K unless otherwise noted. The GC-MS analyses were performed in a Thermo-Scientific Focus DSQ II GC/MS apparatus. The intensities are reported as percentages relative to the base peak after the corresponding *m/z* value. HRMS analyses were carried out on a Bruker Maxis Impact mass spectrometer at the Laboratorio de Técnicas Instrumentales (LTI) of the UVa. Elemental analyses were carried out in a Thermo Scientific FLASH 2000 microanalyzer (at the Parque Científico Tecnológico of the UBU, Burgos, Spain).

Solvents were distilled from appropriate drying agents under nitrogen and stored over 3 Å or 4 Å molecular sieves (toluene) or used directly from the storage with the drying agent (anisole, ethyl benzoate, α,α,α-trifluorotoluene, fluorobenzene and N,N-dimethylaniline). DMA, pinacolone, toluene-d_8 and pyridine were purchased as anhydrous and stored under nitrogen over 3 Å or 4 Å molecular sieves. In the case of DMA, the molecular sieves were changed twice prior to use.

4-Bromobenzotrifluoride, 4-bromotoluene, 4-bromo-*tert*-butylbenzene, 4-bromoanisole, 4-bromofluorobenzene, 4-bromobenzaldehide, 4-chlorobenzotrifluoride, 4-chloroanisole, 4-chlorofluorobenzene, 4-chlorotoluene, cesium carbonate, palladium acetate, tricyclohexylphosphine, triphenylphosphine, tri-*tert*-butylphosphine, 2,2'-bipyridine, 6-hydroxypicolinic acid, acetylglycine, 2-pyridone and X-Phos are commercially available and were purchased from Sigma-Aldrich, Acros Organics, Alfa Aesar, BLD Pharm or Fluorochem. Commercial reagents were used as received unless otherwise noted.

[2,2'-bipyridin]-6(1*H*)-one (Bipy-6-OH),[20] [Pd(bipy-6-OH)Br(C_6F_5)] (**1**),[20] [2,2′-bipyridin]-4(1H)-one (Bipy-4-OH),[20] 6-(2-Pyridinylmethyl)-2(1*H*)-pyridinone (BipyMe-6-OH)[132], 6′-Methyl[2,2′-bipyridin]-6(1*H*)-one (BipyCH_2-6-OH),[133] [Pd(C_6H_4-

[132] Donohoe, T. J.; Fishlock, L. P.; Procopiou, P. A. *Org. Lett.* **2008**, 10, 2, 285-288.
[133] Deng, D.; Hu, B.; Zhang, Z.; Mo, S.; Yang, M.; Chen, D. *Organometallics* **2019**, 38, 9, 2218-2226.

p-CF_3)I(TMEDA)][84], [Pd_2dba_3].$CHCl_3$[83] were prepared according to the procedures in the literature.

3.4.2 Synthesis of palladium complexes

[PdBr(TMEDA)(C_6H_4-*p*-CF_3)]. [Pd(TMEDA)(C_6H_4-*p*-CF_3)I] (120.7 mg, 0.244 mmol) and acetone (2 mL) were introduced in a flask and cooled at -5 °C. In a baker, KBr (34.8 mg, 0.29 mmol) was dissolved in the minimum amount of distilled water and $AgNO_3$ (49.7 mg, 0.29 mmol) was added to the solution. A yellow solid (AgBr) appeared and the liquid phase was removed. The solid was washed twice with distilled water, and added to the reaction mixture. The flask was stirred at -5 °C for 20 h. A white solid appeared and the solution was filtered. The solvent was evaporated and cold Et_2O was added to the residue with vigorous stirring. A yellow solid precipitated, the solution was filtered, and the solid was washed with cold Et_2O and air-dried. Yield: 57 mg, (52 %).

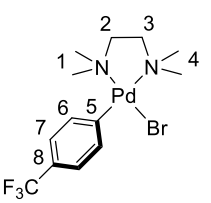

^{1}H NMR (500.13 MHz, δ, $CDCl_3$): 7.44 (d, J = 7.9 Hz, 2H, H^7), 7.18 (d, J = 7.9 Hz, 2H, H^6), 2.77 (m, 2H, H^2), 2.67 (s, 6H, H^4), 2.61 (m, 2H, H^3), 2.43 (s, 6H, H^1). $^{13}C\{^1H\}$ NMR (125.78 MHz, δ, $CDCl_3$): 154.5 (C^5), 135.3 (C^6), 125.5(q, J = 32 Hz, C^8), 124.9 (C^{CF3})*, 122.7 (q, J = 3.8 Hz, C^7), 62.7 (C^2), 58.3 (C^3), 50.7 (C^1), 48.7 (C^4). ^{19}F NMR (470.168 MHz, δ, $CDCl_3$): -61.86 (s, CF_3). *The chemical shift was determined by HSQC ^{13}C-^{19}F. HRMS (ESI-TOF): Calcd. for $C_{13}H_{20}BrF_3N_2NaPd$ $(M+Na)^+$ 468.9689, found 468.9703.

[PdBr(C_6H_4-*p*-CF_3)(PCy_3)$_2$] (8). [PdBr(TMEDA)(C_6H_4-*p*-CF_3)] (76.1 mg, 0.17 mmol) and dry dichloromethane (2 mL) were introduced into a N_2 flushed flask. PCy_3 (95.3 mg, 0.34 mmol) was added and the reaction mixture was stirred at room temperature for 3 h. The solvent was removed and cold Et_2O was added to the residue. A yellow solid appeared. The solution was filtered and the solid was washed with cold Et_2O and air-dried. Yield: 115.7 mg (76 %).

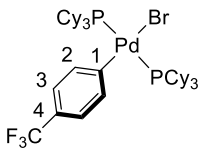

^{1}H NMR (500.13 MHz, δ, $CDCl_3$): 7.55 (d, J = 8.3 Hz, 2H, H^3), 7.16 (d, J = 8.3 Hz, 2H, H^2), 2.10-0.96 (m, 66H, H^{PCy3}). $^{13}C\{^1H\}$ NMR (125.78 MHz, δ, $CDCl_3$): 161.7 (C^1), 138.2 (C^3), 124.9 (C^{CF3})*, 124.2 (C^4), 122.8 (C^2). ^{19}F NMR (470.168 MHz, δ, $CDCl_3$): -62.06 (s, CF_3). $^{31}P\{^1H\}$ NMR (202.31 MHz, δ, $CDCl_3$): 19.8. *The chemical shift was determined by HSQC ^{13}C-^{19}F. HRMS (ESI-TOF): Calcd. for $C_{43}H_{70}F_3P_2Pd$ $(M\text{-}Br)^+$ 811.395, found 811.3946.

[$PdCl_2(PCy_3)_2$][134]**.** $PdCl_2$ (400 mg, 2.3 mmol) was introduced into a round bottom flask. Concentrated HCl (aq) (1.25 mL) and water (3 mL) were added and the mixture was stirred at room temperature. In a two necked flask PCy_3 (1.28 g, 4.6 mmol) was introduced under N_2 and dry acetone (25 mL) was added. The palladium solution was added dropwise to the phosphine solution. The mixture was stirred for 4 h at room temperature. A yellow solid appeared in an orange solution. The solution was filtered, and the solid was washed with acetone and air-dried. Yield: 1.43 g (84 %). HRMS (ESI-TOF): Calcd. for $C_{36}H_{66}ClP_2Pd$ $(M\text{-}Cl)^+$ 701.3368, found 701.3353.

$^{31}P\{^1H\}$ NMR (202.31 MHz, δ, $CDCl_3$): 24.98.

[Pd(C_6H_4-*p*-CF_3)(μ-OH)(PCy_3)]$_2$. Following a similar synthesis described in the literature.[135] [$PdCl_2(PCy_3)$] (410 mg, 0.56 mmol), *p*-$CF_3C_6H_4Cl$ (6 mL), KOH (2.1 g, 37 mmol) and water (6 mL) were introduced into a round bottom flask. It was refluxed 6 h with vigorous stirring. After cooling down the solution, the organic phase was collected and solvent-evaporated. Toluene was added and the mixture was filtered. The solution was evaporated and hexane was added to the residue appearing a white solid. The solution was filtered and the solid was washed with hexane and air-dried. A mixture between two isomers (ratio = 1:0.4) (65 %), aryl halide (15 %) and its homocoupling

[134] Gong, N. Method for preparing bis(tricyclohexylphosphine)palladium dichloride. CN102977151 A, 2013.
[135] Grushin, V. V.; Alper, H. *Organometallics*. **1993**, 12, 1890-1901.

product (20 %) was obtained. The mixture was used without further purification. Yield: 100.1 mg (16 %). The isomers were not fully characterized.

Major isomer: ^{19}F NMR (470.168 MHz, δ, $CDCl_3$): -61.89 (s, CF_3). $^{31}P\{^1H\}$ NMR (202.31 MHz, δ, $CDCl_3$): 37.13.

Minor isomer: ^{19}F NMR (470.168 MHz, δ, $CDCl_3$): -62.04 (s, CF_3). $^{31}P\{^1H\}$ NMR (202.31 MHz, δ, $CDCl_3$): 35.65.

$[Pd(C_6H_4$-*p*-$CF_3)(\mu$-OAc)$(PCy_3)]_2$. Following a similar synthesis described in the literature.[136] $[Pd(C_6H_4$-*p*-$CF_3)(\mu$-OH)$(PCy_3)]_2$ (97.5 mg, 0.09 mmol) was dissolved in toluene (5 mL) and acetic acid (20 µL, 0.35 mmol) was added dropwise to the solution. It was stirred at room temperature for 20 min. The solvent was evaporated and hexane was added to the residue. A white solid appeared, the solution was filtered and the solid was washed with hexane and air-dried. Yield: 102 mg (96 %). A mixture of two isomers was obtained (ratio = 1:0.3) and were not fully characterized.

Major isomer: ^{19}F NMR (470.168 MHz, δ, $CDCl_3$): -62.17 (s, CF_3). $^{31}P\{^1H\}$ NMR (202.31 MHz, δ, $CDCl_3$): 43.04

Minor isomer: ^{19}F NMR (470.168 MHz, δ, $CDCl_3$): -61.98 (s, CF_3). $^{31}P\{^1H\}$ NMR (202.31 MHz, δ, $CDCl_3$): 38.63.

$[Pd(C_6H_4$-*p*-$CF_3)(\mu$-Br$)(PCy_3)]_2$ (10). Following a similar synthesis described in the literature.[137] $[Pd(C_6H_4$-*p*-$CF_3)(\mu$-OAc$)(PCy_3)]_2$ (100 mg, 0.08 mmol) was dissolved in CH_2Cl_2 (1 mL), and NBu_4Br (69 mg, 0.21 mmol) was added to the mixture while stirring. Acetone (10 mL) and water (0.2 mL) were added to the solution. A white solid appeared. The mixture was stirred at room temperature for 3 h. The solution was filtered and the solid was washed with water and acetone and air-dried. Yield: 70 mg (67 %).

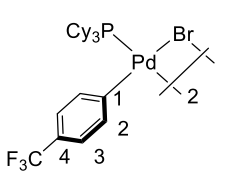

[136] Grushin, V. V.; Bensimon, C.; Alper, H. *Organometallics*. **1995**, 14, 3259-3263.
[137] Grushin, V. V. *Organometallics*. **2000**, 19, 1888-1900.

^{1}H NMR (500.13 MHz, δ, $CDCl_3$): 7.55 (d, J = 7.6 Hz, 2H, H^2), 7.18 (d, J = 7.6 Hz, 2H, H^3), 2.0-0.93 (m, 33H, H^{PCy3}). ^{13}C{^{1}H} NMR (125.78 MHz, δ, $CDCl_3$): 157.4 (C^1), 136.3 (C^2), 125.2 (C^4)*, 124.8 (C^{CF3})*, 122.9 (C^3), 35.1 (d. J = 22 Hz, C^{ipso}, PCy_3), 30.0 (s, C^{meta}, PCy_3), 27.4 (d, J = 11 Hz, C^{ortho}, PCy_3), 26.3 (s, C^{para}, PCy_3). ^{19}F NMR (470.168 MHz, δ, $CDCl_3$): -61.95 (s, CF_3). ^{31}P{^{1}H} NMR (202.31 MHz, δ, $CDCl_3$): 37.74. *The chemical shift was determined by HSQC and HMBC ^{13}C-^{19}F. Anal. Calculated for $C_{50}H_{74}Br_2F_6P_2Pd_2$: C, 49.08 %; H, 6.10 %; found: C, 49.07 %; H, 6.11 %.

3.4.3 Catalytic reactions

General procedure for the direct arylation of arenes.

$Pd(OAc)_2$ (3.8 mg, 0.017 mmol), bipy-6-OH (1.5 mg, 0.0085 mmol) and cesium carbonate (222 mg, 0.68 mmol) were introduced in a Schlenk flask under nitrogen atmosphere. The corresponding aryl halide (0.34 mmol), PCy_3 (4.7 mg, 0.017 mmol) dissolved in the corresponding arene (1.5 mL) and DMA (1.5 mL) were added to the flask. The mixture was stirred at 100 °C and checked by ^{19}F NMR of the crude mixture at the indicated time. When total conversion was observed, the solvent was evaporated in vacuo and the organic product was extracted with a mixture of *n*-hexane (8 mL) and ethyl acetate (2 mL). The extract was filtered through kieselguhr and evaporated to dryness. The product was checked by NMR and GC-MS.

The yields and characterization data for the products obtained are collected below. For known compounds the spectral data conforms to those in the literature (references are given).

Toluene as arene.

ArX = ***p*-$CF_3C_6H_4Br$**. The product was obtained as a white oil, mixture of three isomers in a ratio o:m:p = 1.6:1.1:1. Yield: 0.065 g (80%). ArX = ***p*-$CF_3C_6H_4Cl$**. Ratio of isomers o:m:p = 1.8:1.1:1. Yield: 0.061 g (76%). The characterization of 2-methyl-4'-(trifluoromethyl)-1,1'-biphenyl, 3-methyl-4'-(trifluoromethyl)-1,1'-biphenyl, 4-methyl-4'-(trifluoromethyl)-1,1'-biphenyl has been reported before.[20, 138]

ArX = ***p*-$MeOC_6H_4Br$**. The product was obtained as a white solid, mixture of three isomers in a ratio o:m:p = 1:2.5:1.7. Yield: 0.049 g (73%). ArX = ***p*-$MeOC_6H_4Cl$**. Ratio

[138] *o*-isomer: Shi, S.; Meng, G.; Szostak, M. *Angew. Chem. Int. Ed.* **2016**, *55*, 6959-6963.

of isomers o:m:p = 1.2:1.9:1. Yield: 0.048 g (71%). The characterization of 2-methyl-4'-(methoxy)-1,1'-biphenyl, 3-methyl-4'-(methoxy)-1,1'-biphenyl, 4-methyl-4'-(methoxy)-1,1'-biphenyl has been reported before.[139, 20]

ArX = ***p*-*t*BuC$_6$H$_4$Br**. The product was obtained as a white solid, mixture of three isomers in a ratio o:m:p = 1.3:1:1.5. Yield: 0.064 g (84%). The characterization of 2-methyl-4'-(*t*-butyl)-1,1'-biphenyl, 3-methyl-4'-(*t*-butyl)-1,1'-biphenyl, 4-methyl-4'-(*t*-butyl)-1,1'-biphenyl has been reported before.[140]

ArX = ***p*-FC$_6$H$_4$Br**. The product was obtained as a yellow oil, mixture of three isomers in a ratio o:m:p = 1:2.9:2.2. Yield: 0.047 g (74%). ArX = ***p*-FC$_6$H$_4$Cl**. Ratio of isomers o:m:p = 1:2:1.6. Yield: 0.045 g (71%). The characterization of 2-methyl-4'-(fluoro)-1,1'-biphenyl, 3-methyl-4'-(fluoro)-1,1'-biphenyl, 4-methyl-4'-(fluoro)-1,1'-biphenyl has been reported before.[141]

ArX = ***p*-CHOC$_6$H$_4$Br**. The product was obtained as a yellow oil, mixture of three isomers in a ratio o:m:p = 1.6:1:1. Yield: 0.046 g (69%). The characterization of 2'-methyl-[1,1'-biphenyl]-2-carbaldehyde, 3'-methyl-[1,1'-biphenyl]-2-carbaldehyde and 4'-methyl-[1,1'-biphenyl]-2-carbaldehyde has been reported before.[142]

Trifluoromethylbenzene as arene. ArX = ***p*-MeC$_6$H$_4$Br.** The product was obtained as a white solid, mixture of two isomers in a ratio o:m:p = 0:5:1. Yield: 0.060 g (75%). The characterization of 4-methyl-3'-(trifluoromethyl)biphenyl and 4-methyl-4'-(trifluoromethyl)biphenyl has been reported before.[143]

Pyridine as arene. ArX = ***p*-CF$_3$C$_6$H$_4$Br**. The product was obtained as a yellow oil and only the *metha* isomer. Yield: 0.047 g (63%). The characterization of 3-(3-(trifluoromethyl)phenyl)pyridine has been reported before.[20]

---

[139] *o*-isomer: Gehrtz, P. H.; Geiger, V.; Schmidt, T.; Sršan, L.; Fleischer, I. *Org. Lett.* **2019**, 21, 50-55.
[140] a)*m*-isomer: Arun, V.; Reddy, P. O. V.; Pilania, M.; Kumar, D. *Eur. J. Org. Chem.* **2016**, 2096-2100. b)*o* and *p*-isomers: Chen, Q.; Mao, Z.; Guo, F.; Liu, X. *Tetrahedron Lett.*, **2016**, 57, 3735-3738.
[141] a) *o*-isomer: Shen, A.; Hua, Y-C.; Liu, T-T.; Ni, C.; Luo, Y.; Cao, Y-C. *Tetrahedron Lett*. **2016**, 57, 2055-2058. b) *m*-isomer: Yuen, O. Y.; So, C. M.; Man, H. W.; Kwong, F. Y. *Chem. Eur. J.* **2016**, 22, 6471-6476. c) *p*-isomer: Gombert, A.; McKay, A. I.; Davis, C. J.; Wheelhouse, K. M.; Willis, M. C. *J. Am. Chem. Soc*. **2020**, 142, 3564-3576.
[142] a)*o* and *p*-isomers: Dadras, A.; Naimi-Jamal, M. R.; Moghaddam, F. M.; Ayati, S. E. *Appl. Organometal. Chem.* **2018**, 1-9. b)*m*-isomer: Yan, M. Q.; Yuan, J.; Lan,F.; Zeng, S. H.; Gao, M-Y.; Liu, S-H.; Chena, J.; Yu, G-A. *Org. Biomol. Chem*. **2017**, 15, 3924-3929.
[143] Tang, J.; Biafora, A.; Goossen, L. J. *Angew. Chem. Int. Ed.* **2015**, 54, 13130-13133.

Anisole as arene. ArX = ***p*-$CF_3C_6H_4Br$**. The product was obtained as a yellow oil, mixture of three isomers in a ratio o:m:p = 5.5:1:2.9. Yield: 0.070 g (81%). The characterization of 2-methyl-4'-(trifluoromethyl)-1,1'-biphenyl, 3-methyl-4'-(trifluoromethyl)-1,1'-biphenyl and 4-methyl-4'-(trifluoromethyl)-1,1'-biphenyl has been reported before.[20]

Ethyl benzoate as arene. ArX = ***p*-$CF_3C_6H_4Br$.** The product was obtained as a yellow oil, mixture of three isomers in a ratio o:m:p = 1.5:4:1. Yield: 0.061 g (61%). The characterization of ethyl 4'-(trifluoromethyl)-[1,1'-biphenyl]-2-carboxylate, ethyl 4'-(trifluoromethyl)-[1,1'-biphenyl]-3-carboxylate and ethyl 4'-(trifluoromethyl)-[1,1'-biphenyl]-4-carboxylate has been reported before.[20]

Fluorobenzene as arene. ArX = ***p*-$CF_3C_6H_4Br$.** The product was obtained as a colourless oil, mixture of three isomers in a ratio o:m:p = 14:1.1:1. Yield: 0.061 g (75%). The characterization of 2-fluoro-4'-(trifluoromethyl)-1,1'-biphenyl, 3-fluoro-4'-(trifluoromethyl)-1,1'-biphenyl and 4-fluoro-4'-(trifluoromethyl)-1,1'-biphenyl has been reported before. [20]

***N, N*-dimethylaniline** as arene. ArX = ***p*-$CF_3C_6H_4Br$**. The product was obtained as a yellow oil, mixture of two isomers in a ratio o:m:p = 0:1.4:1. Yield: 0.053 g (59%). The characterization of *N, N*-dimethyl-4'-(trifluoromethyl)[1,1'-biphenyl]-3-amine and *N, N*-dimethyl-4'-(trifluoromethyl)[1,1'-biphenyl]-4-amine has been reported before. [144]

[144] Pinilla, C.; Salamanca, V.; Lledós, A.; Albéniz, A. C. *ACS Catalysis* **2022**, *12*, 14527-14532.

3.4.4 Mechanistic experiments

Active catalyst formation

PCy_3 (5.6 mg, 0.02 mmol) was mixed with 0.6 mL of toluene-d_8 and introduced into a NMR tube. Then, $Pd(OAc)_2$ (2.2 mg, 0.01 mmol) was added to the solution. The species formed at room temperature were examined by $^{31}P\{^1H\}$ NMR (Figure 3.11).

The spectroscopic data of the identified species is given below.

$[Pd(PCy_3)_2(OAc)_2]$: $^{31}P\{^1H\}$ NMR (202.31 MHz, δ, toluene-d_8): 20.81.

9: $^{31}P\{^1H\}$ NMR (202.31 MHz, δ, toluene-d_8): 44.7.

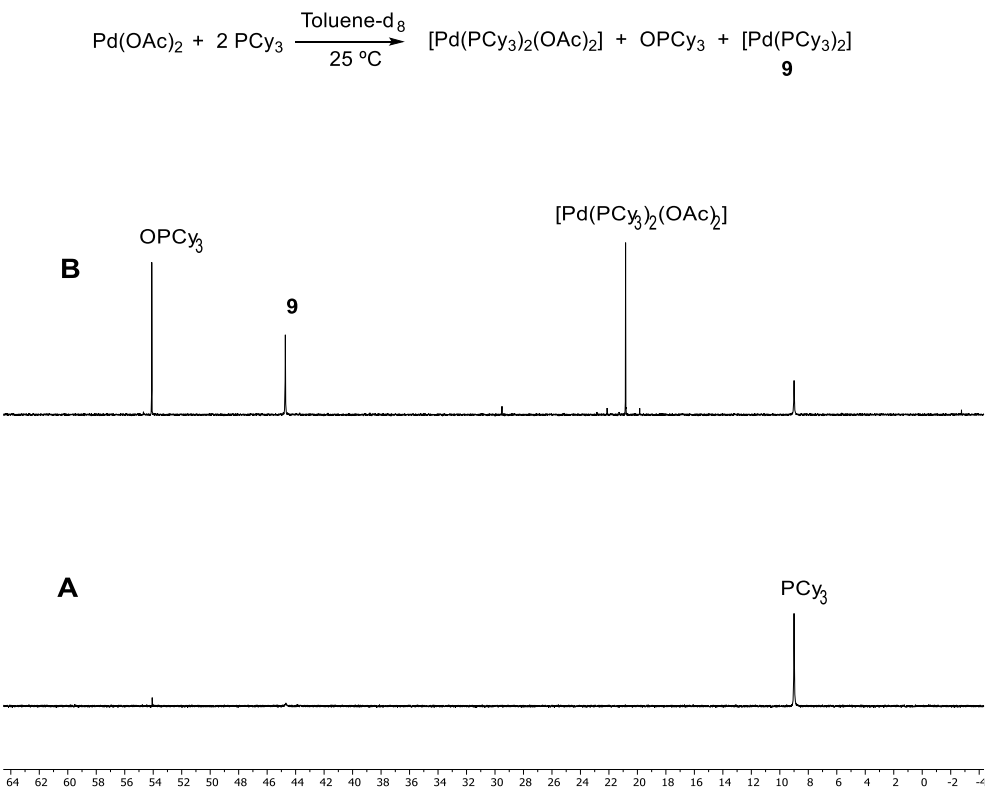

Figure 3.11. $^{31}P\{^1H\}$ NMR spectra (202.31 MHz). A) PCy_3 in toluene-d_8. B) Sample A after adding $Pd(OAc)_2$.

Thermal decomposition of complex 8

Complex **8** (8.9 mg, 0.01 mmol) was dissolved in 0.3 mL of dry toluene and 0.3 mL of dry DMA into a NMR tube along with a sealed glass capillary filled with DMSO-d_6 as

NMR reference. The mixture was heated for 1 h at 100 ºC. The species formed in solution were examined by ^{19}F and $^{31}P\{^{1}H\}$ NMR (Figure 3.12 and Figure 3.13).

The spectroscopic data of the identified species are given below.

8: ^{19}F NMR (470.168 MHz, δ, toluene/DMA (1:1)/DMSO-d_6 capillary): -61.0 (CF_3). $^{31}P\{^{1}H\}$ NMR (202.31 MHz, δ, toluene/DMA (1:1)/DMSO-d_6 capillary): 20.8.

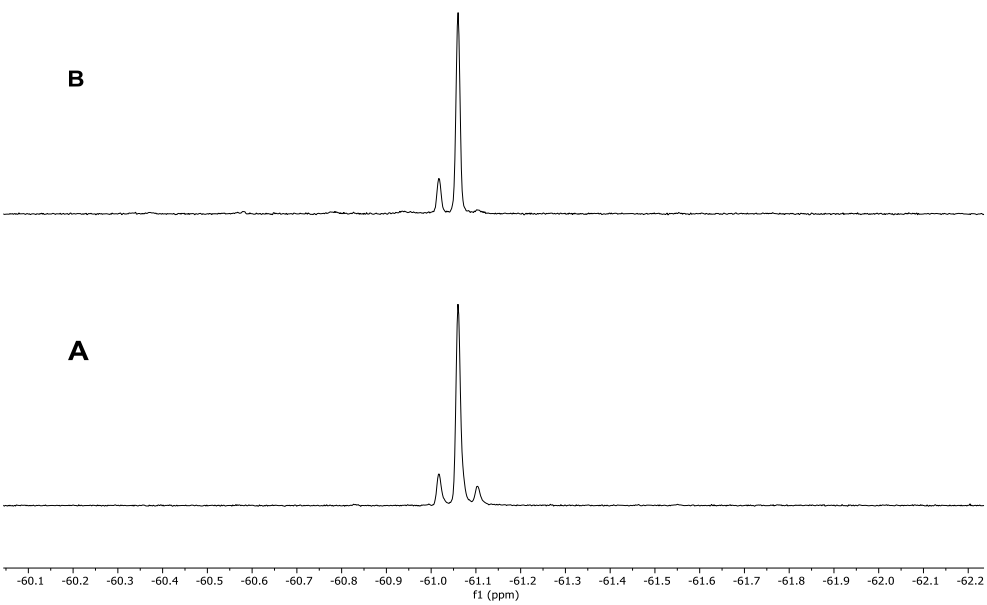

Figure 3.12. ^{19}F NMR spectra (470.168 MHz). A) Complex **8** in toluene:DMA (1:1). B) Sample A after heating 1h at 100°C.

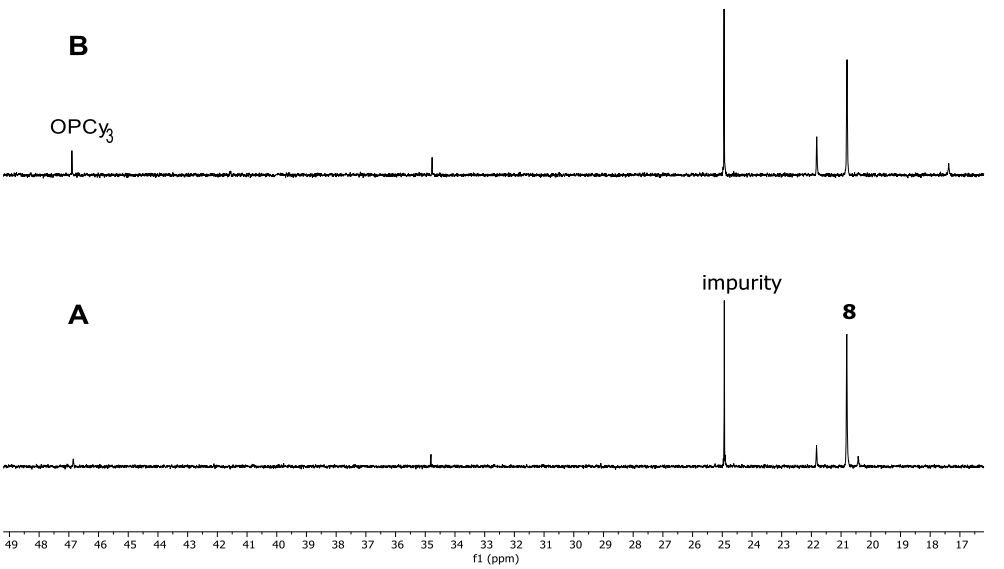

Figure 3.13. $^{31}P\{^{1}H\}$ NMR spectra (202.31 MHz). A) Complex **8** in toluene:DMA (1:1). B) Sample A after heating 1h at 100°C.

Ligand exchange experiments

Complex **1** (6.2 mg, 0.013 mmol) was dissolved in 0.3 mL of dry DMA and 0.3 mL of dry toluene into an NMR tube along with a sealed glass capillary filled with DMSO-d_6 as NMR lock signal. PCy_3 (7.2 mg, 0.026 mmol) was added to the solution. The species formed in solution at room temperature were examined by ^{1}H, ^{19}F and $^{31}P\{^{1}H\}$ NMR (Figure 3.3, Figure 3.14 and Figure 3.15).

The spectroscopic data of the identified species are given below.

1 (mixture of isomers A and B): Isomer A: ^{19}F NMR (470.168 MHz, δ, toluene:DMA (1:1)/DMSO-d_6 capillary): -119.2 (m, 2F, F_{ortho}), -166.5 (m, 1F, F_{para}), -168.3 (m, 2F, F_{meta}). Isomer B: ^{19}F NMR (470.168 MHz, δ, Tol/DMA (1:1)/$DMSO_6$ capillary): -119.2 (m, 2F, F_{ortho}), -161.6 (m, 1F, F_{para}), -164.2 (m, 2F, F_{meta}).

11: ^{19}F NMR (470.168 MHz, δ, toluene:DMA (1:1)/DMSO-d_6 capillary): -108.0 (m, 2F, F_{ortho}), -162.9 (t, J = 21.4 Hz, 1F, F_{para}), -163.8 (m, 2F, F_{meta}). $^{31}P\{^{1}H\}$ NMR (202.31 MHz, δ, toluene:DMA (1:1)/DMSO-d_6 capillary): 28.1.

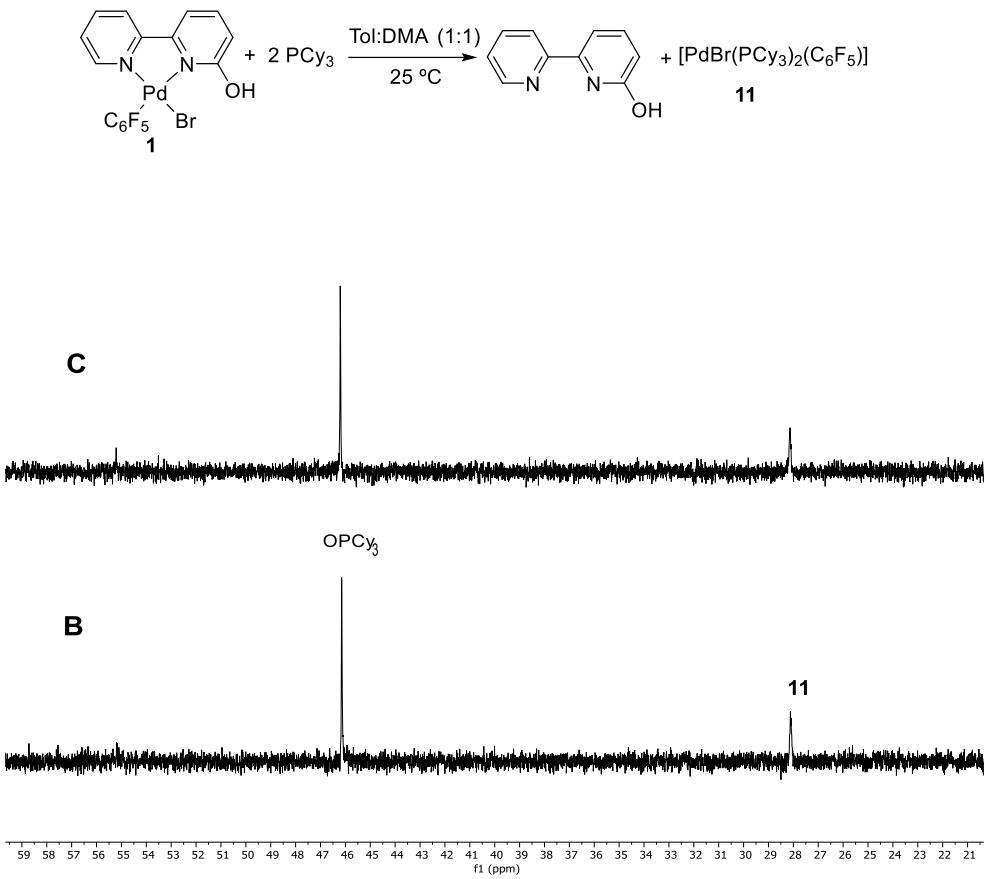

Figure 3.14. $^{31}P\{^{1}H\}$ NMR spectra (202.31 MHz). B) Mixture of complex **1** and 2 equivalents of PCy_3 in toluene:DMA (1:1). C) Sample A after 24 h at room temperature.

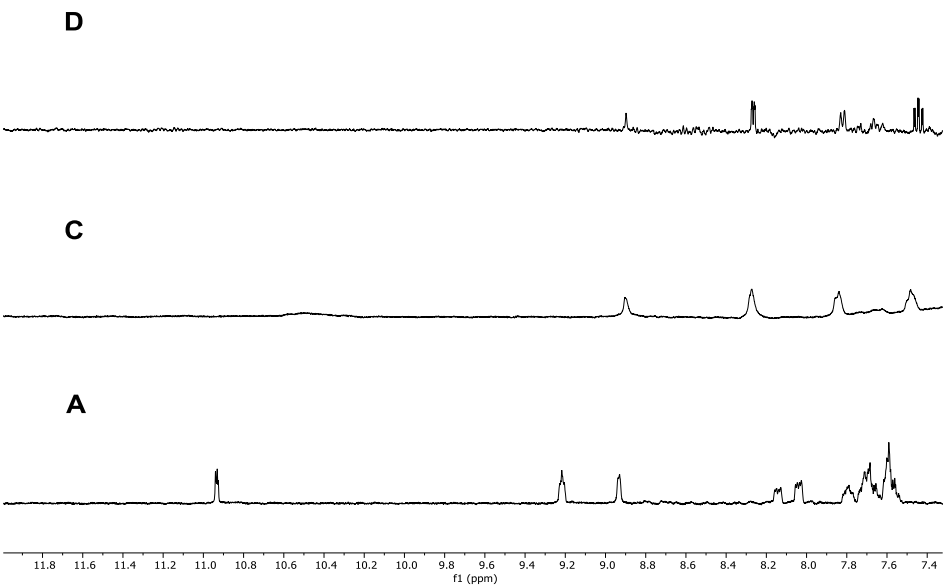

Figure 3.15. ^{1}H NMR spectra (500.13 MHz). A) Complex **1** in toluene:DMA (1:1). C) Sample A after adding 2 equivalents of PCy_3 and being 24h at room temperature. D) Free bipy-6-OH in toluene:DMA (1:1).

Complex **1** (6.2 mg, 0.013 mmol) was dissolved in dry $CDCl_3$ (0.6 mL) in an NMR tube. One equivalent of PCy_3 (3.1 mg, 0.013 mmol) was added to the mixture. The species formed in solution at room temperature were examined by ^{1}H, ^{19}F and $^{31}P\{^{1}H\}$ NMR. Then, a second equivalent of PCy_3 was added (3.1 mg, 0.013 mmol). The species formed in solution at room temperature were examined again by ^{1}H, ^{19}F and $^{31}P\{^{1}H\}$ NMR (Figure 3.16, Figure 3.17 and Figure 3.18).

The spectroscopic data of the identified species are given below.

1: ^{19}F NMR (470.168 MHz, δ, $CDCl_3$): -119.2 (m, 2F, F_{ortho}), -158.8 (t, J = 20.1 Hz, 1F, F_{para}), -161.9 (m, 2F, F_{meta}).

11: ^{19}F NMR (470.168 MHz, δ, $CDCl_3$): -108.2 (m, 2F, F_{ortho}), -161.4 (t, J = 22.0 Hz, 1F, F_{para}), -163.0 (m, 2F, F_{meta}). $^{31}P\{^{1}H\}$ NMR (202.31 MHz, δ, toluene:DMA (1:1)/DMSO-d_6 capillary): 28.1.

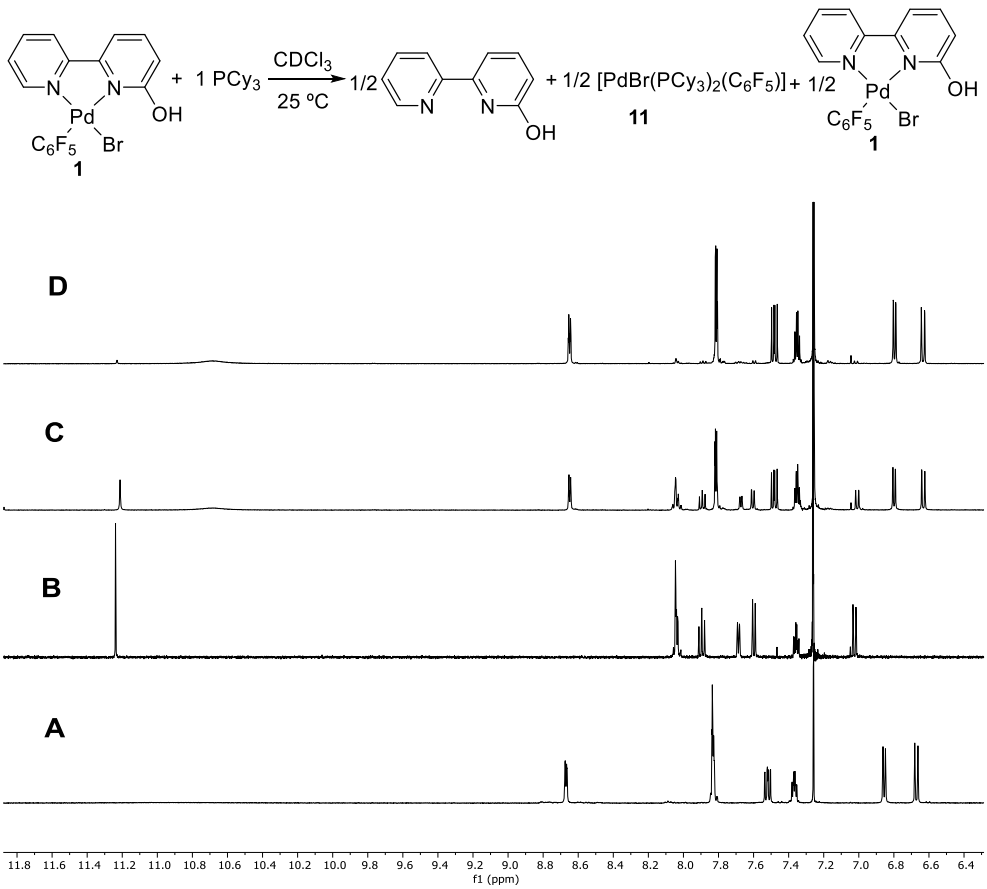

Figure 3.16. ^{1}H NMR spectra (500.13 MHz). A) Free bipy-6-OH in $CDCl_3$. B) Complex **1** in CDC_3. C) Sample B after adding 1 equivalent of PCy_3. D) Sample C after adding 1 more equivalent of PCy_3.

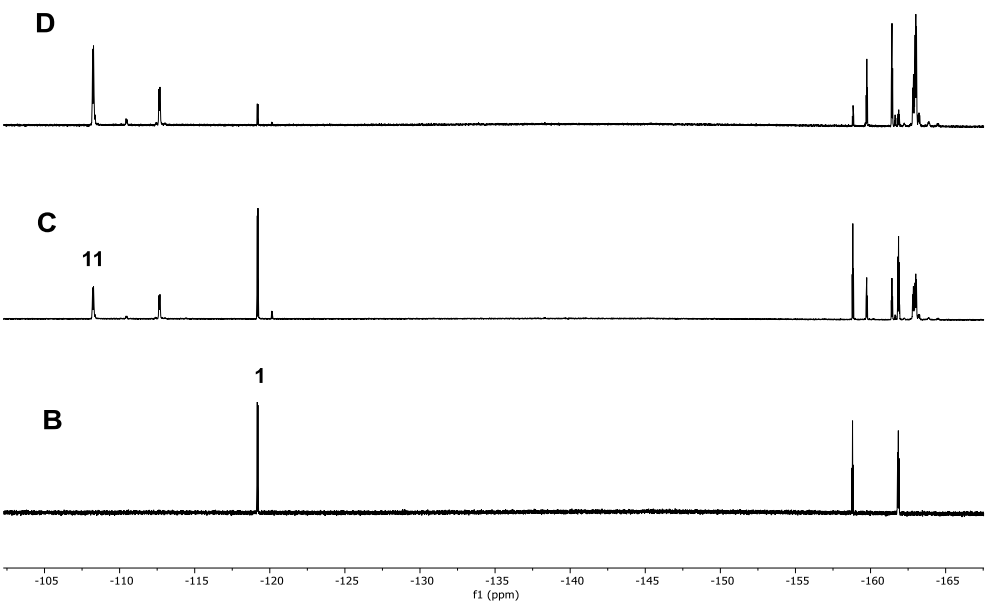

Figure 3.17. ^{19}F NMR spectra (470.168 MHz). B) Complex **1** in $CDCl_3$. C) Sample B after adding 1 equivalent of PCy_3. D) Sample C after adding 1 more equivalent of PCy_3.

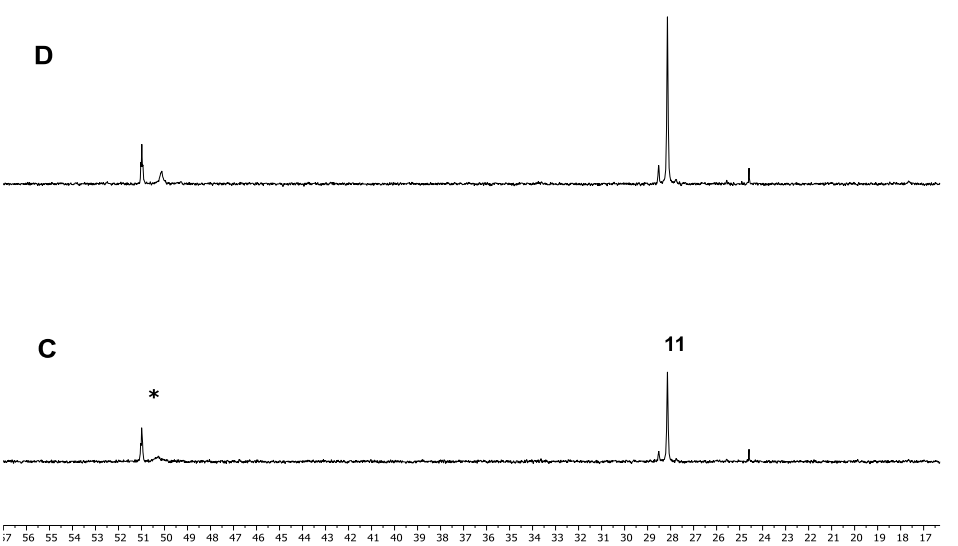

Figure 3.18. $^{31}P\{^1H\}$ NMR spectra (202.31 MHz). C) Complex **1** in $CDCl_3$ after adding 1 equivalent of PCy_3. D) Sample C after adding 1 more equivalent of PCy_3. *Unidetified species.

Complex **12** (7.2 mg, 0.01 mmol) was dissolved in 0.3 mL of dry DMA and 0.3 mL of dry toluene into an NMR tube along with a sealed glass capillary filled with DMSO-d6 as NMR lock signal. Then, PCy_3 (5.6 mg, 0.02 mmol) was added to the mixture. The species formed in solution at room temperature and after heating for 30 min at 100 ºC were examined by ^{1}H, ^{19}F and $^{31}P\{^{1}H\}$ NMR (Figure 3.4, Figure 3.5 and Figure 3.19).

In addition to the species mentioned in former experiments, complexes **12** and **13** were identified.

12: ^{19}F NMR (470.168 MHz, δ, toluene:DMA (1:1)/DMSO-d6 capillary): -118.5 (m, 2F, F_{ortho}), -169.9 (m, 1F, F_{para}), -170.1 (m, 2F, F_{meta}).

13: ^{19}F NMR (470.168 MHz, δ, toluene:DMA (1:1)/DMSO-d6 capillary): -110.9 (m, 2F, F_{ortho}), -163.3 (t, J = 18.4 Hz, 1F, F_{para}), -164.3 (m, 2F, F_{meta}). $^{31}P\{^{1}H\}$ NMR (202.31 MHz, δ, toluene/DMA (1:1)/DMSO-d6 capillary): 21.9.

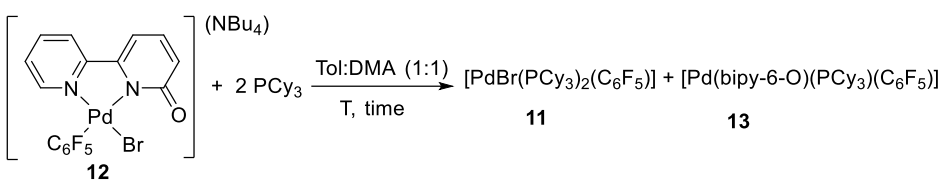

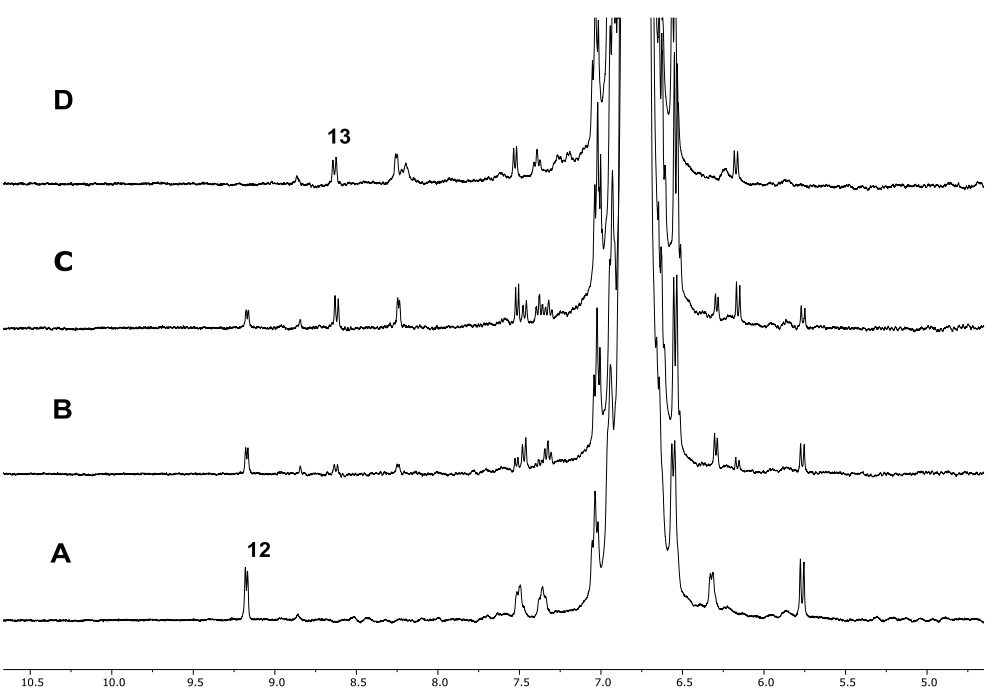

Figure 3.19. ^{1}H NMR spectra (500.13 MHz). Only the aromatic region is showed for clarity. A) Complex **12** in toluene:DMA (1:1). B) Sample A after adding 2 equivalents of PCy_3. C) Sample B after 1 h at room temperature. D) Sample C after heating for 30 min at 100 ºC.

Complex **8** (4.2 mg, 4.7x10^{-3} mmol) was mixed with 0.3 mL of dry DMA and 0.3 mL of dry toluene in an NMR tube along with a sealed glass capillary filled with DMSO-d6 as NMR lock signal. Bipy-6-OH (0.8 mg, 4.7x10^{-3} mmol) was added to the mixture. After checking the species by NMR, Cs_2CO_3 (3.0 mg, 9.4x10^{-3} mmol) was introduced and the tube was shaken vigorously. The species formed in solution at room temperature were examined again by ^{19}F and $^{31}P\{^1H\}$ NMR (Figure 3.20 and Figure 3.21).

The spectroscopic data of the identified species are given in former experimets.

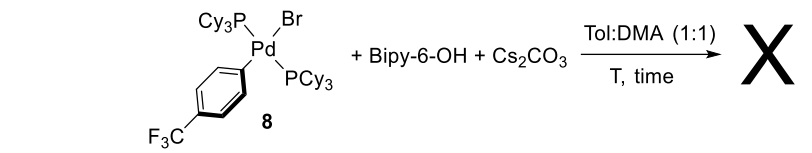

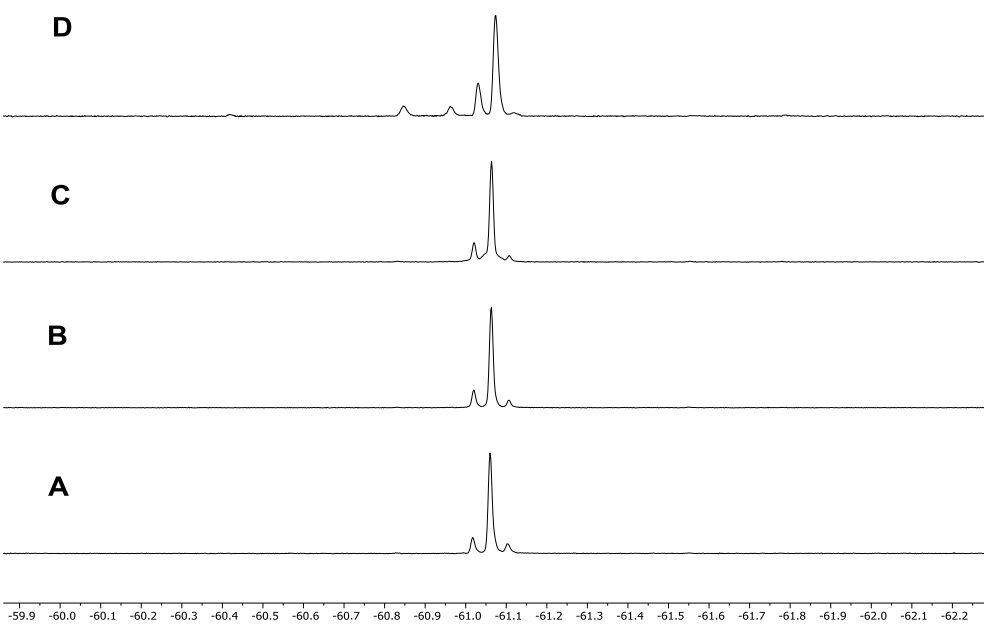

Figure 3.20. ^{19}F NMR spectra (470.168 MHz). A) Complex **8** in toluene:DMA (1:1). B) Sample A after adding 1 equivalent of bipy-6-OH. C) Sample B after adding 2 equivalents of Cs_2CO_3. D) Sample C after heating for 30 min at 100 ºC.

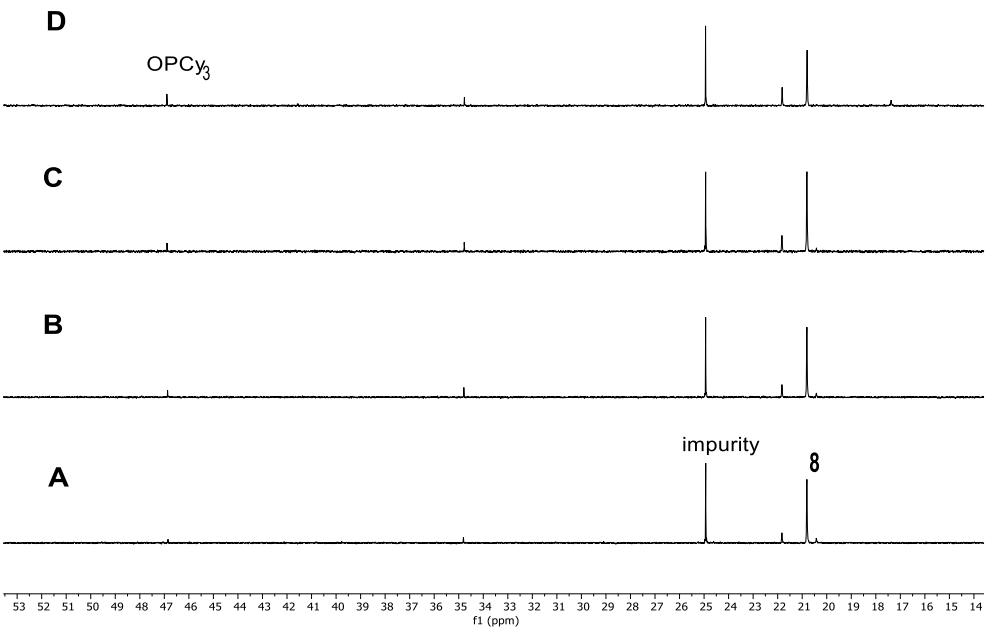

Figure 3.21. $^{31}P\{^{1}H\}$ NMR spectra (202.31 MHz). A) Complex **8** in toluene:DMA (1:1). B) Sample A after adding 1 equivalent of bipy-6-OH. C) Sample B after adding 2 equivalents of Cs_2CO_3. D) Sample C after heating for 30 min at 100 ºC.

Transmetallation experiments

*Reactions of [Pd(bipy-6-O)(C_6F_5)DMA] (**14**) with [PdBr(p-CF_3-C_6H_4)(PCy_3)$_2$] (**8**).*

Complex **1** (5.2 mg, 0.01 mmol) was mixed with 0.6 mL of dry DMA and Ag_2CO_3 (5.5 mg, 0.02 mmol). The mixture was stirred 5 min and then it was filtered. The solution was checked by ^{19}F NMR using a sealed glass capillary filled with DMSO-d6 as NMR lock signal. Complex **8** (8.9 mg, 0.01 mmol) was introduced into the tube. The mixture was heated at 100ºC for the specified time. The species formed in solution at room temperature were examined by ^{19}F and $^{31}P\{^{1}H\}$ NMR (Figure 3.6 and Figure 3.22).

The spectroscopic data of the identified species are given below.

1: (mixture of isomers A and B): Isomer A: ^{19}F NMR (470.168 MHz, δ, DMA/DMSO-d6 capillary): -119.3 (m, 2F, F_{ortho}), -164.4 (m, 1F, F_{para}), -168.4 (m, 2F, F_{meta}). Isomer B: ^{19}F NMR (470.168 MHz, δ, DMA/DMSO-d6 capillary): -119.5 (m, 2F, F_{ortho}), -161.7 (m, 1F, F_{para}), -166.6 (m, 2F, F_{meta}).

14:[25] ^{19}F NMR (470.168 MHz, δ, DMA/DMSO-d6 capillary): -118.8 (m, 2F, F_{ortho}), -162.3 (t, J = 19.6 Hz, 1F, F_{para}), 164.7 (m, 2F, F_{meta}).

8: ^{19}F NMR (470.168 MHz, δ, DMA/DMSO-d6 capillary): -61.87 (CF_3). $^{31}P\{^1H\}$ NMR (202.31 MHz, δ, DMA/DMSO-d6 capillary): 19.93.

11: ^{19}F NMR (470.168 MHz, δ, DMA/DMSO-d6 capillary): -108.0 (m, 2F, F_{ortho}), -162.9 (t, J = 21.4 Hz, 1F, F_{para}), -163.8 (m, 2F, F_{meta}). $^{31}P\{^1H\}$ NMR (202.31 MHz, δ, DMA/DMSO-d6 capillary): 28.1.

C_6F_5-*p*-$(CF_3)C_6H_4$ (C_6F_5-Ar): ^{19}F NMR (470.168 MHz, δ, DMA/DMSO-d6 capillary): -62.75 (s, 3F, F_{CF3}), -144.38 (m, 2F, F_{ortho}), -156.78 (t, J = 21.6 Hz, 1F, F_{para}), -164.11 (m, 2F, F_{meta}).

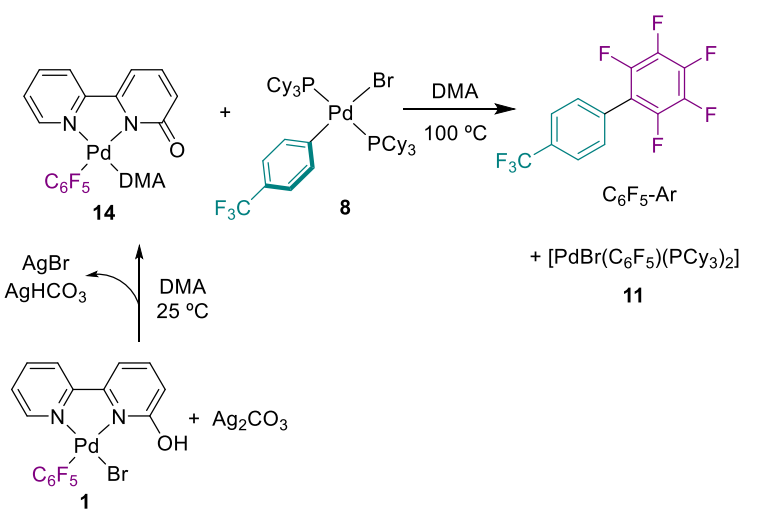

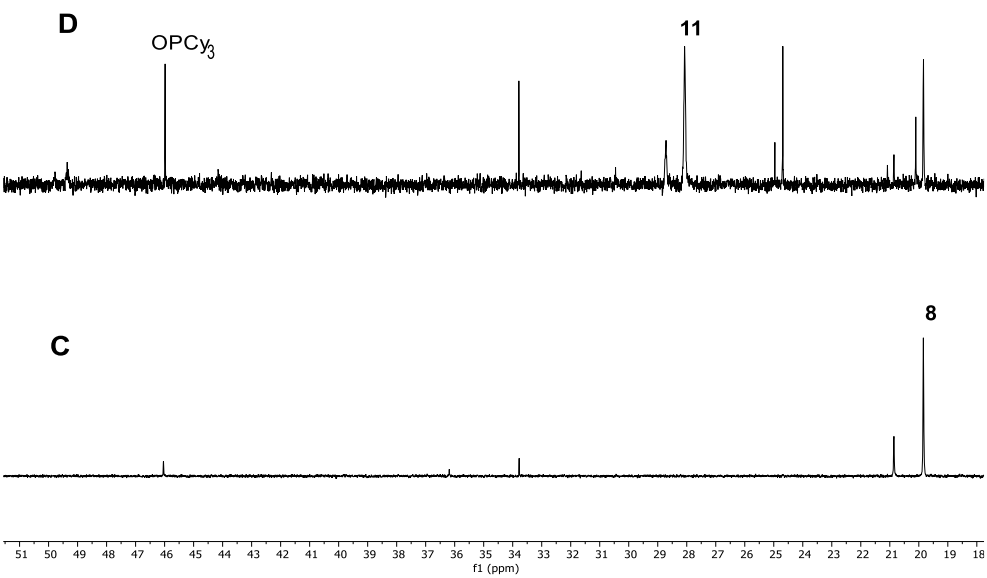

Figure 3.22. $^{31}P\{^{1}H\}$ NMR spectra (202.31 MHz). C) Complex **14** and complex **8** in DMA. D) Sample C after heating for 30 min at 100 °C.

Complex **1** (5.2 mg, 0.01 mmol) was mixed with 0.6 mL of dry DMA and Ag_2CO_3 (5.5 mg, 0.02 mmol). The mixture was stirred 5 min and then it was filtered. The solution was checked by ^{19}F NMR using a sealed glass capillary filled with DMSO-d6 as NMR lock signal. Complex **8** (8.9 mg, 0.01 mmol) and Cs_2CO_3 (6.5 mg, 0.02 mmol) waere introduced into the tube. The mixture was heated at 100ºC for the specified time. The species formed in solution at room temperature were examined by ^{19}F and $^{31}P\{^{1}H\}$ NMR (Figure 3.23 and Figure 3.24).

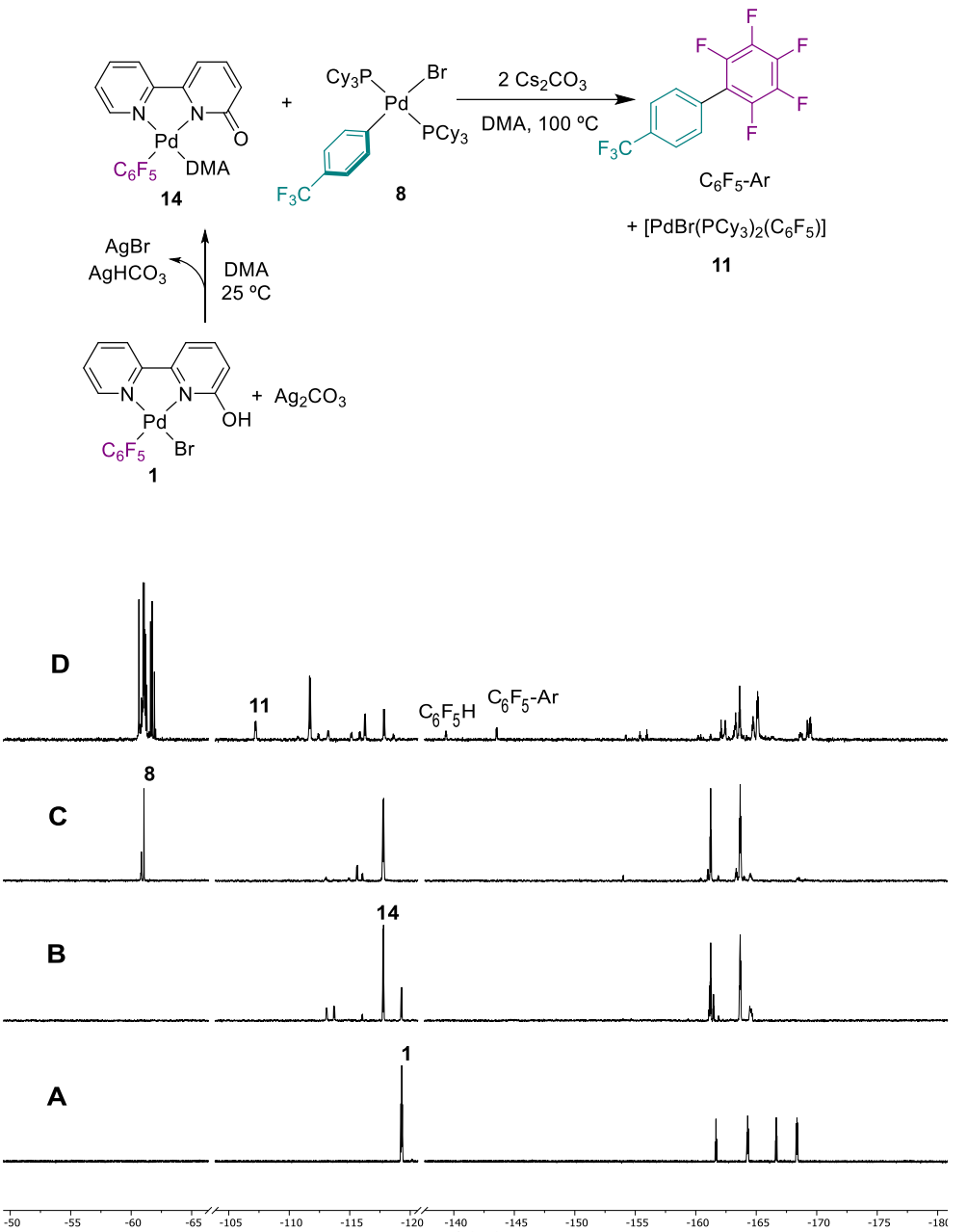

Figure 3.23. ^{19}F NMR spectra (470.168 MHz). A) Complex **1**. B) Sample A + Ag_2CO_3 in DMA. C) Sample B after adding complex **8** and Cs_2CO_3. D) Sample C after heating for 30 min at 100°C. (C_6F_5-Ar 4%)

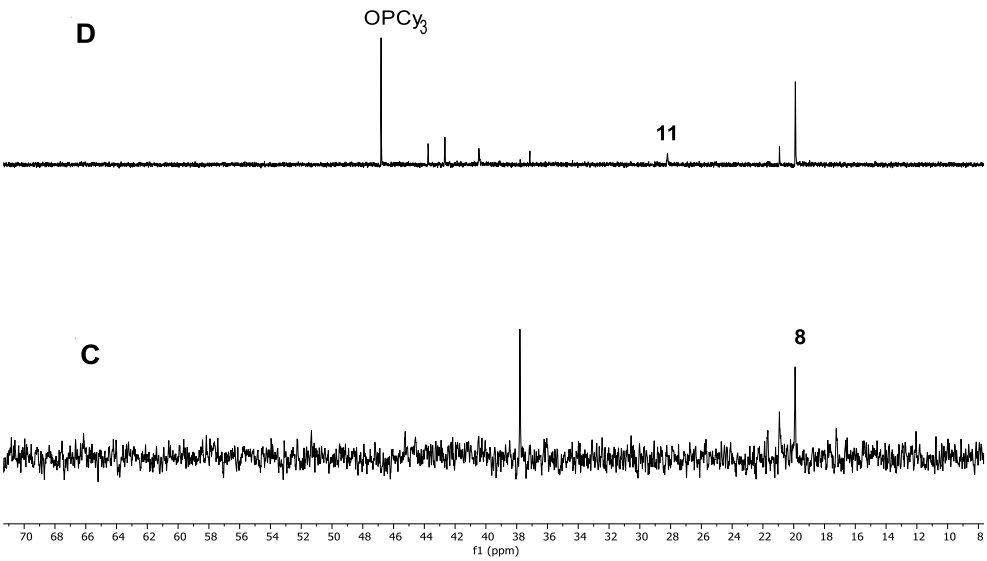

Figure 3.24. $^{31}P\{^{1}H\}$ NMR spectra (202.31 MHz). C) Complex **14**, complex **8** and Cs_2CO_3 in DMA. D) Sample A after heating for 30 min at 100°C.

*Reactions of [Pd(bipy-6-O)(C_6F_5)DMA] (**14**) with [PdBr(p-CF_3-C_6H_4)(PCy_3)]$_2$ (**10**).*

Complex **1** (5.2 mg, 0.01 mmol) was mixed with 0.6 mL of dry DMA and Ag_2CO_3 (5.5 mg, 0.02 mmol). The mixture was stirred 5 min and then it was filtered. The solution was checked by ^{19}F NMR using a sealed glass capillary filled with DMSO-d6 as NMR lock signal. Complex **10** (6.1 mg, 0.001 mmol) was introduced into the tube. The mixture was heated at 100ºC for the specified time. The species formed in solution at room temperature were examined by ^{19}F and $^{31}P\{^{1}H\}$ NMR (Figure 3.7 and Figure 3.25).

The spectroscopic data of the identified species are given below.

10: Slightly soluble.^{19}F NMR (470.168 MHz, δ, DMA/DMSO-d6 capillary): -61.95 (CF_3). $^{31}P\{^{1}H\}$ NMR (202.31 MHz, δ, DMA/DMSO-d6 capillary): 37.74.

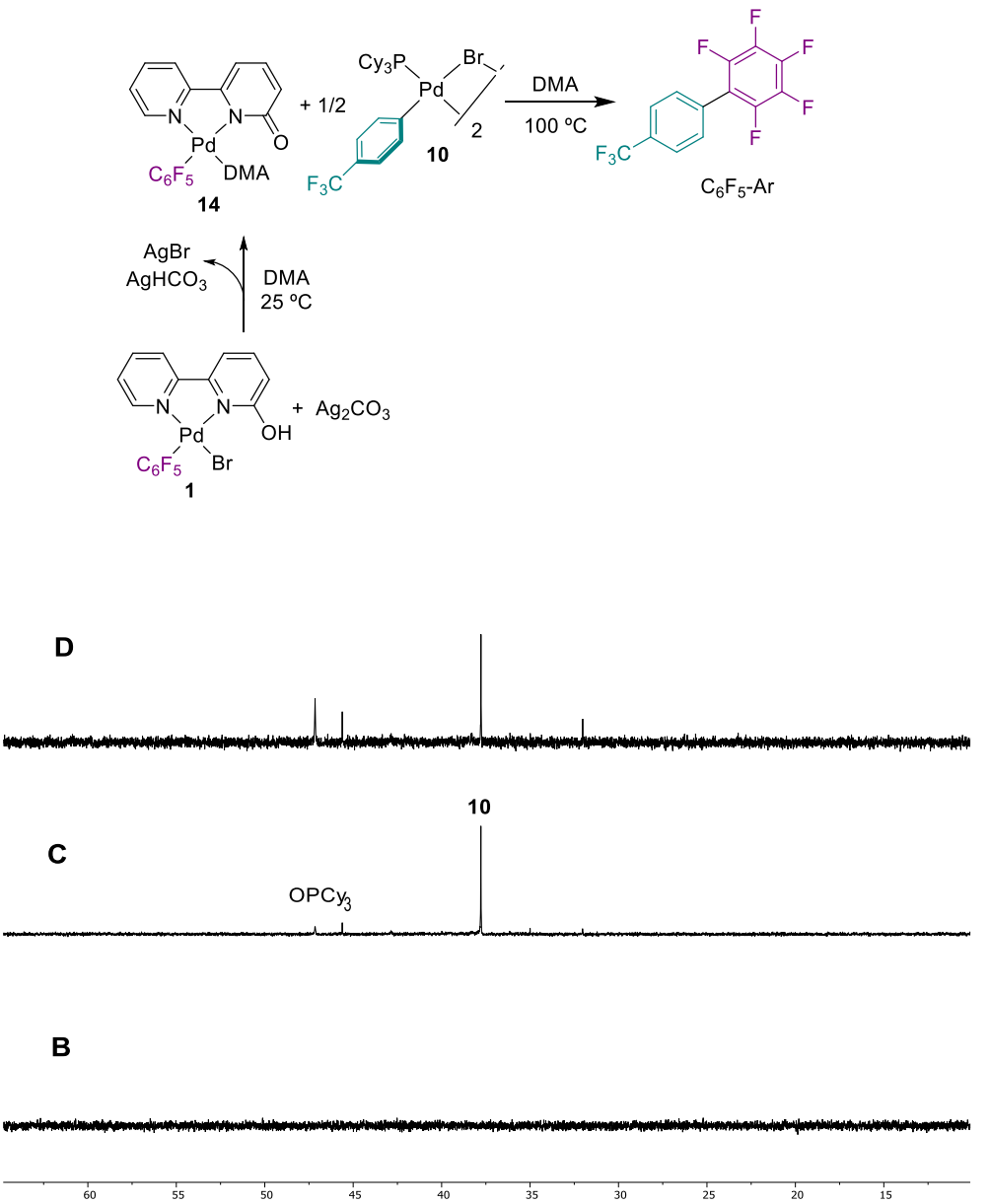

Figure 3.25. $^{31}P\{^{1}H\}$ NMR spectra (202.31 MHz). B) Complex **14** and complex **10** (not soluble) in DMA. C) Sample A after heating for 30 min at 100 °C. D) Sample B after heating for 3 h. * The chemical shift for **10** was assigned by similarity with the characterization in $CDCl_3$.

Complex **1** (2.6 mg, $5x10^{-3}$ mmol) was mixed with 0.6 mL of dry DMA and Ag_2CO_3 (2.7 mg, 0.01 mmol). The mixture was stirred 5 min and then it was filtered. The solution was checked by ^{19}F NMR using a sealed glass capillary filled with DMSO-d6 as NMR lock signal. Complex **10** (3.1 mg, $3.5x10^{-3}$ mmol) and Cs_2CO_3 (3.3 mg, 0.01 mmol) were

introduced into the tube. The mixture was heated at 100 ºC for the specified time. The species formed in solution at room temperature were examined by ^{19}F and $^{31}P\{^{1}H\}$ NMR (Figure 3.26 and Figure 3.27).

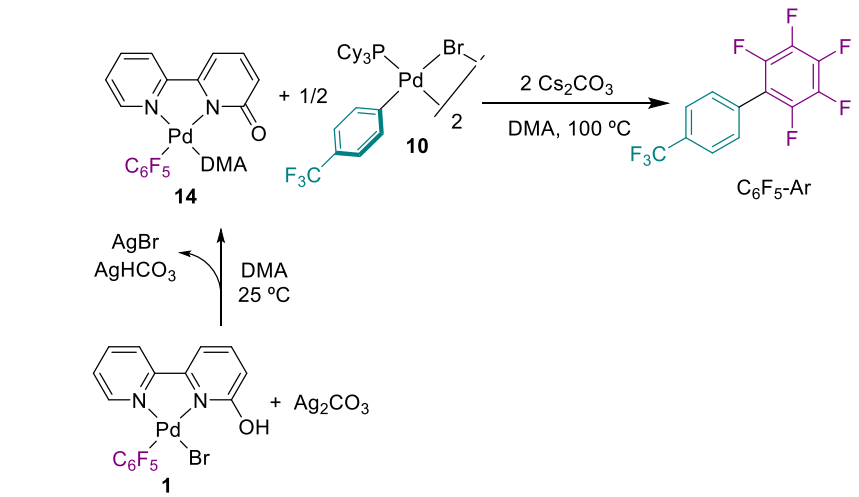

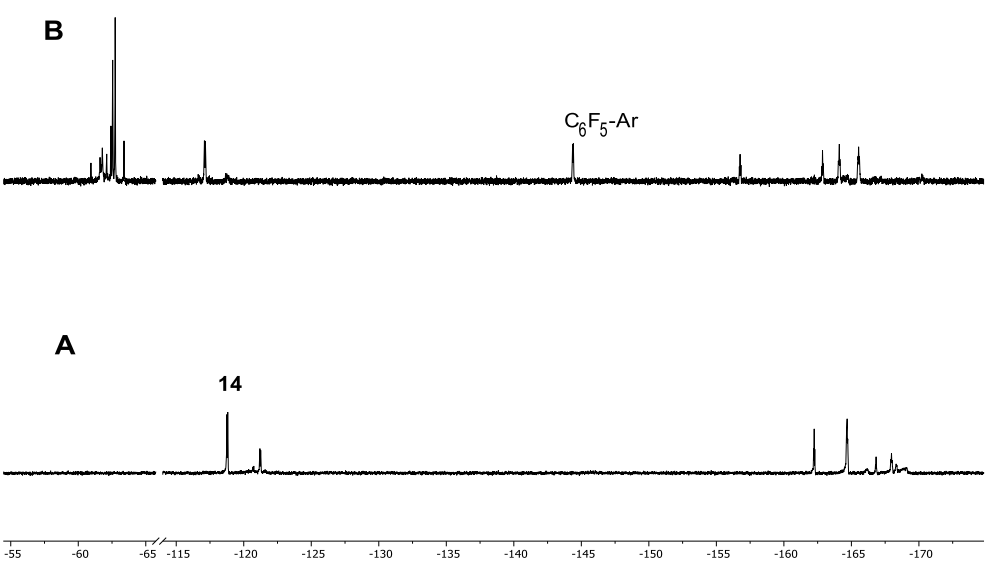

Figure 3.26. ^{19}F NMR spectra (470.168 MHz). A) Complex **14** in DMA. B) Sample A after adding **10** and heating for 30 min a 100 ºC (C_6F_5-Ar 45%).

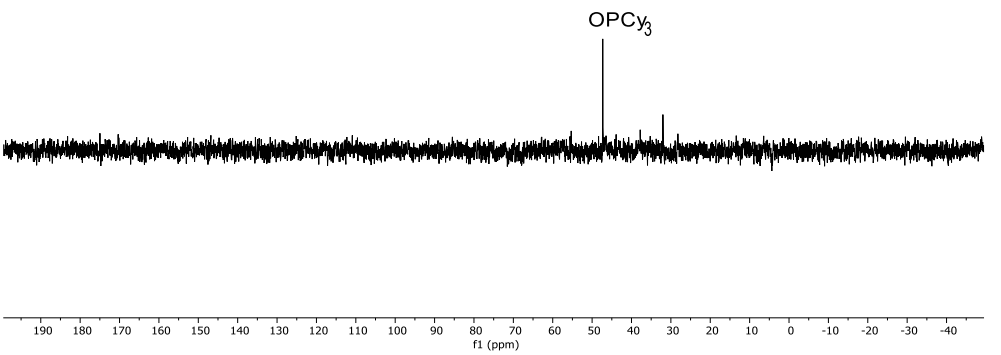

Figure 3.27. $^{31}P\{^{1}H\}$ NMR spectra (202.31 MHz). Mixture of **14**, **10** and Cs_2CO_3 in DMA after heating for 30 min at 100°C.

3.4.5 Kinetic data

Determination of the KIE

Two Schlenk flasks equipped with a septum cap and a Teflon stirring bar were charged with $Pd(OAc)_2$ (3.8 mg, 0.017 mmol), bipy-6-OH (1.5 mg, 0.0085 mmol), PCy_3 (4.7 mg, 0.017 mmol) and cesium carbonate (222 mg, 0.68 mmol) in a nitrogen atmosphere. 4-bromobenzotrifluoride (47 μL, 0.34 mmol) was added to each flask. Then, toluene (1.5 mL) was added to one flask and toluene-d_8 (1.5 mL) to the other. Finally, DMA (1.5 mL) was added to each flasks ($[ArBr]_0$ = 0.12 M). The mixtures were heated at 100 °C with constant stirring. At the indicated time, an aliquot was taken and analysed by ^{19}F NMR adding 0.5 mL of $CDCl_3$ as NMR lock signal. The concentration of the product was determined by integration of the distinct trifluoromethyl signals of reagents and products. The ratio of initial rate constants for both experiments (k_H/k_D) gave the reported KIE value (see below).

Table 3.5. Time and product concentration data for the KIE determining experiments.[a]

	Toluene	**Toluene-d_8**
Time (min)	**[Product] (M)**	**[Product] (M)**
0	0	0
30	0.0045	0.0012
60	0.0102	0.0027
90	0.0193	0.0049
120	0.0295	0.0072
150	0.0408	0.0102
180	0.0533	0.0136

[a]Initial concentration $[ArBr]_0$ = 0.113 M.

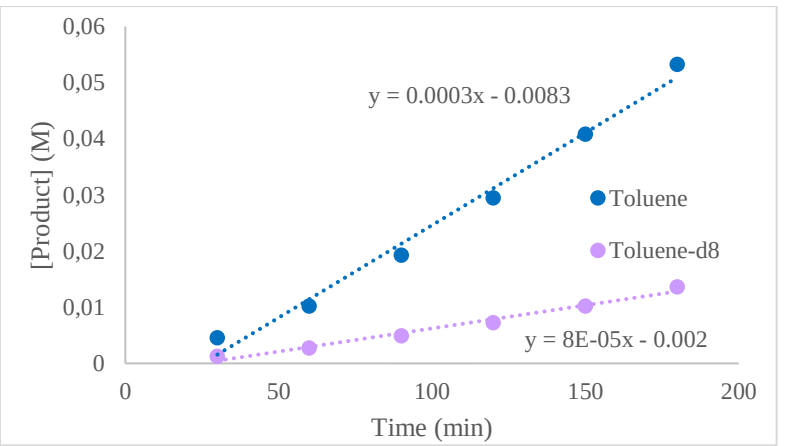

Figure 3.28. Concentration-time plots of the direct arylation of toluene and toluene-d_8.

The ratio of initial reaction rate constants gives the KIE value:

$k_H = 3.3 \pm 0.2 \times 10^{-4}$; $k_D = 8.2 \pm 0.6 \times 10^{-5}$; KIE = $k_H/k_D = 4.0 \pm 0.5$

Kinetic experiments of the direct arylation of toluene

Order in catalyst and aryl bromide

A Schlenk flask equipped with a septum cap and a Teflon stirring bar was charged, in a nitrogen atmosphere, with $Pd(OAc)_2$ (3.8 mg, 0.017 mmol), bipy-6-OH (1.5 mg, 0.0085 mmol), PCy_3 (4.7 mg, 0.017 mmol) and cesium carbonate (222 mg, 0.68 mmol). Then, 4- bromobenzotrifluoride, toluene (1.5 mL) and DMA (1.5 mL) were added. The Schlenk flask was heated at 100 °C with constant stirring. At the indicated time, an aliquot was taken and analysed by ^{19}F NMR adding 0.5 mL of $CDCl_3$ as NMR lock signal. The concentration of the product was determined by integration of the distinct trifluoromethyl signals of reagents and products.

The variable time normalization analysis (VTNA) reported by Burés,[97] was used to determine the order on the reactants for the catalytic reaction (catalyst and aryl bromide). Three experiments were performed each time varying one of the reagent's initial concentrations (Table 3.6). The resulting plots are represented in Figure 3.29.

Table 3.6. Initial concentration values for the kinetic experiments.

Experiment	[Cat][a] (M)	[ArBr] (M)
1	0.0056	0.113
2	0.0028	0.113
3	0.0056	0.227

[a] [Cat] = $Pd(OAc)_2$/ 0.5 bipy-6-OH/ PCy_3; the concentration of each of the three components was halfed in experiment 2. The given concentration corresponds to Pd precursor.

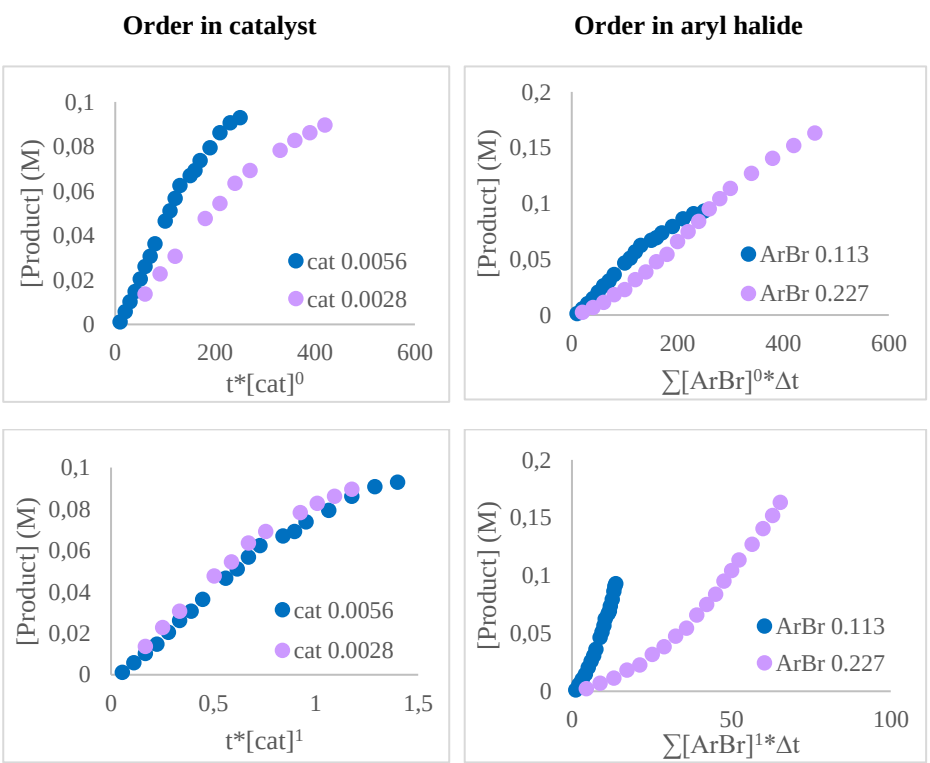

Figure 3.29. Plots derived from the variable time normalization analysis (VTNA). Overlay of plots from two different experiments gives the order in the reagent whose initial concentration is changed (power value in abscissa axis).

Table 3.7. Kinetic data (product concentration at different times) for experiments 1-3 (Table 3.6).

Experiment	Time (min)	[Product] (M)
[Cat] = 0.0056 M [ArBr] = 0.113 M	10	0.0011
	20	0.0057
	30	0.0102
	40	0.0147
	50	0.0204
	60	0.0261
	70	0.0306
	80	0.0363
	100	0.0465
	110	0.0510
	120	0.0567
	130	0.0623
	150	0.0669
	160	0.0691
	170	0.0737
	190	0.0793
	210	0.0861
	230	0.0907
	250	0.0929
[Cat] = 0.0028 M [ArBr] = 0.113 M	60	0.0136
	90	0.0227
	120	0.0306
	180	0.0476
	210	0.0544
	240	0.0635
	270	0.0691
	330	0.0782
	360	0.0827
	390	0.0861
	420	0.0895
	450	0.0941
[Cat] = 0.0056 M [ArBr] = 0.227 M	20	0.0023
	40	0.0068
	60	0.0113
	80	0.0181
	100	0.0227
	120	0.0317
	140	0.0385
	160	0.0476

180	0.0544
200	0.0657
220	0.0748
240	0.0839
260	0.0952
280	0.1042
300	0.1133
340	0.1269
380	0.1405
420	0.1519
460	0.1632

Order in aryl chloride

A Schlenk flask equipped with a septum cap and a Teflon stirring bar was charged, in a nitrogen atmosphere, with $Pd(OAc)_2$ (3.8 mg, 0.017 mmol), bipy-6-OH (1.5 mg, 0.0085 mmol), PCy_3 (4.7 mg, 0.017 mmol) and cesium carbonate (222 mg, 0.68 mmol). Then, 4- chlorobenzotrifluoride, toluene (1.5 mL) and DMA (1.5 mL) were added. The Schlenk flask was heated at 100 °C with constant stirring. At the indicated time, an aliquot was taken and analysed by ^{19}F NMR adding 0.5 mL of $CDCl_3$ as NMR lock signal. The concentration of the product was determined by integration of the distinct trifluoromethyl signals of reagents and products.

Initial rates method was used to determine the order dependence of the aryl chloride. The representation of the product concentration *versus* time gives a line whose slope corresponds to the initial rate for each experiment (Figure 3.30).

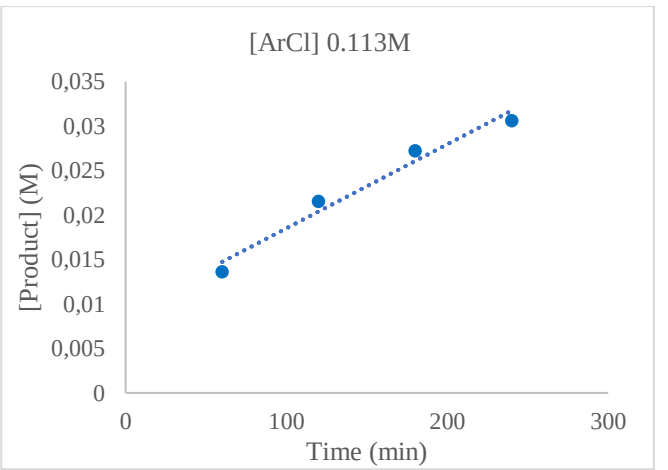

$y = mx + y_0$

$m = 9.4 \pm 1.2 \times 10^{-5}$

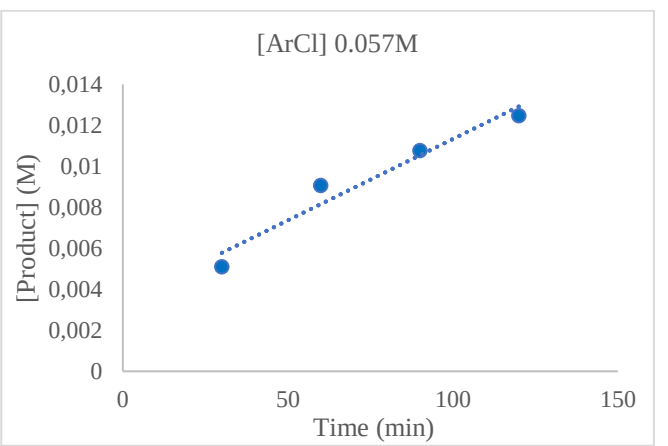

$y = mx + y_0$

$m = 7.9 \pm 1.3 \times 10^{-5}$

Figure 3.30. Concentration-time plots for different concentrations of ArCl.

Table 3.8. Product concentration at different times for experiments in Figure 3.30.

[ArCl] (M)	Time (min)	[Product] (M)	v_0 (min^{-1})
0.113	60	0.0136	$9.4 \pm 1.2 \times 10^{-5}$
	120	0.0215	
	180	0.0272	
	240	0.0306	
0.057	30	0.0051	$7.9 \pm 1.3 \times 10^{-5}$
	60	0.0091	
	90	0.0108	
	120	0.0125	

Effect of the electronic properties of the arenes

Three Schlenk flasks equipped with septum caps and Teflon stirring bars were charged, in a nitrogen atmosphere, with $Pd(OAc)_2$ (3.8 mg, 0.017 mmol), bipy-6-OH (1.5 mg, 0.0085 mmol), PCy_3 (4.7 mg, 0.017 mmol) and cesium carbonate (222 mg, 0.68 mmol). Then, 4- bromobenzotrifluoride (47 µL, 0.34 mmol), the corresponding arene (1.5 mL) and DMA (1.5 mL) were added. The Schlenk flask was heated at 100 °C with constant stirring. At the indicated time, an aliquot was taken and analysed by ^{19}F NMR adding 0.5 mL of $CDCl_3$ as NMR lock signal. The concentration of the product was determined by integration of the distinct trifluoromethyl signals of reagents and products.

Initial rates method was used to determine the kinetic constant for each experiment.

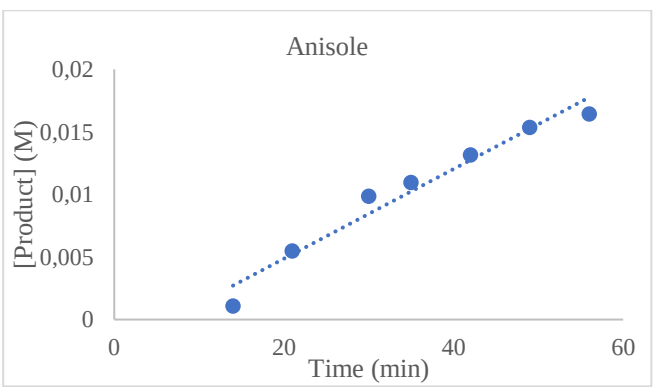

$y = mx + y_0$

$m = 3.6 \pm 0.3 \times 10^{-4}$

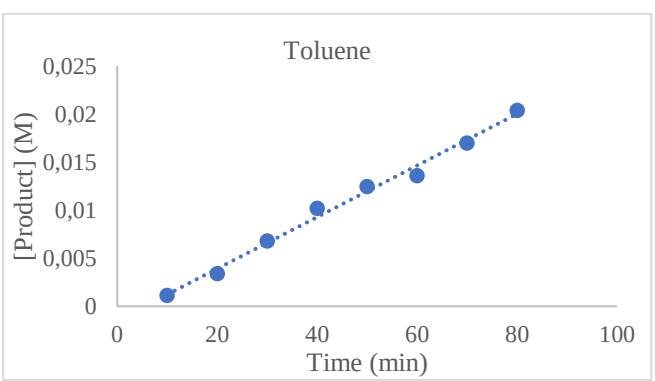

$y = mx + y_0$

$m = 2.7 \pm 0.1 \times 10^{-4}$

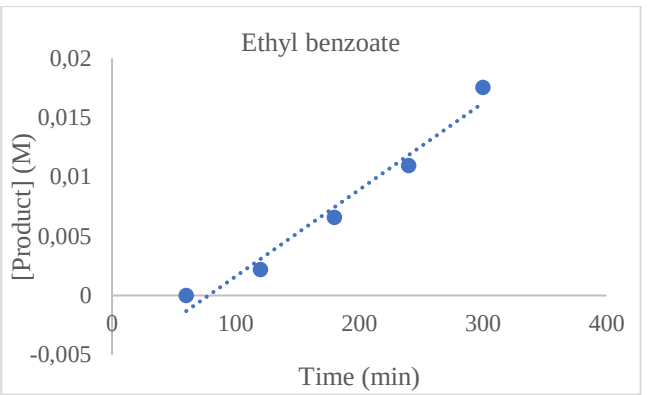

$y = mx + y_0$

$m = 7.3 \pm 0.7 \times 10^{-5}$

Figure 3.31. Concentration-time plots for different arenes.

Table 3.9. Product concentration at different times for experiments in Figure 3.31.

Arene	Time (min)	[Product] (M)	v_0 (min^{-1})
Anisole	14	0.0011	$3.6 \pm 0.3 \times 10^{-4}$
	21	0.0055	
	30	0.0099	
	35	0.0110	
	42	0.0132	
	49	0.0153	
	56	0.0164	
Toluene	10	0.0011	$2.7 \pm 0.1 \times 10^{-4}$
	20	0.0034	
	30	0.0068	
	40	0.0102	
	50	0.0125	
	60	0.0136	
	70	0.0170	
	80	0.0204	
Ethyl benzoate	60	0	$7.3 \pm 0.7 \times 10^{-5}$
	120	0.0022	
	180	0.0066	
	240	0.0110	
	300	0.0175	

3.4.6 Computational details

The DFT studies have been performed with the M06 functional,[102] as implemented in the Gaussian09 program package.[145] The 6-31+G(d) basis set was used for C, O, N, F and H,[103] and LANL2TZ(f) for Pd, Cs and Br[104] (BS I). Solvent effects have been considered trough the continuum model SMD for the experimental solvent, DMA, which was introduced in all the optimizations, frequency calculations and potential energy refinement. All structure optimizations were carried out in solvent phase with no symmetry restrictions. Gibbs energy corrections were calculated at 373.15 K (the experimental temperature) and 10^5 Pa pressure, including zero-point energy corrections (ZPE), and the energies were converted to 1M standard state in solution (adding/subtracting 2.89 kcal mol^{-1} for non-unimolecular processes). Vibrational frequency calculations were performed in order to confirm that the stationary points were minima (without imaginary frequencies) or transition states (with one imaginary frequency). Connectivity of the transition state structures was confirmed by relaxing the transition state geometry towards both the reactant and the product. Final potential energies were refined by performing additional single-point energy calculations (also in solution); Pd, Cs and Br were still described with LANL2TZ(f) basis set, and the remaining atoms were treated with 6-311++G(d,p) basis set (BS II). All energies presented correspond to Gibbs energies in solution, obtained from potential energies (including solvation) with basis set II plus Gibbs energy corrections with basis set I.

Table 3.10. Bond distances comparison between the different TS for the C–H activation step.

	d(C-H) (Å)	**d(C-Pd) (Å)**
TS c2-c3	1.30288	2.14578
TS c5-c6	1.32032	2.16517

[145] Gaussian 09, Revision D.01, Frisch, M. J.; Trucks, G. W.; Schlegel, H. B.; Scuseria, G. E.; Robb, M. A.; Cheeseman, J. R.; Scalmani, G.; Barone, V.; Mennucci, B.; Petersson, G. A.; Nakatsuji, H.; Caricato, M.; Li, X.; Hratchian, H. P.; Izmaylov, A. F.; Bloino, J.; Zheng, G.; Sonnenberg, J. L.; Hada, M.; Ehara, M.; Toyota, K.; Fukuda, R.; Hasegawa, J.; Ishida, M.; Nakajima, T.; Honda, Y.; Kitao, O.; Nakai, H.; Vreven, T.; Montgomery, J. A., Jr.; Peralta, J. E.; Ogliaro, F.; Bearpark, M.; Heyd, J. J.; Brothers, E.; Kudin, K. N.; Staroverov, V. N.; Kobayashi, R.; Normand, J.; Raghavachari, K.; Rendell, A.; Burant, J. C.; Iyengar, S. S.; Tomasi, J.; Cossi, M.; Rega, N.; Millam, J. M.; Klene, M.; Knox, J. E.; Cross, J. B.; Bakken, V.; Adamo, C.; Jaramillo, J.; Gomperts, R.; Stratmann, R. E.; Yazyev, O.; Austin, A. J.; Cammi, R.; Pomelli, C.; Ochterski, J. W.; Martin, R. L.; Morokuma, K.; Zakrzewski, V. G.; Voth, G. A.; Salvador, P.; Dannenberg, J. J.; Dapprich, S.; Daniels, A. D.; Farkas, Ö.; Foresman, J. B.; Ortiz, J. V.; Cioslowski, J.; Fox, D. J. Gaussian, Inc., Wallingford CT, **2009**.

Chapter 4

4 Assessment of the Cooperating Ability of Chelating Ligands in Palladium-Catalysed C–H Activation Reactions.

4.1 INTRODUCTION

Metal-ligand cooperation has been used in the last years as a new strategy to synthesise complex molecules through a different way from traditional synthesis. Usually, the new approaches introduce new reaction pathways or facilitate reaction steps that bring advantages as far as reaction conditions or reactants used are concerned, as commented in the general introduction.

In the previous chapters, the use of the cooperating ligand bipy-6-OH clearly demonstrates the advantages of the metal-ligand cooperation system. The correct choice of the ligand structure and electronic properties is crucial for its role in the reaction. It is also significant to consider the synthesis of the ligand, since an easier synthesis leads to a more accessible process overall.

The use of MPAAs as assisting ligands in palladium-catalysed C–H activation reactions has been widely studied in the last decades as has been previously commented (*Chapter 1.4*). The chelating coordination mode of the ligand and its ability to assist the C–H activation step are essential properties in their role through the reaction.[57, 58, 59]

Taking into account the features that have made MPAAs and bipy-6-OH successful cooperating ligands in C–H activation, the cooperating ability of related 6-hydroxypicolinic acid and amido-pyridine type ligands was assessed and it will be discussed in this chapter. Their structure comparison to the established cooperating ligands mentioned above can be seen in Figure 4.1.

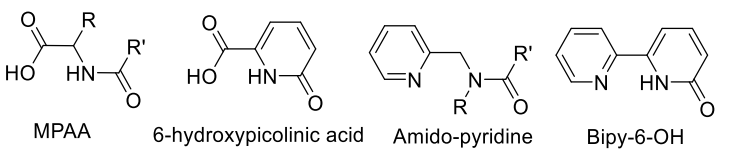

Figure 4.1. Structure similarities between MPAAs, 6-hydroxypicolinic acid, amido-pyridine type ligands and bipy-6-OH.

The compound 6-hydroxypicolinic acid has a similar arrangement as the MPAAs ligands, with the advantage of having a more rigid and delocalized structure due to the pyridine ring. In addition, the cooperating moiety (pyridone group) is equal to that in the bipy-6-OH. The ligand would coordinate in the chelating mode in palladium complexes, plausible key compounds during the catalytic reaction. Moreover, it is commercially available, avoiding the requirement of synthesising the ligand beforehand. This ligand, and its regioisomers, have been used coordinated to iridium for the oxidation of water,[146] and recently a similar derivative has proved to be very effective in the C–H hydroxylation of arenes (Figure 4.2).[147] The ligand reported has one -CR_2- group as a link between the carboxylic acid and the pyridine, forming a six-membered chelate complex when it is coordinated to palladium, Figure 4.3.

[146] a) Bucci, A.; Savini, A.; Rocchigiani, L.; Zuccaccia, C.; Rizzato, S.; Albinati, A.; Llobet, A.; Macchioni, A. *Organometallics*, **2012**, *31*, 8071-8074. b) Menendez Rodriguez, G.; Bucci, A.; Hutchinson, R.; Bellachioma, G.; Zuccaccia, C.; Giovagnoli, S.; Idriss, H.; Macchioni, A. *ACS Energy Lett.* **2017**, *2*, 105-110. c) Dijk, B.; Menendez Rodriguez, G.; Wu, L.; Hofmann, J. P.; Macchioni, A.; Hetterscheid, D. G. H. *ACS Catal*. **2020**, *10*, 4398-4410. d) Menendez Rodriguez, G.; Zaccaria, F.; Dijk, S. V.; Zuccaccia, C.; Macchioni, A. *Organometallics* **2021**, *40*, 3445-3453.
[147] Li, Z.; Park, H. S.; Qiao, J. X.; Yeung, K.-S.; Yu, J.-Q. *J. Am. Chem. Soc*. **2022**, *144*, 18109-18116.

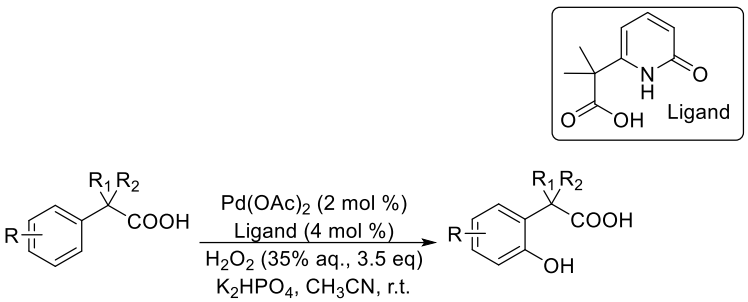

Figure 4.2. C–H hydroxylation of arenes with carboxylic acid as directing groups with aqueous H_2O_2.

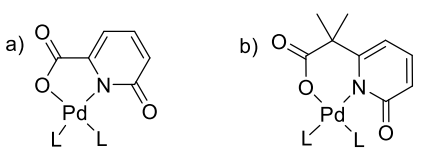

Figure 4.3. a) Five-membered chelate complex of 6-hydroxypicolinic acid as ligand. b) Six-membered chelate derivative reported in ref. 147.

The amido-pyridine derivatives have a structure quite comparable to the bipy-6-OH ligand. Their acyl moiety is similar to the one observed in the MPAAs and potentially cooperating. They could cooperate in palladium-catalysed processes in the same way as the bipy-6-OH with the advantage of a simpler and modular synthetic route, *via* reaction of an amine and a carbonyl compound. Some derivatives of the amido-pyridine ligands have been used in the synthesis of copper complexes for structural studies,[148] or in palladium reactions.[149] There are some precedents of the use of similar ligands, called as acetyl-protected aminoethyl quinolines (APAQ), in C–H activation.[150] A particular example is the enantioselective arylation of methylene C–H bonds of aliphatic amides (Figure 4.4).[151]

---

[148] a) Mondal, A.; Li, Y.; Khan, M. A.; Ross, J. S.; Houser, R. P. *Inorg. Chem.* **2004**, *43*, 7075-7082. b) Chaudhuri, U. P.; Whiteaker, L. R.; Yang, L.; Houser, R. P. *Dalton Trans*., **2006**, 1902-1908. c) Cody, C. C.; Kelly, H. R.; Mercado, B. Q.; Batista, V. S.; Crabtree, R. H.; Brudvig, G. W. *Inorg. Chem*. **2021**, *60*, 14759-14764.

[149] Pérez-Gómez, M.; Azizollahi, H.; Franzoni, I.; Larin, E. M.; Lautens, M.; García-López, J.A. *Organometallics* **2019**, *38*, 973-980.

[150] a) Yang, Y.-F.; Hong, X.; Yu, J.-Q.; Houk, K. N. *Acc. Chem. Res*. **2017**, *50*, 2853-2860. b) Yang, Y.-F.; Chen, G.; Hong, X.; Yu, J.-Q.; Houk, K. N. *J. Am. Chem. Soc*. **2017**, *139*, 8514-8521. c). Hill, D. E.; Pei, Q.-L.; Zhang, E.-X.; Gage, J. R.; Yu, J.-Q.; Blackmond, D. G. *ACS Catal*. **2018**, *8*, 1528-1531. d) Romero, E. A.; Chen, G.; Gembicky, M.; Jazzar, R.; Yu, J.-Q.; Bertrand, G.; *J. Am. Chem. Soc*. **2019**, *141*, 16726-16733.

[151] Chen, G.; Gong, W.; Zhuang, Z.; Andrä, M. S.; Chen, Y.-Q.; Hong, X.; Yang, Y. F.; Liu, T.; Houk, K. N.; Yu, J.-Q. *Science*, **2016**, *353*, 1023-1027.

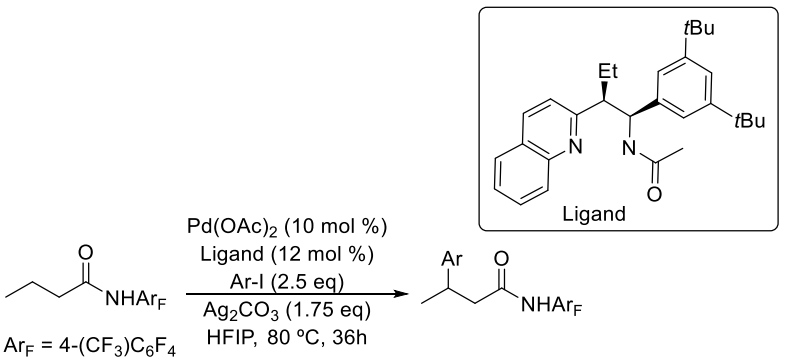

Figure 4.4. Enantioselective methylene C(sp^3) –H bond arylation.

All the ligands (bipy-6-OH, 6-hydroxypicolinic acid and amido-pyridine type ligands) have in common a ketone in their structure in a crucial position. The ketone group is close enough to the metal centre to assist, acting as a base, during the C–H activation step. The proposed TS for the three different ligands can be seen in Figure 4.5.

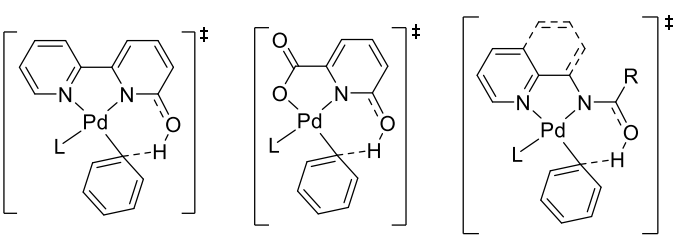

Figure 4.5. Proposed TS for the C-H activation step.

Due to the structural similarity of the proposed ligands to the bipy-6-OH and the MPAAs, their ability to enable the C–H activation step was assessed and they were tested in different catalytic reactions where an accelerating effect was observed when using bipy-6-OH or MPAAs. The chosen reactions are described in the results and discussion section.

4.2 RESULTS AND DISCUSSION

The description of the results and their discussion of this chapter are divided in two main sections: study of the cooperating ability of the ligand 6-hydroxypicolinic acid in direct arylation reactions and the assessment of the cooperating ability of the amido-pyridine ligands in palladium-catalysed C–H functionalization reactions.

4.2.1 Study of the cooperating ability of the ligand 6-hydroxypicolinic acid.

The coordinating ability of 6-hydroxypicolinic acid (pic-6-OH) as ligand to a palladium centre was first tested. The ligand is diprotic and can be deprotonated to act in its mono- and dianionic forms. The reaction between two equivalents of the 6-hydroxypicolinic acid and the palladium dimer $(NBu_4)_2[PdBr(C_6F_5)(\mu\text{-}Br)]_2$ produced a palladium complex with a monoanionic coordinated ligand as can be seen in the Equation 4.1. The complex **15** was obtained as a mixture of two different isomers tentatively assigned to the cis-trans geometries, depending on the position of the bromo atom and the pentafluorophenyl group. The geometry of each isomer could not be assigned and they are named as major isomer (**15M**) and minor isomer (**15m**). **15M** shows broad signals in its NMR spectra indicating that a fluxional process in solution is operating. The ratio of the isolated mixture was **M**:**m** 1:0.4.

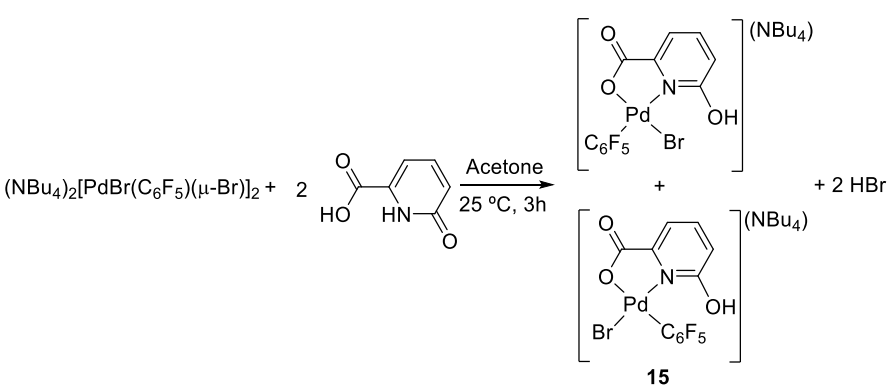

15

Equation 4.1.

The reaction of the isomer mixture with silver carbonate in the presence of pyridine results in an anionic complex with the ligand completely deprotonated and coordinated as a chelate to the metal centre (Equation 4.2.). After the abstraction of the bromine atom with the silver salt, a molecule of pyridine coordinated in the vacant site.

The structure of complex **16** was confirmed by the determination of its molecular structure by X-Ray diffraction (Figure 4.6).

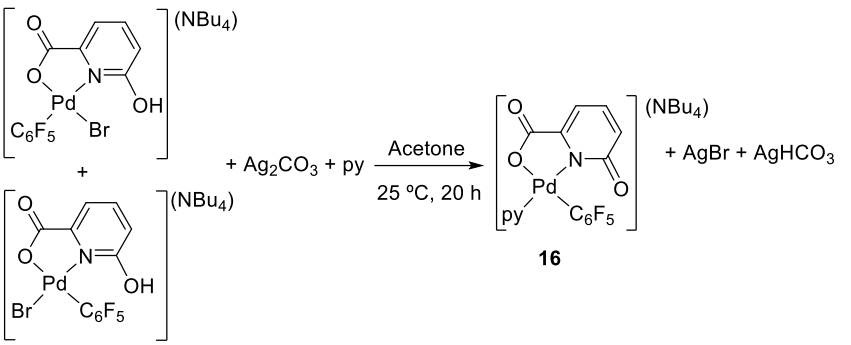

Equation 4.2.

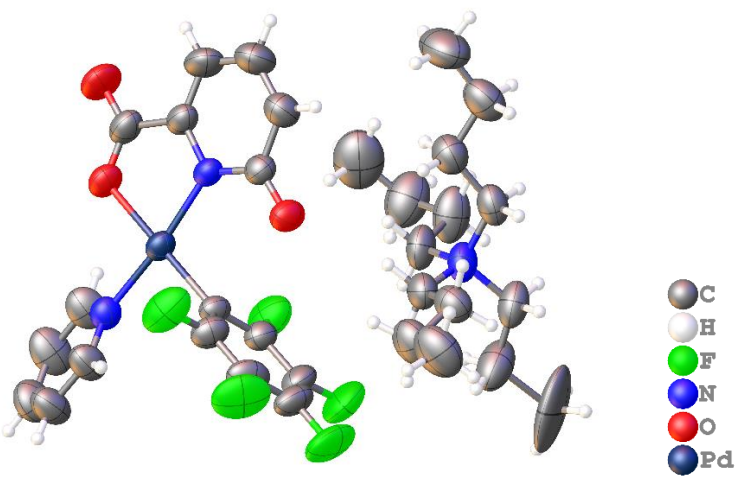

Figure 4.6. X-ray molecular structure of (NBu4)[Pd(6-oxidopicolinato)(C_6F_5)(py)] (**16**). ORTEP plot (40 % probability ellipsoids) is shown.

There are only a few examples in the literature of isolated palladium complexes with an amino acid coordinated or with MPAAs as ligands.[59] The easy isolation of the complex **16** and its stability confirms the better coordination ability of this ligand compared with the MPAAs. This complex was used to study the cooperating ability of the ligand in C–H activation reactions.

The direct arylation of arenes was chosen as model catalytic reaction since it has been thoroughly studied in our research group using bipy-6-OH as cooperating ligand with different arenes, and obtaining excellent results.[20] This reaction would be the perfect candidate due to the large mechanistic knowledge on this reaction gathered in the group.

The arenes selected were pyridine,[152] ethyl benzoate and toluene. They are representative of arenes with different coordination ability (py >> PhCOOEt > PhMe). The reported operating catalytic cycle for the direct arylation of arenes with the cooperating bipy-6-OH can be drawn for the ligand pic-6-OH as shown in Figure 4.7. In a simplified way, it involves four main steps. First the oxidative addition of the aryl halide followed by the coordination of the arene displacing the halide. The intermediate **I₃** will undergo the C–H activation of the arene assisted by the coordinated ligand. Finally, the reductive elimination will release the coupling product and the deprotonation of the ligand recovers the active catalyst.

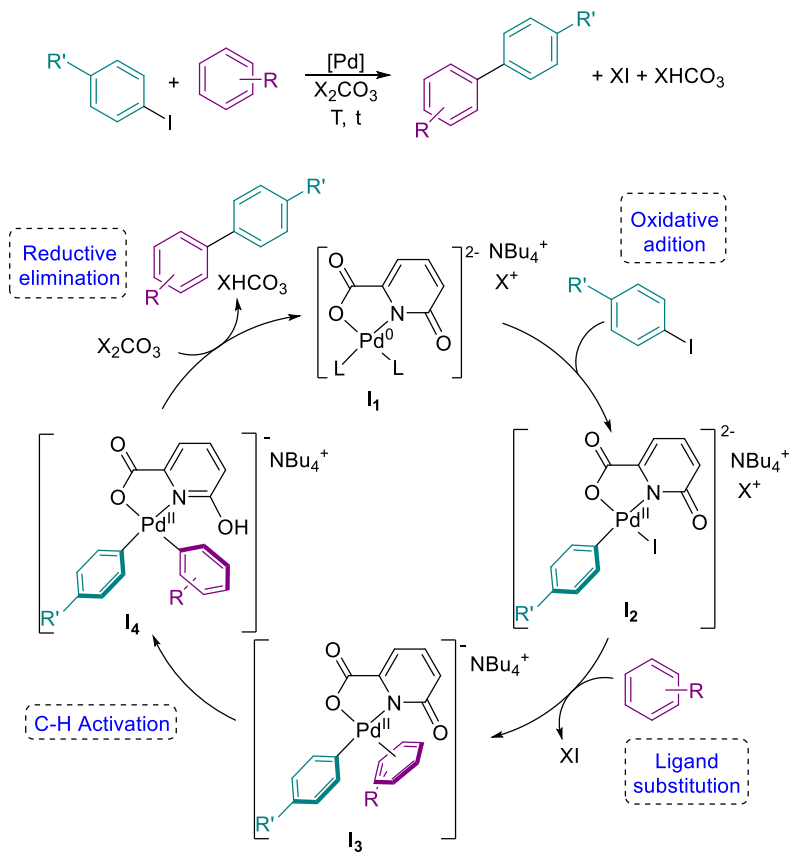

Figure 4.7. Simplified putative catalytic cycle for the direct arylation of arenes with the ligand pic-6-OH.

[152]a) Guo, P.; Joo, J. M.; Rakshit, S.; Sames, D. *J. Am. Chem. Soc.* **2011**, *133*, 16338-16341. b) Ye, M.; Gao, G.-L.; Edmunds, A. J. F.; Worthington, P. A.; Morris, J. A.; Yu, J.-Q. *J. Am. Chem. Soc.* **2011**, *133*, 19090-19093. c) Dai, F.; Gui, Q.; Liu, J.; Yang, Z.; Chen, X.; Guo, R.; Tan, Z. *Chem. Comm.* **2013**, *49*, 4634-4636. d) Gao, G.-L.; Xia, W.; Jain, P.; Yu, J.-Q. *Org. Lett.* **2016**, *18*, 744-747. e) Musaev, D. G.; Haines, B. E. *Chem. Cat. Chem.* **2021**, *13*, 1201-1206.

The complex **16** is similar to the intermediate of the reaction previous to the C–H activation step, **I**$_3$, where the aryl from the aryl halide would be the pentafluorophenyl ring and the arene coordinated, the pyridine. Thus, the monitoring of the reaction described in Equation 4.3 allows to study the C–H cleavage and the cooperation of the ligand during this step.

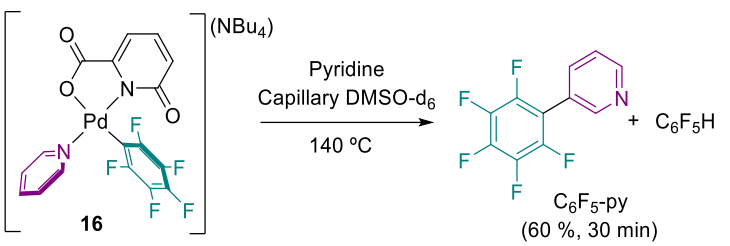

Equation 4.3.

The thermal decomposition of **16** in pyridine at 140 °C in the absence of base, results in the formation of the coupling product *meta*-C_6F_5-py in a 60 % after 30 min, as can be seen in Figure 4.8. The byproduct $[Pd(C_6F_5)_2(py)_2]$ formed by group reorganization between two different palladium complexes was also observed in a 30 % yield. This reorganization is not uncommon for pentafluorophenyl derivatives,[59] and it occurs by transmetalation between palladium centres.[153]

[153] a) Casado, A. L.; Casares, J. A.; Espinet, P. *Organometallics* **1997**, *16*, 5730-5736. b) Albéniz, A. C.; Espinet, P.; López-Cimas, O.; Martín-Ruiz, B. *Chem. Eur. J.* **2005**, *11*, 242-252.

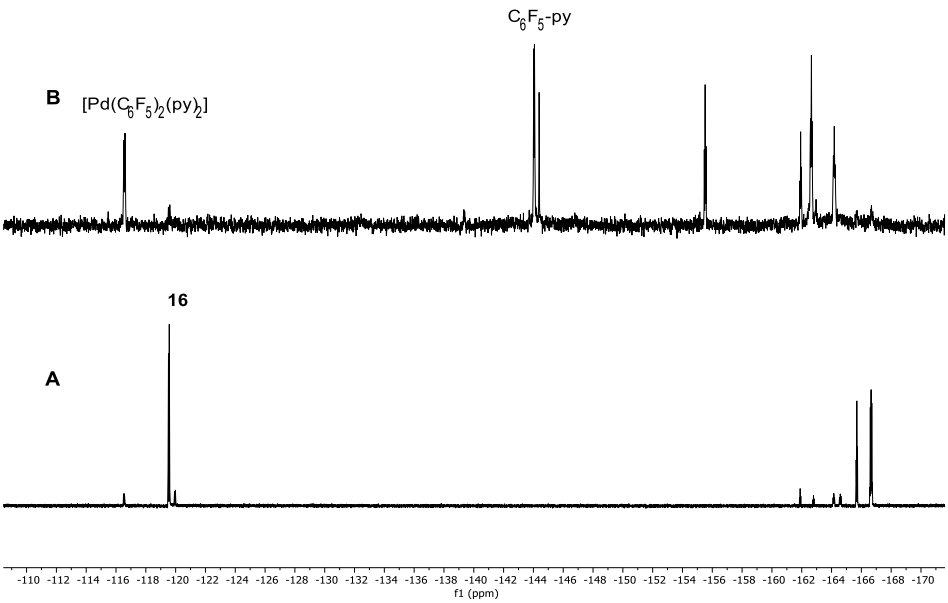

Figure 4.8. ^{19}F NMR spectra (470.168 MHz): A) Complex **16** in pyridine. B) Sample A after heating at 140 °C for 30 min (% mol: **16**, 7 %; $[Pd(C_6F_5)_2(py)_2]$, 33 %; C_6F_5-py, 60 %).

The complex is stable at room temperature even in a coordinating solvent such as pyridine, showing the good coordination ability of the ligand. The experiment clearly demonstrates that the ligand is cooperating in the C–H activation of the arene since there are no additional bases such as carbonates or acetates that could play that role in the reaction media. Moreover, the reductive elimination step in these conditions is fast as in the experiment the coupling product is observed in good yields, even when one of the aryl groups is pentafluoropenyl, which is more reluctant to undergo reductive elimination.

The same experiment was done in toluene (Equation 4.4) and ethyl benzoate (Equation 4.5) as solvents (see Figure 4.9 and Figure 4.10). In toluene, the starting complex is not soluble and an internal standard (C_6F_6) was used during the reaction to quantify the coupling products. Only a 10 % of the coupling product was observed after heating for 30 min. In contrast to pyridine as arene (*meta* coupling) the C–H activation of toluene is not regioselective and a mixture of isomers for the C_6F_5-tol coupling products was obtained (Figure 4.10). This has been observed before for the C–H functionalization reactions with bipy-6-OH as cooperating ligand.[20] Moreover, the pyridine coupling product was also observed (1 %), indicating that the displacement of the pyridine by toluene is not complete even in conditions of large excess. The low

solubility of complex **16** in toluene probably determines the slow rate of the C–H activation and the low amount of C_6F_5-tol coupling product observed after 30 min.

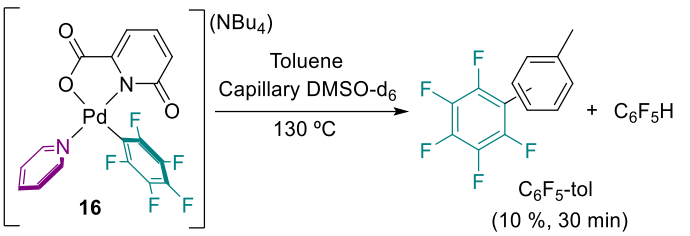

Equation 4.4.

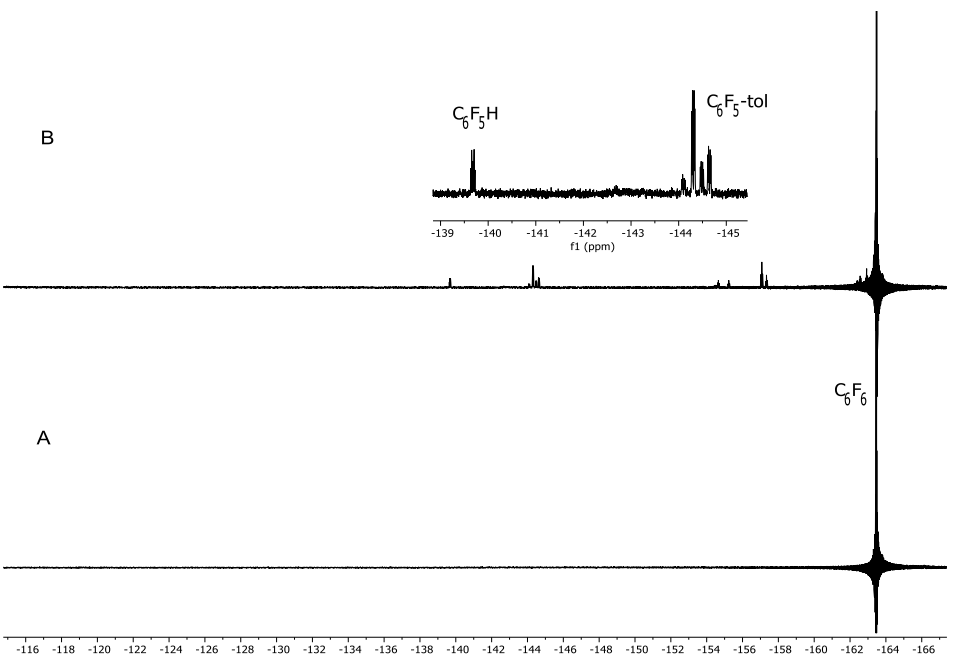

Figure 4.9. ^{19}F NMR spectra (470.168 MHz): A) Complex **16** in toluene with the internal standard (C_6F_6). B) Sample A after heating at 130 °C for 30 min (% mol: C_6F_5-tol, 10 %; C_6F_5H, 2 %; C_6F_5-py, 1 %).

In the case of ethyl benzoate as solvent, complex **16** is soluble and 82 % of the desired coupling products was obtained after heating for 30 min. This demonstrates that the C–H activation of ethyl benzoate assisted by the ligand is possible in excellent yields.

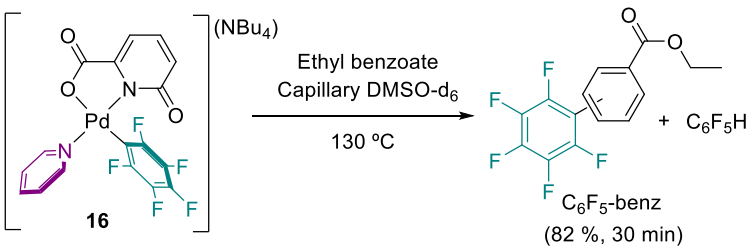

Equation 4.5.

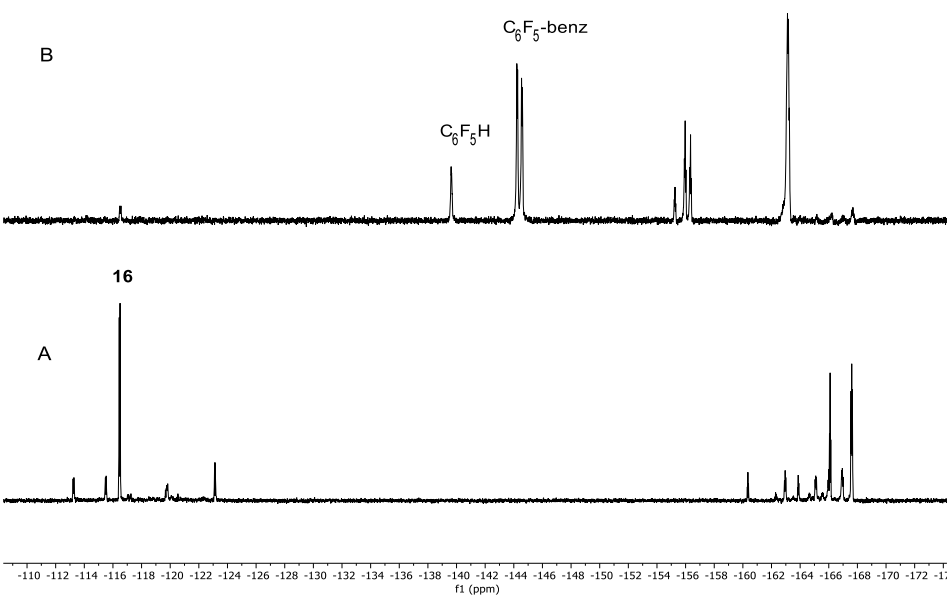

Figure 4.10. ^{19}F NMR spectra (470.168 MHz): A) Complex **16** in ethyl benzoate. B) Sample A after heating at 130 °C for 30 min (% mol: **16,** 4 %; C_6F_5-benz, 82 %; C_6F_5-H, 14%).

DFT calculations at the M06 level were done in order to gather information about the energy requirements for the C–H activation step using pyridine as model arene and trifluoromethylphenyl as aryl group (Figure 4.11). The C–H cleavage is usually the turnover limiting step for the direct arylation reactions, and this was found in the reported example for the direct arylation of pyridine with *p*-$CF_3C_6H_4I$ with bipy-6-OH as ligand (activation Gibbs energy 27.5 kcal mol^{-1}).[20] In our case the energy barrier was found to be 25.4 kcal mol^{-1}, comparable to the former results. This barrier is also in agreement with the conditions needed for the thermal decomposition of the preformed complex. It is clear that the ligand is able to cooperate in the C–H activation of the arene in the same way as the bipy-6-OH ligand does.

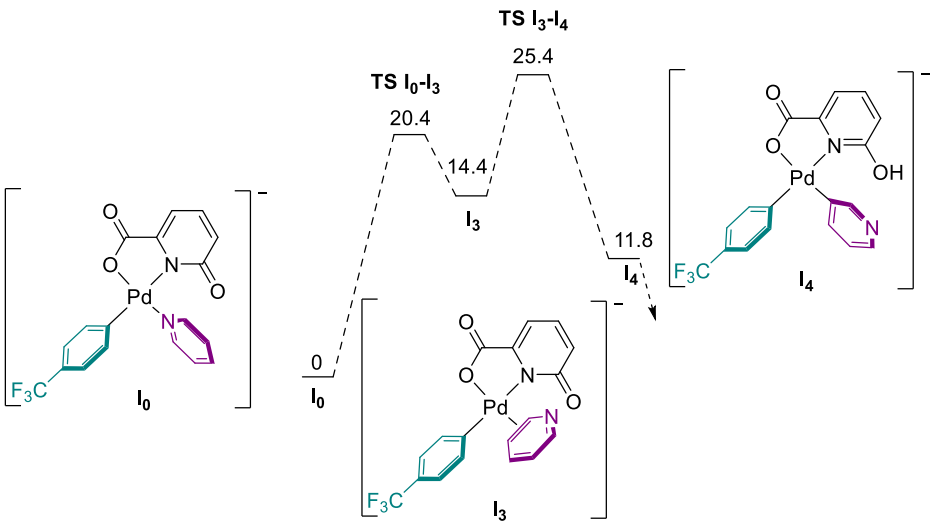

Figure 4.11. Gibbs energy profile for the ligand-assisted cleavage of the *meta* C–H bond of pyridine. Energies in kcal mol^{-1}. Conditions: pyridine as solvent at 140 ºC.

After the experiments described above, we can conclude that the ligand is a good candidate to test in the catalytic C–H functionalization reactions. The model catalytic reaction chosen to test the ligand was the direct arylation of arenes reported by the group as commented before. A reaction scheme is shown in Equation 4.6, where an aryl iodide would be the coupling partner, palladium salts or preformed palladium complexes were used as catalyst and cesium carbonate is usually employed as base.

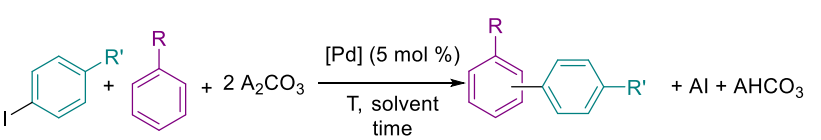

Equation 4.6.

The direct arylation of pyridine has been reported to give the coupling product at the C3 carbon of the pyridine selectively. Equation 4.7 shows the reaction conditions used: an aryl halide in pyridine as solvent at 140 °C and a carbonate as base. The reaction with *p*-iodotrifluorotoluene as aryl halide was thoroughly studied using several bases and additives due to the easy monitorization of the reaction by ^{19}F NMR and it will be discussed below. A few reactions were tested for *p*-iodotoluene and they are collected in the experimental part (Table 4.9).

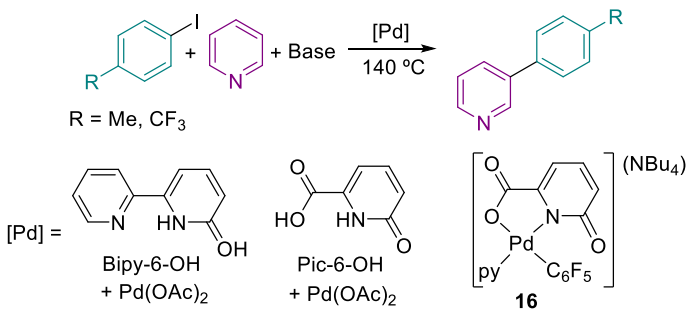

Equation 4.7

As it is shown in Table 4.1, the reaction did not take place when no ligand is used (entry 1, Table 4.1). By adding the ligand bipy-6-OH (entry 2, Table 4.1), the reaction was completed after 2 h. However, the ligand pic-6-OH did not have a significant accelerating effect in the process when it was added either as free ligand (entry 3, Table 4.1) or previously coordinated to palladium (entry 4, Table 4.1). In the latter case, the conversion was higher but large amounts of byproducts were observed (homocoupling product of the aryl halide, Ar-Ar, and reduction product, Ar-H), indicating that the catalyst is not active enough for the target transformation under these conditions.

Different bases were tried in order to see the effect of their solubility or of the nature of the counterion (entries 5 and 6, Table 4.1). Silver carbonate led to a faster reaction but the final yield after 24 h was low. Meanwhile with potassium carbonate the reaction did not take place. In the case of a base with different basicity such as phosphate, no accelerating effect was observed (entry 7, Table 4.1). Looking for a more soluble base, tetrabutylammonium salts were used like acetate and hydrogen phosphate; however higher yields were not obtained (entries 8 and 9, Table 4.1). As carbonate gave the best results, we decided to add tetrabutylammonium chloride as phase transfer agent together with sodium carbonate in order to increase the solubility of the base, but only a 20 % of coupling product was formed (entry 10, Table 4.1). In the same vein, the addition of NBu_4BF_4 to the reaction with cesium carbonate as base resulted in a faster reaction and better yields, (entry 11, Table 4.1). Thus, the solubility of the base is important for this system.

Table 4.1. Direct arylation of pyridine with *p*-iodotrifluorotoluene as aryl halide.[a]

Entry	[Pd]	Base	Additives	Crude yield, % (conv., %), t (h)[b]	Crude yield, % (conv., %), 24 h[b]
1[c]	$Pd(OAc)_2$	Cs_2CO_3	-	0 (0) 6 h	0 (0)
2[c]	$Pd(OAc)_2$ + **bipy-6-OH**	Cs_2CO_3	-	94 (100) 2 h	-
3	$Pd(OAc)_2$ + **pic-6-OH**	Cs_2CO_3	-	0 (6) 6 h	14 (31)
4	**16**	Cs_2CO_3	-	5 (16) 6 h	23 (93)
5	**16**	Ag_2CO_3	-	32 (38) 6 h	32 (44)
6	**16**	K_2CO_3	-	1 (7) 6 h	1 (9)
7	**16**	K_3PO_4	-	4 (4) 6 h	4 (11)
8	**16**	$(NBu_4)OAc$	-	9 (23) 6 h	10 (33)
9[d]	**16**	$(NBu_4)_2HPO_4$	-	13 (34) 6 h	15 (95)
10	**16**	Na_2CO_3	$(NMe_4)Cl$ (0.68 mmol)	8 (27) 6 h	20 (92)
11	**16**	Cs_2CO_3	$(NBu_4)BF_4$ (0.68 mmol)	48 (98) 6 h	-
12[e]	**16**	$(NBu_4)CO_3Me$	-	38 (63) 6 h	40 (75)
13	**16**	$(NBu_4)CO_3Me$	$(NBu_4)I$ (0.34 mmol)	56 (87) 2 h	-
14	**16**	$(NBu_4)CO_3Me$	$(NBu_4)BF_4$ (0.68 mmol)	57 (94) 2 h	-
15[f]	**16**	$(NBu_4)CO_3Me$	DMA (2.5 mL)	41 (100) 2 h	-
16[g]	**16**	$(NBu_4)CO_3Me$	DMA (1.5 mL)	70 (100) 2 h	-
17	**16**	$(NBu_4)_2CO_3$	-	48 (90) 2 h	-
18[g]	**16**	$(NBu_4)_2CO_3$	DMA (1.5 mL)	55 (100) 2 h	-
19	$Pd(OAc)_2$ + **pic-6-OH**	$(NBu_4)_2CO_3$	-	18 (51) 6 h	19 (95)

[a]Reaction conditions: ArI (0.34 mmol), pyridine (3.0 mL), [Pd] (5 mol %), base (0.34 mmol). [b]Crude yields determined by ^{19}F NMR of the reaction mixture. The reduction of the ArI (ArH) and the homocoupling (Ar-Ar) are the observed byproducts.[c] Data taken from the literature.[20] [d]Base (0.68 mmol). [e]Same reaction after 2 h: 35 (68). [f]DMA as solvent, pyridine (0.34 mmol). [g]DMA (1.5 mL) and pyridine (1.5 mL) as solvents.

As a way to use a preformed more soluble carbonate, tetrabutylammonium methyl carbonate and tetrabutylammonium carbonate were synthesised. The reported procedure for the synthesis of $(NBu_4)_2CO_3$ consists on bubbling CO_2 into a solution of NBu_4OH in methanol forming $(NBu_4)HCO_3$.[154] After adding more NBu_4OH and evaporating the solvent a solid, supposedly containing $(NBu_4)_2CO_3$, can be isolated (Scheme 4.1).

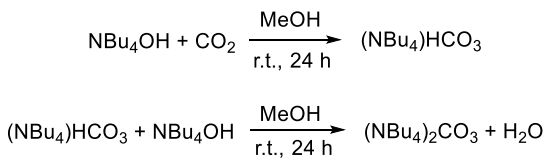

Scheme 4.1. Reported synthesis of tetrabutylammonium carbonate.

However in our hands, after analysing the solid obtained, we found that $(NBu_4)CO_3Me$ was formed. Methanol can also react with CO_2 forming methyl hydrogen carbonate. After an acid-base reaction with NBu_4OH, $(NBu_4)CO_3Me$ can be isolated (Scheme 4.2). We observed a quartet signal of the carbonate carbon in the ^{13}C NMR indicating the formation of $(NBu_4)CO_3Me$ (Figure 4.12) whereas the spectrum of $(NBu_4)_2CO_3$ should show a singlet signal for the carbonate.

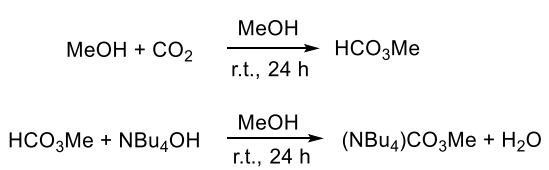

Scheme 4.2. Synthesis of tetrabutylammonium methyl carbonate.

[154] Yang, C.-T.; Fu, Y.; Huang, Y.-B.; Yi, J.; Guo, Q.-X.; Liu, L. *Angew. Chem. Int. Ed.* **2009**, *48*, 7398-7401.

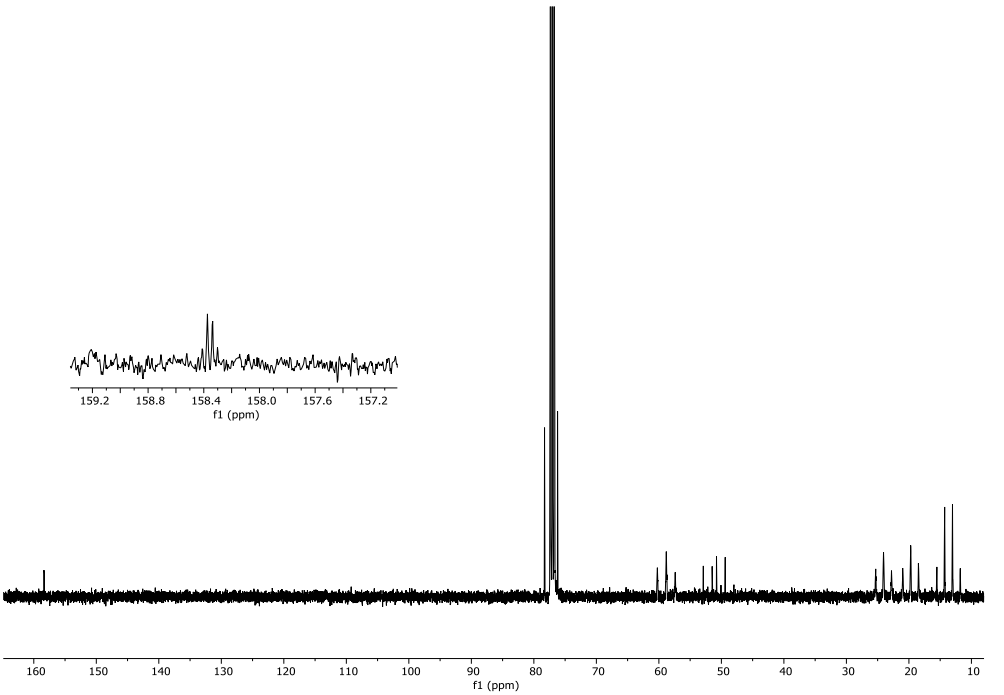

Figure 4.12. ^{13}C NMR of tetrabutylammonium methyl carbonate.

An alternative and more convenient synthesis of tetrabutylammonium carbonate was developed, avoiding the use of methanol as solvent (Scheme 4.3). Tetrabutylammonium hydroxide hydrate was solubilized in dichloromethane and CO_2 was bubbled. After the addition of the second equivalent of NBu_4OH and the evaporation of the solvents, $(NBu_4)_2CO_3$ was isolated.

$$NBu_4OH \cdot 30\ H_2O + CO_2 \xrightarrow[\text{r.t., 24 h}]{CH_2Cl_2} (NBu_4)HCO_3$$

$$(NBu_4)HCO_3 + NBu_4OH \cdot 30\ H_2O \xrightarrow[\text{r.t., 24 h}]{CH_2Cl_2} (NBu_4)_2CO_3 + H_2O$$

Scheme 4.3. New synthesis of tetrabutylammonium carbonate.

The use of $(NBu_4)CO_3Me$ as base in the catalytic reaction led to an increase of the yield of the coupling product and reaction rate when compared to the use of Cs_2CO_3 (entry 4, Table 4.1) but the amount of byproducts is still high (entry 12, Table 4.1). The addition of soluble salts to increase the polarity of the reaction media led to faster reactions and better, but still moderate, yields (entries 13 and 14, Table 4.1). The use of a polar solvent such as DMA and a stoichiometric amount of pyridine did not produce

any better result (entry 15, Table 4.1). Meanwhile if DMA is used as co-solvent together with pyridine the best results were obtained: 70 % of coupling product after 2 h (entry 16, Table 4.1).

When $(NBu_4)_2CO_3$ was used as base the reaction is more efficient than that with methyl carbonate (entries 12 and 17, Table 4.1) but in contrast with the latter, the use of DMA together with $(NBu_4)_2CO_3$ did not give any advantage and similar results were obtained as when no co-solvent was used (entry 18, Table 4.1). Even with the soluble carbonates it is not possible to use the precatalytic mixture $Pd(OAc)_2$ with the free ligand (entry 19, Table 4.1).

The use of soluble bases as carbonate or methyl carbonate clearly increases the product's yield in the direct arylation of pyridine but just moderate values were obtained. The ligand pic-6-OH is able to cooperate in the C–H cleavage of the pyridine coordinated to palladium in its dianionic form (see Equation 4.3) and therefore a high concentration of base may be more important to keep the ligand completely deprotonated and coordinated to the metal in pyridine in comparison to the monoprotic bipy-6-OH. Nevertheless, even under these conditions the accelerating effect of pic-6-OH in the complete reaction is lower and other competing reaction come into play (homocoupling and reduction).

The direct arylation of toluene was next tested. Toluene is a less coordinating arene than pyridine so the problem of displacing the ligand would be less important. However, this advantage could turn into a disadvantage since the coordination of the arene is needed before the C–H activation step. As can be seen in Equation 4.8., *p*-iodotrifluorotoluene was chosen as aryl halide (easy monitoring of the reaction mixture by ^{19}F NMR) and several bases were tried.

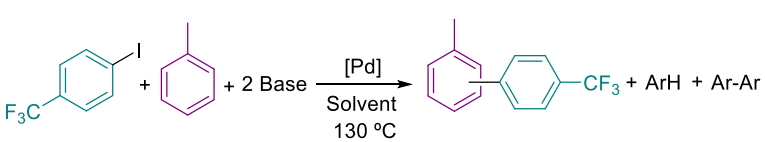

Equation 4.8.

The results are shown in Table 4.2. When no ligand is used the reaction did not take place (entry 1, Table 4.2) and with the ligand bipy-6-OH the reaction is completed after 24 h (entry 2, Table 4.2). The mixture of the ligand pic-6-OH/$Pd(OAc)_2$ or the

preformed complex are not active in the process when toluene is used as solvent (entries 3 and 4, Table 4.2).

Table 4.2. Direct arylation of toluene.[a]

Entry	[Pd]	Base	Solvent	Crude yield, % (conv., %), t h[b]	Crude yield, % (conv., %), 24h[b]
1[c]	$Pd(OAc)_2$	Cs_2CO_3	Tol	0 (0) 6 h	0 (0)
2[c]	$Pd(OAc)_2$+ **bipy-6OH**	Cs_2CO_3	Tol	20 (22) 6 h	91 (100)
3	$Pd(OAc)_2$ + **pic-6-OH**	Cs_2CO_3	Tol	3 (6) 6 h	7 (14)
4	**16**	Cs_2CO_3	Tol	2 (10) 6 h	2 (26)
5	$Pd(OAc)_2$ + **pic-6-OH**	Cs_2CO_3	Tol:Pin (1:1)	7 (15) 6 h	9 (19)
6	**16**	Cs_2CO_3	Tol:Pin (1:1)	18 (78) 6 h	20 (87)
7[d]	$Pd(OAc)_2$ + **pic-6-OH**	$(NBu_4)CO_2Me$	Tol	7 (98) 2 h	-
8[d]	**16**	$(NBu_4)CO_2Me$	Tol	20 (35) 2 h	24 (98)
9[d]	**16**	$(NBu_4)CO_2Me$	Tol:Pin (1:1)	28 (100) 2 h	-
10	$Pd(OAc)_2$ + **pic-6-OH**	$(NBu_4)_2CO_3$	Tol	9 (98) 2 h	-
11	**16**	$(NBu_4)_2CO_3$	Tol	23 (100) 6 h	-

[a]Reaction conditions: ArI (0.34 mmol), solvent (3.0 mL), [Pd] (5 mol %), base (0.68 mmol). [b]Crude yields determined by ^{19}F NMR of the reaction mixture. The reduction of the ArI (ArH), the homocoupling (Ar-Ar) and the coupling with pinacolone (Ar-Pin) are the observed byproducts. [c]Data taken from the literarure. [d]Base (0.51 mmol).

The use of a co-solvent together with toluene to accelerate the reaction was previously described and the best results were obtained with pinacolone.[20] The use of a mixture toluene:pinacolone (1:1 v/v) as solvent only led to an improvement when complex **16** was used as catalyst: a 20 % of the coupling product was formed (entry 6, Table 4.2). However, there were a large amount of byproducts (mixture of reduction of the aryl halide Ar-H, homocoupling Ar-Ar and coupling with pincacolone Ar-Pin).

Cesium carbonate is almost insoluble in toluene so more soluble bases were tried. Tetrabutylammonium methyl carbonate and tetrabutylammonium carbonate gave similar results as cesium carbonate but in lower reaction times (entries 7-11, Table 4.2).

The last reaction explored was the direct arylarion of ethyl benzoate, an arene with a coordinating ability in between toluene and pyridine as commented before (Equation 4.9.). In the same way, *p*-iodotrifluorotoluene was used as aryl halide and different bases were tried. The results are given in Table 4.3.

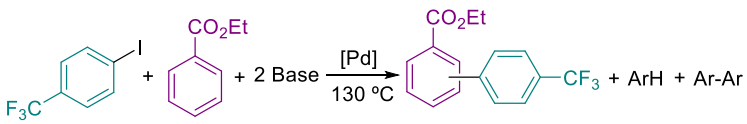

Equation 4.9.

The reaction with palladium acetate and no added ligand led to an almost complete conversion of the ArI but very small amount of the aryl-benzoate coupling product. Large amounts of byproducts, mainly homocoupling of the aryl halide (73 %), were found (entry 1, Table 4.3). The use of bipy-6-OH led to excellent yields of the desired product (entry 2, Table 4.3). Using the mixture pic-6-OH and palladium acetate, moderated yields were observed after 24 h, while with the complex **16** traces of the product were formed (entries 3 and 4, Table 4.3).

Table 4.3. Direct arylation of ethyl benzoate[a].

Entry	[Pd]	Base	Crude yield, % (conv., %), t h[b]	Crude yield, % (conv., %), 24h[b]
1	$Pd(OAc)_2$	Cs_2CO_3	9 (99) 6 h	-
2[c]	$Pd(OAc)_2$ + **bipy-6OH**	Cs_2CO_3	84 (100) 6 h	-
3	$Pd(OAc)_2$ + **pic-6-OH**	Cs_2CO_3	10 (17) 6 h	41 (60)
4	**16**	Cs_2CO_3	3 (35) 6 h	8 (40)
5	**16**	Ag_2CO_3	23 (47) 6 h	50 (97)
6[d]	$Pd(OAc)_2$ + **pic-6-OH**	$(NBu_4)CO_3Me$	38 (97) 2 h	-
7[d]	**16**	$(NBu_4)CO_3Me$	47 (99) 2 h	-
8	$Pd(OAc)_2$ + **pic-6-OH**	$(NBu_4)_2CO_3$	17 (97) 2 h	-
9	**16**	$(NBu_4)_2CO_3$	47 (99) 2 h	-

[a]Reaction conditions: ArI (0.34 mmol), solvent (3.0 mL), [Pd] (5 mol %), base (0.68 mmol). [b]Crude yields determined by ^{19}F NMR of the reaction mixture. The reduction of the ArI (ArH) and the homocoupling (Ar-Ar) are the observed byproducts. [c]Data taken from the literature. [d]Base (0.51 mmol).

Different bases were also evaluated. Silver carbonate led to moderated yields and the relative amount of byproducts was increased (entry 5, Table 4.3). When soluble tetrabutylammonium carbonates were used, the reaction was over after 2 h. The preformed complex seemed to be more active with those bases (entries 7 and 9, Table 4.3) than the mixture of palladium salt and free ligand (entries 6 and 8, Table 4.3). In both cases, the amount of byproducts is over 50 %.

Taking into account all the experiments done, it is clear that the ligand is able to assist in the C–H activation step as has been demonstrated by the thermal decomposition of complex **16** and the DFT calculations. However, in the catalytic reaction the amount of byproducts is really high and the coupling product is obtained in poor to moderate yields in all the cases, even in the best conditions when polar solvents or soluble bases were used. This is in contrast to the related bipy-6-OH, which is highly efficient in these transformations. One of the major byproducts detected is the homocoupling product formed by the reorganization between two palladium aryl complexes prior to the C–H cleavage, i.e. intermediate $\mathbf{I_2}$ in the catalytic cycle or other palladium aryl species (Figure 4.7). This process involves the transmetalation of an aryl group from one palladium centre to another in a dimer to form a bis-aryl complex (Equation 4.13) and may be favoured by pic-6-OH acting in different coordination modes, for example, as a κ^2-O, O monoanionic bridging ligand through the acetato group or in a monodentate form providing an available vacant site. The ligand cooperation in the C–H cleavage occurs when it is bound to the metal in a chelating κ^2-O, N dianionic mode and the importance of this is supported by the beneficial effect of a soluble base in the catalysis which favours the complete deprotonation of the ligand. Pic-6-OH can adopt a higher number of coordination modes than bipy-6-OH and this opens new reaction pathways that can be detrimental for an efficient catalysis.

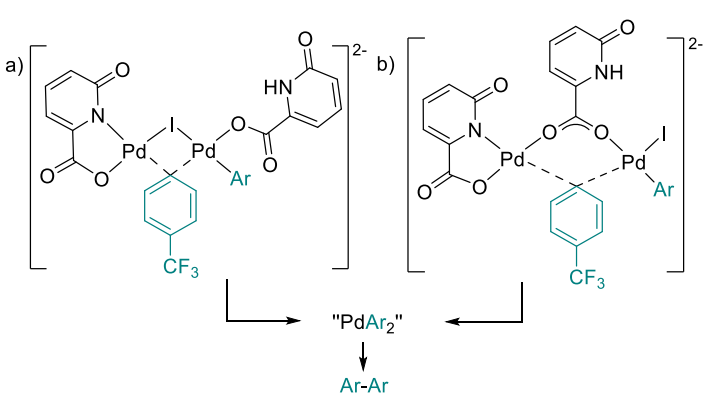

Figure 4.13. Possible transmetallation pathways to form the homocoupling product.

4.2.2 Assessment of the cooperating ability of the amido-pyridine ligands in palladium-catalysed C–H activation reactions.

The amido-pyridine ligands were chosen as potential cooperating ligands in C–H activation reactions due to their structural similarity to the bipy-6-OH and MPAAs, ligands that have demonstrated their accelerating effect in those reactions. The coordination in a chelating mode gives stability to the complexes that are going to be the catalyst of the reaction. In addition, the ketone group close to the metal allows the cooperation during the C–H cleavage. On the other hand, the one-step synthesis and the easy purification make those ligands good candidates to develop more efficient overall synthetic strategies as commented in the introduction.

The general synthesis of the amido-pyridine ligands is shown in Equation 4.10. The amine derivative and triethylamine were cooled at 0 ºC and the acid, acid chloride or anhydride was added dropwise. After a simple work up of the reaction, the product was obtained with good to excellent yields in all the cases. An important characteristic of the synthesis of those ligands is that it is modular and both components, the amine and the carbonyl derivative, can be modified to tailor the ligand according to the requirements of the reaction in which they are going to be used. The amino reagent and the acid/acid chloride/anhydride tolerate different substituents that are going to be part of the final ligand.

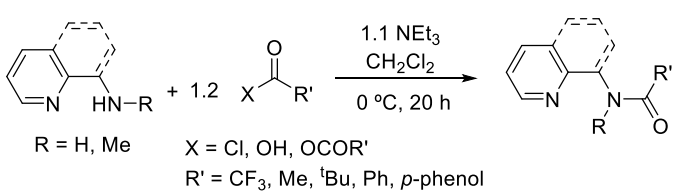

Equation 4.10.

All the amido-pyridine ligands that were synthesised are shown in Figure 4.14. Different R' groups were used, with electron-withdrawing (L1) or electron-donating properties (L2), bulky groups (L3) and phenyl derivatives (L4 and L5). Also, tertiary amines (L6) and a more rigid skeleton (L7 and L8).

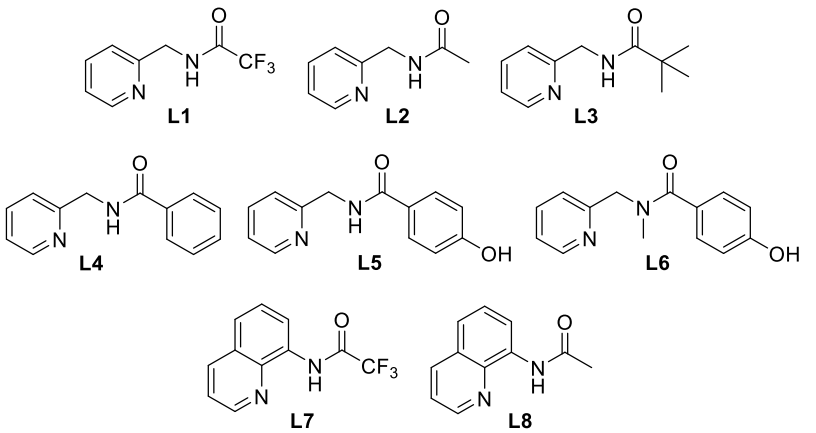

Figure 4.14. Amido-pyridine ligands synthesised.

By adding the OH group to the phenyl moiety in L5, it will increase the basicity of the amidic oxygen of the ligand by resonance and also we get a potentially dianionic ligand (when fully deprotonated). The contributing structures are shown in Figure 4.15. By the deprotonation of the OH group in L5 there is no need to deprotonate the NH. In the case of L6 just the OH can be deprotonated as the nitrogen is protected with a methyl group.

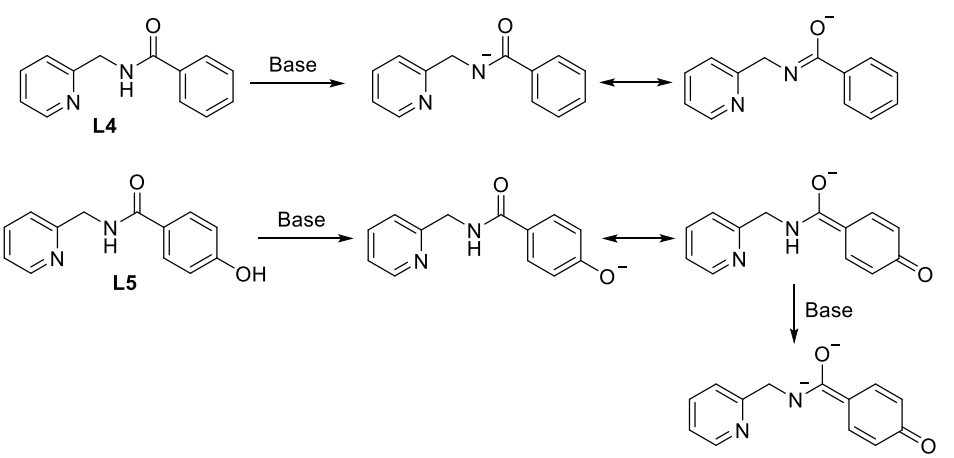

Figure 4.15. Contributing resonant structures in L4 and L5.

Two well-defined palladium complexes containing the ligand L1 were prepared. Following the same synthetic strategy as commented in the first part of this chapter, the reaction between the dimer $(NBu_4)_2[PdBr(C_6F_5)(\mu\text{-}Br)]_2$and L1 in the presence of cesium carbonate results in an anionic complex with the ligand coordinated in a bidentate mode

(**17**, Equation 4.11). The regiochemistry was unequivocally confirmed by a ^{1}H-^{19}F HOESY experiment.

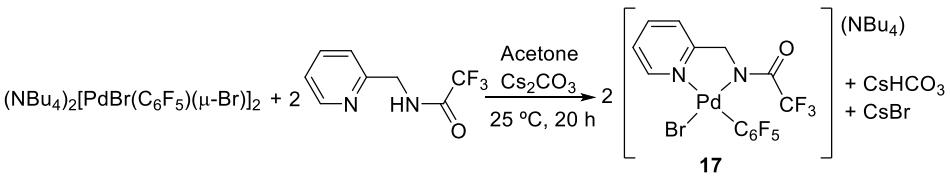

Equation 4.11.

The synthesis of a neutral complex with a coordinated pyridine was achieved through the reaction in Equation 4.12. The easy substitution of labile ligands such as acetonitrile, followed by the removal of the bromine atom with a silver salt and the coordination of a pyridine gave two isomers depending on the relative position of the pentafluorophenyl and pyridine.

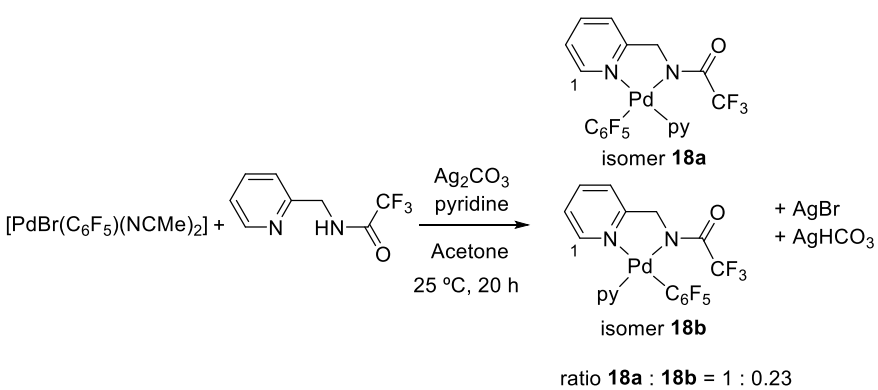

Equation 4.12.

The mixture of isomers was fully characterized and a ^{1}H-^{19}F HOESY experiment shows a cross peak between the F_{ortho} of C_6F_5 and H^1 in the pyridine moiety of the bidentate ligand of isomer **18a**, showing their close proximity **(**Figure 4.16**)**. This cross peak is absent for isomer **18b.** Moreover, a ^{1}H-ROESY shows the proximity of both pyridine rings in **18b**. Crystals suitable for X-Ray diffraction were obtained for the major isomer **18a** (Figure 4.17).

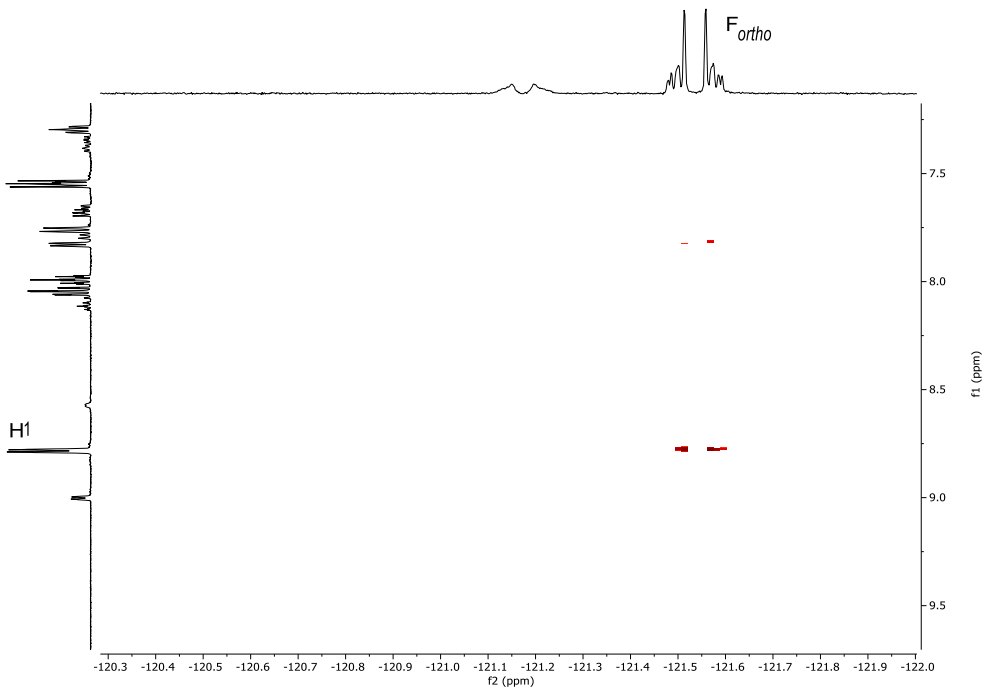

Figure 4.16. ^{1}H-^{19}F HOESY ($(CD_3)_2CO$) of **18a**

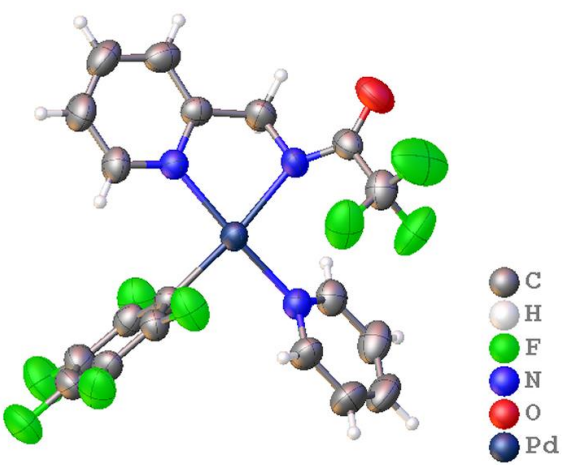

Figure 4.17. X-ray molecular structure of [Pd(2,2,2-trifluoro-N-(pyridin-2-ylmethyl)acetamide)(C_6F_5)(py)] (**18a**). ORTEP plot (40% probability ellipsoids) is shown.

An analogous complex with an MPAA as ligand has been prepared and studied recently in our group (Figure 4.18).[59] The behaviour of this complex can be compared to complex **18**, as it will be mentioned below.

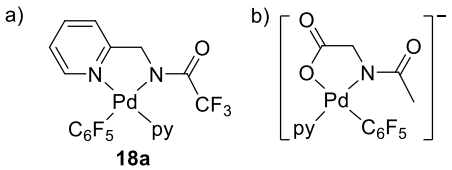

Figure 4.18. a) Major isomer of complex **18**. b) MPAA complex reported previously in the group.

C–H activation in complex 18.

In the same way as in the first part of the chapter, we decided to test the ligands' ability to assist in the C–H activation step. In order to do that, complex **18** was reacted with several arenes in the absence of any additive.

The thermal decomposition of complex **18** was evaluated in pyridine at 140 ºC and the species formed in solution were examined (Equation 4.13).

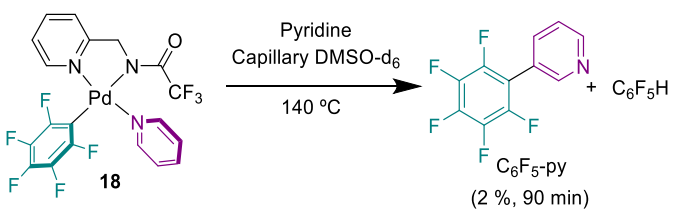

Equation 4.13.

After 90 min only 2 % of the coupling product C_6F_5-py was formed as can be seen in Figure 4.19. About 46 % of the starting material is remaining, so the complex seems to be robust in the reaction conditions. However, two byproducts were observed: 10 % of the pentafluorophenyl ring (C_6F_5H) and 26 % of the complex [$Pd(C_6F_5)_2(py)_2$], formed by the reorganization of two palladium complexes. Similar results have been reported by the thermal decomposition of the analogous MPAA palladium complex in the same conditions, 6 % of coupling product after 30 min.[59]

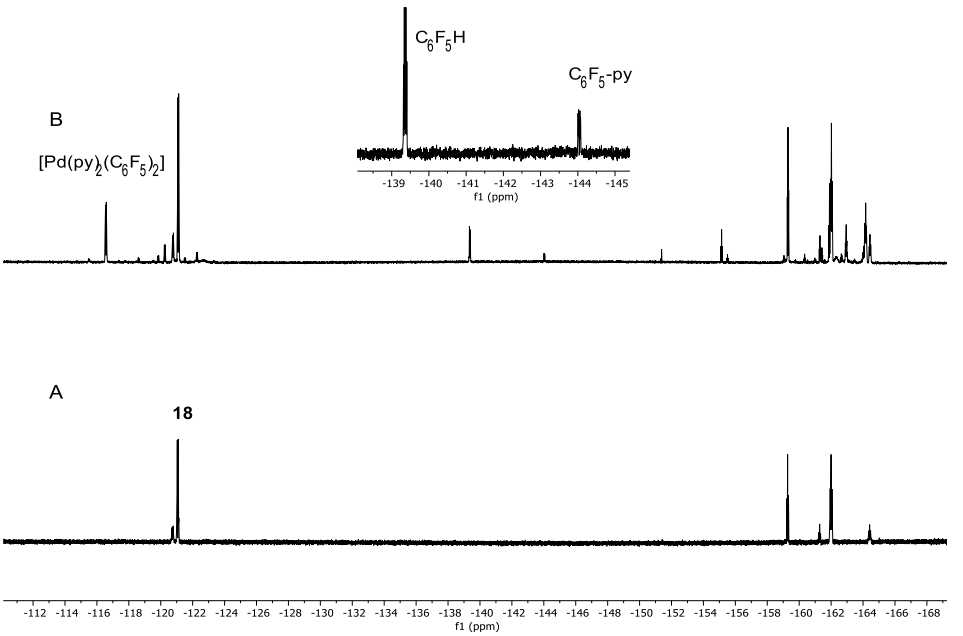

Figure 4.19. ^{19}F NMR spectra (470.168 MHz): A) Complex **18** in pyridine. B) Sample A after heating at 140 °C for 90 min (% mol: **18,** 46 %; $[Pd(C_6F_5)_2(py)_2]$, 26 %; C_6F_5-py, 2 %; C_6F_5H, 10 %).

The experiment clearly demonstrates that the ligand stays coordinated under the reaction conditions, but it is not assisting the C–H activation of pyridine efficiently.

The same experiment was done in toluene (Equation 4.14) and ethyl benzoate (Equation 4.15) as solvent at 130 ºC. In toluene, after 90 min at 130 ºC, 64 % of the coupling product was observed and 89 % after 3.5 h (Figure 4.20, C and D). The results obtained are similar to the complexes reported in the literature for bipy-6-OH (55 % after 1 h)[20] and require longer reaction times compared with the MPAA complex (53 % in 30 min)[59].

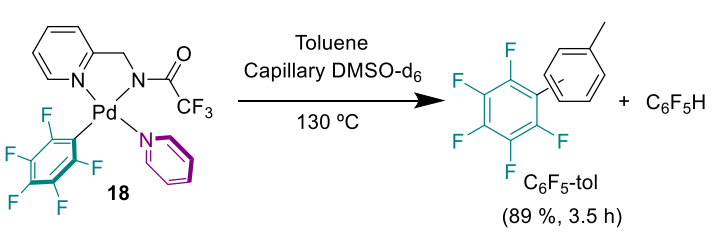

Equation 4.14.

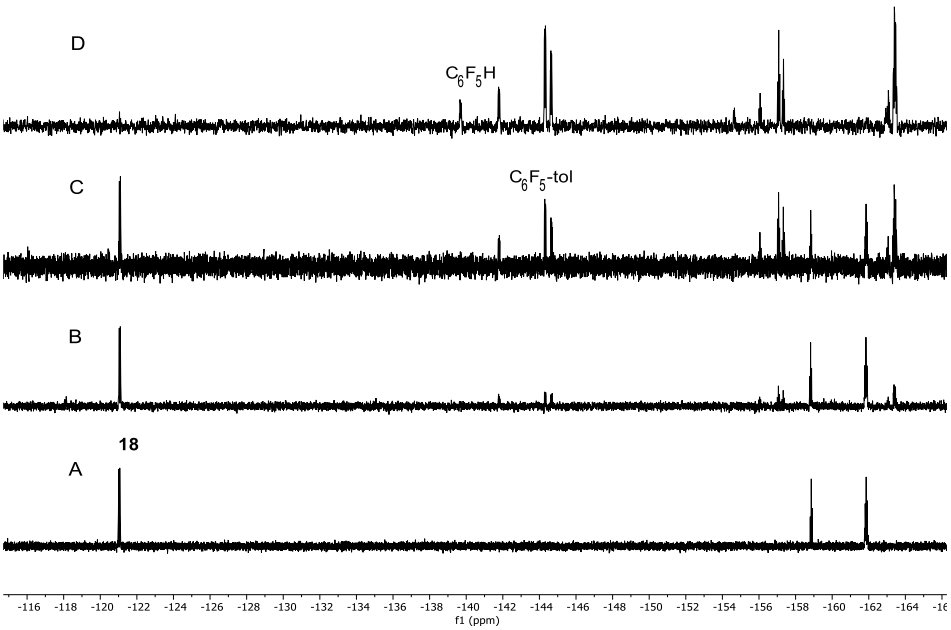

Figure 4.20. ^{19}F NMR spectra (470.168 MHz): A) Complex **18** in toluene. B) Sample A after heating at 130 °C for 30 min (% mol: **18**, 70 %; C_6F_5-tol, 30 %). C) Sample A after heating at 130 °C for 90 min (% mol: **18,** 36 %; C_6F_5-tol, 64 %). D) Sample A after heating at 130 °C for 3.5 h (% mol: C_6F_5-tol, 89 %; C_6F_5H, 11 %).

In ethyl benzoate as solvent (Figure 4.21), 29 % of the coupling product was achieved after heating for 30 min. Moreover, the starting material is still in the reaction mixture in a 50 %. Again, the conversion to the coupling product is slower compared with the reported MPAA complex (83 % after 30 min).

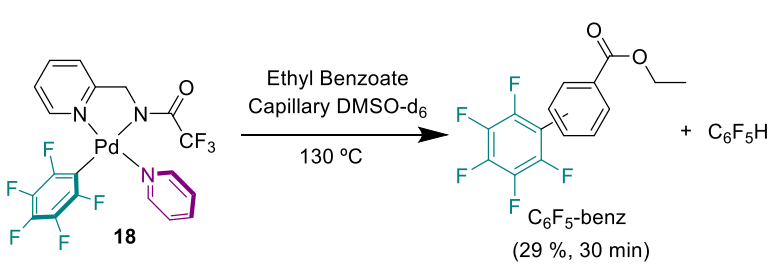

Equation 4.15.

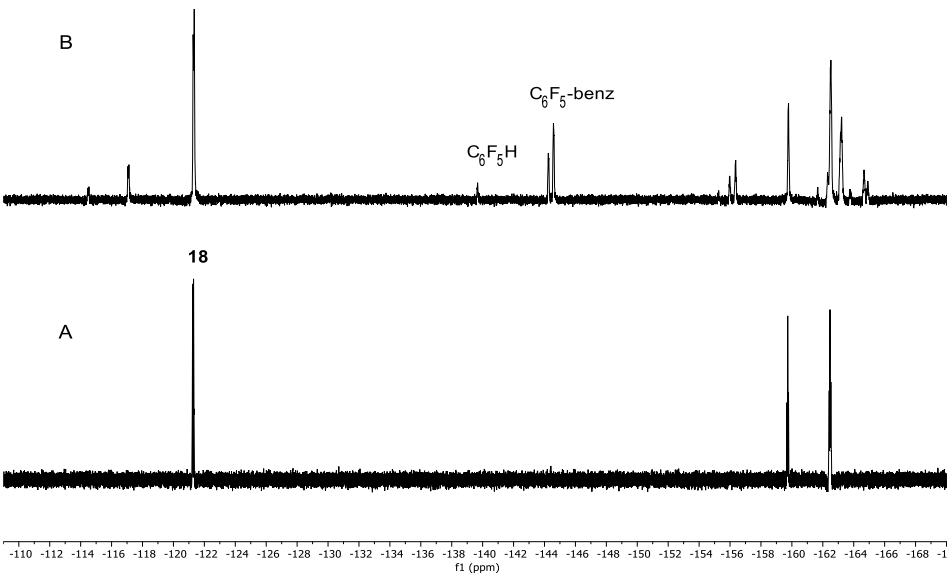

Figure 4.21. ^{19}F NMR spectra (470.168 MHz): A) Complex **18** in ethyl benzoate. B) Sample A after heating at 130 °C for 30 min (% mol: **18,** 50 %; C_6F_5-benz, 29 %; C_6F_5H, 3%).

Taking into account the results observed, the ligand is coordinated to palladium quite strongly, even in coordinating arenes such as pyridine and at high temperatures (140 ºC or 130 ºC). However, it is not efficiently cooperating in the C–H cleavage in the case of pyridine and only a small amount of coupling product was observed. On the other hand, the ligand is able to assist during the C–H activation step of arenes like toluene and ethyl benzoate, as the coupling product has been observed in good yields in the experiments. However, this step seems to be slower compared to the MPAA complexes reported in the literature despite the cooperating moieties of both ligands are quite similar.

DFT calculations at the M06 level were carried out to get more information about the C–H activation step (Figure 4.22). In order to compare the behaviour of this ligand with the data for bipy-6-OH reported in the literature, calculations were performed taking pyridine as model arene and trifluoromethylphenyl as aryl group. First of all, the isomer that has the ketone group away from the metal and the CF_3 substituent of the amido group is close to the arene (**c1**) is more stable than **c2** (ketone group close to the metal) by 2.3 kcal mol^{-1}. The amido group has to rotate around the C–N bond to place the ketone in the correct position to assist during the C–H cleavage. The transition state for this movement was found to be 19.7 kcal mol^{-1}. The next step is the rearrangement

of the pyridine ring from a κ-N to a η^2-pyridine (activation energy 23.7 kcal mol^{-1}). Finally, the TS of the C–H activation assisted by the ligand was found to be 35.5 kcal mol^{-1}, much more energy demanding than the one reported in the literature for the ligand bipy-6-OH (27.5 kcal mol^{-1}).[20]

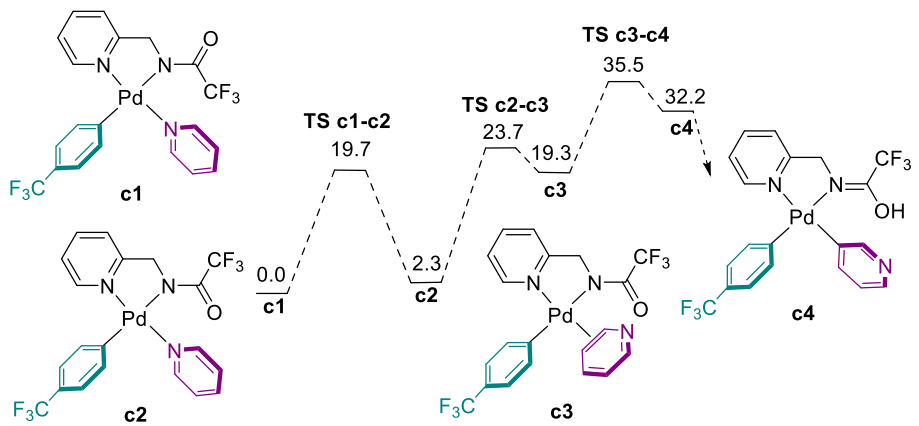

Figure 4.22. Free-energy profile for the L1-assisted cleavage of the *meta* C–H bond of pyridine. Energies in kcal mol^{-1}. Conditions: pyridine as solvent at 140 ºC.

The high activation energy of the process makes the C–H activation step really slow for the pyridine ring. Because of that, the intermediates formed during the reaction evolve through reorganization reactions to give other complexes without the coordinated ligand.

Direct arylation of arenes.

Even though the C–H activation for the pyridine was found to be slow in the thermal decomposition experiment, for toluene and ethyl benzoate the results were quite promising. Because of that, the amido-pyridine ligands and the complexes synthesised were tested in the catalytic direct arylation of arenes. The reaction conditions chosen were the same as in the first part of this chapter: an aryl halide as coupling partner, cesium carbonate as base and the arenes were pyridine (Equation 4.16), toluene (Equation 4.17) and ethyl benzoate (Equation 4.18).

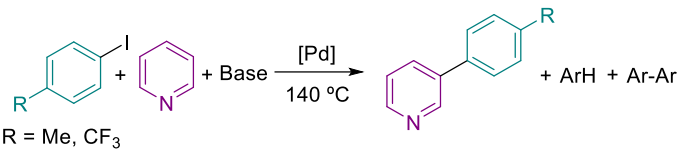

Equation 4.16.

The results obtained with the different catalyst in the direct arylation of pyridine are shown in Table 4.4. The conversions obtained in the control experiment (no ligand) and in that with bipy-6-OH are included for comparison. The cross coupling product obtained correspond to the *meta*-arylation of pyridine exclusively.

Two different arylhalides were tested under the same reaction conditions using cesium carbonate as base and the mixture $Pd(OAc)_2$ + ligand. For *p*-iodotoluene as aryl halide ligands L1 (entry 3, Table 4.4), L2 (entry 4, Table 4.4), L5 (entry 7, Table 4.4) and L6 (entry 8, Table 4.4) are the most active but moderate yields (close to 30 %) were obtained. L4 (entry 6, Table 4.4), and L8 (entry 10, Table 4.4) are less efficient and no conversion with the ligands L3 (entry 5, Table 4.4) and L7 (entry 9, Table 4.4) was observed.

We also used *p*-iodotrifluorotoluene and poor to moderate yields were observed with the complex **18** (entry 13, Table 4.4) or the ligands, L2 (entry 15, Table 4.4), L5 (entry 18, Table 4.4) and L6 (entry 19, Table 4.4). Almost no conversion of the reagent was found with L3 (entry 16, Table 4.4), L4 (entry 17, Table 4.4), L7 (entry 21, Table 4.4) and L8 (entry 22, Table 4.4). The use of soluble bases has no advantage (entries 14 and 19, Table 4.4) not even with L5 that could act as dianionic ligand. Thus, at least the amido pyridine ligands L2, L5 and L6 consistently enable the C–H arylation of pyridine but the reactions are too slow to compete to the more efficient bipy-6-OH ligand.

Table 4.4. Direct arylation of pyridine using different precatalyst.[a]

Entry	[Pd]	Base	R	Crude yield, % (conv., %), 6h[b]	Crude yield, % (conv., %), 24h[b]
1[c]	$Pd(OAc)_2$	Cs_2CO_3	Me	0 (0)	0 (0)
2[c]	$Pd(OAc)_2$ + **bipy-6-OH**	Cs_2CO_3	Me	88 (97)	90 (100)
3	$Pd(OAc)_2$ + **L1**	Cs_2CO_3	Me	17 (33)	25 (35)
4	$Pd(OAc)_2$ + **L2**	Cs_2CO_3	Me	15 (20)	37 (42)
5	$Pd(OAc)_2$ + **L3**	Cs_2CO_3	Me	0 (0)	0 (0)
6	$Pd(OAc)_2$ + **L4**	Cs_2CO_3	Me	13 (18)	17 (22)
7	$Pd(OAc)_2$ + **L5**	Cs_2CO_3	Me	20 (20)	26 (26)
8	$Pd(OAc)_2$ + **L6**	Cs_2CO_3	Me	24 (26)	35 (38)
9	$Pd(OAc)_2$ + **L7**	Cs_2CO_3	Me	0 (0)	4 (9)
10	$Pd(OAc)_2$ + **L8**	Cs_2CO_3	Me	0 (0)	25 (25)
11	$Pd(OAc)_2$	Cs_2CO_3	CF_3	0 (0)	0 (0)
12[c]	$Pd(OAc)_2$ + **bipy-6-OH**	Cs_2CO_3	CF_3	94 (100)[d]	-
13	**18**	Cs_2CO_3	CF_3	5 (6)	13 (14)
14[e]	**18**	$(NBu_4)CO_3Me$		6 (50)	-[x]
15	$Pd(OAc)_2$ + **L2**	Cs_2CO_3	CF_3	21 (21)	32 (35)
16	$Pd(OAc)_2$ + **L3**	Cs_2CO_3	CF_3	0 (0)	9 (10)
17	$Pd(OAc)_2$ + **L4**	Cs_2CO_3	CF_3	7 (7)	8 (9)
18	$Pd(OAc)_2$ + **L5**	Cs_2CO_3	CF_3	16 (16)	27 (27)
19[e]	$Pd(OAc)_2$ + **L5**	$(NBu_4)CO_3Me$		22 (59)	-[x]
20	$Pd(OAc)_2$ + **L6**	Cs_2CO_3	CF_3	20 (20)	30 (31)
21	$Pd(OAc)_2$ + **L7**	Cs_2CO_3	CF_3	1 (2)	4 (5)
22	$Pd(OAc)_2$ + **L8**	Cs_2CO_3	CF_3	2 (3)	10 (11)

[a]Reaction conditions: ArI (0.34 mmol), pyridine (3.0 mL), [Pd] (5 mol %), base (0.34 mmol). [b] Crude yields determined by ^1H or ^{19}F NMR of the reaction mixture. The reduction of the ArI (ArH) and the homocoupling (Ar-Ar) are the observed byproducts. [c]Data taken from the literature. [d]After 2 h. [e]Base (0.51 mmol). [x]Not determined

The direct arylation of toluene was next tried. *p*-Iodotrifluorotoluene was used as aryl halide in all the cases and cesium carbonate as base (Equation 4.17). The results are included in Table 4.5.

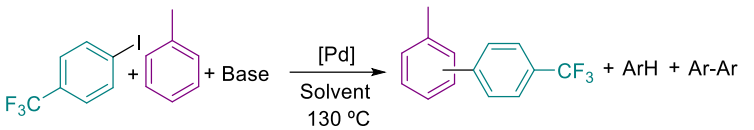

Equation 4.17.

The reaction with no ligand and the model conditions with bipy-6-OH are shown for comparison (entries 1 and 2, Table 4.5). In the case of the amido-pyridine ligands almost no coupling product was observed in all the cases. L1 in toluene showed no reaction (entry 3, Table 4.5). When pinacolone is used as co-solvent (entry 4, Table 4.5), reaction conditions that have shown to accelerate the direct arylation of toluene using bipy-6-OH as enabling ligand,[20] the coupling between the aryl halide and pinacolone is observed in high amounts. To avoid this, DMA was also tried as co-solvent (entry 5, Table 4.5) obtaining the Ar-Ar as major product. In the case on L2 and L3 even with a co-solvent no product was formed (entries 6-9, Table 4.5). Same results were observed with the ligands L4-L8 in toluene (entries 10-15, Table 4.5).

When **17** was used, only in the toluene:pinacolone mixture a 31 % of product was formed (entries 16 and 17, Table 4.5). However, large amounts of byproducts were observed. The use of the soluble base $(NBu_4)CO_3Me$ does not lead to an important increase of the observed yield and induce other competing reactions (entries 12 and 19, Table 4.5). It is clear that the amido-pyridine ligands are not suitable to enable the catalytic direct arylation of toluene.

Table 4.5. Direct arylation of toluene using different precatalyst and solvents.[a]

Entry	[Pd]	Solvent	Crude yield, % (conv., %), 6h[b]	Crude yield, % (conv., %), 24h[b]
1[c]	$Pd(OAc)_2$	Toluene	0 (0)	0 (0)
2[c]	$Pd(OAc)_2$ + **bipy-6-OH**	Toluene	20 (22)	91 (100)
3	$Pd(OAc)_2$ + **L1**	Toluene	2 (2)	6 (6)
4	$Pd(OAc)_2$ + **L1**	Tol:Pin (1:1)	2 (22)	6 (65)
5	$Pd(OAc)_2$ + **L1**	Tol:DMA (1:1)	0 (27)	0 (40)
6	$Pd(OAc)_2$ + **L2**	Toluene	2 (4)	4 (7)
7	$Pd(OAc)_2$ + **L2**	Tol:Pin (1:1)	0 (26)	0 (35)
8	$Pd(OAc)_2$ + **L3**	Toluene	0 (0)	3 (3)
9	$Pd(OAc)_2$ + **L3**	Tol:Pin (1:1)	0 (0)	0 (0)
10	$Pd(OAc)_2$ + **L4**	Toluene	1 (17)	2 (25)
11	$Pd(OAc)_2$ + **L5**	Toluene	0 (5)	0 (5)
12	$Pd(OAc)_2$ + **L5**	Toluene $(NBu_4)CO_3Me$	9 (97)[e]	-
13	$Pd(OAc)_2$ + **L6**	Toluene	0 (16)	0 (19)
14	$Pd(OAc)_2$ + **L7**	Toluene	0 (0)	0 (0)
15	$Pd(OAc)_2$ + **L8**	Toluene	0 (0)	0 (0)
16	**17**	Toluene	0 (7)	0 (9)
17	**17**	Tol:Pin (1:1)	20 (66)	31 (100)
18	**18**	Toluene	0 (6)	0 (8)
19	**18**	Toluene $(NBu_4)CO_3Me$	7 (96)[e]	-

[a]Reaction conditions: ArI (0.34 mmol), solvent (3.0 mL), [Pd] (5 mol %), base (0.68 mmol). [b] Crude yields determined by ^{19}F NMR of the reaction mixture. The reduction of the ArI (ArH), the homocoupling (Ar-Ar) and coupling with pinacolone (Ar-Pin) are the observed byproducts. [c]Data taken from the lireature. [d]After 90 min. [e]Base (0.51 mmol), after 2 h.

Finally, the direct arylation of ethyl benzoate was tried because moderated yields were obtained in the thermal decomposition of complex **18** commented before. The reaction conditions used are shown in Equation 4.18. and the results obtained in Table 4.6.

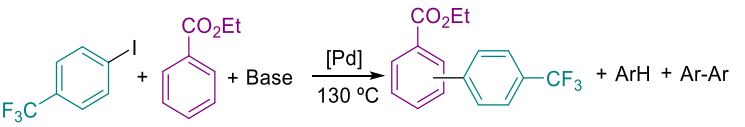

Equation 4.18.

Table 4.6. Direct arylation of ethyl benzoate using different precatalyst.[a]

Entry	[Pd]	Base	Crude yield, % (conv., %), 6h[b]	Crude yield, % (conv., %), 24h[b]
1	$Pd(OAc)_2$	Cs_2CO_3	9 (99)	-
2	$Pd(OAc)_2$ + **bipy-6OH**	Cs_2CO_3	80 (100)	-
3	$Pd(OAc)_2$ + **L1**	Cs_2CO_3	0 (9)	4 (34)
4	$Pd(OAc)_2$ + **L2**	Cs_2CO_3	8 (26)	26 (76)
5	$Pd(OAc)_2$ + **L3**	Cs_2CO_3	8 (10)	7 (13)
6	$Pd(OAc)_2$ + **L4**	Cs_2CO_3	3 (17)	4 (25)
7	$Pd(OAc)_2$ + **L5**	Cs_2CO_3	2 (18)	5 (45)
8	$Pd(OAc)_2$ + **L6**	Cs_2CO_3	0 (7)	0 (13)
9	$Pd(OAc)_2$ + **L7**	Cs_2CO_3	0 (9)	0 (23)
10	$Pd(OAc)_2$ + **L8**	Cs_2CO_3	10 (20)	40 (76)
11	**17**	Cs_2CO_3	1 (21)	5 (46)
12	**18**	Cs_2CO_3	0 (11)	0 (20)
13	**18**	$(NBu_4)CO_3Me$	7 (99)[c]	-
14	$Pd(OAc)_2$ + **L5**	$(NBu_4)CO_3Me$	7 (76)[c]	-

[a]Reaction conditions: ArI (0.34 mmol), pyridine (3.0 mL), [Pd] (5 mol %), base (0.68 mmol). [b]Crude yields determined by ^{19}F NMR of the reaction mixture. The reduction of the ArI (ArH) and the homocoupling (Ar-Ar) are the observed byproducts. [c] Base (0.51 mmol), after 2 h.

As can be seen, only the ligands L2 (entry 4, Table 4.6) and L8 (entry 10, Table 4.6) gave moderate yields in the reaction. When the other ligands and complexes were used, very little amount of the coupling products was observed.

The catalytic reactions did not give good results for any of the arenes, ligands or reaction conditions used. For the pyridine, the C–H cleavage step is really energy demanding and this is shown in the thermal decomposition experiments of complex **18**. In the case of less coordinating arenes, these experiments show that the C–H activation of the arene is possible. However, during the catalytic reaction the intermediates can evolve to the formation of byproducts such as that of aryl homocoupling in most cases

or coupling with pinacolone when it is used as co-solvent. Due to the low efficiency observed in this case we decided to try C–H functionalization reactions different from the direct arylation.

Oxidative Heck reaction of toluene.

The C–H functionalization of arenes *via* the Fujiwara-Moritani or oxidative Heck reaction has been also studied in the group. The coupling reaction is enabled by the bipy-6-OH ligand,[25] so the olefination of arenes would be a good candidate to test the amido-pyridine ligands and compare their effect. This reaction is an example of the coupling between two hydrocarbons as was commented in the general introduction (Section 1). The catalytic cycle for these transformations differs from the direct arylation since there is an oxidation step in the catalytic cycle to recover the active catalyst and therefore the reaction requires an oxidant as reactant. After the C–H activation step of the arene on a Pd(II) complex, the coordination and insertion of the olefin into the Pd-aryl bond occurs, followed by a β-H elimination to give the final product. The palladium hydride formed decomposes to Pd(0) that is reoxidized to Pd(II) and reenters the catalytic cycle.

The reaction conditions chosen can be seen in Equation 4.19. Toluene was selected as coupling partner and *tert*-butyl acrylate as alkene; the reaction is carried out under oxygen as oxidant, using sodium molybdate in catalytic amounts as it is described in the literature.

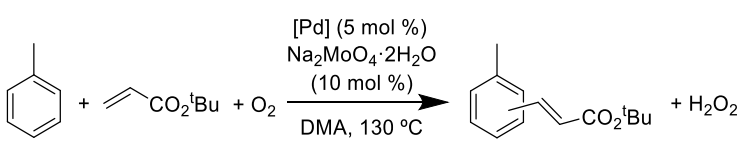

Equation 4.19.

The results obtained can be seen in Table 4.7. The reported data are also included for comparison (entries 1 and 2, Table 4.7). When no ligand was used the reaction affords 47 % of the coupling product. The mixture of $Pd(OAc)_2$ + bipy-6-OH was able to reach a 75 % yield.

Table 4.7. Oxidative Heck reaction of toluene using different precatalyst.[a]

Entry	[Pd]	Crude yield, %, 6h[b]	Crude yield, %, 24h[b]
1[c]	$Pd(OAc)_2$	47	47
2[c]	$Pd(OAc)_2$ + **bipy-6OH**	40	75
3	$Pd(OAc)_2$ + **L1**	16	34
4	$Pd(OAc)_2$ + **L2**	6	10
5	$Pd(OAc)_2$ + **L3**	11	40
6	$Pd(OAc)_2$ + **L4**	0	6
7	$Pd(OAc)_2$ + **L5**	21	21
8	$Pd(OAc)_2$ + **L6**	0	0
9	$Pd(OAc)_2$ + **L7**	20	26
10	$Pd(OAc)_2$ + **L8**	12	14

[a]Reaction conditions: *t*-butyl acrylate (0.34 mmol), toluene (1.5 mL), DMA (1.5 mL), [Pd] (5 mol %), $Na_2MO_2 \cdot 2H_2O$ (0.034 mmol). [b]Crude yields determined by ^1H NMR of the reaction mixture using dodecane as internal standard.[c]Data taken from the literature.

The ligands L1 and L3 led to a moderate yield of the product (entries 3 and 5, Table 4.7). The use of L5 and L7 gave poor results (entries 7 and 9, Table 4.7) and the other ligands almost were even less effective. It is clear that there is no advantage in using amido-pyridine ligands in this process. Even if the ligands have demonstrated to cooperate in the C–H activation of toluene, it is possible that the rate of other elementary steps in the catalytic cycle has been decreased by the coordination of the ligands to the catalyst to the point of hampering the process.[25]

Ortho-C–H alkylation of arylcarboxylic acids and C–H acetoxylation of free carboxylic acids

Finally, we decided to try reactions reported in the literature that use MPAA derivatives as enabling ligands. Due to the similarity of the amido-pyridine ligands with the MPAAs, those reactions could be good candidates to test our catalytic system. The Yu's group has a large experience using these ligands in palladium catalysis, so two of his published procedures were chosen.

The *ortho*-C–H alkylation of arylcarboxylic acids was reported with good yields using a MPAA as ligand.[155] That reaction is a simple way to obtain a large variety of alkyl-aryl coupling products, and some of these skeletons are abundant in natural products or pharmaceuticals. Here we have an oxidative coupling reaction between an arene and an organometallic reagent, a C–C coupling reaction type commented in the general introduction (Section 1). The carboxylic acid moiety in the arene is used as directing group to facilitate the coordination of the reagent to the palladium centre, and control the regioselectivity of the reaction. In the catalytic cycle for this process, after the C–H activation of the arene by a Pd(II) complex there is a transmetallation step of the butyl group from the borate to the palladium catalyst. A reductive elimination and oxidation of the resulting Pd(0) species closes the catalytic cycle. The reaction conditions selected can be seen in Equation 4.20. where [2-(trifluoromethyl)phenyl]acetic acid and potassium butyltrifluoroborate are the coupling partners, lithium carbonate is used as base, silver carbonate as oxidant and DMF as additive.

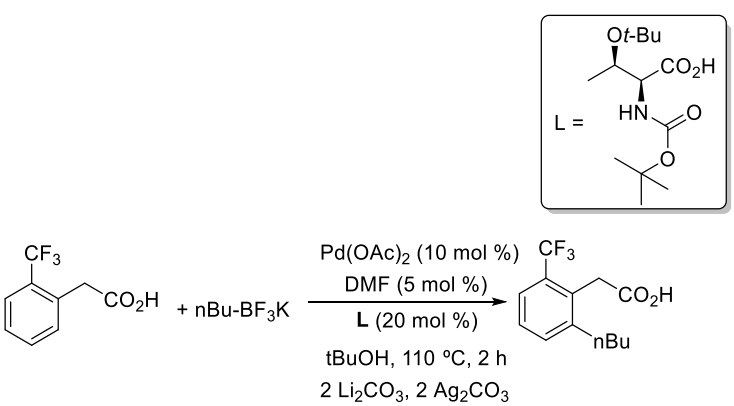

Equation 4.20.

The results obtained are shown in Table 4.8. The reported data is also included for comparison (entries 1 and 2, Table 4.8). With no ligand the conversion obtained was very low. However, when the ligand Boc(L)-Thr(*t*Bu)-OH was used, an 82 % of product is observed after 2 h.

[155] Thuy-Boun, P. S.; Villa, G.; Dang, D.; Richardson, P.; Su, S. and Yu, J-Q. *J. Am. Chem. Soc.* **2013**, 135, 17508-17513.

Table 4.8. Alkylation of arylcarboxylic acids using different precatlyst.[a]

Entry	[Pd]	Crude yield, %, 2h[b]
1[c]	$Pd(OAc)_2$	16
2[c]	$Pd(OAc)_2$ + **Boc(L)-Thr(*t*Bu)-OH**	82
3	$Pd(OAc)_2$ + **L1**	2
4	$Pd(OAc)_2$ + **L2**	2
5	$Pd(OAc)_2$ + **L3**	2
6	$Pd(OAc)_2$ + **L4**	11
7	$Pd(OAc)_2$ + **L5**	2
8	$Pd(OAc)_2$ + **L6**	3
9	$Pd(OAc)_2$ + **L7**	2
10	$Pd(OAc)_2$ + **L8**	1

[a]Reaction conditions: Carboxylic acid (0.5 mmol), alkyl boron reagent (0.75 mmol), tBuOH (2.5 mL), $Pd(OAc)_2$ (0.05 mmol), L (0.1 mmol), Li_2CO_3 (1 mmol), Ag_2CO_3 (1 mmol), DMF (0.025 mmol).[b]Crude yields determined by ^1H and ^{19}F NMR of the crude mixture after the general workup. [c]Data taken from the literature.

None of the amido-pyridine ligands could achieve good yields on this transformation. Moreover, the yields observed were even lower than that reported with no ligand. This means that the ligand is probably slowing down other elementary steps of the catalytic cycle and therefore is not adequate for this transformation.

The second reaction chosen was the C–H acetoxylation of alkyl carboxylic acids, an easy way to synthesise useful molecules using an inexpensive oxidant (TBHP).[156] The reaction conditions tested were 2-methylbutanoic acid as substrate, acetic anhydride, TBHP as oxidant and sodium carbonate as base as can be seen in Equation 4.21. The catalytic cycle proposed for this transformation involves a Pd(II)/Pd(IV) mechanism, different from the Pd(0)/Pd(II) observed in the direct arylation of arenes and the other catalytic reactions tested so far. After the coordination of the carboxylate of the substrate (as directing group) to a Pd(II) complex, the cyclopalladation of the C(sp^3)–H takes place assisted by the MPAA ligand. The oxidative addition of TBHP generates a Pd(IV) complex that, by ligand exchange with Ac_2O, gives the acetate intermediate prior to the reductive elimination of the coupling product.

[156] Zhuang, Z.; Herron, A. N.; Fan, Z. and Yu, J-Q. *J. Am. Chem. Soc.* **2020**, *142*, 6769-6776.

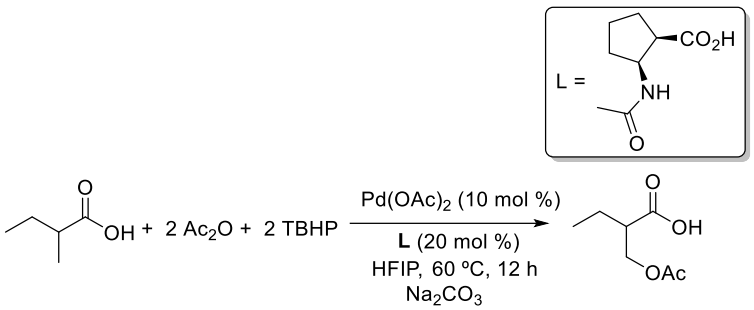

Equation 4.21.

The results observed are included in Table 4.9. The reported data showed a 72 % yield of the product after a reaction time of 12 h using 2-(acetylamino)-cis-cyclopentanecarboxylic acid as ligand (entry 1, Table 4.9).

Table 4.9. Acetoxylation of free carboxylic acids using different precatalyst.[a]

Entry	[Pd]	Crude yield, %, 12h[b]
1	$Pd(OAc)_2$ + **2-(acetylamino)-cis-cyclopentanecarboxylic acid**	72[c]
2	$Pd(OAc)_2$ + **L1**	9
3	$Pd(OAc)_2$ + **L2**	17
4	$Pd(OAc)_2$ + **L3**	8
5	$Pd(OAc)_2$ + **L4**	53
6	$Pd(OAc)_2$ + **L5**	77
7	$Pd(OAc)_2$ + **L6**	23
8	$Pd(OAc)_2$ + **L7**	21
9	$Pd(OAc)_2$ + **L8**	27

[a]Reaction conditions: Carboxylic acid (0.1 mmol), Ac_2O (0.2 mmol), TBHP (0.2 mmol), HFIP (1 mL), $Pd(OAc)_2$ (0.01 mmol), L (0.002 mmol), Na_2CO_3 (0.1 mmol).[b]Crude yields determined by ^1H NMR of the crude mixture after the workup using stilbene as internal standard. [c]Yield data taken from the literature.

The ligands L4 and L5 (entries 5 and 6, Table 4.9) gave the best results, comparative results with the reported ones in the case of L5. The remaining ligands are clearly not efficient. It is worth noting that ligand L5 is the one that is diprotic and therefore analogous to the MPAAs as far as their possibility of acting as a dianionic ligand. This may contribute in this case to stabilize the high-valent Pd(IV) intermediates proposed in the reaction.

Finally, we can conclude that none of the different catalytic transformations tried gave good results when the amido-pyridine ligands were used instead of the model ligands. Even if they seemed to be good candidates due to their similarity with the bipy-6-OH or MPAA ligands and their ability to activate C–H bonds as shown by the stoichiometric decomposition experiments of complex, it is clear that the ligands do not have the right features to make all the steps in the catalytic cycles fast enough to show an accelerating effect.

4.3 CONCLUSIONS

The ligand 6-hydroxypicolinic acid (pic-6-OH) and the amido-pyridine type ligands are efficient cooperating ligands in the C–H activation reaction of arenes. This has been demonstrated by the thermal decomposition of isolated palladium complexes of the type $[Pd(C_6F_5)(ligand)(py]^{n-}$ (**16**, **18**) in different arenes as solvent (pyridine, toluene and ethylbenzoate), that lead to the C_6F_5-arene coupling products. These experimental results and the DFT calculations on the same system (arene = pyridine) collected in Figure 4.11 and Figure 4.22 as well as those in the literature, show the following trend in facilitating the C–H activation step (Gibbs energies of the ligand-assisted CMD transition state in parentheses): pic-6-OH (25.4 kcal mol^{-1}) > bipy-6-OH (27.5 kcal mol^{-1}) > amido-py (35.5 kcal mol^{-1}).

The ligand 6-hydroxypicolinic acid (pic-6-OH) and the amido-pyridine type ligands are not efficient in the catalytic direct arylation of arenes even though they seemed to meet the necessary characteristics for those transformations.

In the case of pic-6-OH an increment of the yield was observed by using soluble bases (tetrabutylammonium methyl carbonate and tetrabutylammonium carbonate) or more polar solvents (DMA), which points to the importance of the chelating dianionic coordination mode of the ligand (favoured by a higher base concentration) for an efficient C–H activation. However, even in these conditions, only moderated yields were observed in the catalytic reaction of the arenes and the ligand seems to promote the formation of a high amount of byproducts, mainly the homocoupling derivative of the aryl halide.

The results for the direct arylation of arenes with amido-pyridine ligands are also poor. The direct arylation of pyridine is difficult since the C–H activation barrier is higher for this type of ligands. However, even for other arenes that have shown a more efficient C–H activation step in the thermal decomposition of complex **18**, the catalytic reactions show a high amount of byproducts indicating that the intermediates evolve through reorganization pathways leading to, for example, homocoupling products.

Other type of coupling reactions different from the direct arylation were tried using the amido-pyridine ligands. In the oxidative Heck reaction of toluene and the *ortho*-C–H alkylation of arylcarboxylic acids using alkyl boronic acids no better results were obtained when the ligands were used. On the other hand, the ligands L4 and L5 achieved good results in the C–H acetoxylation of free alkyl carboxylic acids, but the other ligands gave poor yields.

We can conclude that the ligands proposed in this chapter were not effective in any of the reactions tested although their structure is quite similar compared to the bipy-6-OH and MPAAs. The hypothesis of their cooperation during the C–H cleavage is a fact as this step has been tested independently with isolated palladium complexes. However, their efficiency in the processes is not enough to carry out the complete reactions. The ligand cooperation in the C–H activation is a necessary but not sufficient requirement for an efficient C–H functionalization. In any case, the proved ability of these ligands in the C–H activation step makes them suitable candidates to be considered when developing new catalytic C–H functionalization reactions.

4.4 EXPERIMENTAL PART

4.4.1 General considerations

^{1}H, $^{13}C\{^{1}H\}$ and ^{19}F NMR spectra were recorded on Agilent MR-400 or Agilent MR-500 spectrometers at the *Laboratorio de Técnicas Instrumentales* (LTI) of the UVa. Chemical shifts (in δ units, ppm) were referenced to $SiMe_4$ (^{1}H and ^{13}C) and $CFCl_3$ (^{19}F). The spectral data were recorded at 293 K unless otherwise noted. Homonuclear (^{1}H-COSY, ^{1}H-NOESY and ^{1}H-ROESY) and heteronuclear (^{1}H-^{13}C HSQC and HMBC, ^{19}F-^{13}C HSQC and HMBC and ^{1}H-^{19}F HOESY) experiments were used to help with the signal assignments. Elemental analyses were carried out in a Carlo Erba 1108 microanalyzer (at the Vigo University, Spain). HRMS analyses were carried out on a Bruker Maxis Impact mass spectrometer at the *Laboratorio de Técnicas Instrumentales* (LTI) of the UVa.

Solvents were dried using a solvent purification system SPS PS-MD-5 (THF, Hexane, CH_2Cl_2, Et_2O) or distilled from appropriate drying agents under nitrogen prior to use and stored over 3 Å or 4 Å molecular sieves (acetone, toluene, pyridine, DMA, MeOH, EtOH, ethyl benzoate, pinacolone). NEt_3 was dried, distilled and stored under nitrogen.

6-hydroxypicolinic acid, 4-hydroxypicolinic acid, Cs_2CO_3, Na_2CO_3, K_2CO_3, K_3PO_4, KHMDS, $Pd(OAc)_2$ $(NMe_4)Cl$, $(NBu_4)I$, $(NBu_4)OAc$ and the aryl iodides used are commercially available and were used as received unless otherwise indicated.

$(NBu_4)_2[Pd_2(\mu\text{-}Br)_2Br_2(C_6F_5)_2]$[82] was synthesised according to the procedures in the literature.

4.4.2 Synthesis of amido-pyridine ligands

In a two necked 100 mL flask 2-aminomethylpyridine, N-methyl-2-aminomethylpyridine or 8-aminoquinoline (10 mmol), CH_2Cl_2 (20 mL) and NEt_3 (1.52 mL, 11 mmol) were added under nitrogen. The solution was cooled to 0°C. The corresponding acid chloride, anhydride or acid (12 mmol) was added dropwise while stirring. The mixture was warmed to room temperature and stirred for 20 h. The solution was washed with water (3 x 5 mL), $NaHCO_3$ aq. (3 x 5 mL) and dried with $MgSO_4$. The solvent was evaporated in vacuo. The product was used without further purification in most cases.

2,2,2-trifluoro-N-(pyridin-2-ylmethyl)acetamide (L1)[157]**:** 2-aminomethylpyridine and trifluoroacetic anhydride were used as reagents. Isolated as a yellow solid. Yield: 1.84 g (90.3 %).

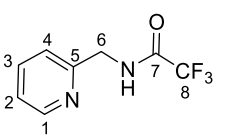

^{1}H NMR (500.13 MHz, δ, $CDCl_3$): 8.54 (d, J = 4.76 Hz, 1H, H^1), 8.07 (br, 1H, H^{NH}), 7.69 (td, J = 7.74 Hz, J = 1.70 Hz, 1H, H^3), 7.27 (d, J = 7.92 Hz, 1H, H^4), 7.26 (dd, J = 7.71 Hz, J = 4.97 Hz, 1H, H^2), 4.61 (d, J = 4.52 Hz, 2H, H^6). ^{13}C{^{1}H} NMR (125.78 MHz, δ, $CDCl_3$): 156.94 (C^7), 153.74 (C^5), 149.26 (C^1), 137.36 (C^3), 123.11 (C^4), 122.22 (C^2), 44.04 (C^6). ^{19}F NMR (470.168 MHz, δ, $CDCl_3$): -75.82 (s, 3F, F^8). HRMS (ESI-TOF): Calcd. for $C_8H_8F_3N_2O$ $[M+H]^+$ 205.0583, found 205.0587.

N-(pyridin-2-ylmethyl)acetamide (L2)[158]**:** 2-aminomethylpyridine and acetyl chloride were used as reagents. Isolated as a colourless semi-solid. Yield: 1.30 g (90.0 %).

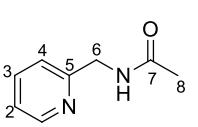

^{1}H NMR (500.13 MHz, δ, $CDCl_3$): 8.47 (dd, J = 4.93 Hz, J = 1.86 Hz, 1H, H^1), 7.61 (td, J =7.62 Hz, J = 1.70 Hz, 1H, H^3), 7.21 (d, J = 7.80 Hz, 1H, H^4), 7.14 (dd, J = 7.47 Hz, J = 5.0 Hz, 1H, H^2), 7.05 (br, 1H, H^{NH}), 4.49 (d, J = 5.28 Hz, 2H, H^6), 2.01 (s, 3H,

[157]Cody, C. C.; Kelly, H. R.; Mercado, B. Q.; Batista, V. S.; Crabtree, R. H.; Brudvig, G. W. *Inorg. Chem.*, **2021**, *60*, 14759-14764.
[158]Mondal, A.; Li, Y.; Khan, M. A.; Ross, J. H.; Houser, R. P. *Inorg. Chem.*, **2004**, *43*, 7075-7082.

H^8).$^{13}C\{^1H\}$ NMR (125.78 MHz, δ, $CDCl_3$): 170.15 (C^7), 156.82 (C^5), 149.04 (C^1), 136.74 (C^3), 122.38 (C^4), 122.09 (C^2), 44.65 (C^6), 23.22 (C^8). HRMS (ESI-TOF): Calcd. for $C_8H_{10}N_2NaO$ $[M+Na]^+$ 173.0685, found 173.0688.

N-(pyridin-2-ylmethyl)pivalamide (L3)[159]**:** 2-aminomethylpyridine and trimethylacetyl chloride were used as reagents. Filtration of the crude through silica gel using EtOAc as eluent was needed. Isolated as yellow semi-solid. Yield: 1.70 g (90.0 %).

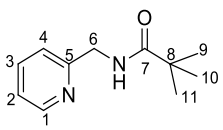

^1H NMR (500.13 MHz, δ, $CDCl_3$): 8.53 (d, 1H, H^1), 7.67 (t, 1H, H^3), 7.27 (d, 1H, H^4), 7.20 (t, 1H, H^2), 7.06 (s, 1H, H^{NH}), 4.53 (d, 2H, H^6), 1.25 (s, 9H, $H^{9,\ 10,\ 11}$).$^{13}C\{^1H\}$ NMR (125.78 MHz, δ, $CDCl_3$): 178.45 (C^7), 156.60 (C^5), 148.64 (C^1), 136.96 (C^3), 122.46 ($C^{2,4}$), 44.31 (C^6), 38.79 (C^8), 27.62 ($C^{9,\ 10,\ 11}$). HRMS (ESI-TOF): Calcd. for $C_{11}H_{16}N_2NaO$ $[M+Na]^+$ 215.1155, found 215.1158.

N-(pyridin-2-ylmethyl)benzamide (L4)[160]**:** 2-aminomethylpyridine and benzoyl chloride were used as reagents. Isolated as a white solid. Yield: 1.84 g (86 %).

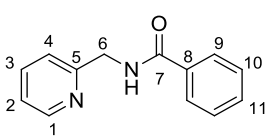

^1H NMR (500.13 MHz, δ, $CDCl_3$): 8.56 (d, J = 4.84 Hz, 1H, H^1), 7.87 (d, J = 8.54 Hz, 2H, H^9), 7.69 (td, J = 7.54, 2.02 Hz, 1H, H^3), 7.66 (br, 1H, H^{NH}), 7.50 (tt, J = 7.32, 1.14 Hz, 1H, H^{11}), 7.44 (t, J = 7.88 Hz, 2H, H^{10}), 7.33 (d, J = 8.13 Hz, 1H, H^4), 7.22 (dd, J = 7.56, 4.88 Hz, 1H, H^2), 4.76 (s, J = 4.80 Hz, 2H, H^6). $^{13}C\{^1H\}$ NMR (125.78 MHz, δ, $CDCl_3$): 167.34 (C^7), 156.15 (C^5), 148.85 (C^1), 136.95 (C^3), 134.34 (C^8), 131.46 (C^{11}), 128.51 (C^{10}), 127.07 (C^9), 122.46 (C^2), 122.29 (C^4), 44.66 (C^6). HRMS (ESI-TOF): Calcd. for $C_{13}H_{12}N_2NaO$ $[M+Na]^+$ 235.0842, found 235.0842.

4-hydroxy-N-(pyridin-2-ylmethyl)benzamide (L5): 2-aminomethylpyridine and 4-hydroxybenzoic acid were used as reagents. Isolated as a white solid. Yield: 2.17 g (95 %).

---

[159] Chaudhuri, U. P.; Whiteaker, L. R.; Yang, L.; Houser, R. P. *Dalton Trans.*, **2006**, 1902-1908.
[160] Kerdphon, S.; Quan, X.; Parihar, V. S.; Andersson, P. G. *J. Org. Chem.* **2015**, *80*, 11529-11537.

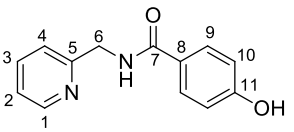

^{1}H NMR (500.13 MHz, δ, DMSO-d_6): 8.47 (d, J = 4.6 Hz, 1H, H^{1}), 7.73 (m, 1H, H^{10}), 7.71 (m, 1H, H^{3}), 7.42 (d, J = 7.8 Hz, 1H, H^{4}), 7.21 (dd, J = 4.92, 7.52 Hz, 1H, H^{2}), 6.76 (m, 1H, H^{9}), 3.83 (s, 2H, H^{6}), 3.5 (br, 2H, NH, OH). ^{13}C{^{1}H} NMR (125.78 MHz, δ, DMSO-d_6): 168.03 (C^{11}), 161.42 (C^{7}), 149.11 (C^{1}), 137.15 (C^{3}), 131.7 (C^{10}), 123.84 (C^{8}), 122.41 (C2), 121.72 (C^{4}), 115.30 (C^{9}), 46.93 (C^{6}). Anal. Calcd. For $C_{13}H_{12}N_2O_2$: C, 68.41 %; H, 5.3 %; N, 12.24 %. Found C, 68.40 %; H, 5.31 %; N, 12.28 %.

4-hydroxy-N-methyl-N-(pyridin-2-ylmethyl)benzamide (L6): N-methyl-2-aminomethylpyridine and 4-hydroxybenzoic acid were used as reagents. Isolated as a white solid. Yield: 2 g (82.6 %).

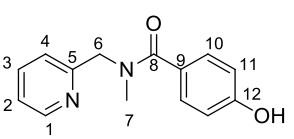

^{1}H NMR (500.13 MHz, δ, DMSO-d_6): 8.46 (d, J = 5.07 Hz, 1H, H^{1}), 7.74 (m, 3H, $H^{3, 10}$), 7.38 (d, J = 7.66 Hz, 1H, H^{4}), 7.22 (dd, J = 7.6 Hz, 4.96 Hz, 1H, H^{2}), 6.77 (m, 2H, H^{11}), 3.75 (s, 2H, H^{6}), 2.29 (s, 3H, H^{7}). ^{13}C{^{1}H} NMR (125.78 MHz, δ, DMSO-d_6): 167.83 (C^{8}), 161.77 (C^{12}), 160.16 (C^{5}), 149.18 (C^{1}), 136.90 (C^{3}), 131.85 (C^{10}), 122.64 (C^{9}), 122.39 (C^{2}), 122.24 (C^{4}), 115.42 (C^{11}), 56.65 (C^{6}), 35.96 (C^{7}). Anal. Calcd. For $C_{14}H_{15}N_2O_2$: C, 69.41 %; H, 5.82 %; N, 11.56 %. Found C, 69.40 %; H, 5.84 %; N, 11.57 %.

2,2,2-trifluoro-N-(quinolin-8-yl)acetamide (L7)[161]: 8-aminoquinoline and trifluoroacetic anhydride were used as reagents. Isolated as a white solid. Yield: 2.20 g (91.7 %).

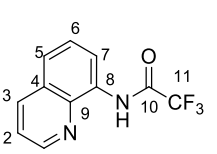

[161]Yang, T.; Cao, X.; Zhang, X.-X.; Ou, Y.; Au, C.-T.; Yin, S.-F.; Qiu, R. *J. Org. Chem.* **2020**, *85*, 12430-12443.

^{1}H NMR (500.13 MHz, δ, $CDCl_3$): 10.74 (br, 1H, H^{NH}), 8.85 (dd, J = 4.43, 1.64 Hz, 1H, H^1), 8.70 (dd, J = 7.49, 1.53 Hz, 1H, H^7), 8.21 (dd, J = 8.18, 1.80 Hz, 1H, H^3), 7.64 (dd, J = 8.35, 1.45 Hz, 1H, H^5), 7.58 (t, J = 7.8 Hz, 1, H^6), 7.51 (dd, J = 8.24, 4.16 Hz, 1H, H^2). ^{13}C{^{1}H} NMR (125.78 MHz, δ, $CDCl_3$): 148.9 (C^1), 138.33 (C^9), 136.49 (C^3), 131.99 (C^8), 127.99 (C^4), 127.07 (C^6), 123.80 (C^5), 122.18 (C^5), 117.62 (C^7). ^{19}F NMR (470.168 MHz, δ, $CDCl_3$): -75.75 (s, 3F, F^{11}). HRMS (ESI-TOF): Calcd. for $C_{11}H_7F_3N_2NaO$ $[M+Na]^+$ 263.0403, found 263.0406.

N-(quinolin-8-yl)acetamide (L8)[162]**:** 8-aminoquinoline and acetyl chloride were used as reagents. Isolated as a white solid. Yield: 1.79 g (96.7 %).

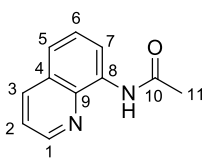

^{1}H NMR(500.13 MHz, δ, $CDCl_3$): 9.79 (br, 1H, H^{NH}), 8.80 (dd, J = 1.8, 4.22 Hz, 1H, H^1), 8.76 (dd, J = 1.56, 7.23 Hz, 1H, H^5), 8.17 (dd, J = 1.6, 8.22 Hz, 1H, H^3), 7.53 (m, 2H, H^6, H^7), 7.45 (dd, J = 43, 8.2 Hz, 1H, H^2), 2.35 (s, 3H, H^{11}). ^{13}C{^{1}H} NMR (125.78 MHz, δ, $CDCl_3$): 168.56 (C^{10}), 148.10 (C^1), 138.13 (C^4), 136.60 (C^3), 134.56 (C^8), 128.10 (C^9), 127.51 (C^6), 121.57 (C^7), 121.43 (C^2), 116.53 (C^5), 25.16 (C^{11}). HRMS (ESI-TOF): Calcd. for $C_{11}H_{10}N_2NaO$ $[M+Na]^+$ 209.0685, found 209.0684.

4.4.3 Synthesis of palladium complexes

$(NBu_4)[PdBr(C_6F_5)$(6-hydroxypicolinato)] (15): In a 100-mL flask 30 mL of acetone, 6-hydroxypicolinic acid (103 mg, 0.74 mmol), $(NBu_4)_2[Pd_2(\mu\text{-}Br)_2Br_2(C_6F_5)_2]$ (500 mg, 0.37 mmol) and Cs_2CO_3 (241 mg, 0.74 mmol) were introduced. The mixture was stirred at room temperature for 3 h. The suspension was filtered and the resulting solution was concentrated in vacuo affording a yellow oil. It was triturated with hexane and a yellow solid appeared. It was filtered and air-dried. Yield: 460 mg (84.9 %). The precipitate proved to be a mixture of two isomers isomer **M**: isomer **m** in ratio 1:0.4 that were tentatively assigned to the cis and trans diastereoisomers. HRMS (ESI-TOF): Calcd. for $C_{12}H_4BrF_5NO_3Pd$ $[M]^-$ 489.8335, found 489.8342.

[162]Pérez-Gómez, M.; Azizollahi, H.; Franzoni, I.; Larin, E. M.; Lautens, M.; García-López, J.-A. *Organometallics*, **2019**, *38*, 973-980.

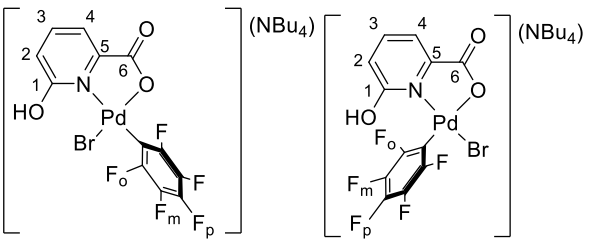

Major isomer (**M**): ^{1}H NMR (500.13 MHz, δ, $(CD_3)_2CO$): 7.27 (br, J = 7 Hz, 1H, H^3), 6.97 (br, J = 7 Hz, 1H, H^4), 5.91 (d, J = 7 Hz, 1H, H^2), 3.45 (m, 8H, H^{NBu4}), 1.83 (m, 8H, H^{NBu4}), 1.43 (m, 8H, H^{NBu4}), 0.98 (t, J = 7.4 Hz, 12H, H^{NBu4}). ^{13}C{^{1}H} NMR (125.78 MHz, δ, $(CD_3)_2CO$): 172.5 (C^6) 168.6 (C^1), 152.6 (C^5), 138.2 (C^3), 116.6 (C^2), 114.3 (C^4). ^{19}F NMR (470.168 MHz, δ, $(CD_3)_2CO$): -118.2 (m, 2F, F_o), -169.2 (br, J = 19.7 Hz, 1F, F_p), -170.1 (br, 2F, F_m).

Minor isomer (**m**): ^{1}H NMR (500.13 MHz, δ, $(CD_3)_2CO$): 7.97 (t, J = 7.4 Hz, 1H, H^3), 7.51 (d, J = 7.0 Hz, 1H, H^4), 6.95 (d, J = 8.0 Hz, 1H, H^2), 3.45 (m, 8H, H^{NBu4}), 1.83 (m, 8H, H^{NBu4}), 1.43 (m, 8H, H^{NBu4}), 0.98 (t, J = 7.4 Hz, 12H, H^{NBu4}). ^{13}C{^{1}H} NMR (125.78 MHz, δ, $(CD_3)_2CO$): 173.3 (C^6), 165.5 (C^1), 150.0 (C^5), 142.0 (C^3), 118.3 (C^4), 114.6 (C^2). ^{19}F NMR (470.168 MHz, δ, $(CD_3)_2CO$): -119.7 (m, 2F, F_o), -164.7 (br, 1F, F_p), -167.3 (br, 2F, F_m).

$(NBu_4)[Pd(C_6F_5)$(6-oxidopicolinato)(py)] (16): In a 50-mL flask $(NBu_4)[PdBr(C_6F_5)$(6-hydroxypicolinate)] (200 mg, 0.27 mmol) and 20 mL of acetone were introduced. Pyridine (90 μL, 1.1 mmol) and Ag_2CO_3 (37 mg, 0.14 mmol) were added. The mixture was stirred at room temperature 20 h protected from light. It was filtered and the solution was concentrated in vacuo affording a yellow oil. It was triturated with hexane and a yellow solid precipitated. It was filtered and air-dried. Yield: 151 mg (76 %).

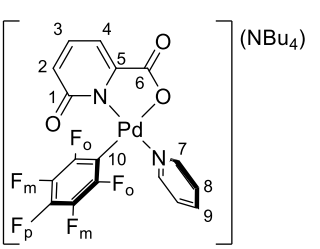

^{1}H NMR (500.13 MHz, δ, $(CD_3)_2CO$): 8.57 (dt, J = 4.9, 1.5 Hz, 2H, H^7), 7.96 (tt, J = 7.7, 1.5 Hz, 1H, H^9), 7.47 (m, 2H, H^8), 6.96 (dd, J = 6.5, 8.6 Hz, 1H, H^3), 6.44 (dd, J = 6.5, 1.5 Hz, 1H, H^4), 5.88 (dd, J = .86, 1.5 Hz, 1H, H^2), 3.42 (m, 8H, H^{NBu4}), 1.80 (m, 8H, H^{NBu4}), 1.42 (m, 8H, H^{NBu4}), 0.97 (t, J = 7.4 Hz, 12H, H^{NBu4}). ^{13}C{^{1}H} NMR (125.78

MHz, δ, $(CD_3)_2CO$): 173.4 (C^6)*, 167.8 (C^1)*, 153.8 (C^5)*, 152.2 (C^7), 147.8 (C^{Fo})*, 138.4 (C^9), 135.9 (C^{Fp})*, 135.5 (C^3), 134.9 (C^{Fm})*, 125.2 (C^8), 120.5 (C^2), 120.3 (C^{10})*, 106.6 (C^4), 58.8 (C^{NBu4}), 23.3 (C^{NBu4}), 19.5 (C^{NBu4}), 13.1 (C^{NBu4}). ^{19}F NMR (470.168 MHz, δ, $(CD_3)_2CO$): -120.25 (m, 2F, F_o), -167.69 (t, J = 19.9 Hz, 1F, F_p), -168.28 (m, 2F, F_m). HRMS (ESI-TOF): Calcd. for $C_{17}H_8F_5N_2O_3Pd$ $[M]^-$ 488.9502, found 488.9521.

*The ^{13}C chemical shifts were determined by ^1H-^{13}C HMBC and ^{19}F-^{13}C HSQC.

(NBu_4)[PdBr(C_6F_5)(2,2,2-trifluoro-N-(pyridin-2-ylmethyl)acetamide)] (17): In a 100-mL flask $(NBu_4)_2[Pd_2(\mu\text{-}Br)_2Br_2(C_6F_5)_2]$ (1.7 g, 1.25 mmol), 30 mL of acetone and 2,2,2-trifluoro-N-(pyridin-2-ylmethyl)acetamide (**L1**) (509 mg, 2.5 mmol) were introduced. Cs_2CO_3 (815 mg, 2.5 mmol) was added to the solution and the mixture was stirred at room temperature 20 h. The solvent was evaporated in vacuo. EtOH (3 mL) and hexane (20 mL) were added to the orange oil and it was stirred vigorously till a yellow solid appears. It was washed with more hexane, filtered and air-dried. Yield: 1.8 g (90.0 %). The complex is a single isomer and the absence of cross-peaks in the ^1H-^{19}F HOESY experiment allows to assign the following structure:.

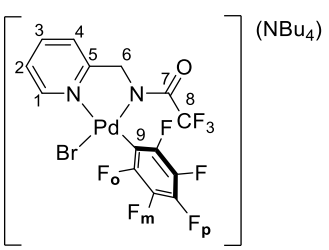

^1H NMR (500.13 MHz, δ, $(CD_3)_2CO$): 8.98 (d, J = 5.4 Hz, 1H, H^1), 7.95 (dt, J = 1.71, 8.26 Hz, 1H, H^3), 7.58 (d, J = 8.26 Hz, 1H, H^4), 7.40 (t, J = 6.27 Hz), 1H, H^2), 5.06 (s, 2H, H^6), 3.46 (m, 8H, H^{NBu4}), 1.83 (m, 8H, H^{NBu4}), 1.43 (m, 8H, H^{NBu4}), 0.98 (t, J = 7.2 Hz, 12H, H^{NBu4}),. $^{13}C\{^1H\}$ NMR (125.78 MHz, δ, $(CD_3)_2CO$): 162.65 (C^7), 149.90 (C^1), 138.56 (C^3), 122.86 (C^3), 120.90 (C^4), 119.78 (C^8), 58.5 (C^{NBu4}), 56.70 (C^6), 23.5 (C^{NBu4}), 19.4 (C^{NBu4}), 12.9 (C^{NBu4}). ^{19}F NMR (470.168 MHz, δ, $(CD_3)_2CO$): -70.43 (s, 3F, F^8), -117.17 (m, 2F, F_o), -166.49 (t, J = 20.21 Hz, 1F, F_p), -168.57 (m, 2F, F_m).). HRMS (ESI-TOF): Calcd. for $C_{14}H_6BrF_8N_2OPd$ $[M]^-$ 554.8576, found 554.8573.

[Pd(C_6F_5)(py)(2,2,2-trifluoro-N-(pyridin-2-ylmethyl)acetamide)] (18): In a 50-mL flask protected from light were introduced 15 mL of acetone, [Pd Br(C_6F_5)$(NCMe)_2$] (175 mg, 0.4 mmol), 2,2,2-trifluoro-N-(pyridin-2-ylmethyl)acetamide (**L1**) (82 mg, 0.4 mmol), pyridine (129.4 µL, 1.6 mmol) and Ag_2CO_3 (55.4 mg, 0.2 mmol). The mixture was stirred at room temperature for 20 h. A brown precipitate appeared and the

suspension was filtered. The resulting yellow solution was evaporated in vacuo obtaining a yellow oil. Cold Et_2O was added and stirred till a yellow precipitate appeared. The precipitate was filtered and air-dried. Yield: 145 mg (65 %). In acetone the precipitate proved to be a mixture of two isomers and after four days the ratio was isomer **a**: isomer **b** 1:0.23. The stereochemistry of the complexes was determined by ^{1}H-^{19}F HOESY NMR and ^{1}H-ROESY NMR. The cross peaks between F_o-H^9 and F_o-H^1 of the major isomer in the ^{1}H-^{19}F HOESY shows it is isomer **a**. Also, a cross peak between F^8-H^9 shows the CF_3 is close to the metal instead of the ketone. In the ^{1}H-ROESY, a cross peak between H^9-H^1 of the minor isomer determines it is isomer **b**. Anal. Calcd. For $C_{19}H_{11}F_8N_3OPd$: C, 41.06 %; H, 2.00 %; N, 7.56 %. Found C, 41.20 %; H, 1.94 %; N, 7.23 %.

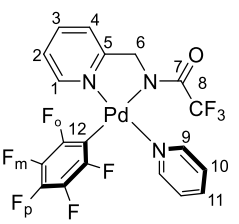

a

Isomer 18a*:* ^{1}H NMR (500.13 MHz, δ, $(CD_3)_2CO$): 8.77 (d, J = 5.57 Hz, 2H, H^9), 8.03 (td, J = 7.35, 1.34 Hz, 1H, H^3), 7.98 (tt, J = 7.79, 1.78 Hz, 1H, H^{11}), 7.81 (d, J = 5.57 Hz, 1H, H^1), 7.74 (d, J = 8.01 Hz, 1H, H^4), 7.53 (t, J = 7.57 Hz, 2H, H^{10}), 7.28 (t, J = 7.12 Hz, 1H, H^2), 5.17 (s, 2H, H^6). ^{13}C{^{1}H} NMR (125.78 MHz, δ, $(CD_3)_2CO$): 165.33 (C^7), 161.30 (C^5), 153.35 (C^9), 151.56 (C^1), 139.89 (C^2), 139.18 (C^{11}), 125.51 (C^{10}), 123.64 (C^3), 122.04 (C^4), 54.67 (C^6). ^{19}F NMR (470.168 MHz, δ, $(CD_3)_2CO$): -71.99 (s, 3F, F^8), -121.53 (m, 2F, F_o), -161.50 (t, J = 19.58 Hz, 1F, F_p), -163.68 (m, 2F, F_m).

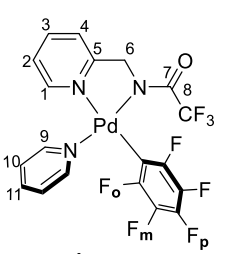

b

Isomer 18b*:* ^{1}H NMR (500.13 MHz, δ, $(CD_3)_2CO$): 9.00 (d, J = 4.05 Hz, 2H, H^9), 8.11 (td, J = 7.85, 1.61 Hz, 1H, H^{11}), 8.07 (tt, J = 7.72, 1.50 Hz, 1H, H^3), 7.79 (d, J = 7.72 Hz, 1H, H^4), 7.68 (d, J = 6.23 Hz, 1H, H^{10}), 7.65 (t, J = 6.46 Hz, 2H, H^1), 7.38 (t, J = 6.57 Hz, 1H, H^2), 5.13 (s, 2H, H^6).). ^{13}C{^{1}H} NMR (125.78 MHz, δ, $(CD_3)_2CO$): 153.10 (C^9), 146.78 (C^1), 139.59 (C^2), 126.81 (C^{11}), 126.67 (C^{10}), 123.44 (C^3), 121.60 (C^4), 56.12

(C^6).* ^{19}F NMR (470.168 MHz, δ, $(CD_3)_2CO$): -70.50 (s, 3F, F^8), -121.15 (m, 2F, F_o), -163.22 (t, J = 18.55 Hz, 1F, F_p), -166.10 (m, 2F, F_m).

*The remaining ^{13}C signals could not be located due to the low concentration of this isomer.

4.4.4 Synthesis of soluble bases and salts.

$(NBu_4)_2CO_3$: $(NBu_4)OH{\cdot}30\ H_2O$ (7.9 g, 9.8 mmol) was introduced into a Schlenk flask under N_2. Dry dichloromethane (40 mL) was added and CO_2 was bubbled into the mixture for 24 h at room temperature taking care to add more solvent when it is evaporating. $(NBu_4)OH{\cdot}30\ H_2O$ (7.9 g, 9.8 mmol) was added to the mixture and was stirred for 24 h at room temperature. After the evaporation of the solvent a white solid was obtained which was washed with cold Et_2O. Yield: 4.9 g (92 %).

$(NBu_4)BF_4$: $(NBu_4)OH$ (2 mL, 1 M in MeOH, 2 mmol) was introduced into a Schlenk flask under N_2. HBF_4 (0.25 mL, 50 wt. % in H_2O, 2 mmol) was added. It was stirred 24 h at room temperature. After the evaporation of the solvent a white solid was obtained and washed with cold Et_2O. Yield: 0.58 g (94 %).

$(NBu_4)_2HPO_4$: $(NBu_4)OH{\cdot}$ (4.4 mL, 40 wt % in H_2O, 6.8 mmol) was introduced into a Schlenk flask under N_2. H_3PO_4 (0.24 mL, 84 wt. % in H_2O, 3.4 mmol) was added. It was stirred 24 h at room temperature. After the evaporation of the solvent a white solid was obtained. Yield: 1.8 g (91 %).

4.4.5 Catalytic reactions

General procedure for the direct arylation of arenes.

$Pd(OAc)_2$ (3.8 mg, 0.017 mmol), ligand (0.017 mmol) and base (0.68 mmol) were introduced in a Schlenk flask under a nitrogen atmosphere. Then, the Ar-I (0.34 mmol) and the corresponding arene (3.0 mL) were added to the flask. The reaction mixture was stirred at the specified temperature and checked by ^1H or ^{19}F NMR of the crude mixture after 6 h and 24 h. The spectroscopic data for the coupling products and byproducts were compared with the literature data.[20]

The results for the direct arylation reactions are collected in the Tables in the main text. Additional data are collected in Table 4.10.

Table 4.10. Direct arylation of pyridine with *p*-iodotoluene as aryl halide using the pic-6-OH ligand.[a]

Entry	[Pd]	Crude yield, % (conv., %), 6h[b]	Crude yield, % (conv., %), 24h[b]
1[c]	$Pd(OAc)_2$	0 (0)	0 (0)
2[c]	$Pd(OAc)_2$ + **bipy-6OH**	88 (97)	90 (100)
3	$Pd(OAc)_2$ + **pic-6-OH**	0 (0)	4 (5)
4	**16**	15 (25)	27 (39)

[a]Reaction conditions: ArI (0.34 mmol), pyridine (3.0 mL), [Pd] (5 mol %), Cs_2CO_3 (0.34 mmol); 140 ˚C. [b]Crude yields determined by ^1H NMR of the reaction mixture. The reduction of the ArI (ArH) is the observed byproduct. [c]Data taken from the literature.

General procedure for the oxidative Heck reaction of arenes.

In a Schlenk flask, $Pd(OAc)_2$ (3.8 mg, 0.017 mmol), the corresponding ligand (0.017 mmol) and sodium molybdate dihydrate (8.3 mg, 0.034 mmol) were introduced. The flask was purged of air and backfilled with oxygen. *tert*-Butyl acrylate (50 µL, 0.34 mmol), dodecane (40 µL, 0.18 mmol) as internal standard, toluene (1.5 mL) and DMA (1.5 mL) were added to the mixture. Oxygen was bubbled during 5 minutes. The flask was introduced into an oil bath at 120 ºC and stirred. The reaction mixture was checked by ^1H NMR of the crude after 6 h and 24 h. The spectroscopic data were compared with the literature.[25]

General procedure for the alkylation of arylcarboxylic acids.

2-(Trifluoromethyl)benzeneacetic acid (105.2 mg, 0.5 mmol), potassium butyltrifluoroborate (127 mg, 0.75 mmol), Li_2CO_3 (73.1 mg, 1.0 mmol), Ag_2CO_3 (275.8 mg, 1.0 mmol), $Pd(OAc)_2$ (11.2 mg, 0.05 mmol), the corresponding ligand (0.1 mmol) and DMF (40 µL, 0.5 mmol) were introduced into a Schlenk flask. ^{t}BuOH (2.5 mL) was added to the mixture. It was purged of air and backfilled with N_2 and stirred at 110 ºC for 2 h. The vessel was transferred to an ice bath, the reaction quenched with 2M $HCl_{(aq)}$, and extracted with Et_2O (3 x 25 mL). The organic phase was concentrated in vacuo and checked by ^1H and ^{19}F NMR. The spectroscopic data were compared with those in the literature.[155]

General procedure for the acetoxylation of free carboxylic acids.

2-Methylbutanoic acid (11 µL, 0.1 mmol), Na_2CO_3 (10.6 mg, 0.1 mmol), $Pd(OAc)_2$ (2.2 mg, 0.01 mmol) and the corresponding ligand (0.02 mmol) were introduced into a Schlenk flask which was purged and filled with N_2. Then, HFIP (1 mL), TBPH (37 µL, 0.2 mmol) and Ac_2O (20 µL, 0.2 mmol) were added to the mixture. It was stirred 3 min at room temperature and then heated at 60 ºC for 12 h. After cooling down, AcOH (0.05 mL) was added and the solution was evaporated to dryness. The residue was dissolved in MeOH (1 mL) and $TMSCHN_2$ (0.1 mL, 0.2 mmol) was added. The mixture was stirred at room temperature 1 h and concentrated in vacuo. The crude mixture was checked by ^1H NMR and the spectroscopic data were compared with the literature.[156]

4.4.6 Mechanistic experiments: thermal decomposition of 16 and 18 under catalytic conditions.

Complex **16** (7.3 mg, 0.01 mmol) was added into an NMR tube along with a sealed glass capillary filled with DMSO-d_6 as NMR lock signal. Then, 0.6 mL of solvent were added. The species formed in solution at room temperature were examined by ^{19}F NMR. Then, the mixture was heated for the specified time. The experiment in toluene was done adding an internal standard (2 eq of C_6F_6) due to the low solubility of **16**. The ^{19}F NMR signals of the decomposition products conform to those in the literature.[20]

Pyridine as solvent.

16: ^{19}F NMR (470.168 MHz, δ, pyridine/DMSO-d_6 capillary): -119.54 (m, 2F, F_{ortho}), -165.7 (t, J = 19.8 Hz, 1F, F_{para}), -166.65 (m, 2F, F_{meta}).

Ethyl benzoate as solvent

16: ^{19}F NMR (470.168 MHz, δ, ethyl benzoate/DMSO-d_6 capillary): -116.43 (m, 2F, F_{ortho}), -166.10 (t, J = 16.7 Hz, 1F, F_{para}), -167.60 (m, 2F, F_{meta}).

Complex **18** (7.0 mg, 0.013 mmol) was added into an NMR tube along with a sealed glass capillary filled with DMSO-d_6 as NMR lock signal. Then, 0.6 mL of solvent were added. The species formed in solution at room temperature were examined by ^{19}F NMR. Then, the mixture was heated for the specified time.

Pyridine as solvent

18: ^{19}F NMR (470.168 MHz, δ, pyridine/DMSO-d_6 capillary): -121.06 (m, 2F, F_{ortho}), 159.28 (t, J = 26 Hz, 1F, F_{para}), 162.00 (m, 2F, F_{meta}).

Toluene as solvent

18: ^{19}F NMR (470.168 MHz, δ, toluene/DMSO-d_6 capillary): -121.03 (m, 2F, F_{ortho}), -158.85 (t, J = 19 Hz, 1F, F_{para}), 161.86 (m, 2F, F_{meta}).

Ethyl benzoate as solvent

18: ^{19}F NMR (470.168 MHz, δ, ethyl benzoate/DMSO-d_6 capillary): -121.28 (m, 2F, F_{ortho}), 159.73 (t, J = 24 Hz, 1F, F_{para}), 162.47 (m, 2F, F_{meta}).

4.4.7 Computational details

The DFT studies have been performed with the M06 functional,[102] as implemented in the Gaussian09 program package.[146] The 6-31+G(d) basis set was used for C, O, N, F and H,[103] and LANL2TZ(f) for Pd,[104] (Basis set I). Solvent effects have been considered through the continuum model SMD for the experimental solvent, pyridine (ε = 12.3 at 25 ºC), which was introduced in all the optimizations, frequency calculations and potential energy refinement. All structure optimizations were carried out in solvent phase with no symmetry restrictions. Gibbs energy corrections were calculated at 413.15 K (the experimental temperature) and 105 Pa pressure, including zero point energy corrections (ZPE), and the energies were converted to 1M standard state in solution (adding/subtracting 1.89 kcal mol^{-1} for non-unimolecular processes). Vibrational frequency calculations were performed in order to confirm that the stationary points were minima (without imaginary frequencies) or transition states (with one imaginary frequency). Final potential energies were refined by performing additional single-point energy calculations (also in solution); Pd was still described with LANL2TZ(f) basis set, and the remaining atoms were treated with 6-311++G(d,p) basis set (Basis set II). All energies presented correspond to free energies in solution, obtained from potential energies (including solvation) with basis set II plus Gibbs energy corrections with basis set I and are given in kcal mol^{-1}.

4.4.8 Data for X-Ray structure determinations

Crystals suitable for X-ray analyses were obtained by slow evaporation of the solvent of a solution of complex (NBu_4)[Pd(6-oxidopicolinate)(C_6F_5)(py)] (**16**) in acetone at room temperature and by slow evaporation of the solvent of a solution of complex [Pd(2,2,2-trifluoro-N-(pyridin-2-ylmethyl)acetamide)Py(C_6F_5)] (**18**) in CH_2Cl_2 at room temperature. The crystals were attached to glass fibers and transferred to an Agilent Supernova diffractometer with an Atlas CCD area detector. Data collection was performed with Mo Kα radiation (0.71073 Å) at 298 K. Data integration and empirical absorption correction were carried out using the CrysAlisPro program package.[98] The structures were solved by direct methods and refined by full-matrix least squares against F2 with SHELX,[99] using Olex2.[100] The non-hydrogen atoms were refined anisotropically and hydrogen atoms were constrained to ideal geometries and refined with fixed isotropic displacement parameters. Refinement proceeded smoothly to give the residuals shown in Table 4.11.

Table 4.11. Crystal data and structure refinement for complex **16** and **18**.

Compound name	**16**	**18**
Empirical formula	$C_{33}H_{44}N_2O_3F_5Pd$	$C_{19}H_{11}N_3OF_8Pd$
Formula weight	718.10	555.71
Temperature/K	298	298
Crystal system	monoclinic	triclinic
Space group	$P2_1/n$	P-1
a/Å	9.6445(4)	7.8652(7)
b/Å	17.1990(7)	8.1503(7)
c/Å	21.3233(9)	15.9688(16)
α/°	90	99.910(8)
β/°	100.365(4)	95.532(8)
γ/°	90	92.609(7)
Volume/Å^3	3479.3(3)	1001.67(16)
Z	4	2
ρ_{calc}g/cm^3	1.371	1.842
μ/mm^{-1}	0.593	1.016
F(000)	1484.0	544.0
Crystal size/mm^3	0.336 × 0.277 × 0.111	0.464 × 0.355 × 0.154
Radiation	MoKα (λ = 0.71073)	MoKα (λ = 0.71073)
2Θ range for data collection/°	6.72 to 58.928	6.602 to 58.928
Index ranges	$-10 \leq h \leq 13$, $-17 \leq k \leq 23$, $-27 \leq l \leq 25$	$-8 \leq h \leq 10$, $-11 \leq k \leq 10$, $-22 \leq l \leq 13$
Reflections collected	19423	8273
Independent reflections	8309 [R_{int} = 0.0371, R_{sigma} = 0.0623]	4660 [R_{int} = 0.0389, R_{sigma} = 0.0707]
Data/restraints/parameters	8309/0/401	4660/0/289
Goodness-of-fit on F^2	1.054	1.047
Final R indexes [I>=2σ (I)]	R_1 = 0.0555, wR_2 = 0.1430	R_1 = 0.0466, wR_2 = 0.0877
Final R indexes [all data]	R_1 = 0.1027, wR_2 = 0.1753	R_1 = 0.0789, wR_2 = 0.1080
Largest diff. peak/hole / e Å^{-3}	0.98/-0.76	0.61/-0.72

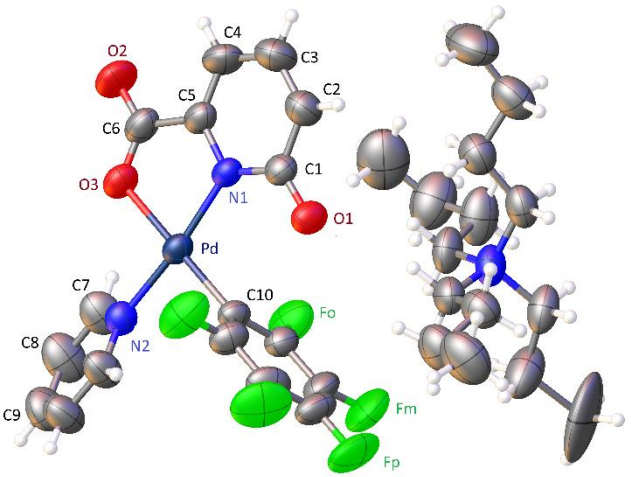

Figure 4.23. X-ray molecular structure of **16** (ORTEP 40 % probability ellipsoids).

Table 4.12. Selected bond lengths for complex **16.** Numbering scheme in Figure 4.23.

Bond	**d (Å)**
Pd-N_1	2.014
Pd-N_2	2.038
Pd-O_3	2.050
Pd-C_{10}	1.980
C_1-O_1	1.244

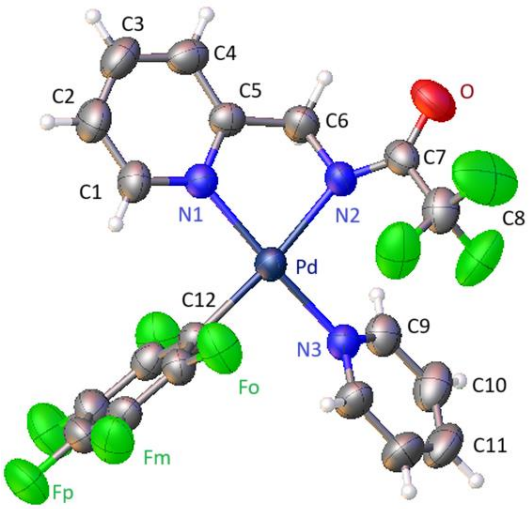

Figure 4.24. X-ray molecular structure of **18a** (ORTEP 40 % probability ellipsoids).

Table 4.13. Selected bond lengths for complex **18a.** Numbering scheme in Figure 4.24.

Bond	**d (Å)**
Pd-N_1	2.026
Pd-N_2	2.067
Pd-N_3	2.030
Pd-C_{12}	2.009
N_2-C_7	1.298
N_2-C_6	1.473
C_7-O	1.229

Conclusions

The work developed during this thesis includes two new synthetic methodologies of metal-ligand cooperation for the direct arylation of arenes and the assessment of potential cooperating ligands in C–H activation. The conclusions are described for each topic are the following.

Unprotected anilines can be selectively arylated in the *ortho* position using the Pd/[2,2′-bipyridin]-6(1H)-one (bipy-6-OH) catalyst system, avoiding the protection-deprotection additional steps commonly used in the literature. Substituted anilines with different electronic properties or even with bulky substituents can be functionalized. The *ortho* isomer was obtained selectively for all the primary and secondary anilines but for tertiary anilines no *ortho* coupling product was formed. It has been demonstrated by mechanistic studies that the cooperating role of the bipy-6-OH in the C–H cleavage step is crucial for the chemoselectivity, affording the C–C coupling product. Computational studies have shown the operation of an anionic route where the C–H activation occurs on an amido complex, which has a lower activation energy than the C–N reductive elimination. The relative energy barriers for both processes eliminates the competition of the C–N coupling product (amination) and explain the chemoselectivity observed. The regioselectivity of primary and secondary anilines can be also explained by the anionic route, which favours the *ortho* isomer.

A new dual ligand approach (bipy-6-OH/PCy_3) allows to use milder reaction conditions than the reported ones in the literature for the direct arylation of simple arenes. Electron-donating and electron-withdrawing groups are tolerated in the arene and aryl halide scaffold. In addition, aryl chlorides can be used as coupling partners. The reaction rate depends directly on the electronic properties of the arene and a higher reaction rate was observed for electron rich arenes (anisole). Mechanistic studies allow to propose a bimetallic reaction mechanism where a bipy-6-OH-palladium complex and a PCy_3-containing complex operates simultaneously. The transmetallation step between those two species has been demonstrated by independent experiments. The palladium species responsible for the C–H activation are more electrophilic than in the reported monoligand systems and an *e*CMD mechanism is possible as supported by computational studies and the higher reactivity of electron rich arenes. The regioselectivity of the reaction depends on the arene and aryl halide used, and the isomer ratio observed seems to be influenced by the rate of the transmetallation step.

The ligand 6-hydroxypicolinic acid (pic-6-OH) and the amido-pyridine type ligands are efficient cooperating ligands in the C–H activation reaction of arenes as has

been demonstrated by the thermal decomposition of isolated palladium complexes and the DFT calculations. Nevertheless, those ligands are not efficient in the catalytic direct arylation of arenes even though they seemed to meet the necessary characteristics for those transformations.

In the case of pic-6-OH an increment of the yield was observed by using soluble bases or more polar solvents, which points to the importance of the chelating dianionic coordination mode of the ligand for an efficient C–H activation. However, the ligand seems to promote the formation of a high amount of byproducts.

For the amido-pyridine ligands, the catalytic reactions show a high amount of byproducts indicating that the intermediates evolve through reorganization pathways. Other type of coupling reactions were also tried. In the oxidative Heck reaction of toluene and the *ortho*-C–H alkylation of arylcarboxylic acids using alkyl boronic acids no better results were obtained when the ligands were used. On the other hand, some of the ligands achieved good results in the C–H acetoxylation of free alkyl carboxylic acids.

It seems that the efficiency of pic-6-OH and the amido-pyridine ligands in the processes is not enough to carry out the complete reactions. The ligand cooperation in the C–H activation is a necessary but not sufficient requirement for an efficient C–H functionalization. In any case, the proved ability of these ligands in the C–H activation step makes them suitable candidates to be considered when developing new catalytic C–H functionalization reactions.

Summary

The formation of new C–C bonds is a versatile tool in the synthesis of interesting compounds such as drugs, pesticides, cosmetics and so on. To improve the step economy of the processes, several efforts have been made during the last decades in order to use hydrocarbons as reagents. They require a C–H activation step in their mechanism but this is not easy due to the low reactivity of the C–H bonds. To achieve those high energy demanding processes, cooperating ligands have been developed with the role of assisting during the C–H activation of the reactants. The work in this thesis is focused on the use of cooperating ligands in C–C coupling reactions with C–H activation.

Chapter 2: The chemo- and regioselective arylation of primary anilines in the aromatic ring is achieved. By using the cooperating ligand 2,2'-bipiridin-6(1*H*)-one, the competitive amination reaction (Buchwald-Hartwig reaction) is not occurring, and the *ortho* C–C coupling product is obtained without the need of protecting the amine group. The reaction can be extended anilines with different electronic properties. An exhaustive computational study of the reaction mechanism explaining the chemo- and regioselectivity observed was done in collaboration with Prof. Agustí Lledós from Universidad Autónoma de Barcelona.

Chapter 3: The use of the cooperating ligand 2,2'-bipiridin-6(1*H*)-one in combination with PCy_3 allows to use milder reaction conditions than the reported ones in the direct arylation of simple arenes. Several functional groups are tolerated in the arene and in the aryl halide derivative (even aryl chlorides). The preliminary mechanistic studies show an operating bimetallic catalytic cycle and the transmetallation step has been demonstrated by independent experiments. The reaction rate depends on the electronic properties of the arene being higher for electronrich arenes. Moreover, the isomer ratio seems to be determined by the rate fo the trasnmetallation step.

Chapter 4: 6-hydroxypicolinic acid and the amido-pyridine type ligands have a similar scaffold to the cooperating ligand 2,2'-bipiridin-6(1*H*)-one or the widely reported *N*-monoprotected amino acids (MPAAs). Because of that, we have studied their cooperating ability in C–H activation processes. Independent experimental studies and DFT calculations showed the possibility of their cooperation in the direct arylation of arenes. However, in the catalytic reaction high ammounts of byproducts were obtained in all the reaction coditions tested (base, solvent and additives), pointing that the intermediates evolve through reorganization pathways. It seems that the ligand cooperation in the C–H activation is a necessary but not sufficient requirement for an efficient C–H functionalization

Resumen

Prefacio

El desarrollo de procesos de síntesis más sostenibles es uno de los mayores desafíos en el ámbito de la química hoy en día. El principal objetivo de esta tésis es mejorar las condiciones de reacción buscando alternativas más eficaces para las reacciones de acoplamiento C–C. La formación de nuevos enlaces C–C es una herramienta muy útil a la hora de sintetizar compuestos de alto valor añadido como pueden ser fármacos, cosméticos, pesticidas… etcétera. Las reacciones convencionales de acoplamiento C–C catalizadas por paladio generalmente requieren de un compuesto organometálico y un derivado halogenado, ambos necesitan ser sintetizados previamente desde los hidrocarburos comerciales. Durante las últimas décadas se han desarrollado diferentes alternativas que utilizan los hidrocarburos directamente, evitando los pasos de funcionalización previa de los reactivos. Las nuevas reacciones requieren de una etapa de activación C–H en su mecanismo y esto no es fácil debido a la baja reactividad de los enlaces C–H. Para conseguir rebajar la energía de activación de estos procesos se han desarrollado ligandos cooperativos que puedan asistir durante la etapa de activación C–H. El trabajo recogido en esta tésis se centra en el uso de ligandos cooperativos en las reacciones de acoplamiento C–C con activación C–H.

El *Capítulo 1* contiene una introducción general de las reacciones de acoplamiento C–C con activación C–H. En este capítulo se incluyen las diferentes alternativas a las reacciones de acoplamiento convencionales y los mecanismos descritos más relevantes para la etapa de activación C–H. También se describen algunas de las estrategias desarrolladas para controlar la regioselectividad de las reacciones.

Los *Capítulos 2* y *3* se centran en el uso del ligando cooperativo 2,2'-bipiridin-6(1*H*)-one en la arilación directa de arenos. En el *Capítulo 2* se incluye la arilación directa de anilinas en el anillo aromático quimio- y regioselectivamente. El uso del ligando cooperativo evita la formación del producto competitivo de la reacción de aminación de Buchwal-Hartwig, obteniéndose únicamente el producto de acoplamiento C–C sin la necesidad de proteger el grupo amino. El mecanismo de la reacción ha sido estudiado experimentalmente y mediante cálculos computacionales en colaboración con el Profesor Agustí Lledós de la Universidad Autónoma de Barcelona.

La arilación directa de arenos simples mediante un sistema dual de ligandos se describe en el *Capítulo 3*. El uso del ligando cooperativo 2,2'-bipiridin-6(1*H*)-one en

conjunto con PCy_3 permite rebajar la temperatura de la reacción de arilación de arenos ya descrita en la bibliografía. La reacción tolera diferentes grupos funcionales tanto en el areno como en el haluro de arilo utilizados como reactivos. Lo estudios del mecanismo indican un posible ciclo catalítico bimetálico.

El *Capítulo 4* describe el estudio de los ligandos ácido 6-hidroxipicolínico y amido-piridina y su capacidad de asistir en la etapa de activación C–H de diferentes reacciones. Ambos ligandos tienen una estructura similar a la de 2,2'-bipiridin-6(1*H*)-one y los aminoácidos monoprotegidos (MPAA) muy utilizados en este tipo de reacciones.

Esta tésis contiene un apéndice con una lista de abreviaturas y un índice de los compuestos descritos. Las referencias se encuentran como notas al pié en cada uno de los capítulos y en una lista en el apéndice.

Capítulo 1: Introducción

Las reacciones de acoplamiento C–C son una herramienta indispensable en la síntesis química hoy en día. Las reacciones de acoplamiento convencionales catalizadas por paladio generalmente utilizan un compuesto organometálico (M-R') y un derivado halogenado (R-X) como reactivos (Figura 1, a).[1]

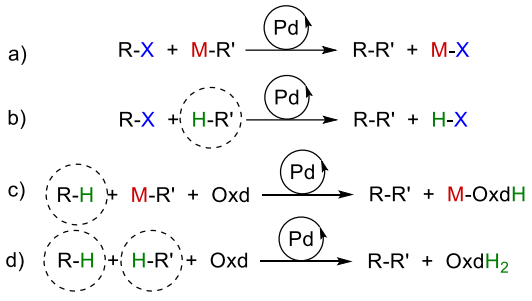

Figura 1. a) Acoplamiento C–C convencional. b) Acoplamiento entre un hidrocarburo y un derivado halogenado. c) y d) Acoplamiento oxidativo.

Para evitar los diferentes pasos de síntesis previa de los reactivos, durante las últimas décadas se han desarrollado alternativas más eficaces que utilizan los hidrocarburos de partida como reactivos para la reacción de acoplamiento.[2] En las reacciones de acoplamiento tradicionales el compuesto organometálico se comporta como nucleófilo y el haloderivado como electrófilo. Una de las alternativas consiste en sustituir el compuesto organometálico por el hidrocarburo correspondiente, en este caso el hidrocarburo seguirá comportándose como nucleófilo (Figura 1, b).[3] En el caso de sustituir el derivado halogenado por un hidrocarburo, ambos reactivos tendrán carácter nucleófilo por lo que un oxidante es necesario (Figura 1, c).[4] Finalmente, cuando ambos

[1] a) Mizoroki, T.; Ozaki, M. A. *Bull. Chem. Soc. Jpn.* **1971**, 44, 581-584. b) Heck, R. F. *J. Am. Chem. Soc.* **1968**, *90*, 5518-5526. c) Heck, R. F. *Org. React.* **1982**, *27*, 345-390. c) Kumada, M. *Pure Appl. Chem.* **1980**, 52, 669-679. d) Negishi, E.-I., *Ass. Chem. Res.* **1982**, 15, 340-348. e) Miyaura, N.; Yanagi, T.; Suzuki, A. *Synth. Commun.* **1981**, 11, 513-519. f) Miyaura, N.; Suzuki, A. *Chem. Rev.* **1995**, 95, 2457-2483. g) Stille, J. K. *Angew. Chem. Int. Ed.* **1986**, 25, 508-524. h) Stille, J. K. *Angew. Chem.* **1986**, 98, 504-519. i) Hiyama, T.; Shirakawa, E. *Top. Curr. Chem*. **2002**, 219, 61-85. j) Hiyama, T.; *J. Organomet. Chem*. **2002**, 653, 58-61.

[2] Campeau, L.-C.; Hazari, N. *Organometallics* **2019**, 38, 3-35.

[3] a) Vicente, R.; Kapdi, A. R.; Ackermann, L. *Angew. Chem. Int. Ed*. **2009**, 48, 9792-9826. b) Salamanca, V.; Toledo, A.; Albéniz, A. C. *J. Am. Chem. Soc*. **2018**, 140, 17851-17856. c) Salamanca, V.; Albéniz, A. C. *Org. Chem. Front*., **2021**, 8, 1941-1951.

[4] a) Luan, Y.-X.; Zhang, T.; Yao, W.-W.; Lu,, K.; Kong, L.-Y.; Lin, Y.-T.; Ye, M. *J. Am. Chem. Soc*. **2017**, 139, 1786-1789. b) Wang, D.; Salazar, C. A.; Stahl, S. S. *Organometallics*, **2021**, 40, 2198-2203. c) Salazar, C. A.; Gair, J. J.; Flesch, K. N.; Guzei, I. A.; Lewis, J. C.; Stahl, S. S. *Angew. Chem. Int. Ed.*, **2020**, 59 (27), 10873-10877.

reactivos son sustituidos por hidrocarburos, de nuevo un oxidante es necesario en la reacción (Figura 1, d).[5]

El mecanismo de las reacciones convencionales puede resumirse en tres etapas elementales: adición oxidante del derivado halogenado, transmetalación del organometálico al catalizador y finalmente la eliminación reductora dando lugar al producto de acoplamiento (Esquema 1, a). Cuando se sustituye el organometálico por un hidrocarburo, la etapa de transmetalación se sustituye por una etapa de activación del enlace C–H (Esquema 1, b). En el caso de sustituir ambos reactivos por hidrocarburos, dos etapas de activación C–H son necesarias además de una etapa de oxidación para recuperar el catalizador (Esquema 1, c).

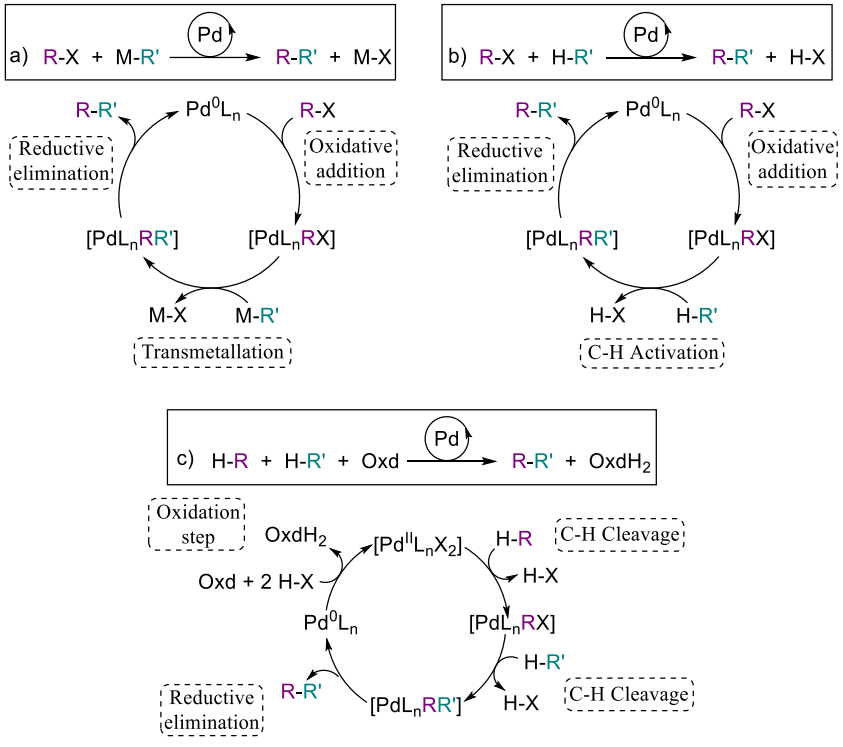

Esquema 1. Ciclo catalítico simplificado. a) Acoplamiento convencional. b) Acoplamiento entre un hidrocarburo y un derivado halogenado. c) Acoplamiento entre dos hidrocarburos.

El trabajo recogido en esta tésis se centra en las reacciones de arilación directa de arenos. El uso de hidrocarburos (arenos) como reactivos conlleva dos principales

[5] a) S. Kancherla, K. B. Jorgensen, M. A. Fernández-Ibáñez, *Synthesis* **2019**, 51, 643-663. b) W. Ali, G. Prakash, D. Maiti, *Chem. Sci.* **2021**, *12*, 2735-2759. c) Yang, Y.; Lan, J.; You, J. *Chem. Rev*. **2017**, 117, 8787-8863. d) Villalba, F.; Albéniz, A. C. *Adv. Synth.Catal*. **2021**,363, 4795-4804. e) Stuart, D. R. ; Fagnou, K. *Science* **2007**, 316, 1172-1175.

problemas: la funcionalización de un enlace C–H concreto (regioselectividad) y la poca reactividad del enlace C–H. En los últimos años se han desarrollado diferentes estrategias para conseguir que las reacciones sean regioselectivas. Una de ellas es el uso de grupos directores.[6] El grupo director presente en el sustrato se coordina a paladio y dirige la funcionalización a un enlace C–H cercano. Finalmente, el grupo director debe eliminarse para obtener el producto deseado. Para evitar los pasos de añadir y eliminar el grupo director se desarrollaron los grupos directores transitorios, los cuales son añadidos y eliminados del producto en el medio de reacción, sin la necesidad de pasos adicionales.[7] Otra estrategia es el uso de ligandos plantilla, los cuales tienen una estructura específica para dirigir la funcionalización a un enlace C–H concreto mediante impedimento estérico o interacciones no covalentes con el sustrato.[8] El uso de ligandos que pueden ser insertados en el enlace Pd–C reversiblemente, como norborneno, es otra de las estrategias utilizadas y da lugar a la funcionalización de un enlace C–H consecutivo al que sufre la primera activación C–H.[9] Estos ligandos son llamados grupos mediadores transitorios.

El mecanismo por el que se produce la activación del enlace C–H de arenos más aceptado en los últimos años es el de metalación-deprotonación concertada.[10] Este

---

[6] a) Neufeldt, S. R.; Sanford, M. S. *Acc. Chem. Res.* **2012** 45, 936-946. b) Tang, K.-X.; Wang, C.-M.; Gao, T.-H.; Chen., L.; Fan, L.; Sun, L.-P. *Adv. Synth. Catal*. **2019**, 361 (1), 26-38. c) Tomberg, A.; Muratore, M. E.; Johansson, M. M.; Terstiege, I.; Sköld, C. Norrby P.-O. *iScience*, **2019**, 20, 373-391. d) Murali, K.; Machado, L. A.; Carvalho, R. L.; Pedrosa, L. F.; Mukherjee, R.; Da Silva, E. N.; Maiti, D. *Chem. Eur. J.* **2021**, 27 (49), 12453-12508. e) Tang, K.-X.; Wang, C.-M.; Gao, T.-H.; Pan, C.; Sun, L.-P. *Org. Chem. Front*., **2017**, 4, 2167-2169.

[7] a) Gandeepan, P.; Ackermann, L. *Chem*, **2018**, 4, 199-222. b) Jacob, C.; Maes, B. U. W.; Evano, G. *Chem. Eur. J*. **2021**, 27 (56), 13899-13952. c) Xu, W.; Zhang, Y.; Wu, Y.; Wuan, J.; Lu, X.; Zhou, Y.; Zhang F.-L. *J. Org. Chem*. **2022**, 87, 10807-10814. d) Zhang, F.-L.; Hong, K.; Li, T.-J.; Park, H.; Yu, J.-Q. *Science*, **2016**, 351, 252-256. e) Xu, J.; Liu, Y.; Wang, Y.; Li, Y.; Xu, X.; Jin, Z. *Org. Lett*. **2017**, 19, 1562-1565.

[8] a) Zhang, Z.; Tanaka, K.; Yu, J.-Q. *Nature*, **2017**, 543, 538–542. b) Achar, T. K.; Ramakrishna, K.; Pal, T.; Porey, S.; Dolui, P.; Biswas, J. P.; Maiti, D. *Chem. Eur. J.*, **2018**, 24 (68), 17906-17910. c) Achar, T. P.; Biswas, J. P.; Porey, S.; Pal, T.; Ramakrishna, K.; Maiti, S.; Maiti, D. *J. Org. Chem*. **2019**, 84, 8315-8321. d) Shi, H.; Lu, Y.; Weng, J.; Bay, K. L.; Chen, X.; Tanaka, K.; Verma, P.; Houk, K. N.; Yu, J.-Q. *Nat. Chem*. **2020**, 2, 399-404. e) Dhankhar, J.; Hofer, M. D.; Linden, A.; Čorić, I. *Angew. Chem. Int. Ed*. **2022**, 61, e2022054.

[9] a) Catellani, M.; Chiusoli, G. P.; Costa, M. *J. Organomet. Chem*. **1995**, 500, 69-80. b) Catellani, M. *Synlett* **2003**, 298-313. c) Della Ca',N.; Fontana, M.; Motti, E.; Catellani, M. *Acc. Chem. Res.* **2016**, 49, 1389-1400. a) Wang, X.-C.; Gong, W.; Fang, L.-Z.; Zhu, R.-Y.; Li, S.; Engle, K. M.; Yu, J.-Q. *Nature*, **2015**, 519, 334-338. b) Dong, Z.; Wang, J.; Dong, G. *J. Am. Chem. Soc*. **2015**, 137, 5887-5890. c) Dutta, U.; Porey, S.; Pimparkar, S.; Mandal, A.; Grover, J.; Koodan, A.; Maiti, D. *Angew. Chem. Int. Ed.* **2020**, 59 (47), 20831-20836. d) Liu, S.; Wang, Q.; Huang, F.; Wang, W.; Yang, C.; Liu, J. Chen, D. *Org. Chem. Front.*, **2022**, 9, 129-139. e) Sukowski, V.; Borselen, M. V.; Mathew, S.; Fernández-Ibáñez, M. A. *Angew. Chem., Int. Ed.* **2022**, 61, e202201750.

[10] a) Fagnou, K.; Lapointe, D. *Chem. Lett*. **2010**, 39, 1118-1126. b) Akermann, L. *Chem. Rev*. **2011**, 111, 1315-1345. c) McMullin, C. L.; Davies, D. L.; Macgregor, S. A. *Chem. Rev*. **2017**, 117, 8649-8709. d) Sampson, J.; Wang, L.; Carrow, B. P. *Isr. J. Chem*. **2020**, 60, 230-258. e) Davies, D. L.; Donald, S. M. A.; Macgregor, S. A. *J. Am. Chem. Soc*. **2005**, 127, 13754-13755. f) Boutadla, Y.; Davies, D. L.; Macgregor, S. A.; Poblador-Bahamonde, A. I. *Dalton Trans*, **2009**, 5820-5831. g)

mecanismo consiste en que una base externa se coordina al centro metálico e interacciona con el enlace C–H del areno también coordinado al metal (Figura 2, a). Para abordar el problema de la baja reactividad de los enlaces C–H, se han desarrollado nuevos catalizadores que sean capaces de acelerar la etapa de activación C–H. Una estrategia muy utilizada es el uso de ligandos cooperativos. Estos ligandos pueden interactuar con el sustrato y sufrir cambios estructurales reversibles de manera que sean capaces de activar enlaces poco reactivos.[11] Uno de los ejemplos más interesantes es el uso de aminoácidos monoprotegidos.[12] Estos ligandos coordinados al metal pueden actuar como base y activar el enlace C–H, evitando la necesidad de que la base externa se coordine al metal (Figura 2, b).

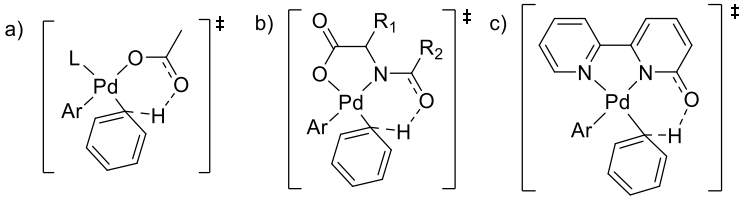

Figura 2. Comparación de estados de transición para la etapa de activación C–H. a) Metalación-deprotonación concertada. b) Activación C–H asistida por aminoácidos monoprotegidos. c) Activación C–H asistida por el ligando bipy-6-OH.

En este contexto se encuentra el trabajo recogido en esta tésis. El efecto acelerador del ligando [2,2′-bipyridin]-6(1H)-one (bipy-6-OH) ha sido demostrado anteriormente en reacciones de arilación directa de arenos (Figura 2, c).[13] El estudio de este ligando ha sido ampliado en esta tésis en la reación de arilación de anilinas (*Capítulo 2*). También se han conseguido mejorar las reacciones de arilación de arenos mediante

García-Cuadrado, D.; Braga, A. A. C.; Maseras, F.; Echavarren, A. M. *J. Am. Chem. Soc*. **2006**, 128, 1066-1067.

[11] a) Khusnutdinova, J. R.; Milstein, D. *Angew. Chem. Int. Ed.* **2015**, 54, 12236-12273. b) Higashi, T.; Kusumoto, S.; Nozaki, K. *Chem. Rev*. **2019**, 119, 18, 10393-10402. c) Gunanathan, C.; Milstein, D. *Acc. Chem. Res.* **2011**, 44 (8), 588-602. d) Kusumoto, S.; Akiyama, M.; Nozaki, K. *J. Am. Chem. Soc*. **2013**, 135, 18726-18729.

[12] a) Shao, Q.; Wu, K.; Zhuang, Z.; Qian, S.; Yu, J.-Q. *Acc. Chem. Res*. **2020**, 53, 833-851. b) G. J. Cheng, Y. F. Yang, P. Liu, P. Chen, T. Y. Sun, G. Li, X. Zhang, K. N. Houk, J. Q. Yu; Y. D. Wu, *J. Am. Chem. Soc*., **2014**, 136, 894-897. c) B. E. Haines, J. Q. Yu; D. G. Musaev, *ACS Catal*., **2017**, 7, 4344-4354. d) P. Wedi, M. Farizyan, K. Bergander, C. Mück-Lichtenfeld; M. Gemmeren, *Angew. Chem. Int. Ed*., **2021**, 60, 15641-15649. e) K. Mukherjee, N. Grimblat, S. Sau, K. Ghosh, M. Shankar, V. Gandon ; A. K. Sahoo, *Chem. Sci*., **2021**, 12, 14863-14870. f) L. P. Xu, Z. Zhuang, S. Qian, J. Q. Yu; D. G. Musaev, *ACS Catal*., **2022**, 12, 4848-4858. g) Fernández-Moyano, S.; Salamanca, V.; Albéniz, A. C. *Chem. Sci*., **2023**,14, 6688-6694.

[13] a) Salamanca, V.; Toledo, A.; Albéniz, A. C. *J. Am. Chem. Soc*. **2018**, *140*, 17851-17856. b) Salamanca, V.; Albéniz, A. C. *Org. Chem. Front*., **2021**, *8*, 1941-1951.

el uso de bipy-6-OH y PCy_3 (*Capítulo 3*). Además, se han estudiado diferentes ligandos y su capacidad asistir durante la etapa de activación C–H (*Capítulo 4*).

Capítulo 2: Arilación en orto de anilinas no protegidas catalizada por paladio

La funcionalización directa de anilinas es una transformación muy interesante sintéticamente debido a que su estructura se encuentra presente en importantes compuestos bioactivos. Muchos de los procesos publicados para funcionalizar anilinas en el anillo aromático requieren de la protección del grupo amino previo a la reacción de acoplamiento.[1] Generalmente el grupo protector tiene también función de grupo director, permitiendo la funcionalización de anilinas selectiva a uno de los regioisómeros. La funcionalización C–H en la posición *para* de anilinas protegidas ha sido publicado por Fernández-Ibáñez incluyendo algún ejemplo de funcionalización en de anilinas primarias *orto*-disustituidas.[2] Sin embargo, no existen muchos más ejemplos, ya que cuando se hacen reaccionar un haluro de arilo y un grupo amino se produce fácilmente el producto de aminación de Buchwald-Hartwing (C–N). Por ello, la protección del grupo amino de anilinas es una práctica común para conseguir el producto de acoplamiento C–C.

En este capítulo se describe la arilación directa de anilinas no protegidas selectivamente en *orto* catalizada por paladio. El ligando cooperativo bipy-6-OH es responsable tanto de la activación C–H como de favorecer la quimioselectividad de la reacción hacia el acoplamiento C–C en lugar del C–N.

La reacción representada en la Ecuación 1 se utilizó como modelo. Las mejores condiciones de reacción encontradas fueron: DMA como disolvente, carbonato de cesio

---

[1] a) Tischler, M. O.; Tóth, M. B.; Novák, Z. *Chem. Rec*. **2017**, 17, 184-199. b) Leitch, J. A.; Frost, C. G. *Synth*. **2018**, 50, 2693-2706. Usando Ar-X: c) Daugulis, O.; Zaitsev, V. G. Angew. *Chem. Int. Ed*. **2005**, 44, 4046-4048. d) Scarborough, C. C.; McDonald, R. I.; Hartmann, C.; Sazama, G. T.; Bergant, A.; Stahl, S. S. *J. Org. Chem*. **2009**, 74, 2613-2615. e) Wan, C.; Zhao, J.; Xu, M.; Huang, J. *J. Org. Chem*. **2014**, 79, 4751-4756. f) Kwak, S. H.; Gulia, N.; Daugulis, O. *J. Org. Chem*. **2018**, 83, 5844-5850. g) Lichte, D.; Pirkl, N.; Heinrich, G.; Dutta, S.; Goebel, J. F.; Koley, D.; Goossen, L. J. *Angew, Chem, Int. Ed*. **2022**, 61 (47), e202210009. Usando sales de diarilyodonio: h) Kalyani, D.; Deprez, N. R.; Desai, L. V.; Sanford, M. S. *J. Am. Chem. Soc*. **2005**, 127, 7330-7331. i) Phipps, R. J.; Gaunt, M. J. *Science*, **2009**, 323, 1593-1597. j) Ciana, C. L.; Phipps, R. J.; Brandt, J. R.; Meyer, F. M.; Gaunt, M. J. *Angew. Chem. Int. Ed.* **2011**, 50, 458-462. Arilación oxidtiva con arenos: k) Li, B. J.; Tian, S. L.; Fang, Z.; Shi, Z. J. *Angew. Chem. Int. Ed.* **2008**, 47 (6), 1115-1118. l) Yeung, C. S.; Zhao, X.; Borduas, N.; Dong, V. M. *Chem. Sci*. **2010**, 1, 331-336. m) Brasche, G.; García-Fortanet, J.; Buchwald, S. L. *Org. Lett*. **2008**, 10, 2207-2210. Arilación oxidativa con ácidos borónicos: n) Nishikata, T.; Abela, A. R.; Huang, S.; Lipshutz, B. H. *J. Am. Chem. Soc*. **2010**, 132, 4978-4979. ñ) Koley, M.; Dastbaravardeh, N.; Schnürch, M.; Mihovilovic, M. D. *ChemCatChem* **2012**, 4 (9), 1345-1352.

[2] Naksomboon, K.; Poater, J.; Bickelhaupt, F. M.; Fernández- Ibáñez, M. A. *J. Am. Chem. Soc*. **2019**, 141, 6719-6725.

como base y 5 % mol de catalizador (complejo **1**) a 130 ºC, obteniendo 83 % de producto de acoplamiento tras 6 h de reacción.

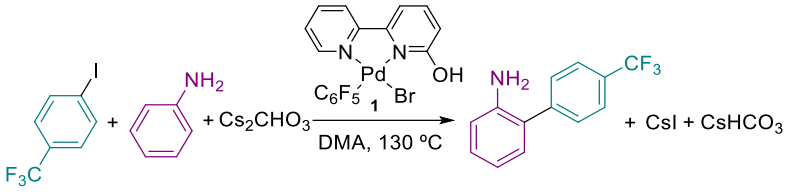

Ecuación 1.

El producto competitivo resultante de la reacción de aminación de Buchwald-Hartwig (C–N) se detectó únicamente en un 5 %. Este compuesto puede sintetizarse de manera selectiva si se modifican las condiciones de reacción, utilizando como catalizador Pd_2dba_3 y el ligando XPhos, en DMF a 65 ºC durante 18 h (Ecuación 2).

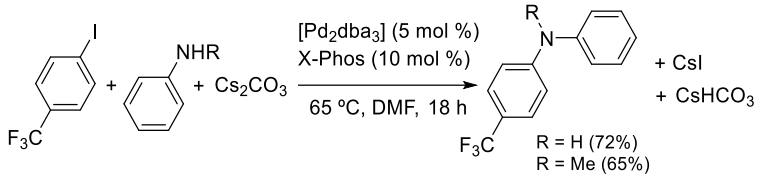

Ecuación 2.

La reacción de *orto* arilación de anilinas puede extenderse para diferentes compuestos (Esquema 2). La reacción tolera grupos electro-dadores y electro-atractores tanto en la anilina como en el haluro de arilo. En todos los casos se observa el producto de acoplamiento selectivo en *orto*. En el caso de anilinas secundarias se obtiene mezcla de los tres regioisómeros: *orto*, *meta* y *para*, siendo el *orto* mayoritario. Para *N*,*N*-dimetilanilina solo se observó producto de acoplamiento en *meta* y *para*.

Esquema 2. Arilación de anilinas con el complejo **1**.

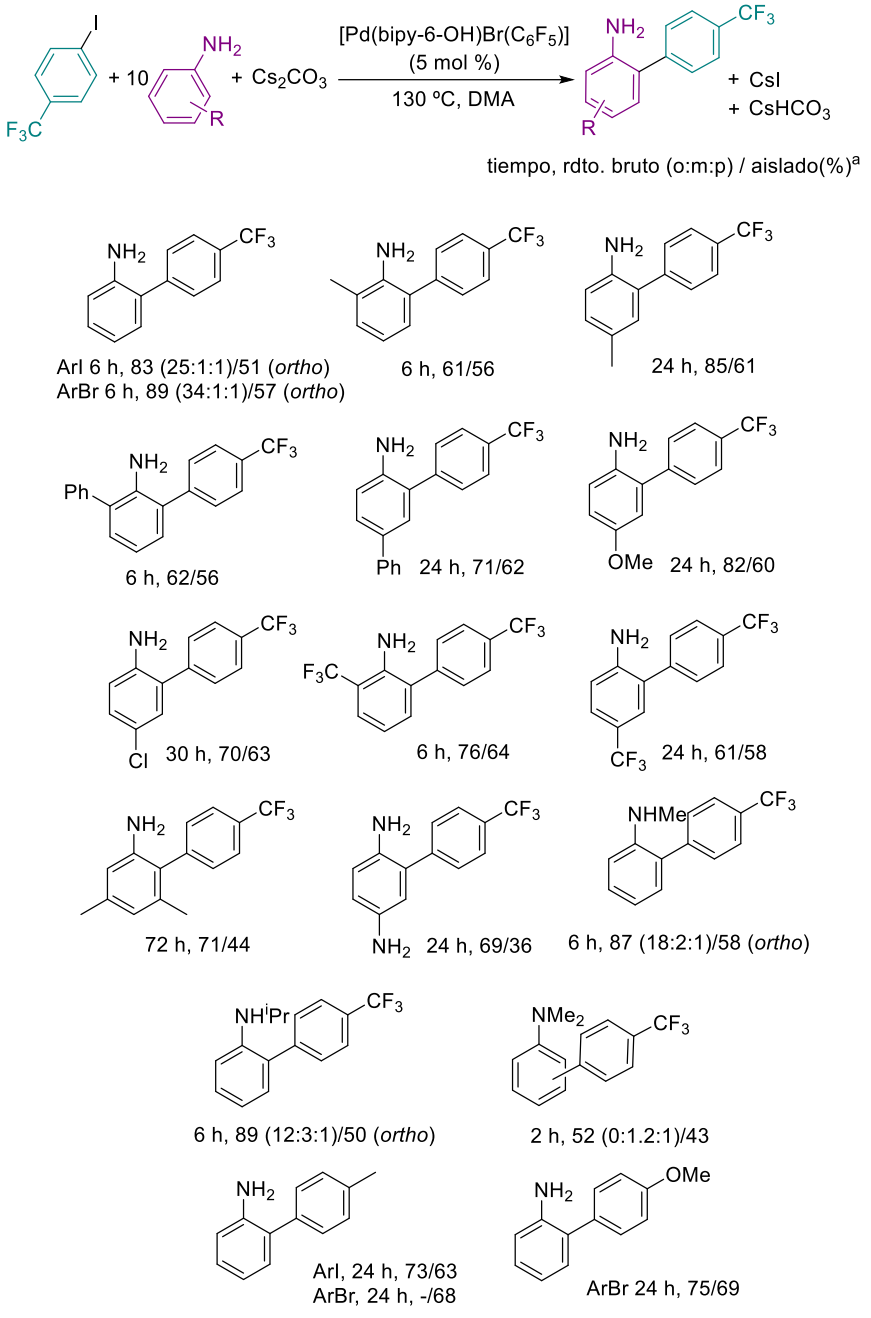

La reacción en Ecuación 1 se utilizó como modelo en varios experimentos mecanísticos. Se sintetizó el complejo **6** y se probó como catalizador en la reacción modelo, obteniendo 90 % de rendimiento en 6 h. La descomposición térmica de **6** en las condiciones catalíticas dio lugar a un 61 % del producto de acoplamiento (Ecuación 3). Por lo tanto, puede ser un intermedio presente en ciclo catalítico.

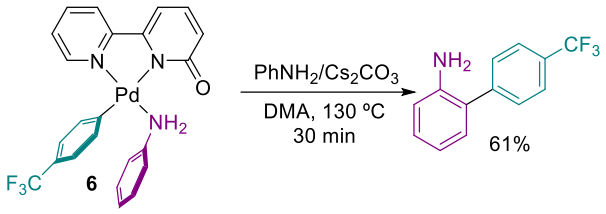

Ecuación 3.

Mediante experimentos cinéticos se encontró que la reacción era de primer orden respecto del catalizador **1**, y que la velocidad de reacción no dependía del haluro de arilo ni de la cantidad de anilina (dentro del rango utilizado). Se observó un efecto cinético isotópico de 4.2 ± 0.2, indicando que la activación C–H es la etapa limitante de la reacción. La reacción modelo (Ecuación 1) también se llevó a cabo en presencia de D_2O. Debido al fácil intercambio H/D en el ligando protonado, una incorporación de deuterio en el producto significaría una activación C–H reversible. Al no observarse incorporación de deuterio se puede asumir una etapa de activación C–H irreversible.

Por último, se realizaron cálculos computacionales para obtener más información sobre el mecanismo. Debido a la complejidad de los cálculos, estos se realizaron en colaboración con el Profesor Agustí Lledós de la Universidad Autónoma de Barcelona. Todas las energías recogidas en el texto se han obtenido mediante cálculos *single point* en el nivel DLPNO-CCSD(T)/def2-TZVp, añadiendo las energías de solvatación obtenidas en el nivel M06/BS1 (consultar la parte experimental para más detalles). Sin embargo, se encontró que era necesaria la modelización explícita de la base (carbonato de cesio) y de varias moléculas de disolvente (DMA). El perfil de energía completo para el isómero *orto* se muestra en Figura 3. La reorganización de la anilina transforma **6** en **c1*orto***. La rápida deprotonación de la anilina (**c1NH*orto***) da lugar a un estado de transición para la activación C–H más bajo en energía (12.1 kcal mol^{-1}) que desde el intermedio protonado **c1*orto*** (16.0 kcal mol^{-1}). Después, el grupo NH se protona, recuperándose el grupo amino (**c2*orto***) y el ligando es deprotonado por la base externa, dando lugar al intermedio **c2b*orto***. Finalmente, la eliminación reductora libera el producto de acoplamiento. Se encontró que la formación del producto competitivo C–N está desfavorecida y tiene una barrera de 14.1 kcal mol^{-1}. En cuanto a la regioselectividad observada (Figura 4), se encontró que el camino de menor energía corresponde a intermedios amiduro y favorece el isómero *orto.*

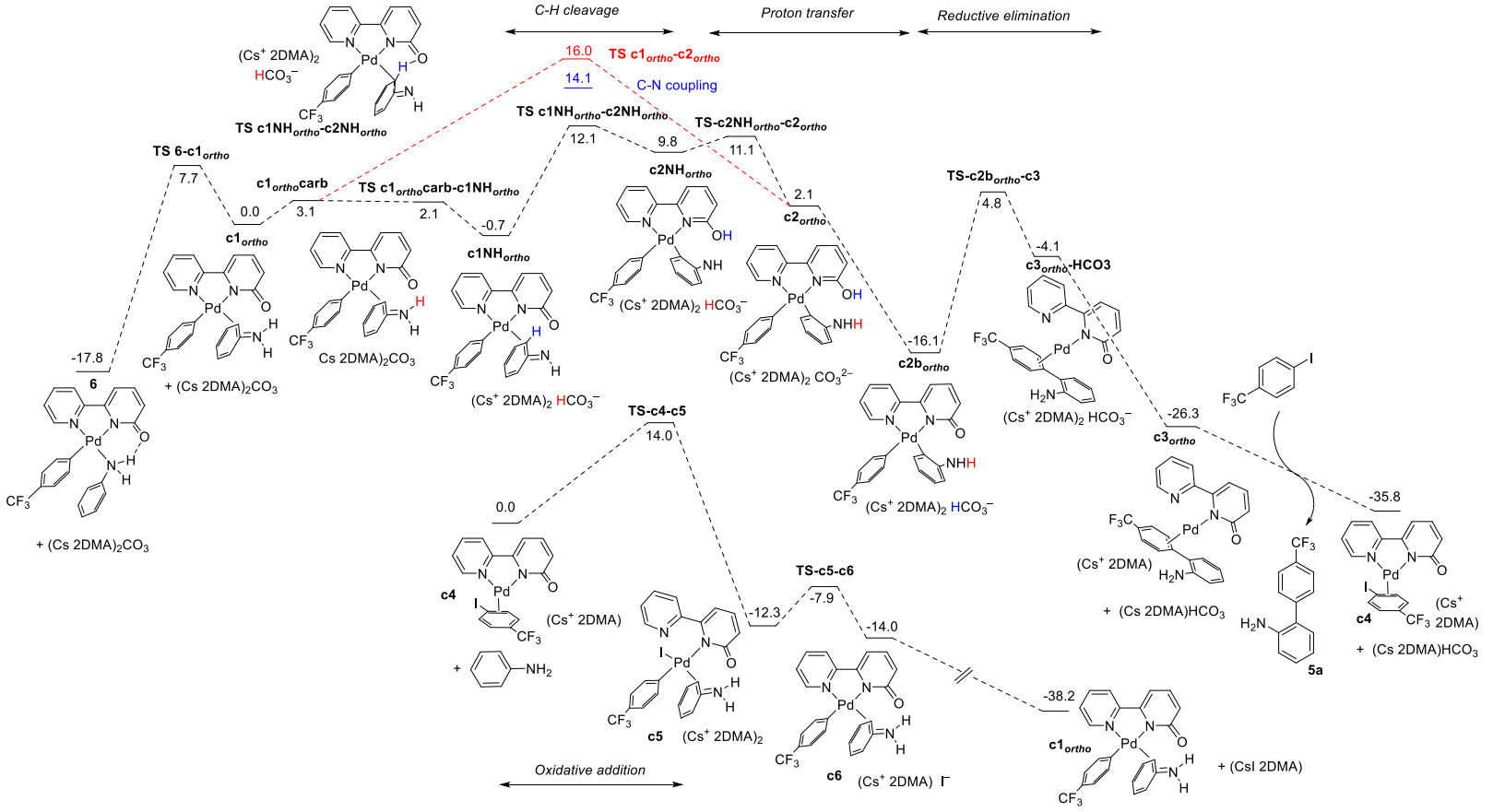

Figura 3. Perfil de energía para la arilación directa de anilina en la posición *orto* catalizada por paladio y asistida por el ligando bipy-6-OH. (Energías en kcal mol^{-1}).

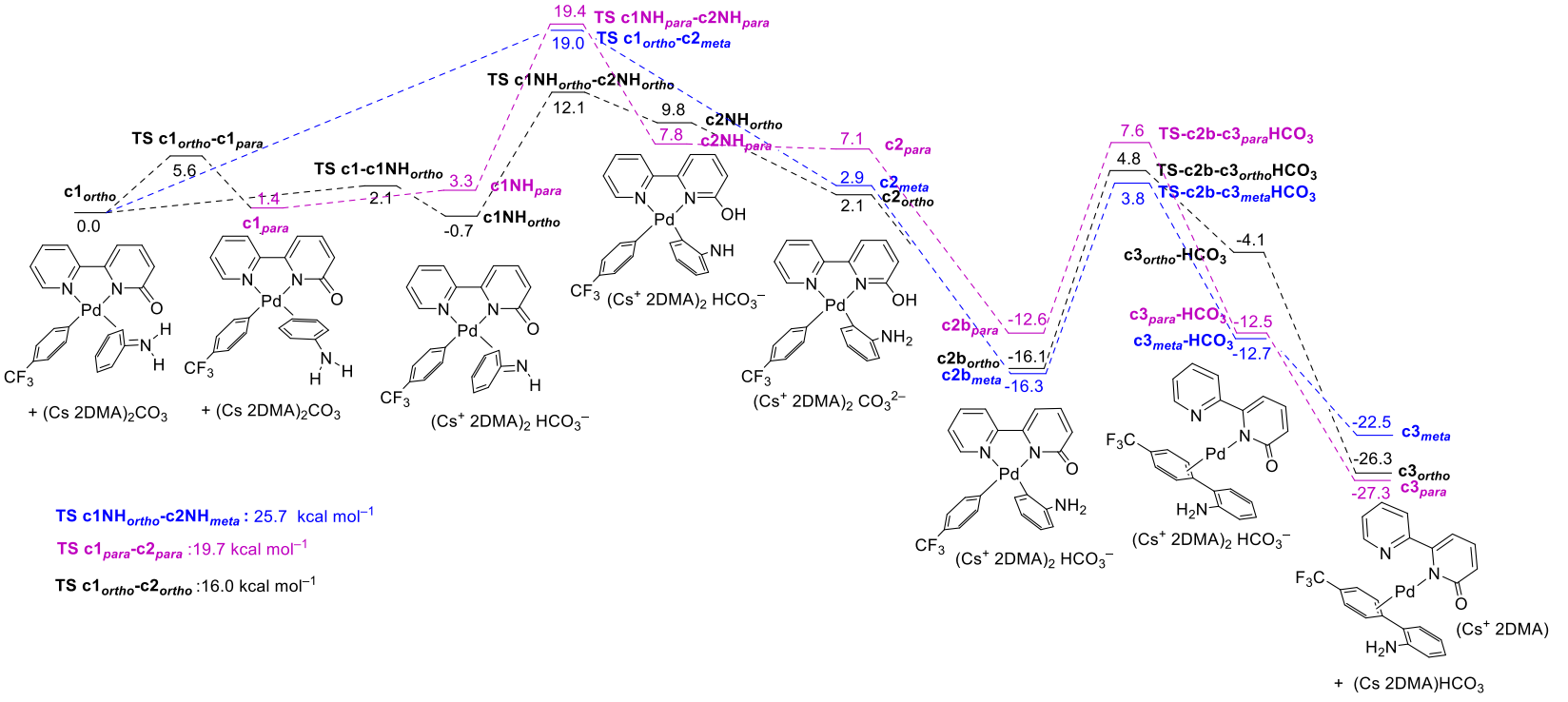

Figura 4. Perfil de energía para la activación C–H y eliminación reductora de los diferentes regioisómeros. Para los isómeros *orto* (negro) y *para* (rosa) el camino desde los intermedios amiduro es más bajo en energía mientras que para el isómero *meta* (azul), el camino desde la anilina protonada es preferido. Para simplificar la figura solo el isómero *orto* se ha dibujado. (Energías en kcal mol^{-1}).

Capítulo 3: Arilación directa de arenos simples catalizada por paladio a través de un sistema de ligandos dual

El concepto de sistema dual de ligandos describe reacciones en las que se usan dos ligandos diferentes, combinando de las propiedades de ambos en un mismo proceso catalítico. Cada ligando tiene unas características específicas y tendrá un papel concreto en el mecanismo de la reacción. Uno de los primeros ejemplos utilizando esta estrategia en reacciones de funcionalización C–H catalizadas por paladio es el uso de *N*-acetil glicina (un aminoácido monoprotegido, MPAA) para la activación C–H de arenos junto a un ligando derivado de la piridina.[1] Desde entonces se han publicado varios ejemplos de este tipo de reacciones, combinando norborneno y piridina,[2] aminoácidos monoprotegidos y derivados piridona,[3] e incluso el uso de fosfinas con derivados piridona.[4]

En este capítulo se ha estudiado un sistema dual de ligandos para la arilación directa de arenos simples, consiguiendo condiciones de reacción más suaves que las publicadas en la bibliografía para un solo ligando.[5] Además, los estudios mecanísticos llevan a un posible mecanismo bimetálico.

El ciclo catalítico más común para las reacciones de acoplamiento cruzado se ha descrito en la introducción general. Sin embargo, hay algunos ejemplos donde se ha encontrado un mecanismo bimetálico. En estos casos, dos especies de paladio están involucradas y cada una de ellas es responsable de etapas específicas del mecanismo. Hartwig *et al.* encontraron que la arilación de *N*-óxidos de piridina catalizada por paladio y P^tBu_3 como ligando ocurría a través de un mecanismo bimetálico.[6] Por una parte, un complejo con P^tBu_3 coordinada era responsable de la adición oxidante y eliminación

---

[1] a) Chen, H.; Wedi, P.; Meyer, T.; Tavakoli, G.; Gemmeren, M. V. *Angew. Chem. Int. Ed*. **2018**, 57 (9), 2497-2501. b) Wedi, P.; Farizyan, M.; Bergander, K.; Mgck-Lichtenfeld, C.; Gemmeren, M. V. *Angew. Chem. Int. Ed*. **2021**, 60, 15641-15649.

[2] a) Liu, L.-Y.; Qiao, Y. X.; Yeung, K.-S.; Ewing, W. R.; Yu Y.-Q. *J. Am. Chem. Soc*. **2019**, 141, 14870-14877. b) Liu, L.-Y.; Qiao, J. X.; Yeung, K.-S. Ewing, W. R.; Yu, Y.-Q. *Angew. Chem. Int. Ed.*, **2020**, 53 (33), 13831-13835.

[3] a) Park, H. S.; Fan, Z.; Zhu, R.-Y.; Yu, J.-Q. *Angew. Chem. Int. Ed.*, **2020**, 59 (31), 12853-12859. b) Sinha, S. K.; Panja, S.; Grover, J.; Hazra, P.S.; Pandit, S.; Bairagi, Y.; Zhang, X.; Maiti, D. *J. Am. Chem. Soc*. **2022**, 144, 12032-12042.

[4] Beckers, I.; Bugaev, A.; De Vos, D. *Chem. Sci*., **2023**,14, 1176-1183.

[5] a) Salamanca, V.; Toledo, A.; Albéniz, A. C. *J. Am. Chem. Soc*. **2018**, *140*, 17851-17856. b) Salamanca, V.; Albéniz, A. C. *Org. Chem. Front*., **2021**, *8*, 1941-1951.

[6] a) Tan, Y.; Barrios-Landeros, F.; Hartwig, J. F. *J. Am. Chem. Soc*. **2012**, 134, 3683-3686. b) Gorelsky, S. I. *Organometallics*, **2012**, 31, 4631-4634.

reductora del ciclo. Por otro lado, un complejo con la fosfina metalada y acetato como ligando era responsable de la activación C–H del areno. Otro ejemplo es la síntesis oxidativa de biarilos publicada por Stahl *et al.* donde observaron dependencia de segundo orden para concentraciones bajas del catalizador.[7] Un mecanismo bimetálico similar fue publicado por Hong *et al.* unos años después para la arilación directa de arenos operado por un ligando de tipo diimina y ácido piválico.[8]

La arilación directa de tolueno representada en Ecuación 4 se utilizó como reacción modelo. Los resultados obtenidos en diferentes condiciones de reacción se muestran en la Tabla 1.

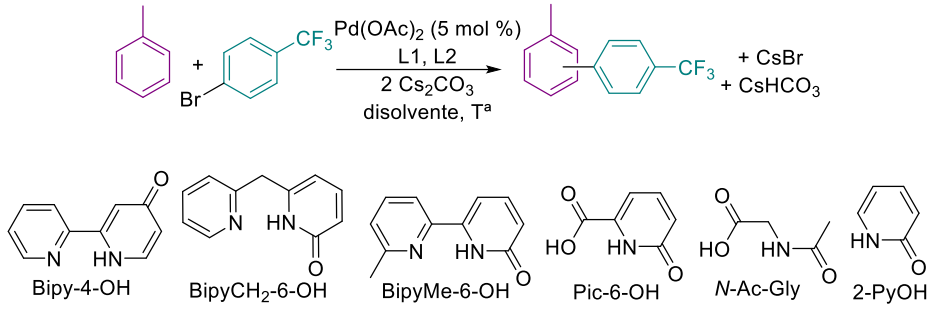

Ecuación 4.

Las condiciones de reacción publicadas en la bibliografía usando solo bipy-6-OH (*p*-$CF_3C_6H_4I$) se encuentran en la entrada 1, Tabla 1 (130 ºC, tolueno como disolvente), consiguiendo 91 % de rendimiento tras 24 h.[5] Al añadir PCy_3 como ligando la reacción es más rápida que sin fosfina consiguiendo conversión completa tras 6 h (entrada 2, Tabla 1). Cuando se utiliza *p*-$CF_3C_6H_4Br$ como haluro de arilo la reacción sin fosfina llega a un 16 % tras 6 h (entrada 3, Tabla 1), mientras que con el sistema dual la velocidad de reacción es mayor (56 % tras 6 h, entrada 4, Tabla 1). El ligando bipy-6-OH es necesario en la reacción para realizar la activación C–H, cuando no se utiliza la reacción no avanza hacia los productos de acoplamiento (entrada 5, Tabla 1). Se utilizó DMA como co-disolvente, de la misma manera que en el *Capítulo 2*, obteniendo excelentes rendimientos tras 90 min de reacción, mucho más rápido que usando solo tolueno como disolvente (entrada 6, Tabla 1). Usando la mezcla tolueno:DMA se puede rebajar la temperatura a 100 ºC y se obtiene 90 % del producto en 3 h (entrada 7, Tabla 1). En estas condiciones de reacción (tolueno:DMA a 100 ºC) se probaron diferentes

[7] Wang, D.; Izawa, Y.; Stahl, S. S. *J. Am. Chem. Soc*. **2014**, 136, 9914-9917.
[8] a) Kim, J.; Hong, S. H. *ACS Catal.* **2017**, 7, 3336-3343. b) Kim, D.; Choi, G.; Kim, W.; Kim, D.; Kang, Y. K.; Hong, S. H. *Chem. Sci*., **2021**, 12, 363-373.

ligandos similares a bipy-6-OH. La presencia del grupo piridona es necesaria (entrada 8, Tabla 1) y debe estar en la posición 6 ya que al utilizar el ligando bipy-4-OH con el grupo piridona lejos del centro metálico no se obtuvo producto de acoplamiento (entrada 9, Tabla 1).

Tabla 1. Diferentes disolventes y catalizadores probados en la reacción de arilación de tolueno.

Entrada	Disolvente	L1 (mol %)	L2 (mol %)	Rdto. bruto, %, (Conv, %), 6 h[b]	Rdto. bruto, %, (Conv, %), 24 h[b]
130 ºC					
1[c,d]	Tolueno	Bipy-6-OH (5)	-	20 (22)	91 (100)
2[d]	Tolueno	Bipy-6-OH (2.5)	PCy_3 (5)	90 (100)	
3	Tolueno	Bipy-6-OH (5)	-	16 (16)	75 (75)
4	Tolueno	Bipy-6-OH (2.5)	PCy_3 (5)	59 (65)	90 (100)
5	Tolueno	-	PCy_3 (10)	3 (6)	3 (7)
6	Tolueno:DMA	Bipy-6-OH (2.5)	PCy_3 (5)	88 (100)[e]	
100 ºC					
7	Tolueno:DMA	Bipy-6-OH (2.5)	PCy_3 (5)	90 (94)[f]	
8	Tolueno:DMA	Bipy (2.5)	PCy_3 (5)	0 (22)	0 (100)
9	Tolueno:DMA	Bipy-4-OH (2.5)	PCy_3 (5)	0 (0)	0 (100)
10	Tolueno:DMA	Bipy-6-OH (2.5)	PPh_3 (5)	38 (45)	41 (49)
11	Tolueno:DMA	Bipy-6-OH (2.5)	P^tBu_3 (5)	4 (9)	14 (19)
12	Tolueno:DMA	Bipy-6-OH (2.5)	XPhos (5)	80 (85)	88 (92)
13	Tolueno:DMA	Bipy-6-OH (2.5)	$HPCy_3$ BF_4 (5)	93 (97)[f]	
14	Tolueno:DMA	Bipy-6-OH (5)	PCy_3 (5)	78 (84)[f]	
15	Tolueno:DMA	Bipy-6-OH (5)	PCy_3 (10)	31 (40)	85 (91)
16	Tolueno:DMA	Bipy-6-OH (2.5)	PCy_3 (7.5)	46 (54)	78 (89)
17	Tolueno:DMA	Bipy-6-OH (2.5)	PCy_3 (2.5)	35 (38)	79 (87)

[a]Condiciones de reacción: *p*-$CF_3C_6H_4Br$ (0.34 mmol), Cs_2CO_3 (0.68 mmol), disolvente (3 mL). [b]Rendimientos brutos obtenidos por ^{19}F RMN de la mezcla de reacción. The reduction or theLa reducción del bromuro de arilo (ArH) y el homoacoplamiento (Ar-Ar) son los subproductos observados. [c]Datos de la bibliografía. [d]*p*-$CF_3C_6H_4I$. [e]Tras 90 min. [f]Tras 3 h.

Se probaron otras fosfinas y se encontró que sólo XPhos era capaz de dar buenos resultados, pero en tiempos de reacción de reacción más largos. La sal de fosfonio $HPCy_3 \cdot BF_4$ da resultados comparables a PCy_3 (entradas 10-13, Tabla 1). También se modificaron las cantidades de ligandos, en el caso de bipy-6-OH no produjo ningún efecto (entrada 14, Tabla 1) pero un exceso o defecto de PCy_3 lleva a mayores tiempos de reacción (entradas 15-17, Tabla 1).

Con las mejores condiciones de reacción (Tabla 1, entrada 7), se probaron diferentes haluros de arilo y arenos con el objetivo de estudiar el alcance de la reacción. Se toleran tanto grupos electro-dadores como electro-atractores en el areno y el haluro de arilo. Además, los cloruros de arilo también dan buenos resultados, lo que no ocurre cuando se emplea el sistema Pd/bipy-6-OH sin fosfina (Esquema 3).

Esquema 3. Reacción de arilación de arenos con diferentes bromuros y cloruros de arilo.

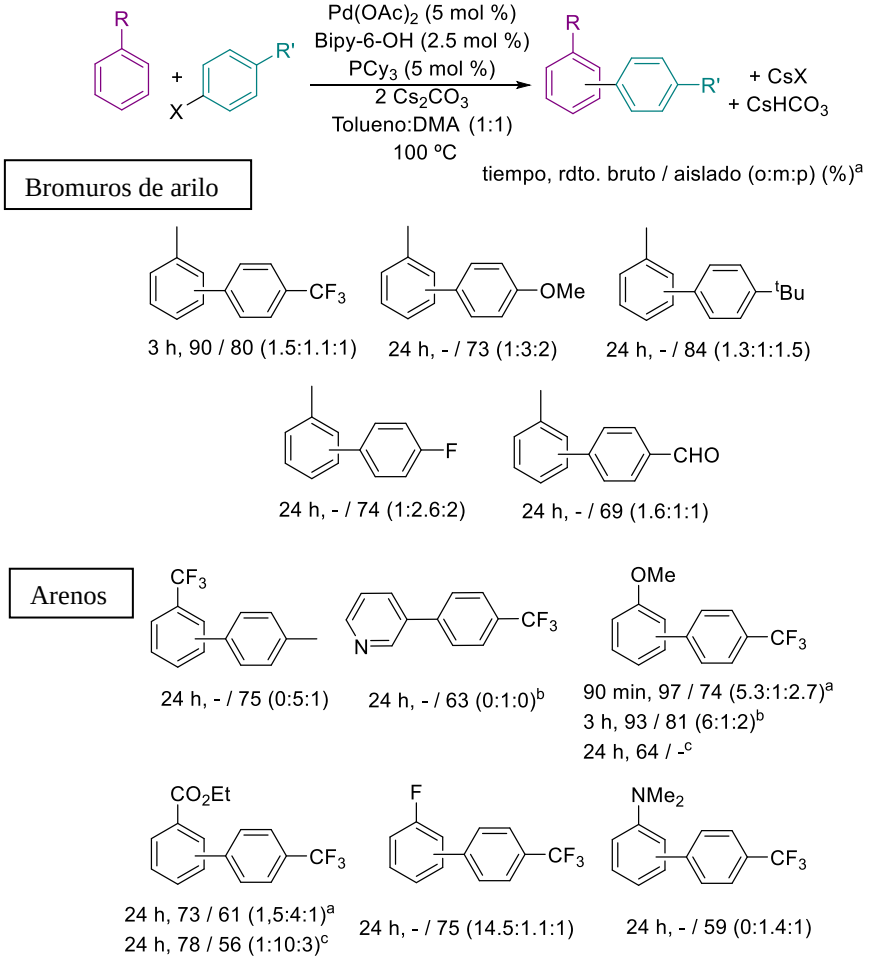

Cloruros de arilo

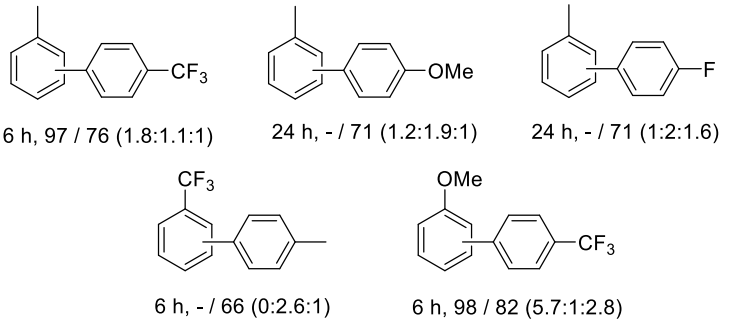

[a]Condiciones de reacción en Tabla 1. [b]Areno (3.4 mmol), DMA (3 mL). [c]Areno (3 mL).

La regioselectividad de la reacción cambia en función del areno y del haluro de arilo utilizado, en la mayoría de los casos la reacción no es selectiva y se obtiene mezcla de isómeros *orto*, *meta* y *para*. Los mejores resultados se obtuvieron para trifluorotolueno y benzoato de etilo, donde el isómero *meta* es mayoritario, y para la piridina donde el isómero *meta* es único. La reacción es regioselectiva en el caso anisol y fluorobenceno, donde isómero *orto* es el mayoritario. La regioselectividad no está relacionada con las propiedades electrónicas del areno. No se observó producto de acoplamiento C–C cuando se utilizaron anilina (se obtiene el producto de acoplamiento C–N) o benzonitrilo como arenos. Tampoco para de *p*-bromobenzonitrilo o ácido *p*-bromobenzoico como haluros de arilo. En el caso de *p*-bromoclorobenceno, se obtuvo el producto de acoplamiento donde habían reaccionado tanto el enlace C–Br como el enlace C–Cl.

Para obtener más información acerca del mecanismo de la reacción, se llevaron a cabo diversos experimentos. Se encontró que la mezcla $Pd(OAc)_2$ + 2 PCy_3 daba lugar a los complejos $[Pd(OAc)_2(PCy_3)_2]$ y $[Pd(PCy_3)_2]$ mediante la oxidación de la fosfina. Este podría ser la vía de formación de una de las especies catalíticamente activas. Por otra parte, se realizaron experimentos de sustitución de ligandos ya que dos ligandos están involucrados en la reacción. Se encontró que el ligando bipy-6-OH, tanto en su forma protonada como deprotonada, se desplazaba por PCy_3. Sin embargo, la fosfina no es desplazada por bipy-6-OH ni por bipy-6-O. Por lo tanto, el intercambio de ligandos sobre el mismo centro de paladio durante el ciclo catalítico no es probable como mecanismo de reacción. La posibilidad de un mecanismo bimetálico con una etapa de transmetalación se comprobó mediante la reacción en la Ecuación 5. Se obtuvo un 48 % del producto de acoplamiento entre los arilos de ambos complejos, demostrando que la

transmetalación entre un complejo con bipy-6-OH y un complejo con PCy_3 es posible y puede ser una etapa elemental del mecanismo.

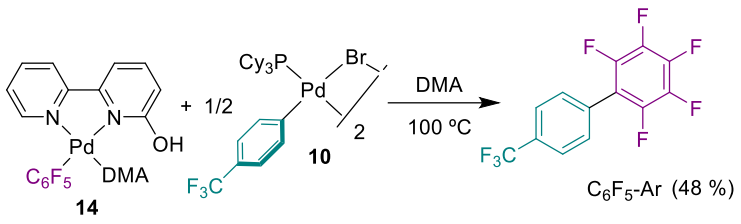

Ecuación 5.

En la reacción modelo (entrada 6, Tabla 1) se observó un efecto cinético isotópico de 4.0 ± 0.5, indicando que la etapa de activación C–H es la etapa limitante de la reacción. Además, en las condiciones catalíticas. la velocidad de reacción muestra una dependencia de primer orden respecto del catalizador, pero es independiente respecto de la concentración de bromuro o cloruro de arilo. Para observar el efecto de las propiedades electrónicas del areno, se midieron las velocidades iniciales con anisol, tolueno y benzoato de etilo. Se encontró que la k_{obs} era $3.1 \pm 0.3\ 10^{-4}$, $2.3 \pm 0.1\ 10^{-4}$ y $5.8 \pm 0.7\ 10^{-5}$ respectivamente, indicando que la reacción es más rápida para arenos más ricos en densidad electrónica.

Con todos estos datos, el posible mecanismo bimetálico para estas transformaciones se representa en el Esquema 4. Las etapas de adición oxidante y eliminación reductora se producen en un complejo de paladio con la fosfina coordinada. Por otro lado, la etapa de activación C–H es asistida por la bipy-6-OH en otro complejo de paladio, que después transmetala el arilo al otro complejo desde donde se produce la eliminación reductora. La activación C–H ha sido estudiada mediante cálculos computacionales, encontrando una barrera energética de 26.9 kcal mol^{-1}, en concordancia con las condiciones de reacción necesarias. Esta barrera es más baja que la encontrada para los intermedios formados en un sistema monoligando ([Pd(bipy-6-O)(Ar)(tolueno)], en vez de **I_2**). El centro de paladio en **I_2** es más electrofílico y el estado de transición de la ruptura C–H tiene más carácter eCMD y está más favorecido para arenos ricos en densidad electrónica, como se ha observado experimentalmente.

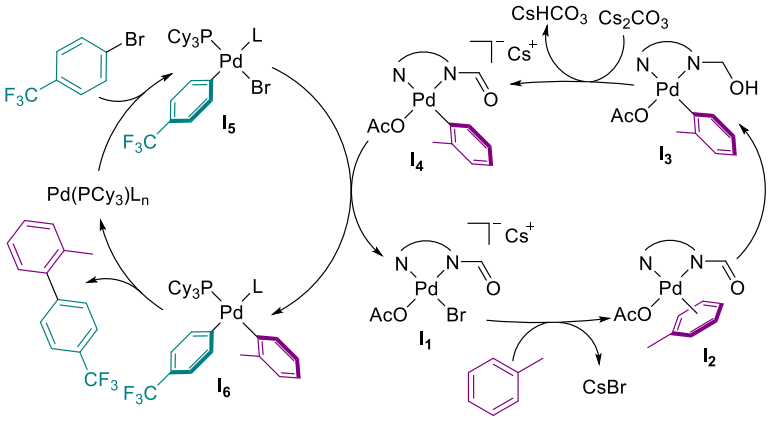

Esquema 4. Posible ciclo catalítico para la arilación directa de arenos catalizada por un sistema dual de ligandos.

Capítulo 4: Estudio de ligandos quelato para asistir en las reacciones de activación C–H catalizadas por paladio

La cooperación metal-ligando es una estrategia muy usada en los últimos años para conseguir catalizadores capaces de sintetizar moléculas complejas por vías diferentes de las comúnmente utilizadas. Las nuevas estrategias generalmente aportan ventajas como condiciones de reacción más suaves o funcionalización de sustratos poco reactivos. En los capítulos anteriores, el ligando cooperativo bipy-6-OH ha demostrado las ventajas de este tipo de sistemas. También se ha comentado en la introducción general el aumento del uso de aminoácidos monoprotegidos (MPAA) como ligandos en las reacciones de activación C–H. Dentro de este contexto, en este capítulo se ha examinado la capacidad cooperativa de ligandos con estructura similar a la bipy-6-OH y los MPAAs como son el ácido 6-hidrocipicolínico y ligandos del tipo amido-piridina.

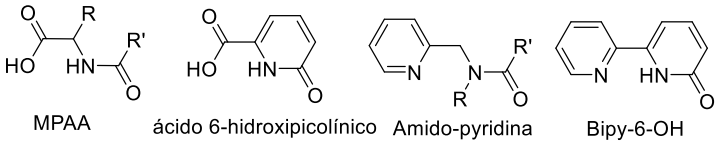

Figura 5. Comparativa estructural de MPAA, ácido 6-hidroxipicolínico, ligandos amido-piridina y bipy-6-OH.

El ácido 6-hidroxipicolínico tiene un esqueleto muy parecido a los MPAAs con la ventaja de tener una estructura que podría hacer de él un mejor ligando quelato. Además, el grupo cooperativo (piridona) es igual al de bipy-6-OH y es un compuesto comercial y muy accesible. Este ligando y algunos regioisómeros se han utilizado coordinados a iridio para la oxidación de agua.[1] También se ha utilizado un derivado muy similar en la hidroxilación de arenos.[2]

Los derivados de amido-piridina tienen una estructura similar a la bipy-6-OH y el grupo acilo se parece bastante al grupo que poseen los MPAAs. Además, tienen la ventaja de que sus síntesis es simple y modular. Algunos derivados se han utilizado para

[1] a) Bucci, A.; Savini, A.; Rocchigiani, L.; Zuccaccia, C.; Rizzato, S.; Albinati, A.; Llobet, A.; Macchioni, A. *Organometallics,* **2012**, *31*, 8071-8074. b) Menendez Rodriguez, G.; Bucci, A.; Hutchinson, R.; Bellachioma, G.; Zuccaccia, C.; Giovagnoli, S.; Idriss, H.; Macchioni, A. *ACS Energy Lett.* **2017**, *2*, 105-110. c) Dijk, B.; Menendez Rodriguez, G.; Wu, L.; Hofmann, J. P.; Macchioni, A.; Hetterscheid, D. G. H. *ACS Catal*. **2020**, *10*, 4398-4410. d) Menendez Rodriguez, G.; Zaccaria, F.; Dijk, S. V.; Zuccaccia, C.; Macchioni, A. *Organometallics* **2021**, *40*, 3445-3453.
[2] Li, Z.; Park, H. S.; Qiao, J. X.; Yeung, K.-S.; Yu, J.-Q. *J. Am. Chem. Soc*. **2022**, *144*, 18109-18116.

la formación de complejos de cobre en estudios estructurales[3] o en reacciones de complejos de paladio.[4] En activación C–H se ha publicado el uso de ligandos con estructura similar, llamados generalmente APAQ (*acetyl-protected aminoethyl quinolines*).[5]

Debido a las similitudes estructurales entre los ligandos propuestos y bipy-6-OH o los MPAAs, se ha estudiado la capacidad de los nuevos ligandos de asistir en reacciones de activación C–H donde se haya observado un efecto acelerador por parte de bipy-6-OH o MPAA.

Estudio de la capacidad cooperativa del ligando ácido 6-hidroxipicolínico

Se estudió la capacidad coordinante del ligando 6-hidroxipicolínico (pic-6-OH). Es un compuesto diprótico que puede actuar de forma mono- o dianiónica. Se sintetizaron dos complejos de paladio con el ligando coordinado. El complejo **15** se obtuvo como una mezcla de isómeros dependiendo de la posición del átomo de bromo y el grupo pentafluorofenilo donde el ligando actúa como monoaniónico (Ecuación 6, a). Tras precipitar el átomo de bromo con carbonato de plata en presencia de piridina se obtuvo el complejo **1**, donde el ligando está coordinado como dianiónico (Ecuación 6, b).

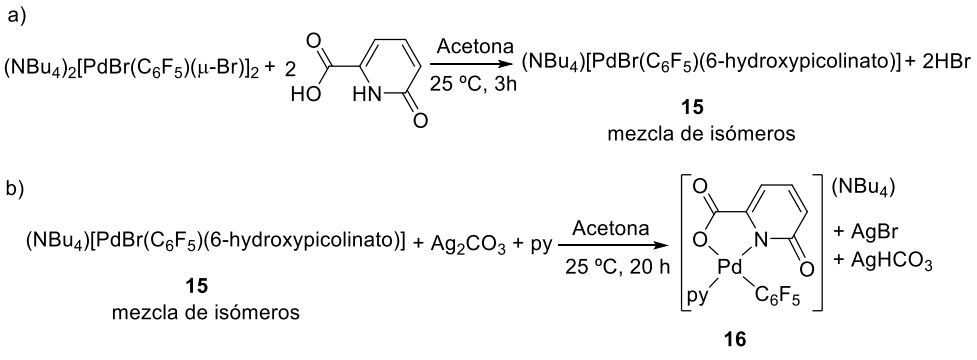

Ecuación 6.

[3] a) Mondal, A.; Li, Y.; Khan, M. A.; Ross, J. S.; Houser, R. P. *Inorg. Chem.* **2004**, *43*, 7075-7082. b) Chaudhuri, U. P.; Whiteaker, L. R.; Yang, L.; Houser, R. P. *Dalton Trans*., **2006**, 1902-1908. c) Cody, C. C.; Kelly, H. R.; Mercado, B. Q.; Batista, V. S.; Crabtree, R. H.; Brudvig, G. W. *Inorg. Chem*. **2021**, *60*, 14759-14764.

[4] Pérez-Gómez, M.; Azizollahi, H.; Franzoni, I.; Larin, E. M.; Lautens, M.; García-López, J.A. *Organometallics* **2019**, *38*, 973-980.

[5] a) Yang, Y.-F.; Hong, X.; Yu, J.-Q.; Houk, K. N. *Acc. Chem. Res*. **2017**, *50*, 2853-2860. b) Yang, Y.-F.; Chen, G.; Hong, X.; Yu, J.-Q.; Houk, K. N. *J. Am. Chem. Soc*. **2017**, *139*, 8514-8521. c). Hill, D. E.; Pei, Q.-L.; Zhang, E.-X.; Gage, J. R.; Yu, J.-Q.; Blackmond, D. G. *ACS Catal*. **2018**, *8*, 1528-1531. d) Romero, E. A.; Chen, G.; Gembicky, M.; Jazzar, R.; Yu, J.-Q.; Bertrand, G.; *J. Am. Chem. Soc*. **2019**, *141*, 16726-16733. e) Chen, G.; Gong, W.; Zhuang, Z.; Andrä, M. S.; Chen, Y.-Q.; Hong, X.; Yang, Y. F.; Liu, T.; Houk, K. N.; Yu, J.-Q. *Science*, **2016**, *353*, 1023-1027.

La arilación directa de arenos se escogió como reacción modelo para probar este ligando debido a que su mecanismo ha sido estudiado anteriormente en el grupo de investigación.[6] Los arenos probados fueron piridina, benzoato de etilo y tolueno por su diferente habilidad de coordinación (piridina>>benzoato de etilo>tolueno). Para probar la capacidad cooperativa del ligando pic-6-OH, se llevó a cabo la descomposición térmica del complejo **16** (posible intermedio de reacción) en los diferentes arenos como disolvente (Ecuación 7). Como se puede observar en la Tabla 2, el ligando pic-6-OH es capaz de realizar la activación C–H de piridina y benzoato de etilo con muy buenos resultados. En el caso de tolueno, la activación C–H tiene lugar, pero es un proceso mucho más lento que para los otros arenos. Esto puede deberse a la poca solubilidad del complejo **16** en tolueno que puede ralentizar el proceso completo.

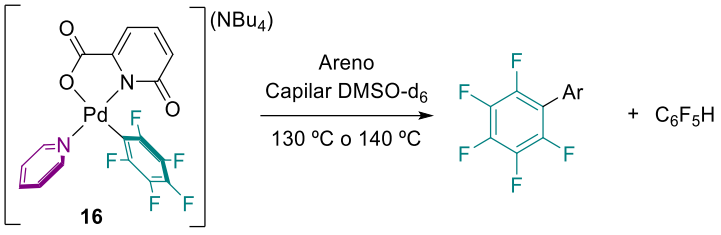

Ecuación 7.

Tabla 2. Resultados obtenidos de la descomposición térmica de **16.**

Areno	Temperatura	% C_6F_5-Ar (tiempo)
Piridina	140 ºC	60 % (30 min)
Benzoato de etilo	130 ºC	82 % (30 min)
Tolueno	130 ºC	10 % (30 min)

Se llevaron a cabo cálculos computacionales para obtener más información acerca de la etapa de activación C–H, ya que normalmente es la etapa limitante de la reacción. Se utilizó como modelo un complejo de paladio con el ligando coordinado, piridina como areno y *p*-$CF_3C_6H_4$ como arilo coordinado. Para la activación C–H con el ligando pic-6-OH se encontró una barrera energética de 25.4 kcal mol^{-1}, más baja que la correspondiente a la activación C–H con bipy-6-OH (27.5 kcal mol^{-1}), publicada en la bibliografía.[6]

[6] a) Salamanca, V.; Toledo, A.; Albéniz, A. C. *J. Am. Chem. Soc*. **2018**, *140*, 17851-17856. b) Salamanca, V.; Albéniz, A. C. *Org. Chem. Front*., **2021**, *8*, 1941-1951.

Con estos datos experimentales y computacionales, queda demostrada la capacidad del ligando pic-6-OH de asistir durante la etapa de activación C–H. Por lo tanto, es un buen candidato a probar en las reacciones catalíticas de acoplamiento C–C con activación C–H.

Los arenos probados en la reacción catalítica fueron los mismos que para las reacciones de descomposición (Ecuación 8): piridina (140 ºC), benzoato de etilo y tolueno (130 ºC). Se probaron diferentes bases y aditivos.

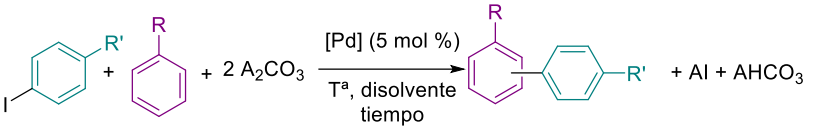

Ecuación 8.

Los resultados obtenidos se recogen en la Tabla 3. La arilación directa de piridina utilizando pic-6-OH como ligando y carbonato de cesio como base lleva solo a un 14 % de producto tras 24 h (entrada 1, Tabla 3). Cuando se utiliza **16** como catalizador el rendimiento aumenta hasta un 23 %, sin embargo, la cantidad de subproductos también se ve aumentada (entrada 2, Tabla 3). Cuando se utiliza carbonato de plata como base el rendimiento es ligeramente superior tras 24 h (32 %, entrada 3, Tabla 3). La adición de $(NBu_4)BF_4$ como agente de transferencia de fase y para aumentar la solubilidad de la base resulta en un aumento del producto obtenido, pero también de los subproductos (entrada 4, Tabla 3). Teniendo en cuenta que la solubilidad de la base puede ser un factor importante, se probaron bases solubles como carbonato de tetrabutilamonio y metilcarbonato de tetrabutilamonio (entradas 5-9, Tabla 3). En ambos casos los tiempos de reacción disminuyeron a 2 h. Los mejores resultados se obtuvieron cuando se utilizó DMA como co-disolvente y metilcarbonato de tetrabutilamonio como base (entrada 7, Tabla 3); en el resto de reacciones se observaron rendimientos moderados con elevadas cantidades de subproductos.

En la arilación directa de tolueno casi no se obtuvo producto de acoplamiento cuando se utilizó la mezcla ligando pic-6-OH + $Pd(OAc)_2$ o el complejo **16** con carbonato de cesio como base (entradas 10 y 11, Tabla 3). El uso de pinacolona como co-disolvente (una estrategia utilizada anteriormente en el grupo)[6] con **16** como catalizador resulta en un 18 % de acoplamiento tras 6 h (entrada 12, Tabla 3). Con el uso de bases solubles no se consiguieron mejores resultados (entradas 13-15, Tabla 3).

Tabla 3. Arilación directa de arenos.[a]

Entrada	[Pd]	Base	Aditivos	Rdto bruto, % (conv., %), t (h)[b]	Rdto bruto, % (conv., %), 24 h[b]
			Piridina		
1	$Pd(OAc)_2$ + **pic-6-OH**	Cs_2CO_3	-	0 (6) 6 h	14 (31)
2	**16**	Cs_2CO_3	-	5 (16) 6 h	23 (93)
3	**16**	Ag_2CO_3	-	32 (38) 6 h	32 (44)
4	**16**	Cs_2CO_3	$(NBu_4)BF_4$ (0.68 mmol)	48 (98) 6 h	-
5	**16**	$(NBu_4)CO_3Me$	-	35 (68) 2 h	-
6	**16**	$(NBu_4)CO_3Me$	$(NBu_4)BF_4$ (0.68 mmol)	57 (94) 2 h	-
7[c]	**16**	$(NBu_4)CO_3Me$	DMA (1.5 mL)	70 (100) 2 h	-
8	**16**	$(NBu_4)_2CO_3$	-	48 (90) 2 h	-
9[c]	**16**	$(NBu_4)_2CO_3$	DMA (1.5 mL)	55 (100) 2 h	-
			Tolueno		
10	$Pd(OAc)_2$ + **pic-6-OH**	Cs_2CO_3	-	3 (6) 6 h	7 (14)
11	**16**	Cs_2CO_3	-	2 (10) 6 h	2 (26)
12[c]	**16**	Cs_2CO_3	Pinacolona (1.5 mL)	18 (78) 6 h	20 (87)
13[d]	**16**	$(NBu_4)CO_2Me$	-	20 (35) 2 h	24 (98)
14[cd]	**16**	$(NBu_4)CO_2Me$	Pinacolona (1.5 mL)	28 (100) 2 h	-
15	**16**	$(NBu_4)_2CO_3$	-	23 (100) 6 h	-
			Benzoato de etilo		
16	$Pd(OAc)_2$ + **pic-6-OH**	Cs_2CO_3	-	10 (17) 6 h	41 (60)
17	**16**	Cs_2CO_3	-	3 (35) 6 h	8 (40)
18[d]	**16**	$(NBu_4)CO_3Me$	-	47 (99) 2 h	-
19	**16**	$(NBu_4)_2CO_3$	-	47 (99) 2 h	-

[a]Condiciones de reacción: ArI (0.34 mmol), disolvente (3.0 mL), [Pd] (5 mol %), base (piridina: 0.34 mmol, tolueno y benzoato de etilo: 0.68 mmol). [b]Rdto bruto determinado por ^{19}F RMN de la mezcla de reacción. La reducción del ArI (ArH), homoacoplamiento (Ar-Ar) y acoplamiento con

pinacolona (Ar-Pin) son los subproductos observados. [c]Codisolvente (1.5 mL) y areno (1.5 mL). [d]Base (0.51 mmol).

Finalmente, en la arilación de benzoato de etilo, la mezcla pic-6-OH + $Pd(OAc)_2$ lleva a un 41 % de producto tras 24 h (entrada16, Tabla 3). El uso de **16** resulta en peores resultados (entrada 17, Tabla 3). La adición de bases solubles lleva a mejores rendimientos sin embargo la cantidad de subproductos también se ve aumentada (entradas 18 y 19, Tabla 3).

Estudio de la capacidad cooperativa de los ligandos amido-piridina.

La síntesis modular de los ligandos de tipo amido-piridina se encuentra en la Ecuación 9. La reacción tolera diferentes grupos tanto en la estructura de la amina como en el derivado de ácido, de esta forma se pueden sintetizar ligandos con diferentes características electrónicas y estéricas. Además el procedimiento de la reacción es muy sencillo y el producto se puede aislar fácilmente con buenos rendimientos.

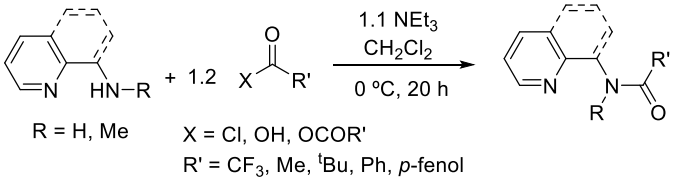

Ecuación 9.

Todos los ligandos sintetizados se muestran en la Figura 6. Se utilizaron diferentes grupos R': electro-atractores (L1), electro-dadores (L2), con impedimento estérico (L3), derivados de fenilo (L4), dianiónicos (L5), aminas terciarias (L6) y derivados de quinolinas (L7 y L8).

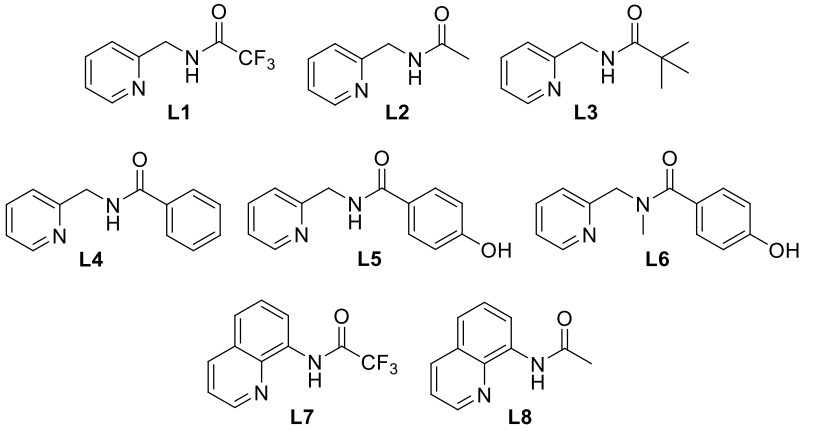

Figura 6. Ligandos amido-piridina sintetizados.

Se sintetizó un complejo bien definido de paladio utilizando el ligando L1 a través de la ruta sintética en Ecuación 10. Se obtuvo una mezcla de isómeros **18a** y **18b** que fueron completamente caracterizados.

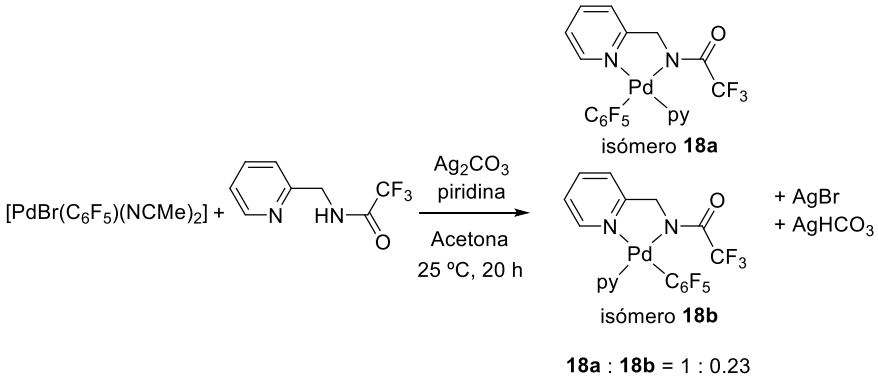

Ecuación 10.

Mediante la descomposición térmica del complejo 18, se llevó a cabo el estudio de la capacidad de este ligando para asistir en la etapa de activación C–H (Ecuación 11). Como se observa en la

Tabla 4, el ligando no es eficaz en la activación C–H de piridina. En el caso de benzoato de etilo y tolueno se forma producto de acoplamiento, pero en tiempos de reacción más largos comparado con reacciones similares publicadas para bipy-6-OH[6] ó MPAAs.[7]

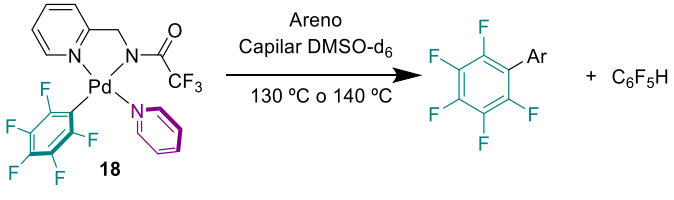

Ecuación 11.

Tabla 4. Resultados obtenidos de la descomposición térmica de **18.**

Areno	Temperatura	% C_6F_5-Ar (tiempo)
Piridina	140 ºC	2 % (90 min)
Benzoato de etilo	130 ºC	29 % (30 min)
Tolueno	130 ºC	30 % (30 min) 89 % (3.5 h)

[7] Fernández-Moyano, S.; Salamanca, V.; Albéniz, A. C. *Chem. Sci*., **2023**,*14*, 6688-6694.

Se realizaron cálculos computacionales para obtener más información acerca de la etapa de activación C–H. Se utilizó como modelo un complejo de paladio con L1 coordinado, piridina y un *p*-$CF_3C_6H_4$ como arilo coordinado. Se encontró una barrera de 35.5 kcal mol^{-1} para la activación C–H (mucho mayor que la publicada para bipy-6-OH, 27.5 kcal mol^{-1}).[6]

Se eligió la arilación directa de arenos para estudiar la actividad de los ligandos en reacciones catalíticas con activación C–H (Ecuación 12). Se probaron diferentes arenos: piridina, tolueno y benzoato de etilo, y diferentes condiciones de base y disolvente. Sin embargo, ninguno de los ligandos o complejos probados llevó a rendimientos mayores del 40 % en el producto de acoplamiento.

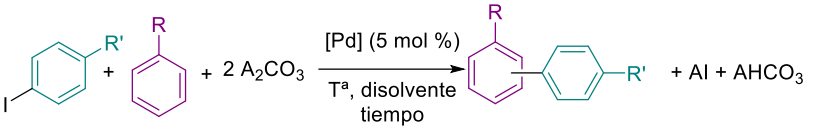

Ecuación 12.

Debido a la baja actividad de los ligandos en las reacciones de arilacion directa de arenos, se decidió probar su efectividad en otras reacciones que tengan activación C–H. La reacción de Heck oxidativa ha sido estudiada en el grupo de investigación utilizando tolueno como areno y *tert*-butil acrilato como alqueno (Ecuación 13).[8] Esta reacción es un acoplamiento entre dos hidrocarburos, un tipo de reacción comentada en la introducción general. Ninguno de los ligandos sintetizados fue capaz de acelerar la reacción modelo. El mejor dato que se observó fue utilizando L3 como ligando donde llegó a un 40 % de acoplamiento tras 24 h, lejos del 75 % publicado con bipy-6-OH.

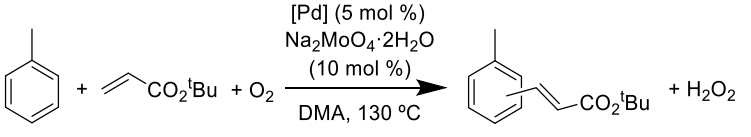

Ecuación 13.

Seguidamente se probó el efecto de los ligandos en una reacción entre un areno y un derivado organometálico, otro tipo de reacción oxidativa comentado en la

[8] Villalba, F.; Albéniz, A. C. *Adv. Synth.Catal*. **2021**, *363*, 4795-4804.

introducción. En este caso, la reacción de derivados bencílicos de ácidos carboxílicos con alquil trifluoroboratos se veía acelerada por el uso de un ligando de tipo MPAA (Boc(L)-Thr(*t*Bu)-OH, Ecuación 14).[9] En este caso, ninguno de los ligandos amido-piridina probados pudo conseguir buenos resultados para esta transformación.

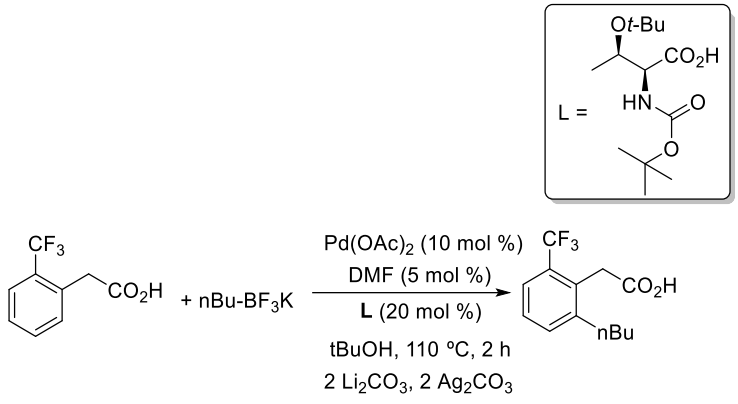

Ecuación 14.

Por último, se probó la acetoxilación de derivados alquílicos de ácidos carboxílicos catalizada por paladio y acelerada por un ligando de tipo MPAA (Ecuación 15).[10] El mecanismo descrito para esta transformación involucra un ciclo catalítico Pd(II)/Pd(IV). Algunos de los ligandos probados dieron buenos resultados en esta reacción. En el caso de L4 se obtuvo un 53 % del producto de acoplamiento y para el ligando L5, un 77 %, rendimiento comparable con el publicado para la reacción modelo (72 %).

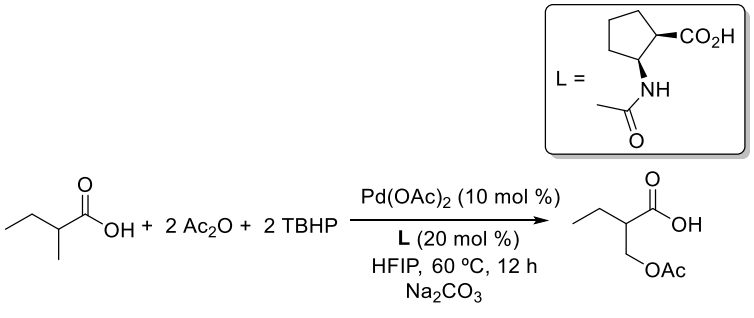

Ecuación 15.

[9] Thuy-Boun, P. S.; Villa, G.; Dang, D.; Richardson, P.; Su, S. and Yu, J-Q. *J. Am. Chem. Soc.* **2013**, 135, 17508-17513.
[10] Zhuang, Z.; Herron, A. N.; Fan, Z. and Yu, J-Q. *J. Am. Chem. Soc.* **2020**, *142*, 6769-6776.

Finalmente se puede concluir que los ligandos de tipo amido-piridina no han dado buenos resultados en ninguna de las transformaciones probadas. Aunque los ligandos parecían tener las características necesarias para asistir en las reacciones de activación C–H, no han sido eficaces en la aceleración de esta etapa en las reacciones catalíticas.

Conclusiones generales

Capítulo 2: El sistema catalítico Pd/bipy-6-OH permite la arilación directa de anilinas primarias selectivamente en *orto*, sin competencia de la reacción de aminación Buchwald-Hartwig permitiendo evitar, por primera vez, los pasos de protección y desprotección adicionales usados hasta ahora. Se encontró que las mejores condiciones eran DMA como disolvente, carbonato de cesio como base a 130 ºC. La reacción tolera diferentes propiedades electrónicas tanto en la anilina como en el haluro de arilo. Se ha demostrado mediante estudios mecanísticos experimentales y computacionales, que la reacción transcurre a través de intermedios aniónicos y la activación C–H se produce en un derivado amiduro de paladio tras la deprotonación de la anilina. La barrera para este proceso es menor que la eliminación reductora arilo-amiduro, evitando así la formación del producto de aminación. Así, el ligando bipy-6-OH es crucial para la quimioselectividad. La activación C–H en orto está favorecida en el intermedio aniónico tipo amiduro y esto explica que la reacción sea regioselectiva en *orto* para anilinas primarias y secundarias pero no para terciarias.

Capítulo 3: Se ha desarrollado un sistema dual de ligandos para la arilación directa de arenos simples. El uso del ligando bipy-6-OH en conjunto con PCy_3 permite usar condiciones de reacción más suaves que las correspondientes al uso de un solo ligando (30 ˚C inferior). La reacción tolera bromuros y cloruros de arilo como reactivos, además de grupos electro-dadores y electro-atractores tanto en el areno como en el haluro de arilo. La reacción es más rápida para arenos ricos en densidad electrónica. Mediante experimentos mecanísticos se pueden descartar etapas de intercambio de ligandos sobre el mismo metal en el ciclo catalítico. El mecanismo probable es bimetálico, donde un complejo Pd/PCy_3 es responsable de la adición oxidante mientras la activación C–H tiene lugar en un complejo Pd/bipy-6-O. La etapa de transmetalación entre estos dos complejos de paladio con arilos diferentes llevaría a la formación de un derivado bis-arilo con PCy_3 coordinada, y al producto final tras la eliminación reductora. Esta etapa ha sido demostrada mediante experimentos independientes con complejos análogos. La ventaja de usar un sistema dual es que la especie responsable de la etapa de activación C–H, la más lenta del ciclo catalítico, es diferente a la que opera en un mecanismo con sólo bipy-6-OH. Esta especie es previsiblemente [Pd(bipy-6-O)(OAc)(Tolueno)] en la que el centro de Pd es más electrofílico y el estado de transición con carácter eCMD tiene una barrera más baja que en intermedios [Pd(bipy-6-O)(Ar)(Tolueno)], responsables de la activación C–H en el sistema monoligando.

Capítulo 4: El ligando pic-6-OH y los ligandos de tipo amido-piridina son capaces de asistir en la etapa de activación C–H como ha sido demostrado experimental y computacionalmente. Sin embargo, no son efectivos en las reacciones catalíticas de funcionalización C–H. El ligando pic-6-OH lleva a rendimientos mayores en la arilación directa de arenos cuando se utilizan bases solubles o disolventes polares, lo que parece indicar la importancia de que el ligando esté coordinado en su forma dianiónica para producir la activación C–H. Los ligandos amido-piridina tampoco dan buenos resultados en la arilación de arenos, ni en reacciones de acoplamiento C–C oxidativas de arenos. Tan sólo en la acetoxilación de ácidos alquil-carboxílicos uno de los ligandos (L5) fue capaz de dar resultados comparables con los publicados. La cooperación del ligando en la activación C–H es una condición necesaria pero no suficiente para una funcionalización C–H eficaz, como lo demuestran los resultados obtenidos para los dos tipos de ligandos ensayados. Es un hecho que ambos son capaces de facilitar la activación C–H y pueden ser candidatos para ensayar otro tipo de reacciones catalíticas de funcionalización de hidrocarburos.

Appendix

List of abbreviations and acronyms

AMLA	Ambiphilic Metal Ligand Activation
An	aniline
Anal.	Elemental Analysis
Ar	Aryl group
benz	ethyl benzoate
bipy	2,2'-bipyridine
bipy-4-OH	[2,2′-Bipyridin]-4(1H)-one
bipy-6-OH	[2,2'-bipyridin]-(1H)-one
bipyMe-6-OH	6′-Methyl[2,2′-bipyridin]-6(1H)-one
bipyCH_2-6-OH	6-[(6-Methyl-2-pyridinyl)methyl]-2(1H)-pyridinone
br	broad
CCD	Charge Coupled Device
CMD	Concerted Metalation-Deprotonation
COPASI	COmplex PAthway SImulator
COSY	COrrelation SpectroscopY
d	doublet
dba	*trans*,*trans*-Dibenzylideneacetone
DFT	Density Functional Theory
DG	Directign Grorup
DMA	*N*,*N*-dimethylacetamide
DMF	*N*,*N*-dimethylformamide
DMSO	Dimethyl sulfoxide
eq	Equivalent
ESI-TOF	Electrospray Ionization-Time-Of.-Flight
GC	Gas Chromatography
HFIP	Hexafluoroisopropanol
HMBC	Heteronuclear Multiple Bond Correlation
HOAc	Acetic acid
HOESY	Heteronuclear Overhauser Effect Spectroscopy
HRMS	High Resolution Mass Spectrometry
HSQC	Heteronuclear Single Quantum Coherence Spectroscopy
IR	Infrared
J	Coupling constant

KHMDS	Potassium bis(trimethylsilyl)amide
KIE	Kinetic Isotope Effect
L4-OH	4-hydroxypicolinic acid
L6-OH	6-hydroxypicolinic acid
m	multiplet
MLC	Metal Ligand Cooperation
m.p.	Melting point
MPAA	Mono Protected AminoAcid
MS	Mass Spectrometry
NMR	Nuclear Magnetic Resonance
NOESY	Nuclear Overhauser Effect Spectroscopy
OAc	Acetate
ORTEP	Oak Ridge Thermal Ellipsoid Plot
Ox	Oxidant
pin	pinacolone
Pf	Pentafluorophenyl group
Phen-2-OH	[1,10-phenanthrolin]-2(1H)-one
ppm	Parts per millon
py	pyridine
Rf	Retention factor
s	singlet
SMD	Solvation Moled based on Density
Solv	Solvent
t	triplet
TBHP	Tert-Butyl hydroperoxide
TDG	Transient Directing Group
TMSCHN2	Trimethylsilyldiazomethane
tol	toluene
TS	Transition State
XPhos	2-Dicyclohexylphosphino-2′,4′,6′-triisopropylbiphenyl

Compound index

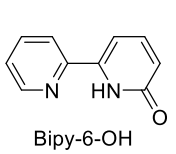

Bipy-6-OH

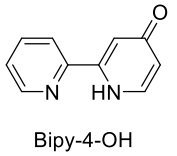

Bipy-4-OH

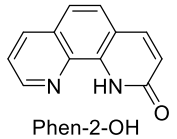

Phen-2-OH

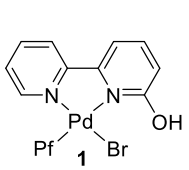

1

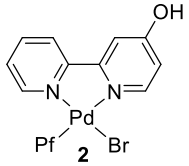

2

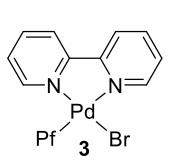

3

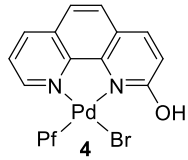

4

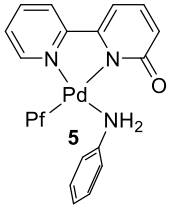

5

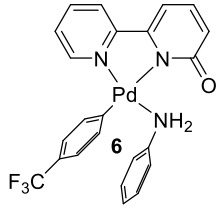

6

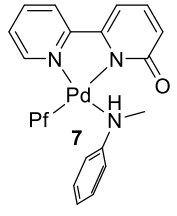

7

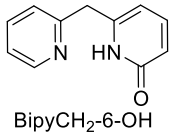

$BipyCH_2$-6-OH

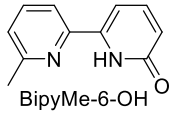

BipyMe-6-OH

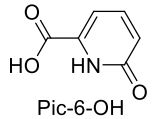

Pic-6-OH

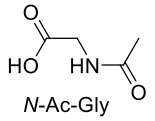

N-Ac-Gly

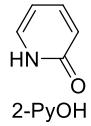

2-PyOH

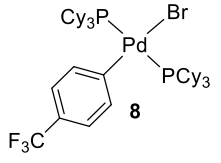

8

$[Pd(PCy_3)_2]$

9

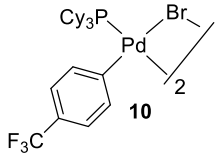

10

$[PdBr(PCy_3)_2Pf]$

11

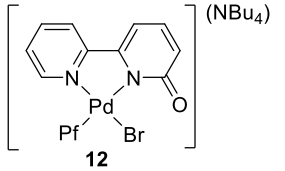

12

$[Pd(Bipy\text{-}6\text{-}O)(PCy_3)Pf]$

13

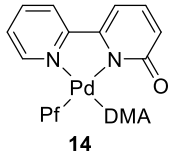

14

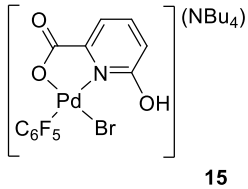

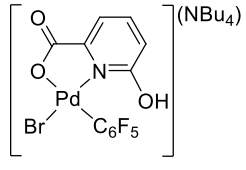

15

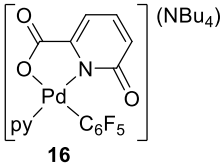

16

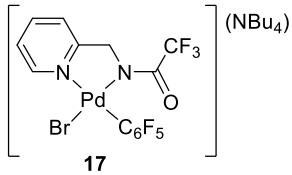

17

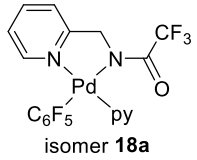

isomer **18a**

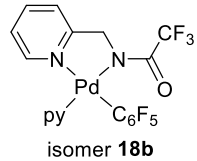

isomer **18b**

References

[1]Wu, X.-F.; Anbarasan, P.; Neumann, H.; Beller, M. *Angew. Chem. Int. Ed.* **2010**, *49*, 9047-9050.
[2]a) Mizoroki, T.; Ozaki, M. A. *Bull. Chem. Soc. Jpn.* **1971**, *44*, 581-584. b) Heck, R. F. *J. Am. Chem. Soc.* **1968**, *90*, 5518-5526. c) Heck, R. F. *Org. React.* **1982**, *27*, 345-390.
[3]Kumada, M. *Pure Appl. Chem.* **1980**, *52*, 669-679.
[4]Negishi, E.-I., *Ass. Chem. Res.* **1982**, *15*, 340-348.
[5]a) Miyaura, N.; Yanagi, T.; Suzuki, A. *Synth. Commun.* **1981**, *11*, 513-519. b) Miyaura, N.; Suzuki, A. *Chem. Rev*. **1995**, *95*, 2457-2483.
[6]a) Stille, J. K. *Angew. Chem. Int. Ed.* **1986**, *25*, 508-524. b) Stille, J. K. *Angew. Chem.* **1986**, *98*, 504-519.
[7]a) Hiyama, T.; Shirakawa, E. *Top. Curr. Chem*. **2002**, *219*, 61-85. b) Hiyama, T.; *J. Organomet. Chem*. **2002**, *653*, 58-61.
[8]a) Sonogashira, K.; Tohda, Y.; Hagihara, N. *Tetrahedron Lett.* **1975**, 4467-4470. b) Sonogashira, K. in *Comprehensive organic Synthesis* (Eds.: B. M. Trost, I. Fleming), Pergamon Press, Oxford, **1991**, *3*, 521-549.
[9]Campeau, L.-C.; Hazari, N. *Organometallics* **2019**, *38*, 3-35.
[10]https://scifinder.cas.org (accessed June 5, 2023).
[11]He, J.; Wasa, M.; Chan, K. S. L.; Shao, Q.; Yu, J.-Q. *Chem. Rev.* **2017**, *117*, 8754-8786.
[12]Newton, C. G.; Wang, S.-G.; Oliveira, C. C.; Cramer, N. *Chem. Rev*. **2017**, *117*, 8908-8976.
[13]Seo, T.; Kubota, K.; Ito, H. *J. Am. Chem. Soc*. **2023**, *145*, 12, 6823-6837.
[14]a) Kalyani, D.; McMurtrey, K. B.; Neufeldt, S. R.; Sanford, M. S. *J. Am. Chem. Soc*. **2011**, *133*, 18566-18569. b) Liang, L.; Xie, M. S.; Wang, H. X.; Niu, H. Y.; Qu, G. R.; Guo, H. M. *J. Org. Chem*. **2017**, *82*, 5966-5973. c) Sahoo, M. K.; Rana, J.; Subaramanian, M.; Balaraman, E. *ChemistrySelect* **2017**, *2*, 7565-7569.
[15]Dhawa, U.; Kaplaneris, N.; Ackermann, L. *Org. Chem. Front*., **2021**, *8*, 4886-4913.
[16]Mandal, T.; Mondal, M.; Choudhury, J. *Organometallics* **2021**, *40*, 2443-2449.
[17]Gandeepan, P.; Müller, T.; Zell, D.; Cera, G.; Warratz, S.; Ackermann, L. *Chem. Rev*. **2019**, *119*, 2192-2452.
[18]Yadav, P.; Velmurugan, N.; Luscombe, C. K. *Synthesis* **2023**, *55*, 1-26.
[19]Vicente, R.; Kapdi, A. R.; Ackermann, L. *Angew. Chem. Int. Ed*. **2009**, *48*, 9792-9826.
[20]a) Salamanca, V.; Toledo, A.; Albéniz, A. C. *J. Am. Chem. Soc*. **2018**, *140*, 17851-17856. b) Salamanca, V.; Albéniz, A. C. *Org. Chem. Front*., **2021**, *8*, 1941-1951.
[21]a) Luan, Y.-X.; Zhang, T.; Yao, W.-W.; Lu,, K.; Kong, L.-Y.; Lin, Y.-T.; Ye, M. *J. Am. Chem. Soc.* **2017**, *139*, 1786-1789. b) Wang, D.; Salazar, C. A.; Stahl, S. S. *Organometallics*, **2021**, *40*, 2198-2203.
[22]Salazar, C. A.; Gair, J. J.; Flesch, K. N.; Guzei, I. A.; Lewis, J. C.; Stahl, S. S. *Angew. Chem. Int. Ed.*, **2020**, *59*, 10873-10877.
[23]a) Kancherla,S.; Jorgensen, K. B.; Fernández-Ibáñez, M. A. *Synthesis* **2019**, *51*, 643-663. b) Ali, W.; Prakash, G.; Maiti, D. *Chem. Sci.* **2021**, *12*, 2735-2759. c) Ortiz-de-Elguea, V.; Carral-Menoyo, A.; Simón-Vidal, L.; Martinez-Nunes, M.; Barbolla, I.; Lete, M. G.; Sotomayor, N.; Lete, E. *ACS Omega*, **2021**, *6*, 29483-29494.
[24]Yang, Y.; Lan, J.; You, J. *Chem. Rev*. **2017**, *117*, 8787-8863.

[25]Villalba, F.; Albéniz, A. C. *Adv. Synth.Catal*. **2021**, *363*, 4795-4804.
[26]Stuart, D. R. ; Fagnou, K. *Science* **2007**, *316*, 1172-1175.
[27]a) Xu, L.-M.; Li, B.-J.; Yang, Z.; Shi, Z.-J., *Chem. Soc. Rev*. **2010**, *39*, 712-733. b) Juliá-Hernández, F.; Arcas, A.; Vicente, J. *Chem. Eur. J.*, **2011**, *18*, 7780-7786. c) Topczewski, J. J.; Sanford, M. S. *Chem. Sci.*, **2015**, *6*, 70-76. d) Liu, S.; Zhuang, Z; Qiao, J. X.; Yeung, K.-S.; Su, S.; Cherney, E. C.; Ruan, Z.; Ewing, W. R.; Poss, M. A.; Yu, Y.-Q. *J. Am. Chem. Soc*. **2021**, *143*, 21657-21666.
[28]a) Arcas, A.; Juliá-Hernández, F.; Bautista, D.; Vicente, J. *Angew. Chem. Int. Ed.*, **2011**, *50*, 6896-6899. b) Whitehurst, W. G.; Gaunt, M. J., *J. Am. Chem. Soc.* **2020**, *142*, 14169-14177.
[29]Poveda, S.; Alonso, I.; Fernández-Ibáñez, M. A. *Chem. Sci*., **2014**, *5*, 3873-3882.
[30]a) Neufeldt, S. R.; Sanford, M. S. *Acc. Chem. Res.* **2012,** *45*, 936-946. b) Tang, K.-X.; Wang, C.-M.; Gao, T.-H.; Chen., L.; Fan, L.; Sun, L.-P. *Adv. Synth. Catal*. **2019**, *361*, 26-38. c) Tomberg, A.; Muratore, M. E.; Johansson, M. M.; Terstiege, I.; Sköld, C. Norrby P.-O. *iScience*, **2019**, *20*, 373-391. d) Murali, K.; Machado, L. A.; Carvalho, R. L.; Pedrosa, L. F.; Mukherjee, R.; Da Silva, E. N.; Maiti, D. *Chem. Eur. J.* **2021**, *27*, 12453-12508. e) Urruzuno, I.; Andrade-Sampedro, P.; Correa, A. *Eur. J. Org. Chem*. **2023**, *26*, e202201489.
[31]Tang, K.-X.; Wang, C.-M.; Gao, T.-H.; Pan, C.; Sun, L.-P. *Org. Chem. Front*. **2017**, *4*, 2167-2169.
[32]a) Gandeepan, P.; Ackermann, L. *Chem*, **2018**, *4*, 199-222. b) Jacob, C.; Maes, B. U. W.; Evano, G. *Chem. Eur. J*. **2021**, *27*, 13899-13952. c) Xu, W.; Zhang, Y.; Wu, Y.; Wuan, J.; Lu, X.; Zhou, Y.; Zhang F.-L. *J. Org. Chem*. **2022**, *87*, 10807-10814.
[33]Zhang, F.-L.; Hong, K.; Li, T.-J.; Park, H.; Yu, J.-Q. *Science*, **2016**, *351*, 252-256.
[34]Xu, J.; Liu, Y.; Wang, Y.; Li, Y.; Xu, X.; Jin, Z. *Org. Lett*. **2017**, *19*, 1562-1565.
[35]a) Zhang, Z.; Tanaka, K.; Yu, J.-Q. *Nature*, **2017**, *543*, 538–542. b) Achar, T. K.; Ramakrishna, K.; Pal, T.; Porey, S.; Dolui, P.; Biswas, J. P.; Maiti, D. *Chem. Eur. J*., **2018**, *24*, 17906-17910. c) Achar, T. P.; Biswas, J. P.; Porey, S.; Pal, T.; Ramakrishna, K.; Maiti, S.; Maiti, D. *J. Org. Chem*. **2019**, *84*, 8315-8321.
[36]Shi, H.; Lu, Y.; Weng, J.; Bay, K. L.; Chen, X.; Tanaka, K.; Verma, P.; Houk, K. N.; Yu, J.-Q. *Nat. Chem*. **2020**, *2*, 399-404.
[37]Dhankhar, J.; Hofer, M. D.; Linden, A.; Čorić, I. *Angew. Chem. Int. Ed*. **2022**, *61*, e2022054.
[38]a) Catellani, M.; Chiusoli, G. P.; Costa, M. *J. Organomet. Chem*. **1995**, *500*, 69-80. b) Catellani, M. *Synlett* **2003**, 298-313. c) Della Ca',N.; Fontana, M.; Motti, E.; Catellani, M. *Acc. Chem. Res.* **2016**, *49*, 1389-1400.
[39]a) Wang, X.-C.; Gong, W.; Fang, L.-Z.; Zhu, R.-Y.; Li, S.; Engle, K. M.; Yu, J.-Q. *Nature*, **2015**, *519*, 334-338. b) Dong, Z.; Wang, J.; Dong, G. *J. Am. Chem. Soc*. **2015**, *137*, 5887-5890. c) Dutta, U.; Porey, S.; Pimparkar, S.; Mandal, A.; Grover, J.; Koodan, A.; Maiti, D. *Angew. Chem. Int. Ed.* **2020**, *59*, 20831-20836. d) Liu, S.; Wang, Q.; Huang, F.; Wang, W.; Yang, C.; Liu, J. Chen, D. *Org. Chem. Front.* **2022**, *9*, 129-139.
[40]Sukowski, V.; Borselen, M. V.; Mathew, S.; Fernández-Ibáñez, M. A. *Angew. Chem., Int. Ed*. **2022**, *61*, e202201750.
[41]Altus, K. M.; Love, J. A. *Commun. Chem.* **2021**, *4*, 173. https://doi.org/10.1038/s42004-021-00611-1.

[42]a) Jia, C.; Piao, D.; Oyamada, J.; Lu, W.; Kitamura, T.; Fujiwara, Y. *Science*, **2000**, *287*, 1992-1995. b) Martín-Matute, B.; Mateo, C.; Cárdenas, D. J; Echavarren, A. M. *Chem. Eur. J*. **2001**, *7*, 2341-2348. c) Lane, B. S.; Brown, M. A.; Sames, D. *J. Am. Chem. Soc.* **2005**, *127*, 8050-8057.
[43]Capito, E.; Browna, J. M.; Ricci, A. *Chem. Commun*. **2005**, 1854-1856.
[44]a) Murai, S.; Kakiuchl, F.; Seklne, S.; Tanaka, Y.; Kamatani, A.; Sonoda M.; Chatani, N. *Nature*, **1993**, *336*, 529-531. b) Zhang, X.; Kanzelberger, M.; Emge, T. J.; Goldman, A. S. *J. Am. Chem. Soc*. **2004**, *126*, 13192-13193. c) Pabst, T. P.; Chirik, P. J. *Organometallics*, **2021**, *40*, 7, 813-831.
[45]a) Thompson, M. E.; Baxter, S. M.; Bulls, A. R.; Burger, B. J.; Nolan, M. C.; Santarsiero, B. D.; Schaefer, W. P.; Bercaw, J. E. *J. Am. Chem. Soc.* **1987**, *109*, 203-219. b) Sadow, A. D.; Tilley, T. D. *J. Am. Chem. Soc*. **2005**, *127*, 643-656. c) Waterman, R. *Organometallics*, **2013**, *32*, 7249-7263. d) Soller, B. S.; Salzinger, S.; Jandl, C.; Pöthig, A.; Rieger, B. *Organometallics*, **2015**, *34*, 2703-2706. e) Parker, K.; Weragoda, G. K.; Canty, A. J.; Polyzos, A.; Ryzhov, V.; O'Hair, R. A. J. *Organometallics*, **2020**, *39*, 4027-4036. f) Perutz,R. N.; Sabo-Etienne, S.; Weller, A. S. *Angew. Chem. Int. Ed*. **2022**, *61*, e202111462.
[46]a) Fagnou, K.; Lapointe, D. *Chem. Lett.* **2010**, *39*, 1118-1126. b) Akermann, L. *Chem. Rev*. **2011**, *111*, 1315-1345. c) McMullin, C. L.; Davies, D. L.; Macgregor, S. A. *Chem. Rev*. **2017**, *117*, 8649-8709. d) Sampson, J.; Wang, L.; Carrow, B. P. *Isr. J. Chem*. **2020**, *60*, 230-258.
[47]Davies, D. L.; Donald, S. M. A.; Macgregor, S. A. *J. Am. Chem. Soc*. **2005**, *127*, 13754-13755.
[48]Boutadla, Y.; Davies, D. L.; Macgregor, S. A.; Poblador-Bahamonde, A. I. *Dalton Trans*, **2009**, 5820-5831.
[49]García-Cuadrado, D.; Braga, A. A. C.; Maseras, F.; Echavarren, A. M. *J. Am. Chem. Soc*. **2006**, *128*, 1066-1067.
[50]a) Lafrance, M.; Rowley, C. N; Woo, T. K.; Fagnou, K. *J. Am. Chem. Soc*. **2006**, *128*, 8754-8756. b) Gorelsky, S. I.; Lapointe, D.; Fagnou, K. *J. Am. Chem. Soc*. **2008**, *130*, 10848-10849. c) Gorelsky, S. I.; Lapointe, D.; Fagnou, K. *J. Org. Chem*. **2012**, *77*, 658-668.
[51]Gorsline, B. J.; Wang, L.; Ren, P.; Carrow, B. P. *J. Am. Chem. Soc*. **2017**, *139*, 9605-9614.
[52]Wang, L.; Carrow, B. P. *ACS Catal*. **2019**, *9*, 6821-6836.
[53]a) Khusnutdinova, J. R.; Milstein, D. *Angew. Chem. Int. Ed.* **2015**, *54*, 12236-12273. b) Higashi, T.; Kusumoto, S.; Nozaki, K. *Chem. Rev*. **2019**, *119*, 18, 10393-10402.
[54]Gunanathan, C.; Milstein, D. *Acc. Chem. Res.* **2011**, *44*, 588-602.
[55]Kusumoto, S.; Akiyama, M.; Nozaki, K. *J. Am. Chem. Soc*. **2013**, *135*, 18726-18729.
[56]Clerc, A.; Marelli, E.; Adet, N.; Monot, J.; Martín-Vaca, B.; Bourissou, D. *Chem. Sci*., **2021**, *12*, 435-441.
[57]Shao, Q.; Wu, K.; Zhuang, Z.; Qian, S.; Yu, J.-Q. *Acc. Chem. Res*. **2020**, *53*, 833-851.
[58]a) Cheng, G. J.; Yang, Y. F.; Liu, P.; Chen, P.; Sun, T. Y.; Li, G.; Zhang, X.; Houk, K. N.; Yu J.-Q.; Wu, Y. D. *J. Am. Chem. Soc*., **2014**, *136*, 894-897. b) Haines, B. E.; Yu; J.-Q.; Musaev, D. G. *ACS Catal*., **2017**, *7*, 4344-4354. c) Wedi, P.; Farizyan, M.; Bergander, K.; Mück-Lichtenfeld C.; Gemmeren, M. *Angew. Chem. Int. Ed*., **2021**, *60*, 15641-15649. d) Mukherjee, K.; Grimblat, N.; Sau, S.; Ghosh, K.; Shankar, M.; V. Gandon ;

Sahoo, A. K. *Chem. Sci*., **2021**, *12*, 14863-14870. e) Xu, L. P.; Zhuang, Z.; Qian, S.; Yu, J.-Q.; Musaev, D. G. *ACS Catal*., **2022**, *12*, 4848-4858.
[59]Fernández-Moyano, S.; Salamanca, V.; Albéniz, A. C. *Chem. Sci*., **2023**,*14*, 6688-6694.
[60]a) Wang, P.; Verma, P.; Xia, G.; Shi, J.; Qiao, J. X.; Tao, S.; Cheng, P. T. W.; Poss, A.; Farmer, M. E.; Yeung, K.-S.; Yu, J.-Q. *Nature*, **2017**, *551*, 489-494. b) Zhu, R.-Y.; Li, Z.-Q.; Park, H. S.; Senanayake, C. H.; Yu, J.-Q. *J. Am. Chem. Soc*. **2018**, *140*, 3564-3568. c) Fan, Z.; Bay, K. L.; Chen, X.; Zhuang, Z.; Park, H. S.; Yeung, K.-S.; Houk, K. N.; Yu, J.-Q. *Angew. Chem., Int. Ed.* **2020**, *59*, 4770-4777. d) Li, Y.-H. Ouyang, Y.; Chekshin, N.; Yu, J.-Q. *ACS Catal.* **2022**, *12*, 10581-10586.
[61]a) Wang, Z.; Hu, L.; Chekshin, N.; Zhuang, Z.; Qian, S.; Qiao, J. X.; Yu, J.-Q. *Science* **2021**, *374*, 1281-1285. b) Chan, H. S. S.; Yang, J.-M.; Yu, J.-Q. *Science*. **2022**, *376*, 1481-1487. c) Hu, L.; Meng, G.; Yu, J.-Q. *J. Am. Chem. Soc*. **2022**, *144*, 20550-20553.
[62]a) Tischler, M. O.; Tóth, M. B.; Novák, Z. *Chem. Rec*. **2017**, *17*, 184-199. b) Leitch, J. A.; Frost, C. G. *Synth*. **2018**, *50*, 2693-2706.
[63]a) Boele, M. D. K.; Van Strijdonck, G. P. F.; De Vries, A. H. M.; Kamer, P. C. J.; De Vries, J. G.; Van Leeuwen, P. W. N. M. *J. Am. Chem. Soc*. **2002**, *124*, 1586-1587. b) Mizuta, Y.; Obora, Y.; Shimizu, Y.; Ishii, Y. *ChemCatChem* **2012**, *4*, 187-191. c) Yao, Q. J.; Xie, P. P.; Wu, Y. J.; Feng, Y. L.; Teng, M. Y.; Hong, X.; Shi, B. F. *J. Am. Chem. Soc*. **2020**, *142*, 18266-18276.
[64]Naksomboon, K.; Poater, J.; Bickelhaupt, F. M.; Fernández- Ibáñez, M. A. *J. Am. Chem. Soc*. **2019**, *141*, 6719-6725.
[65]Direct arylation using ArX: a) Daugulis, O.; Zaitsev, V. G.Angew. *Chem. Int. Ed*. **2005**, *44*, 4046-4048. b) Scarborough, C. C.;McDonald, R. I.; Hartmann, C.; Sazama, G. T.; Bergant, A.; Stahl, S. S. *J. Org. Chem*. **2009**, *74*, 2613-2615. c) Wan, C.; Zhao, J.; Xu, M.; Huang, J. *J. Org. Chem*. **2014**, *79*, 4751-4756. d) Kwak, S. H.; Gulia, N.; Daugulis, O. *J. Org. Chem*. **2018**, *83*, 5844-5850. e) Lichte, D.; Pirkl, N.; Heinrich, G.; Dutta, S.; Goebel, J. F.; Koley, D.; Goossen, L. J. *Angew, Chem, Int. Ed*. **2022**, *61*, e202210009.
[66]Arylation using diaryliodonium salts: a) Kalyani, D.; Deprez, N. R.; Desai, L. V.; Sanford, M. S. *J. Am. Chem. Soc*. **2005**, *127*, 7330-7331. b) Phipps, R. J.; Gaunt, M. J. *Science*, **2009**, *323*, 1593-1597. c) Ciana, C. L.; Phipps, R. J.; Brandt, J. R.; Meyer, F. M.; Gaunt, M. J. *Angew. Chem. Int. Ed.* **2011**, *50*, 458-462.
[67]Oxidative arylation with arenes: a) Li, B. J.; Tian, S. L.; Fang, Z.; Shi, Z. J. *Angew. Chem. Int. Ed.* **2008**, *47*, 1115-1118. b) Yeung, C. S.; Zhao, X.; Borduas, N.; Dong, V. M. *Chem. Sci*. **2010**, 1, 331-336. c) Brasche, G.; García-Fortanet, J.; Buchwald, S. L. *Org. Lett*. **2008**, *10*, 2207-2210.
[68]Oxidative arylation with arylboronic derivatives: a) Nishikata, T.; Abela, A. R.; Huang, S.; Lipshutz, B. H. *J. Am. Chem. Soc*. **2010**, *132*, 4978-4979. b) Koley, M.; Dastbaravardeh, N.; Schnürch, M.; Mihovilovic, M. D. *ChemCatChem* **2012**, *4*, 1345-1352.
[69]Ghorai, D.; Finger, L. H.; Zanoni, G.; Ackermann, L. *ACS Catal*. **2018**, *8*, 11657-11662.
[70]Deng, K. Z.; Jia, W. L.; Fernández-Ibáñez, M. A. *Chem. Eur. J.* **2022**, *28*, e202104107.
[71]Chan, C. W.; Zhou, Z.; Yu, W. Y. *Adv. Synth. Catal*. **2011**, *353*, 2999-3006.
[72]Tang, R. -Y.; Li, G.; Yu, J. -Q. *Nature* **2014**, *507*, 215-220.

[73]Raju, S.; Hsiao, H. C.; Thirupathi, S.; Chen, P. L.; Chuang, S. C. *Adv. Synth. Catal.* **2019**, *361*, 683-689.
[74]a) Wetzel, A.; Ehrhardt, V.; Heinrich, M. R. *Angew. Chem. Int. Ed.* **2008**, *47*, 9130-9133. b) Jiang, T.; Chen, S. Y.; Zhuang, H.; Zeng, R. S.; Zou, J. P. *Tetrahedron Lett.* **2014**, *55*, 4549-4552.
[75]Pirali, T.; Zhang, F.; Miller, A. H.; Head, J. L.; McAusland, D.; Greaney, M. F. *Angew. Chem. Int. Ed.* **2012**, *51*, 1006-1009.
[76]Truong, T.; Daugulis, O. *Org. Lett.* **2012**, *14*, 5964-5967.
[77]Rieck, H.; Dunkel, R.; Elbe, H. L.; Wachendorff-Neumann, U.; Mauleer-Machnik, A.; Kuck, K. H. US 7186862 B2, 2007.
[78]a) Dhanak, D.; Knight, S. D.; Moore, M. L.; Newlander, K.A. WO 2006/005063 A2, 2006. b) Schmidt, A. W.; Reddy, K. R.; Knölker , H. J. *Chem. Rev.* **2012**, *112*, 3193-3328. c) Suzuki, C.; Hirano, K.; Satoh, T.; Miura, M. *Org. Lett.* **2015**, *17*, 1597-1600.
[79]Braun, H.J.; Chassot, L. US 6500213 B1, 2002.
[80]Sparta, M.; Riplinger, C.; Neese, F. *J. Chem. Theory Comput*. **2014**, *10*, 1099-1108.
[81]Cusumano, A. Q.; Stoltz, B. M.; Goddard, III, W. A. *J. Am. Chem. Soc.* **2020**, *142*, 13917-13933.
[82]Espinet, P.; Albéniz, A. C.; Usón, R.; Forniés, J.; Nalda, J. A.; Lozano, M. *J. Inorg. Chim. Acta*, **1989**, *156*, 251-256.
[83]Ishii, Y.; Hasegawa, S.; Kimura, S.; Itoh, K. *J. Organomet. Chem.* **1974**, *73*, 411-418.
[84]Yamashita, M.; Cuevas Vicario, J.; Hartwig, J. F. *J. Am. Chem. Soc.* **2003**, *125*, 16347-16360.
[85]Tomon, T.; Koizumi, T.; Tanaka, K. *Eur. J. Inorg. Chem*. **2005**, 285-293
[86]Chen, H.; Wang, L.; Han, J. *Chem. Commun*., **2020**, *56*, 5697-5700.
[87]Benting, J.; Desbordes, P.; Gary, S.; Greul, J.; Tsuchiya, T.; Wachendorff-Neumann, U. US 9206137 B2, 2015.
[88]Parrish, C. A.; Adams, N. D.; Auger, K. D.; Burgess, J. L.; Carson, J. D.; Chaudhari, A. M.; Copeland, R. A.; Diamond, M. A.; Donatelli, C. A.; Duffy, K. J.; Faucette, L. F.; Finer, J. T.; Huffman, W. F.; Hugger, E. D.; Jackson, J. R.; Knight, S. D.; Luo, L.; Moore, M. L.; Newlander, K. A.; Ridgers, L. H.; Sakowicz, R.; Shaw, A. N.; Sung, C. M.; Sutton, D.; Wood, K. W.; Zhang, Y.-S.; Zimmerman, M. N.; Dhanak, D. *J. Med. Chem.* **2007**, *50*, 4939-4952.
[89]Dai, W.; Yang, B.; Xu, S.; Wang, Z. *J. Org. Chem.* **2021**, *86*, 2235-2243.
[90]Zuo, Z.; Liu, J.; Nan, J.; Fan, L.; Sun, W.; Wang, Y.; Luan, X. *Angew. Chem. Int. Ed*. **2015**, 54, 15385-15389.
[91]Gillespie, J. E.; Morrill, C.; Phipps, R. J. *J. Am. Chem. Soc.* **2021**, *143*, 9355-9360.
[92]Maity, A.; Frey, B. L.; Hoskinson, N. D.; Powers, D. C. *J. Am. Chem. Soc*. **2020**, *142*, 4990-4995.
[93]a) Ohshita, K.; Ishiyama, H.; Oyanagi, K.; Nakatab, H.; Kobayashi, J. *Bioorg. Med. Chem.* **2007**, *15*, 3235-3240. b) Surry, D. S.; Buchwald, S. L. *Angew. Chem. Int. Ed.* **2008**, *47*, 6338-6361.
[94]a) Sharma, C.; Srivastava, A. K.; Sharma, K. S.; Joshi, R. K. *Org. Biomol. Chem.*, **2020**,*18*, 3599-3606. b) Srivastava, A. K.; Sharma, C.; Joshi, R. K. *Green Chem*., **2020**, *22*, 8248-8253.

[95]a) Li, J.; Huang, C.; Wen, D.; Zheng, Q.; Tu, B.; Tu, T. *Org. Lett.* **2021**, *23*, 687-691. b) Tröndle, S.; Freytag, M.; Jones, P. G.; Tamm, M. *Eur. J. Inorg. Chem.* **2019**, 2569-2576.
[96]Fuchita Y.; Tsuchiya, H.; Miyafuji, A. *Inorg. Chim. Acta*. **1995**, 233, 91-96.
[97]a) Burés, J. *Angew. Chem. Int. Ed.* **2016**, *55*, 16084-16087. b) Burés, J., A. *Angew. Chem. Int. Ed.* **2016**, *55*, 2028-2031.
[98]CrysAlisPro Software system, version 1.171.33.51, **2009**, Oxford Diffraction Ltd, Oxford, UK.
[99]Sheldrick, G. M. *Acta Cryst.* **2015**, *C71*, 3-8.
[100]Dolomanov, O. V.; Bourhis, L. J.; Gildea, R. J.; Howard J. A. K.; Puschmann, H. *J. Appl. Crystallogr.* **2009**, *42*, 339-341.
[101]Gaussian 16, Revision C.01, Frisch, M. J.; Trucks, G. W.; Schlegel, H. B.; Scuseria, G. E.; Robb, M. A.; Cheeseman, J. R.; Scalmani, G.; Barone, V.; Petersson, G. A.; Nakatsuji, H.; Li, X.; Caricato, M.; Marenich, A. V.; Bloino, J.; Janesko, B. G.; Gomperts, R.; Mennucci, B.; Hratchian, H. P.; Ortiz, J. V.; Izmaylov, A. F.; Sonnenberg, J. L.; Williams-Young, D.; Ding, F.; Lipparini, F.; Egidi, F.; Goings, J.; Peng, B.; Petrone, A.; Henderson, T.; Ranasinghe, D.; Zakrzewski, V. G.; Gao, J.; Rega, N.; Zheng, G.; Liang, W.; Hada, M.; Ehara, M.; Toyota, K.; Fukuda, R.; Hasegawa, J.; Ishida, M.; Nakajima, T.; Honda, Y.; Kitao, O.; Nakai, H.; Vreven, T.; Throssell, K.; Montgomery, J. A., Jr.; Peralta, J. E.; Ogliaro, F.; Bearpark, M. J.; Heyd, J. J.; Brothers, E. N.; Kudin, K. N.; Staroverov, V. N.; Keith, T. A.; Kobayashi, R.; Normand, J.; Raghavachari, K.; Rendell, A. P.; Burant, J. C.; Iyengar, S. S.; Tomasi, J.; Cossi, M.; Millam, J. M.; Klene, M.; Adamo, C.; Cammi, R.; Ochterski, J. W.; Martin, R. L.; Morokuma, K.; Farkas, O.; Foresman, J. B.; Fox, D. J. Gaussian, Inc., Wallingford CT, **2016**.
[102](a) Zhao, Y.; Truhlar, D. G. J. *Chem. Phys.* **2006**, *125*, 194101-194118. (b) Zhao, Y.; Truhlar, D. G. *Theor. Chem. Acc.* **2006**, *120*, 215-241.
[103](a) Francl, M. M; Petro, W. J.; Hehre, W. J.; Binkley, J. S.; Gordon, M. S.; DeFrees, D. J.; Pople, J. A. *J. Chem. Phys.* **1982**, *77*, 3654- 3665. (b) Clark, T.; Chandrasekhar, J.; Schleyer, P. V. R. J. *J. Comput. Chem.* **1983**, *4*, 294-301.
[104](a) Ehlers, A. W.; Böhme, M.; Dapprich, S.; Gobbi, A.; Höllwarth, A.; Jonas, V.; Köhler, K. F.; Stegmann, R.; Veldkamp, A.; Frenking, G. *Chem. Phys. Lett.* **1993,** *208*, 111-114. (b) Roy, L. E.; Hay, P. J.; Martin, R. L. J. *J. Chem. Theory Comput.* **2008**, *4*, 1029-1031.
[105]Hay, P. J.; Wadt, W. R. *J. Chem. Phys.* **1985**, *82*, 270-283.
[106]Norjmaa, G.; Ujaque, G.; Lledós. *Top. Catal.* **2022**, *65*, 118-140.
[107]Marenich, A. V.; Cramer, C. J.; Truhlar, D. G. *J. Phys. Chem. B* **2009**, *113*, 6378-6396.
[108](a) Riplinger, C.; Neese, F. *J. Chem. Phys.* **2013**, *138*, 034106. (b) Riplinger, C.; Sandhoefer, B.; Hansen, A.; Neese, F. *J. Chem. Phys.* **2013**, *139*, 134101. (c) Riplinger, C.; Pinski, P.; Becker, U.; Valeev, E. F.; Neese, F.. *J. Chem. Phys.* **2016**, 144, 024109.
[109]a) Neese, F. WIREs Comput. Mol. Sci. 2012, 273-78. (b) Neese, F. WIREs Comput. Mol. Sci. 2018, 8, e1327.
[110](a) Schäfer, A.; Horn, H.; Ahlrichs, R. *J. Chem. Phys.* **1992**, *97*, 2571-2577. (b) Weigend, F.; Ahlrichs, R. *Phys. Chem. Chem. Phys.* **2005**, *7*, 3297-3305. (c) Weigend, F. *Phys. Chem. Chem. Phys.* **2006**, *8*, 1057-1065.

[111]Neese, F.; Wennmohs, F.; Hansen, A.; Becker, U. *Chem. Phys.* **2009**, *356*, 98-109.
[112](a) Andrae, D.; Häussermann, U.; Dolg, M.; Stoll, H.; Preuss, H. *Theoret. Chim. Acta* **1990**, *77*, 123-141. (b) Leininger, T.; Nicklass, A.; Kuechle, W.; Stoll, H.; Dolg, M.; Bergner, A. *Chem. Phys. Lett.* **1996**, *255*, 274-280.
[113]Bryantsev, V. S.; Diallo, M. S.; Goddard III, W. A. Calculation of Solvation Free Energies of Charged Solutes Using Mixed Cluster/Continuum Models. *J. Phys. Chem. B* **2008**, *112*, 9709-9719.
[114]Legault, C. Y. CYLview20; Université de Sherbrooke, **2020**; http://www.cylview.org
[115]COmplex PAthway Simulator (COPASI) is an easily available free software: Hoops, S.; Sahle, S.; Gauges, R.; Lee, C.; Pahle, J.; Simus, N.; Singhal, M; Xu, L.; Mendes, P.; Kummer, U. COPASI–A COmplex PAthway SImulator *Bioinformatics*, **2006**, *22*, 3067-3074.
[116]a) Chen, H.; Wedi, P.; Meyer, T.; Tavakoli, G.; Gemmeren, M. v. *Angew. Chem. Int. Ed*. **2018**, *57*, 2497-2501. b) Wedi, P.; Farizyan, M.; Bergander, K.; Mgck-Lichtenfeld, C.; Gemmeren, M. V. *Angew. Chem. Int. Ed*. **2021**, *60*, 15641-15649.
[117]Chen, H.; Mondal, A.; Wedi, P.; Gemmeren, M. v. *ACS Catal.* **2019**, *9*, 1979-1984.
[118]Mondal, A.; Chen, H.; Flämig, L.; Wedi, P.; Gemmeren, M. v. *J. Am. Chem. Soc*. **2019**, *141*, 18662-18667.
[119]Kaltenberger, S.; Gemmeren, M. v. *Acc. Chem. Res*. **2023**, *56*, 2459-2472.
[120]Yin, B.; Fu, M.; Wang, L.; Liu, J.; Zhu, Q. *Chem. Commun.*, **2020**, *56*, 3293-3296.
[121]a) Liu, L.-Y.; Qiao, Y. X.; Yeung, K.-S.; Ewing, W. R.; Yu, Y.-Q. *J. Am. Chem. Soc*. **2019**, *141*, 14870-14877. b) Liu, L.-Y.; Qiao, J. X.; Yeung, K.-S. Ewing, W. R.; Yu, Y.-Q. *Angew. Chem. Int. Ed.*, **2020**, *53*, 13831-13835.
[122]Park, H. S.; Fan, Z.; Zhu, R.-Y.; Yu, J.-Q. *Angew. Chem. Int. Ed.***, 2020**, *59*, 12853-12859.
[123]Sinha, S. K.; Panja, S.; Grover, J.; Hazra, P.S.; Pandit, S.; Bairagi, Y.; Zhang, X.; Maiti, D. *J. Am. Chem. Soc*. **2022**, *144*, 12032-12042.
[124]Meng, G.; Wang, Z.; Chan, H. S. S.; Chekshin, N.; Li, Z.; Wang, P.; Yu, J.-Q. *J. Am. Chem. Soc.* **2023**, *145*, 8198-8208.
[125] a) Beckers, I.; Bugaev, A.; De Vos, D. *Chem. Sci*., **2023**, *14*, 1176-1183. b) Beckers, I.; De Vos, D. *iScience*, **2023**, *26*, 105790.
[126]a) Barder, T. E.; Walker, S. D.; Martinelli, J. R.; Buchwald, S. L. *J. Am. Chem. Soc.* **2005**, *127*, 4685-4696. b) Martin, R.; Buchwald, S. L. *Acc. Chem. Res.* **2008**, *41*, 1461-1473.
[127]a) Sun, H.-Y.; Gorelsky, S. I.; Stuart, D. R.; Campeau, L.-C.; Fagnou, K. *J. Org. Chem*. **2010**, *75*, 8180-8189. b) Liegault, B.; Petrov, I.; Gorelsky, S. I.; Fagnou, K. *J. Org. Chem*. **2010**, *75*, 1047-1060. c) Yamajala, K. D. B.; Patil, M.; Banerjee, S. *J. Org. Chem*. **2015**, *80*, 3003-3011. d) Yuen; O. Y; Charoensak, M.; So, C. M.; Kuhakarn C.; Kwong, F. Y. *Chem. Asian J.*, **2015**, *10*, 857-861. e) Ji, Y.; Plata, R. E.; Regens, C. S.; Hay, M.; Schmidt, M.; Razler, T.; Qiu, Y.; Geng, P.; Hsiao, Y.; Rosner, T.; Eastgate, M. D.; Blackmond, D. G. *J. Am. Chem. Soc*. **2015**, *137*, 13272-13281.
[128]a) Tan, Y.; Barrios-Landeros, F.; Hartwig, J. F. *J. Am. Chem. Soc*. **2012**, *134*, 3683-3686. b) Gorelsky, S. I. *Organometallics*, **2012**, *31*, 4631-4634.
[129]Wang, D.; Izawa, Y.; Stahl, S. S. *J. Am. Chem. Soc*. **2014**, *136*, 9914-9917.
[130]a) Kim, J.; Hong, S. H. *ACS Catal.* **2017**, *7*, 3336-3343. b) Kim, D.; Choi, G.; Kim, W.; Kim, D.; Kang, Y. K.; Hong, S. H. *Chem. Sci*., **2021**, *12*, 363-373.
[131]Hattori, H.; Ogiwara, Y.; Sakai, N. *Organometallics* **2022**, 41, 1509-1518.

[132]Donohoe, T. J.; Fishlock, L. P.; Procopiou, P. A. *Org. Lett.* **2008**, 10, 2, 285-288.
[133]Deng, D.; Hu, B.; Zhang, Z.; Mo, S.; Yang, M.; Chen, D. *Organometallics* **2019**, 38, 9, 2218-2226.
[134]Gong, N. Method for preparing bis(tricyclohexylphosphine)palladium dichloride. CN102977151 A, 2013.
[135]Grushin, V. V.; Alper, H. *Organometallics*. **1993**, 12, 1890-1901.
[136]Grushin, V. V.; Bensimon, C.; Alper, H. *Organometallics*. **1995**, 14, 3259-3263.
[137]Grushin, V. V. *Organometallics*. **2000**, 19, 1888-1900.
[138]*o*-isomer: Shi, S.; Meng, G.; Szostak, M. *Angew. Chem. Int. Ed.* **2016**, *55*, 6959-6963.
[139]*o*-isomer: Gehrtz, P. H.; Geiger, V.; Schmidt, T.; Sršan, L.; Fleischer, I. *Org. Lett.* **2019**, 21, 50-55.
[140]a)*m*-isomer: Arun, V.; Reddy, P. O. V.; Pilania, M.; Kumar, D. *Eur. J. Org. Chem.* **2016**, 2096-2100. b)*o* and *p*-isomers: Chen, Q.; Mao, Z.; Guo, F.; Liu, X. *Tetrahedron Lett.*, **2016**, 57, 3735-3738.
[141]a) *o*-isomer: Shen, A.; Hua, Y-C.; Liu, T-T.; Ni, C.; Luo, Y.; Cao, Y-C. *Tetrahedron Lett.* **2016**, 57, 2055-2058. b) *m*-isomer: Yuen, O. Y.; So, C. M.; Man, H. W.; Kwong, F. Y. *Chem. Eur. J.* **2016**, 22, 6471-6476. c) *p*-isomer: Gombert, A.; McKay, A. I.; Davis, C. J.; Wheelhouse, K. M.; Willis, M. C. *J. Am. Chem. Soc*. **2020**, 142, 3564-3576.
[142]a)*o* and *p*-isomers: Dadras, A.; Naimi-Jamal, M. R.; Moghaddam, F. M.; Ayati, S. E. *Appl. Organometal. Chem.* **2018**, 1-9. b)*m*-isomer: Yan, M. Q.; Yuan, J.; Lan,F.; Zeng, S. H.; Gao, M-Y.; Liu, S-H.; Chena, J.; Yu, G-A. *Org. Biomol. Chem*. **2017**, 15, 3924-3929.
[143]Tang, J.; Biafora, A.; Goossen, L. J. *Angew. Chem. Int. Ed.* **2015**, 54, 13130-13133.
[144]Pinilla, C.; Salamanca, V.; Lledós, A.; Albéniz, A. C. *ACS Catalysis* **2022**, *12*, 14527-14532
[145]Gaussian 09, Revision D.01, Frisch, M. J.; Trucks, G. W.; Schlegel, H. B.; Scuseria, G. E.; Robb, M. A.; Cheeseman, J. R.; Scalmani, G.; Barone, V.; Mennucci, B.; Petersson, G. A.; Nakatsuji, H.; Caricato, M.; Li, X.; Hratchian, H. P.; Izmaylov, A. F.; Bloino, J.; Zheng, G.; Sonnenberg, J. L.; Hada, M.; Ehara, M.; Toyota, K.; Fukuda, R.; Hasegawa, J.; Ishida, M.; Nakajima, T.; Honda, Y.; Kitao, O.; Nakai, H.; Vreven, T.; Montgomery, J. A., Jr.; Peralta, J. E.; Ogliaro, F.; Bearpark, M.; Heyd, J. J.; Brothers, E.; Kudin, K. N.; Staroverov, V. N.; Kobayashi, R.; Normand, J.; Raghavachari, K.; Rendell, A.; Burant, J. C.; Iyengar, S. S.; Tomasi, J.; Cossi, M.; Rega, N.; Millam, J. M.; Klene, M.; Knox, J. E.; Cross, J. B.; Bakken, V.; Adamo, C.; Jaramillo, J.; Gomperts, R.; Stratmann, R. E.; Yazyev, O.; Austin, A. J.; Cammi, R.; Pomelli, C.; Ochterski, J. W.; Martin, R. L.; Morokuma, K.; Zakrzewski, V. G.; Voth, G. A.; Salvador, P.; Dannenberg, J. J.; Dapprich, S.; Daniels, A. D.; Farkas, Ö.; Foresman, J. B.; Ortiz, J. V.; Cioslowski, J.; Fox, D. J. Gaussian, Inc., Wallingford CT, **2009**.
[146]a) Bucci, A.; Savini, A.; Rocchigiani, L.; Zuccaccia, C.; Rizzato, S.; Albinati, A.; Llobet, A.; Macchioni, A. *Organometallics*, **2012**, *31*, 8071-8074. b) Menendez Rodriguez, G.; Bucci, A.; Hutchinson, R.; Bellachioma, G.; Zuccaccia, C.; Giovagnoli, S.; Idriss, H.; Macchioni, A. *ACS Energy Lett.* **2017**, *2*, 105-110. c) Dijk, B.; Menendez Rodriguez, G.; Wu, L.; Hofmann, J. P.; Macchioni, A.; Hetterscheid, D. G. H. *ACS Catal*. **2020**, *10*, 4398-4410. d) Menendez Rodriguez, G.; Zaccaria, F.; Dijk, S. V.; Zuccaccia, C.; Macchioni, A. *Organometallics* **2021**, *40*, 3445-3453.

[147]Li, Z.; Park, H. S.; Qiao, J. X.; Yeung, K.-S.; Yu, J.-Q. *J. Am. Chem. Soc*. **2022**, *144*, 18109-18116.
[148]a) Mondal, A.; Li, Y.; Khan, M. A.; Ross, J. S.; Houser, R. P. *Inorg. Chem.* **2004**, *43*, 7075-7082. b) Chaudhuri, U. P.; Whiteaker, L. R.; Yang, L.; Houser, R. P. *Dalton Trans*., **2006**, 1902-1908. c) Cody, C. C.; Kelly, H. R.; Mercado, B. Q.; Batista, V. S.; Crabtree, R. H.; Brudvig, G. W. *Inorg. Chem*. **2021**, *60*, 14759-14764.
[149]Pérez-Gómez, M.; Azizollahi, H.; Franzoni, I.; Larin, E. M.; Lautens, M.; García-López, J.A. *Organometallics* **2019**, *38*, 973-980.
[150]a) Yang, Y.-F.; Hong, X.; Yu, J.-Q.; Houk, K. N. *Acc. Chem. Res*. **2017**, *50*, 2853-2860. b) Yang, Y.-F.; Chen, G.; Hong, X.; Yu, J.-Q.; Houk, K. N. *J. Am. Chem. Soc*. **2017**, *139*, 8514-8521. c). Hill, D. E.; Pei, Q.-L.; Zhang, E.-X.; Gage, J. R.; Yu, J.-Q.; Blackmond, D. G. *ACS Catal*. **2018**, *8*, 1528-1531. d) Romero, E. A.; Chen, G.; Gembicky, M.; Jazzar, R.; Yu, J.-Q.; Bertrand, G.; *J. Am. Chem. Soc*. **2019**, *141*, 16726-16733.
[151]Chen, G.; Gong, W.; Zhuang, Z.; Andrä, M. S.; Chen, Y.-Q.; Hong, X.; Yang, Y. F.; Liu, T.; Houk, K. N.; Yu, J.-Q. *Science*, **2016**, *353*, 1023-1027.
[152] a) Guo, P.; Joo, J. M.; Rakshit, S.; Sames, D. J. Am. Chem. Soc. 2011, 133, 16338-16341. b) Ye, M.; Gao, G.-L.; Edmunds, A. J. F.; Worthington, P. A.; Morris, J. A.; Yu, J.-Q. J. Am. Chem. Soc. 2011, 133, 19090-19093. c) Dai, F.; Gui, Q.; Liu, J.; Yang, Z.; Chen, X.; Guo, R.; Tan, Z. Chem. Comm. 2013, 49, 4634-4636. d) Gao, G.-L.; Xia, W.; Jain, P.; Yu, J.-Q. Org. Lett. 2016, 18, 744-747. e) Musaev, D. G.; Haines, B. E. Chem. Cat. Chem. 2021, 13, 1201-1206.
[153]a) Casado, A. L.; Casares, J. A.; Espinet, P. *Organometallics* **1997**, *16*, 5730-5736. b) Albéniz, A. C.; Espinet, P.; López-Cimas, O.; Martín-Ruiz, B. *Chem. Eur. J*. **2005**, *11*, 242-252.
[154]Yang, C.-T.; Fu, Y.; Huang, Y.-B.; Yi, J.; Guo, Q.-X.; Liu, L. *Angew. Chem. Int. Ed.* **2009**, *48*, 7398-7401.
[155]Thuy-Boun, P. S.; Villa, G.; Dang, D.; Richardson, P.; Su, S. and Yu, J-Q. *J. Am. Chem. Soc*. **2013**, 135, 17508-17513.
[156]Zhuang, Z.; Herron, A. N.; Fan, Z. and Yu, J-Q. *J. Am. Chem. Soc*. **2020**, *142*, 6769-6776.
[157]Cody, C. C.; Kelly, H. R.; Mercado, B. Q.; Batista, V. S.; Crabtree, R. H.; Brudvig, G. W. *Inorg. Chem.*, **2021**, *60*, 14759-14764.
[158]Mondal, A.; Li, Y.; Khan, M. A.; Ross, J. H.; Houser, R. P. *Inorg. Chem.*, **2004**, *43*, 7075-7082.
[159]Chaudhuri, U. P.; Whiteaker, L. R.; Yang, L.; Houser, R. P. *Dalton Trans.*, **2006**, 1902-1908.
[160]Kerdphon, S.; Quan, X.; Parihar, V. S.; Andersson, P. G. *J. Org. Chem.* **2015**, *80*, 11529-11537.
[161]Yang, T.; Cao, X.; Zhang, X.-X.; Ou, Y.; Au, C.-T.; Yin, S.-F.; Qiu, R. *J. Org. Chem*. **2020**, *85*, 12430-12443.
[162]Pérez-Gómez, M.; Azizollahi, H.; Franzoni, I.; Larin, E. M.; Lautens, M.; García-López, J.-A. *Organometallics*, **2019**, *38*, 973-980.